The response of tumour-infiltrating myeloid cells to the chemotherapy-treatment of tumours

Reuben Harwood

Department of Oncology

University of Sheffield

Thesis submitted for the degree of Doctor of Philosophy

December 2013

Declaration

No part of the work referred to in this thesis has been included in submissions for other qualifications of this or any other University or Institute of Learning.

ACKNOWLEDGEMENTS

The work presented in this thesis would not have been possible without the support and collaboration of many friends and colleagues. First, my thanks go to the University of Sheffield (UoS), UK, and the Agency for Science, Technology and Research (A*STAR), Singapore, for funding my PhD. Living and working in Singapore for two years was an excellent learning experience – both professionally and personally – for which I will always be thankful.

Secondly, my gratitude extends to my supervisors, Professor Claire Lewis (UoS) and Dr. Subhra Biswas (A*STAR), whose guidance, challenging and general support during my PhD kept me focussed and continually learning. Their more recent assistance in the preparation of this thesis is also very much appreciated and I thank them for the many opportunities they have given me.

Furthermore, I would like to acknowledge the tremendous amount of support I have received from friends/colleagues in the lab, particularly Dr. Russell Hughes, who have put up with a less competent scientist at the start of this PhD and have supported me through till the end. They are extremely fun to work alongside and I will miss the dim sum lunchtime outings and, of course, the Francis Newton lecture series. Additionally, I thank Dr. Munitta Muthana and Dr. Russell Hughes for their provision of ASV-B and LLC murine tumour samples used in this thesis. I also thank my less-squeamish colleagues in A*STAR who volunteered to donate blood for the isolation of neutrophils, although they got at least as much blood from me as I did from them, so I count us even!

I am also very grateful to Dr. Joan Massagué, Dr. Swarnali Acharyya and Dan Macalinao (Memorial Sloan-Kettering Cancer Center, USA) for their collaboration and generous provision of PyMT murine tumour samples. The tumour samples and data provided by them are clearly cited in the chapters that follow, but I also wish to acknowledge their helpful correspondence and continued collaboration since more mouse studies are currently ongoing.

Needless to say, the support of my family goes well beyond the boundaries of this PhD, but in these past years they have remained thoroughly

encouraging and supportive. They have been a source of love and reassurance in my times of stress and panic, even when I was thousands of miles away in Singapore. I am also proud of each of you for your own achievements. I thank my parents for giving me the opportunity to reach where I am today, and despite not understanding much of it, I also thank then for sperl checking my thebis.

And finally… Lydie. I first met you in Sheffield when I started my PhD and now you're my wife! So much has happened in between then and now and marrying you was the highlight, even though you can be a grumpy old trout at times, and trying to understand you is a futile endeavour. You have given me a good kicking when I needed it, and you have waited impatiently those two years I was in Singapore. I can't thank you enough for all your support and I pray you never change.

As is the aspiration of every cancer research scientist, I hope that my blood (extracted from me for experiments), sweat (in the ridiculous humidity of Singapore) and tears (of joy when an experiment worked) add a significant contribution to the fight against cancer.

CONTENTS

LIST OF FIGURES

LIST OF TABLES

ABBREVIATIONS

5-FU 5-fluorouracil

4T1 murine breast cancer cells

A549 human lung adenocarcinoma cells

ANG-2 angiopoietin-2

APCs antigen presenting cells

APRIL a proliferation-inducing ligand

ARG1 arginase 1

ASV-B Transgernic mice of the antitrobin III-SV40T lineage that develop liver tumours

BAFF B cell-activating factor

bFGF basic fibroblast growth factor

C5a complement 5a

CCL1 chemokine (C-C motif) ligand 1

CCL2 chemokine (C-C motif) ligand 2

CCL3 chemokine (C-C motif) ligand 3

CCL7 chemokine (C-C motif) ligand-7

CCL8 chemokine (C-C motif) ligand 8

CCL16 chemokine (C-C motif) ligand 16

CCL17 chemokine (C-C motif) ligand 17

CCL18 chemokine (C-C motif) ligand 18

CCL22 chemokine (C-C motif) ligand 22

CCL24 chemokine (C-C motif) ligand24

CCR2 chemokine (C-C motif) receptor 2

CD3-ζ cluster of differentiation 3-zeta

CD4 cluster of differentiation 4

CD8 cluster of differentiation 8

CD44 cluster of differentiation 44

CD80 cluster of differentiation 80

CD86 cluster of differentiation 86

CD163 cluster of differentiation 163

CINC-1 (also known as CXCL1/Groα/KC) cytokine-induced neutrophil chemoattractant-1

COX-2 cyclooxygenase-2

CSF-1 colony-stimulating factor-1

CSF1R colony-stimulating factor 1 receptor

CTL cytotoxic T lymphocyte

CTSB cathepsin B

CTSC cathepsin C

CTSL cathepsin L

CTSS cathepsin S

CXCL1 (also known as Groα/KC/CINC-1) chemokine (C-X-C motif) ligand 1

CXCL2 (also known as Groβ/MIP-2) chemokine (C-X-C motif) ligand 2

CXCL3 (also known as Groγ) chemokine (C-X-C motif) ligand 3

CXCL5 (also known as ENA-78) chemokine (C-X-C motif) ligand 5

CXCL8 (also known as IL-8) chemokine (C-X-C motif) ligand 8

CXCL13 chemokine (C-X-C motif) ligand 13

DC dendritic cell

DEG differentially expressed gene

DMEM Dulbecco's modified eagle medium

DMSO dimethyl sulphoxide

DOX/CTX doxorubicin and cyclophosphamide combined chemotherapy treatment

ECM extracellular matrix

EGF epidermal growth factor

ELISA enzyme-linked immunosorbent assay

ELR glutamic acid-leucine-arginine

EMT epithelial–mesenchymal transition

ERK extracellular signal-regulated kinases

FACS fluorescence-activated cell sorting

FOV field-of-view

G-CSF granulocyte colony-stimulating factor

GC glucocorticoid

GM-CSF granulocyte-macrophage colony-stimulating factor

GMP granulocyte-macrophage progenitor

Gr-1 granulocyte-differentiation antigen-1

Groα (also known as CXCL1/KC/CINC-1) growth-related oncogene alpha

Groβ (also known as CXCL2/MIP-2) growth-related oncogene beta

Groγ (also known as CXCL3) growth-related oncogene gamma

H&E hematoxylin and eosin stain

HGF hepatocyte growth factor

HIF-1α hypoxia inducible factor-1 alpha

HNP-1 human neutrophil peptide-1

HNP-3 human neutrophil peptide-3

HSC hematopoietic stem cell

ICAM-1 intercellular adhesion molecule-1

IFN-β interferon beta

IFN-γ interferon gamma

IL-1 interleukin-1

IL-1ra interleukin-1 receptor antagonist

IL-1β interleukin-1 beta

IL-4 interleukin-4

IL-6 interleukin-6

IL-8 (also known as CXCL8) interleukin-8

IL-10 interleukin-10

IL-12 interleukin-12

IL-13 interleukin-13

IL-13Rα2 interleukin-13 receptor, alpha 2

IL-22 interleukin-22

IL-23 interleukin-23

iMC immature myeloid cell

IMDM Iscove's modified Dulbecco's medium

iNKT invariant natural killer T

iNOS inducible nitric oxide synthase

IRF5 interferon regulatory factor 5

KC (also known as CXCL1/Groα/CINC-1) keratinocyte chemoattractant

LBT4 leukotriene B4

LLC murine Lewis lung carcinoma cells

LPS lipopolysaccharide

Ly6B.2 lymphocyte antigen B.2

Ly6C lymphocyte antigen 6C

Ly6G lymphocyte antigen 6G

MDM monocyte-derived macrophage

MDP macrophage-dendritic cell progenitor

MDSC myeloid-derived suppressor cell

MHC I major histocompatibility complex I

MHC II major histocompatibility complex II

MMP13 matrix metalloprotease 13

MMP19 matrix metalloprotease 19

MMP9 matrix metalloprotease 9

MMTV-PyMT mouse mammary tumour virus-driven polyoma middle T transgenic mouse

MPS mononuclear phagocyte system

mRNA messenger ribonucleic acid

MyD88 myeloid differentiation factor 88

NE neutrophil elastase

NET neutrophil extracellular trap

NF-kB nuclear factor-kappa B

NK natural killer

NLR NOD-like receptor

NO nitric oxide

NSCLC non-small cell lung cancer

P53 tumour protein 53

PAMP pathogen-associated molecular pattern

PDAC pancreatic ductal adenocarcinoma

PGE2 prostaglandin E2

PMN polymorphonuclear cells

PR3 proteinase 3

PRR pattern recognition receptor

PSGL-1 P-selectin glycoprotein ligand-1

PTX paclitaxel

PTX3 pentraxin 3

PyMT (see MMTV-PyMT)

qPCR quantitative polymerase chain reaction

RLR RIG-I-like receptor

RNS reactive nitrogen species

ROS reactive oxygen species

RT-PCR real-time polymerase chain reaction

rTNF recombinant tumour necrosis factor

SAA1 serum amyloid A1

SDF-1 stromal-derived factor-1

SGD neutrophil-specific granule deficiency

STAT signal transducer and activator of transcription

TAM tumour-associated macrophage

TAN tumour-associated neutrophil

TCR T cell receptor

TGF-β transforming growth factor-beta

TGF-βR transforming growth factor-beta receptor

TLR Toll-like receptor

TNFRI tumour necrosis factor receptor 1

TNFRII tumour necrosis factor receptor 2

TNFα tumour necrosis factor alpha

TRAF tumour necrosis factor receptor-associated factor

TRAIL tumour necrosis factor-related apoptosis-inducing ligand

Tregs regulatory T cells

TUNEL terminal transferase-mediated dUTP nick end labelling

uPA urokinase-type plasminogen activator

uPAR urokinase-type plasminogen activator receptor

VEGF vascular endothelial growth factor

WHO World Health Organisation

WNT5A wingless-type MMTV integration site family, member 5A

w.r.t with respect to

ABSTRACT

Myeloid cells are a major component of most forms of malignant tumour. The plasticity of such cells means that they can alter their phenotype in response to changes in the tumour microenvironment, including the pronounced ones that take place after chemotherapy. Tumour cell death, as well as the various cytokines and chemokines released by cells in tumours after such treatments, are now known to alter both the recruitment and function of myeloid cells. Recent studies have shown that monocytes recruited into tumours during/following chemotherapy can promote tumour chemoresistance and metastasis. The data presented in this thesis suggest that, following chemotherapy, tumour-associated macrophages (TAMs) may increase their expression of the neutrophil-recruiting chemokines, CXCL1, CXCL2 and CXCL5, and possibly stimulate the intratumoural accumulation of neutrophils. Responding to these CXC chemokines (and possibly other secreted factors in chemotherapy-treated tumours), neutrophils may then upregulate their expression of such inflammatory cytokines as TNFα, CCL2 and CCL3. Furthermore, data from *in vitro* invasion assays suggest that neutrophil-derived TNFα is capable of inducing tumour cell invasiveness. Notably, the number of tumour-infiltrating neutrophils was significantly increased after chemotherapy in 3 of the 4 mouse tumour models used. Furthermore, in all 4 tumour models there were significantly more $TNF\alpha^+$ neutrophils after chemotherapy compared to control tumours. Combined treatment with chemotherapy and SB 265610, a CXCR2 antagonist that inhibits CXCL1, CXCL2 and CXCL5 signalling, successfully reduced both the number of these tumour-infiltrating, $TNF\alpha^+$ neutrophils, and the overall level of immunodetectable TNFα in tumours after chemotherapy. Although TNFα is known to be capable of supporting tumour growth, angiogenesis and metastasis, it remains to be seen whether such an increase in neutrophil TNFα expression contributes significantly to the post-chemotherapy regrowth of either primary or metastatic tumours. This could be achieved by giving chemotherapy to mice in which TNFα has been selectively knocked out/down in neutrophils. Data presented here suggest that combining chemotherapy with CXCR2 inhibitors like SB 265610 to inhibit the above neutrophil-mediated events could improve patient tumour responsiveness to chemotherapy and reduce tumour relapse.

1 INTRODUCTION

1.1 BASICS OF THE IMMUNE SYSTEM

The body is protected from invading pathogens by the immune system, a complex network of cells, humoral factors, tissues and organs. It consists of adaptive and innate immunity. Both rely on cells called 'white blood cells' or 'leukocytes', including monocytes, macrophages and neutrophils. These cells are professional phagocytes and key to the processes of inflammation and tissue repair. They share a common lineage in early stages of myeloid cell development, and are derived mainly from haematopoietic stem cells (HSCs) in the bone marrow (**Fig 1.1**). Under some conditions, bone marrow-derived HSCs can also accumulate at extramedullary sites, such as the spleen, which can also then become an important site for monocyte production [1].

1.2 ORIGINS OF MACROPHAGES AND NEUTROPHILS

Macrophages and neutrophils are classically categorised as belonging to the haematopoietic stem cell (HSC) lineage in the bone marrow, and a temporal sequence of progenitor cells that ultimately lead to macrophage and neutrophil differentiation has been described [2-5]. However, in recent years gathering evidence has challenged former understanding [6], rewriting the ontology of myeloid cells at least in mice. The mononuclear phagocyte system (MPS) – a family of cells that includes monocytes, macrophages and dendritic cells [7] – has been shown to derive from at least three sources (**Fig 1.1**). Firstly, resident macrophages of the central nervous system called 'microglia' were identified as arising from yolk sac progenitors in mice, and thus were an ontogenically distinct population in the MPS [8]. In contrast, murine Langerhans cells – the dendritic cells of the epidermis – were shown to derive mainly from progenitors in the foetal liver, with only a minor contribution from the yolk sac [9].

Furthermore, a key study demonstrated that the transcription factor, Myb, which is essential in bone marrow haematopoiesis, is functionally irrelevant in yolk sac macrophages and for several F4/80^{hi} yolk sac-derived tissue macrophage populations that persist in adult mice [10]. In this way, the

major F4/80^{hi} resident macrophage populations in liver, skin, spleen, pancreas, brain and lung, were identified as arising from yolk sac progenitors (**Fig 1.1**). Additionally, kidney (Kupffer) macrophages and lung (alveolar) macrophage populations were found to include F4/80^{lo} cells, but also some F4/80^{hi} cells, suggesting a mixed origin from both the bone marrow and yolk sac [10]. The smaller F4/80^{lo} macrophage population and classical dendritic cells are continually seeded by bone marrow haematopoiesis. Taken together, these data

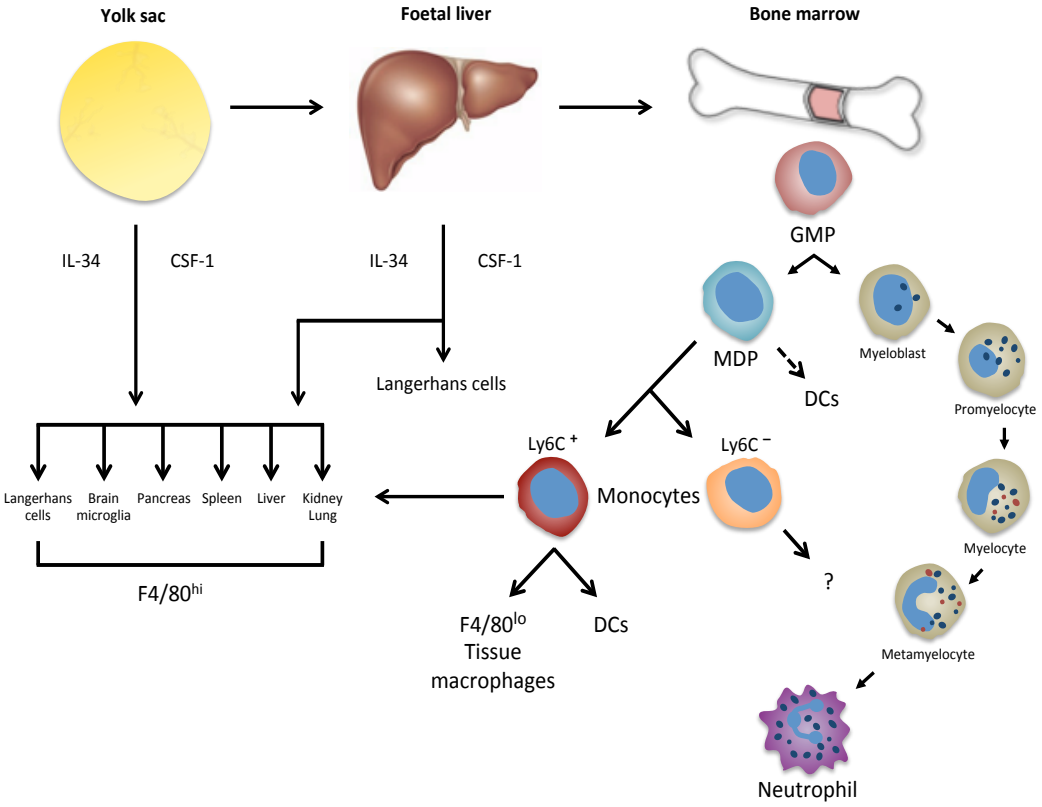

Figure 1.1 Myeloid cell lineage. Macrophages and neutrophils are thought to derive from common progenitors. Recent evidence shows that the mononuclear phagocyte system in adult mice derives from at least three sources: the yolk sac, the foetal liver, and the bone marrow. Progenitors from the yolk sac can seed to all tissues and are thought to give rise to F4/80^{hi} resident macrophages, under the guidance of IL-34 and CSF-1. The foetal liver also contributes to production of Langerhans cells, possibly via a progenitor cell from the yolk sac. Circulating monocytes, F4/80^{lo} macrophages and dendritic cells derive from the classic 'bone marrow lineage'. In certain organs, including kidney and lung, F4/80^{lo} tissue macrophages derived from the bone marrow, and F4/80^{hi} tissue macrophages from the yolk sac, coexist and produce chimeric organs. The exact roles of patrolling Ly6C^{-} monocytes is currently unclear. GMP, granulocyte-monocyte progenitor; MDP, monocyte dendritic cell progenitor. Adapted from [6] and [11].

suggest that murine macrophages originate from three sources, and further studies are needed to better understand the role of circulating Ly6C$^-$ monocytes, given that murine Ly6C$^-$ monocytes do not seem to be important for seeding adult tissues with macrophages [6]. In support of this, the loss of the analogous 'resident' monocyte population in humans – supposedly important for rapid response to infection (see **section 1.2.2.2**) – appears to have little effect on patient susceptibility to infection [12].

1.2.1 MONOCYTE AND NEUTROPHIL RELEASE INTO THE BLOOD

Mobilisation of monocytes from the bone marrow into the blood is controlled, in part, by C-C chemokine receptor type 2 (CCR2) expressed on monocytes, in addition to activating and recruiting them from the blood to sites of inflammation [13, 14]. The CCR2 ligands that direct these processes include such C-C chemokine ligands as CCL7 and CCL2 [13].

Neutrophil production and release into the blood – a process called granulopoiesis - is also regulated by soluble cytokines like granulocyte-colony stimulating factor (G-CSF), which regulates neutrophil numbers in the blood [15]. Neutrophils leave the bone marrow as part of steady-state homeostasis. However, large pools of mature neutrophils are also retained, forming bone marrow reserves [16]. During inflammation, such pro-inflammatory cytokines as CXCL-1 [16], CXCL-2 [17], CXCL-8 [18], TNFα, leukotriene B4 (LTB4) and complement 5a (C5a) [19] are increased in the blood, inducing a rapid release of neutrophils from bone marrow reserves. Both monocytes and to a lesser extent, neutrophils, express the chemokine receptor CXCR4, for which one of the ligands is stromal-derived factor-1 (SDF-1 or CXCL12). As its name suggests, SDF-1 was first identified as a factor released by stromal cells of the bone marrow [20]. The binding of CXCR4 by SDF-1 is important for the retention of monocytes and neutrophils in the bone marrow, acting as a negative regulator of their release [16, 21]. Once released from the bone marrow, circulating monocytes migrate into tissues under homeostatic and inflammatory conditions. Under typical inflammatory conditions, growth factors, cytokines and any microbial products present locally in the tissues induce phenotypic changes, and the differentiation of monocytes into macrophages and dendritic cells.

1.2.2 MACROPHAGE LINEAGE AND MONOCYTE SUBSETS

Monocytes can be distinguished from other leukocytes through their expression of CD11b, Csf-1 receptor (CD115) and chemokine receptor CX_3CR1, and lack of expression of CD15, CD19, Nkp-46 or CD3. Within the monocyte population, accumulating evidence suggests that phenotypically discrete subsets exist. In mice and humans, two major populations of monocytes have been described: inflammatory and resident monocytes, as shown in **Table 1.1**. The resident population of monocytes patrol tissue microvasculatures for danger, while the other describes the classical inflammatory monocytes that accumulate at inflammatory sites, and have a shorter lifespan than the resident population [22, 23].

	Inflammatory or Classical	Resident or Non-classical
Human	$CD14^{++}$	$CD14^{+}$
	$CD16^{-}$	$CD16^{+}$
	CX_3CR1^{lo}	CX_3CR1^{hi}
	$CCR2^{+}$	$CCR2^{-}$
	Shorter lived	Longer lived
Murine	CX_3CR1^{lo}	CX_3CR1^{hi}
	$CCR2^{+}$	$CCR2^{-}$
	$Gr1^{+}$	$Gr1^{-}$
	$CD62L^{+}$	$CD62L^{-}$
	Shorter lived	Longer lived

Table 1.1 Monocyte populations in humans and mice. This table shows the markers and features that identify the inflammatory (classical) and resident (non-classical) populations of human and murine monocytes. Human inflammatory monocytes can be identified as $CD14^{++}CD16^{-}$ cells, and $CD14^{+}CD16^{+}$ cells as human resident monocytes. In mice, inflammatory and resident monocytes are identified as $CX_3CR1^{lo}CCR2^{+}Gr1^{+}$ and $CX_3CR1^{hi}CCR2^{-}Gr1^{-}$ cells, respectively. Adapted from [22].

1.2.2.1 INFLAMMATORY MONOCYTES

The 'inflammatory' monocyte population are identified by expression of CCR2, which is important for their recruitment to sites of inflammation, and of Gr1, a myeloid differentiation antigen. They also exhibit low expression of CX_3CR1, a chemokine receptor that is involved in monocyte adhesion and migration [22] (**Table 1.1**). Recruited to sites of inflammation, these

$CX_3CR1^{lo}CCR2^{+}Gr1^{+}$ monocytes have been shown to specialise in the production of pro-inflammatory cytokines tumour necrosis factor (TNF), reactive oxygen species (ROS), nitric oxide (NO), and type 1 interferon, but marginal anti-inflammatory cytokine interleukin (IL)-10 in response to bacterial and viral infection, as has been discussed elsewhere [24, 25]. This inflammatory monocyte population also have a shorter survival of approximately 48 hours [14]. In line with their production of pro-inflammatory molecules, classical monocytes can differentiate into immunostimulatory dendritic cells (DCs), which are professional antigen presenting cells (APCs) that communicate with the adaptive immune system. Furthermore, these cells are also believed to give rise to myeloid-derived suppressor cells (MDSCs), which are important in the resolution of acute inflammation [26].

Similar monocyte subsets have been described in humans, whereby the more abundant inflammatory or 'classical' monocyte population are identified by high expression of CD14 (**Table 1.1**), a co-receptor that detects conserved bacterial motifs including lipopolysaccharide (LPS) [27], and an absence of Fc receptor CD16 expression [28, 29]. Such $CD14^{++}CD16^{-}$ classical monocytes share commonalities in their surface marker expression and gene expression with murine inflammatory monocytes [22].

1.2.2.2 Resident Monocytes

Conversely, 'resident' or 'non-classical' monocytes are characterised in mice by the expression of CX_3CR1, which binds to its ligand CX_3CL1 [30] and is important in recruitment of resident monocytes into non-inflamed tissue [22] (**Table 1.1**). They also exhibit greatly reduced CCR2 and Gr1 expression, and therefore are identified as $CX_3CR1^{hi}CCR2^{-}Gr1^{-}$ cells [22]. In humans, (low) expression of CD14 and high expression of CD16 identifies a similar, non-classical subset of macrophages [29]. Analogous to murine resident monocytes, human $CD14^{++}CD16^{-}$ monocytes are also $CCR2^{-}$ [31] and the $CD14^{+}CD16^{+}$ monocyte phenotype can additionally be defined by CX_3CR1^{hi} expression in humans [22]. $CD14^{+}CD16^{+}$ monocytes exhibit patrolling behaviour in blood vessels [32] similar to that shown in mice [23], whereby they roll along the

surface of endothelial cells to allow for a very rapid response to damage and/or infection.

1.2.3 NEUTROPHIL LINEAGE

Neutrophils arise through the process of granulopoiesis, sharing a common myeloid lineage with bone marrow-derived monocytes and macrophages [2-5] (**Fig 1.1**). Granulopoiesis involves the differentiation of granulocyte-monocyte progenitors (GMPs) into myeloblasts, the first of the granulocyte precursors, which are capable of differentiating into neutrophils, eosinophils and basophils [11, 33, 34]. Tracking the neutrophil lineage, myeloblasts differentiate further into promyelocytes, myelocytes and then metamyelocytes, which ultimately mature into neutrophils (**Fig 1.1**).

Neutrophils are produced in the bone marrow at a rate of $\sim 10^6$ per second in humans and circulate in the blood at a concentration of between 3 and 6 million cells per millilitre in a healthy human [35]. They are far more abundant than monocyte/macrophage phagocytes, but have a much shorter lifespan. It is generally believed that neutrophils survive less than a day in the body, showing a half-life of approximately 8-10 hours in mice [36] and 10 hours in humans [37-39]. Other studies have suggested that under homeostatic conditions neutrophils may in fact live up to 12.5 hours and 5.4 days *in vivo* in mice and humans, respectively [40]; however, the methodology used (^2H_2O-labelled water) was later criticised since it is likely to label bone marrow neutrophils as well as circulating cells, thus augmenting the measure of neutrophil longevity in the blood [41]. Communication between the complex networks of cells, tissues, and organs that make up the immune system is required to coordinate an effective immune response.

In humans, neutrophil pools are sustained by steady state granulopoiesis under homeostatic conditions. Infection and inflammation, however, triggers neutrophilia via the release of neutrophils from pools in the bone marrow, and increases the rate of neutrophil generation in a process termed 'emergency' granulopoiesis [42]. This is partially stimulated by macrophage and neutrophil

release of G-CSF, CXCL1 and CXCL8 [43, 44] upon detection of infection, supporting increased neutrophil release from the bone marrow.

1.3 INNATE RESPONSE TO INFECTION

After penetrating the skin and other external defences (e.g. mucous membranes, gut lining etc.), microbes must traverse the epithelial barrier where they will encounter components of the innate immune system. Initially, pathogens are recognised by the innate components of the immune system. These macrophages and neutrophils are capable of discriminating between different types of infectious pathogen, but are not capable of immunological memory. Immunological memory is important for a rapid response to previously encountered infectious agents and involves the specific arm of the immune system.

The outcome of microbial invasion is very much dependent upon the interaction between the microbe and host. In cases where the host generates a balanced immune response to control and destroy microbes, infectious disease can be avoided. Should the microbial attack mechanisms favour the microbe, pathogenic infection may occur. The host response to the presence of microbes is also governed by the damage done to the host through toxins and enzymes, which may lead to host cell apoptosis and necrosis, or support the transition to malignancy [45].

1.3.1 PATTERN RECOGNITION RECEPTORS

The innate arm of the immune system responds rapidly to common motifs present on microbes called 'pathogen-associated molecular pattern' (PAMPs) using germline-encoded pattern recognition receptors (PRRs). Some of the most important PRRs are Toll-like receptors, or TLRs, of which there are 10 functional receptors identified in humans and 12 in mice, and TLRs 1-9 are conserved between humans and mice [46, 47]. Human TLRs 1, 2, 4, 5, 6 and 10 are expressed on the cell surface, primarily binding to components of microbial membranes and cell walls, whereas TLRs 3, 7, 8 and 9 are incorporated into the membranes of endosomes and predominantly detect foreign nucleic acids. Additionally, TLR10 is only expressed in humans and TLR11 only in mice.

Experimental models have been used to observe the effects of the deletion of each TLR individually and to identify ligands of these receptors, including a diverse array of protein, lipoprotein, lipid and nucleic acid components of microorganisms [48]. Activation of TLRs on innate immune cells characteristically leads to the production of such inflammatory cytokines as TNFα, IL-1, IL-6, and IL-12 [49-51].

Other PRRs that have been identified include RIG-I-like receptors (RLRs), which detect viral RNA species [52], and a large family of receptors called Nod-like receptors (NLRs) [53], which also detect a wide range of PAMPs that are expressed on, or are part of, infectious agents. The intracellular signalling that results from the binding of PRRs, and upregulation of pro-inflammatory cytokine expression, are the first steps towards initiating an immune response [54].

1.3.2 PHAGOCYTOSIS

Phagocytosis – the engulfing of cells – is also a key feature of innate immunity. The process was initially described in 1883 by Ilya Metchnikoff who shared a Nobel prize for his discovery of the cells that he and his colleagues termed phagocytes [55].

Metchnikoff noted that phagocytes could: (i) rapidly detect microbes, (ii) phagocytose foreign material like fungal spores, and (iii) exert antimicrobial activity, which he postulated was through some sort of secretion. The main professional phagocytes are macrophages (literally meaning 'big eaters') and neutrophils [56, 57]. Their ability to engulf material is not just important for eradication of pathogens, but also for the clearing of dead cells and debris as part of normal tissue homeostasis and conditions like wound healing [58, 59].

Macrophages and neutrophils are complementary and cooperative partners, ingesting the invading microbes they encounter and coordinating an immune response against them. Their arsenal of anti-microbial mechanisms includes the production of reactive oxygen and nitrogen species (ROS and RNS), granule proteins, and iron-withholding molecules [60, 61]. Detection and phagocytosis of material by macrophages and neutrophils also leads to their production of pro-inflammatory cytokines TNFα, IL-1, IL-6, CXCL2 and CCL5

[62], through which they recruit other inflammatory cells to the site of infection and activate their anti-microbial functions, and then begin to communicate with the specific (or adaptive) arm of the immune system.

The highly specialised adaptive system is made up of T- and B-lymphocytes that each express a unique antigen receptor. This receptor diversity is achieved through accelerated mutation and recombination of gene segments that encode these receptors [63]. The incredible array of unique receptor-carrying T and B cells helps protect against infection since, even before they encounter any microbes, a receptor that can bind an epitope somewhere on the invading microbe already exists. Therefore, when antigen-presenting cells (APCs) present microbial components, specific T- and B-lymphocytes can bind to particular epitopes via their unique antigen receptors and initiate an adaptive immune response. This crucial step in an immune response leads to the activation and subsequent clonal expansion of cells bearing a receptor that specifically binds the fragment, and therefore will be effective in targeting the invading pathogen. The host produces large quantities of effector and memory lymphocytes that eliminate the invading microbe and protect against future infection [64].

1.4 NORMAL PHYSIOLOGICAL ROLE OF NEUTROPHILS

Neutrophils are known to express an abundance of PRRs, which are key to their identification and phagocytosis of microorganisms as well as their detection of tissue damage. In humans, neutrophils express TLRs 1, 2, 4, 5, 6, 7, 8, 9, and 10 – all the TLRs except TLR3 – which when activated lead to neutrophil cytokine release, enhanced phagocytosis of opsonised latex beads, and inhibition of IL-8–mediated chemotaxis [65].

Under inflammatory conditions, activated neutrophils are also known to produce ROS; such proteolytic enzymes as neutrophil elastase (NE), proteinase 3 (PR3) and cathepsin G [66, 67]; and such antimicrobial proteins as myeloperoxidase, hydrogen peroxide and chloride [68], which they store in intracellular granules. Upon phagocytosis of encountered microbes, these granules fuse with phagosomes to form phagolysosomes, and the resultant

exposure to proteolytic enzymes, antimicrobial proteins, acidic pH, and ROS further support the degradation and killing of microorganisms.

These factors can also be released by active neutrophils into the extracellular environment as an alternative mechanism for attacking microorganisms. Paradoxically, however, this can also lead to host tissue damage and has been implicated in various diseases [33].

Activated neutrophils (e.g. via TLR ligands or CXCR2 ligands) are capable of expressing a wide array of cytokines [69, 70], including:

- TNF superfamily members; including, but not limited to, TNFα, TRAIL, APRIL, BAFF
- Pro-inflammatory cytokines; IL-1, IL-6
- Anti-inflammatory cytokines; IL-1ra, TGF-β
- Immunoregulatory cytokines; IFN, IL-22, IL-23
- CC chemokines; CCL2, CCL3
- CXC chemokines; CXCL1, CXCL2
- Granulocyte colony-stimulating factor; G-CSF
- Fibrogenic and angiogenic factors; HGF, VEGF and IL-8

However, neutrophils are well known for their ability to recruit and activate monocytes at sites of inflammation [71], specifically the inflammatory $CX_3CR1^{lo}CCR2^{+}Gr1^{+}$ monocyte subset in mice [72]. Similar chemotactic effects have been observed towards macrophages and T cells, mediated by neutrophil-derived CCL2 released in skin wounds [73].

The role of neutrophils in angiogenesis is also well established. In such sites as inflamed tissues and malignant tissues, neutrophils can promote angiogenesis, in part driven by their release of matrix metalloprotease-9 (MMP9) and VEGF, and release of VEGF from extracellular stores in the extracellular matrix [74, 75].

1.4.1 Neutrophil Extracellular Traps

Besides phagocytosis and cytokine expression, neutrophils also combat microorganisms via the production of microbial traps in tissues called

'neutrophil extracellular traps' or 'NETs'. By actively extruding chromatin bound to granular proteins to create an extracellular fibrillary network, neutrophils can immobilise and disarm invading pathogens [76]. The DNA is bound by such antimicrobial factors as neutrophil elastase, myeloperoxidase and histones, which – due to their high concentration in NETs – readily bind, immobilise and kill microorganisms.

The exact mechanisms leading to the formation of NETs are not currently known, but several factors could be involved including platelet interaction [77]; the presence of gram positive and gram negative bacteria [76], or fungi [78]; even the cytokines TNFα, IL-1β and IL-8, through the activation of NADPH oxidase and myeloperoxidase [79].

1.5 MACROPHAGE/NEUTROPHIL CROSSTALK

Given their shared origin, it is not surprising that macrophages and neutrophils have many shared characteristics, as summarised in **Table 1.2**.

Feature	**Refs.**
Phagocytic capabilities and an arsenal of anti-microbial functions (e.g. ROS, RNS)	[80, 81]
Expression of similar transcription patterns and co-expressed genes (e.g. CSF-1R, F4/80, COX-2)	[82, 83]
Similar cytokine and chemokine secretion profiles, common surface receptors and antigen expression, making them difficult to target independently (e.g. IL-1β, TNFα, PRRs, CD11b, Ly6C)	[48, 58, 84, 85]
Neutrophils can contribute to scavenging of necrotic cells and debris, particularly when macrophages are overwhelmed	[86]
Mobilisation of macrophages and neutrophils to sites of infection follow a similar pattern	[56]

Table 1.2 Shared characteristics of macrophages and neutrophils. Macrophages and neutrophils share a common lineage in early stages of development. This table summarises key characteristics shared by murine macrophages and neutrophils. Most, but not all, are conserved in humans.

The interaction of neutrophils and macrophages can also occur – with the former helping to recruit the latter under some conditions like inflammation. Neutrophils are often the first responders to sites of infection and inflammation, and are capable of secreting factors that recruit macrophages and additional neutrophils, but can also recruit other such immune cells as T cells, mast cells and dendritic cells. For example, neutrophil release of human neutrophil peptide (HNP)-1 and 3 – natural antibiotic peptides, known as alpha-defensins – was shown to strongly attract macrophages as well as T cells and mast cells [87]. Production of these factors by neutrophils is important in inflammatory diseases including Crohn's disease, inflammatory cardiac disease and inflammatory bowel disease. Furthermore, such peptides also induce TNFα and IL-1β expression in monocytes within the context of Staphylococcus aureus infection [88].

These neutrophil-derived chemotactic molecules explain why a patient with neutrophil-specific granule deficiency (SGD) – characterised by a lack of neutrophil granules that are key to their protein secretion – exhibits reduced monocyte migration into Rebuck skin windows (slides that are applied to abraded skin areas to allow visualisation of leukocyte infiltration) [89]; and why neutropenia, induced by injection of neutrophil-depleting antibody RB6-8C5 or 1A8, caused a significant reduction in the mobilisation of inflammatory monocytes in mice, which could be restored by local injection of secretions isolated from activated neutrophils [72].

Additionally, monocyte-derived macrophages from neutropenic patients were found to express lower levels of cytokines than healthy control volunteers; this included expression of TNFα, IL-6, IL-10 and IL-1RA, indicating a deactivation of macrophages in the absence of neutrophils [90]. Neutrophils, and their granule proteins, are key to the proper function of monocytes/macrophages [91].

Interestingly, tissue resident macrophages at sites of inflammation have been shown in mice to play an important role in the recruitment of neutrophils, by releasing CXCL1 and CXCL2 chemokines [92]. Resident macrophages were shown to upregulate CXC cytokines via signalling dependent upon TLR adaptor

proteins, MyD88 and TRIF, both of which are used by TLR4. Macrophage TLR4 signalling was therefore found to be responsible for the robust chemoattraction of neutrophils, leading to their accumulation at sites of inflammation or injury, which is an essential early step in the immune response. The use of blocking monoclonal antibodies to these chemokines demonstrated *in vitro* and *in vivo* that neutrophil chemotaxis was dependent upon them, thus suggesting that at sites of inflammation or injury, tissue macrophages cause neutrophil accumulation in a CXCL1/CXCL2-dependent manner [93]. Importantly, however, macrophages are also known to stimulate endothelial cells [94]; it is possible therefore that the pro-inflammatory actions of macrophages stimulate epithelial cells to release chemokines via the pro-inflammatory actions of macrophages, and are themselves a major source of neutrophil chemokines [95].

The production of CXCL8 by human blood monocytes upon stimulation with bacterial products, LPS and polyhydroxyalkanoate (PHA), was identified [96]. Two key responses of neutrophils to CXCL8-containing conditioned media were observed: the release of specific granules/exocytosis, and the induction of a respiratory burst (the swift release of reactive oxygen species to combat invading pathogens they encounter). Human and murine macrophages have also been found to express CXCL8 under hypoxic conditions, such as those found in tumours [97]. This correlates with the finding that, in (7 day old) rats where hypoxia/ischaemia was induced by occlusion of the left carotid artery and exposure to a 7.7% oxygen atmosphere, increased numbers of neutrophils were seen in the infarct region [98].

As previously mentioned, neutrophils do not survive long in the blood or following extravasation into tissues and their activation. A tightly regulated apoptotic programme controls their survival, and thus, acts as a mechanism for resolving acute inflammation. Clearance of apoptotic/necrotic neutrophils and associated debris, which is called efferocytosis, is a process in which macrophages play a crucial part as expert scavengers and phagocytes [99, 100]. Interestingly, such pro-inflammatory factors as LPS and TNFα can not only manipulate the rate of apoptosis and promote the survival of macrophages and

neutrophils during infection/inflammation, but have also been demonstrated to inhibit efferocytosis of neutrophils by macrophages [100].

1.6 CELLULAR PLASTICITY

Cells of the MPS share a common feature of plasticity – the ability to adapt and change characteristics in different environments – governed by the combinations of local chemical signals and receptor binding [58, 101]. Plasticity is important for maintaining homeostasis, since tissue repair, regeneration and resolution of inflammation require a dynamic interaction between multifaceted immune cells and resident cells.

1.6.1 M1 AND M2 POLARISATION OF MACROPHAGES

Macrophages display considerable functional plasticity. The conventional paradigm has been that macrophages are antigen-presenting phagocytes that secrete antimicrobial and pro-inflammatory factors. However, it is now known that in response to their environment macrophages can alter their functional phenotype. Initially, two disparate macrophage phenotypes were described, which – although an oversimplification of the true phenotypic diversity – provide a useful framework for the study of macrophage plasticity.

The nomenclature M1 and M2 were ascribed to classically activated and alternatively activated macrophages, respectively. In line with T helper 1 and T helper 2 type immune responses, the M1 macrophage phenotype can be skewed by lipopolysaccharide (LPS) and interferon gamma (IFN-γ), and the M2 phenotype by interleukin-4 (IL-4) and interleukin-13 (IL-13) [101-103], as shown in **Fig 1.2**. In both mice and humans, the pro-inflammatory M1 population of macrophages can be broadly described as being IL-12^{hi}IL-10^{lo}, whereas the generally immunosuppressive M2 population are IL-12^{lo}IL-10^{hi} [104-106]. M1 macrophages have dominant microbicidal and tumouricidal functions, and conversely, M2 macrophages are involved in parasite clearance, immunoregulation in order to supress hypersensitivity and maintain homeostatic conditions, and can promote tissue remodelling and tumour progression.

In addition to high IL-12 and low IL-10 expression, the human M1 macrophage phenotype is further characterised by high expression of such pro-inflammatory molecules as TNFα, IL-1β, IL-6, IL-23 and reactive nitrogen and oxygen species [107, 108], and expression of TLRs 2 and 4, and CD80 and CD86, which are important for detection of pathogens and macrophage direct and indirect killing activities. Additionally, M1 macrophages express high levels of major histocompatibility complex (MHC) I and II, and express CCL5, CCL16, CXCL9, CXCL10 and CXCL11, which together indicate communication with other cells and recruitment of other members of the innate and adaptive immune system to generate strong immune responses [106]. In mice and humans, the transcription factor interferon regulatory factor (IRF) 5 was shown to control the upregulation and downregulation of M1 and M2 marker expression on macrophages [109]. High expression of IRF5 is associated with an M1 macrophage phenotype.

Conversely, M2 macrophages share a low expression of IL-12 and IL-23, and increased expression of scavenger receptor and mannose receptor [102, 103]. Importantly, it was established that M1 and M2 macrophage phenotypes are not simply due to different activation states, but are the outcome of two separate metabolic programmes [110]. Later, a more complex description of macrophage behaviour was suggested, which extrapolated beyond the basic M1 and M2 phenotypes. This acknowledged the array of phenotypes that can be adopted in response to changes in their environment, suggesting that rather than the existence of two distinct subsets, macrophages can 'reversibly and progressively change the pattern of functions that they express' and adopt an array of different phenotypes [111].

In line with this, the M2 population of macrophages has been further divided into three subsets in both mice and humans termed M2a, M2b and M2c, depending upon their environmental stimulation, as shown in **Fig 1.2**. Stimulated with the Th2 cytokines IL-4 and IL-13, macrophages can be polarised to an M2a phenotype, whereby they express IL-1ra to reduce IL-1 inflammatory signalling, and anti-inflammatory cytokine IL-10. They also express scavenger receptor CD163, growth factor TGF-β [102, 112], and cytokines CCL17, CCL22

and CCL24, which lead to recruitment of eosinophils, basophils and Th2 cells and result in a type II response [106].

In contrast, the M2b phenotype is induced by LPS and immune complexes (IC), and by exposure to IL-1ra. M2b macrophages retain their expression of such inflammatory genes as IL-1, IL-6 and TNFα [106], as shown in **Fig 1.2**. Additionally, M2b macrophages are characterised by CCL1 expression, a

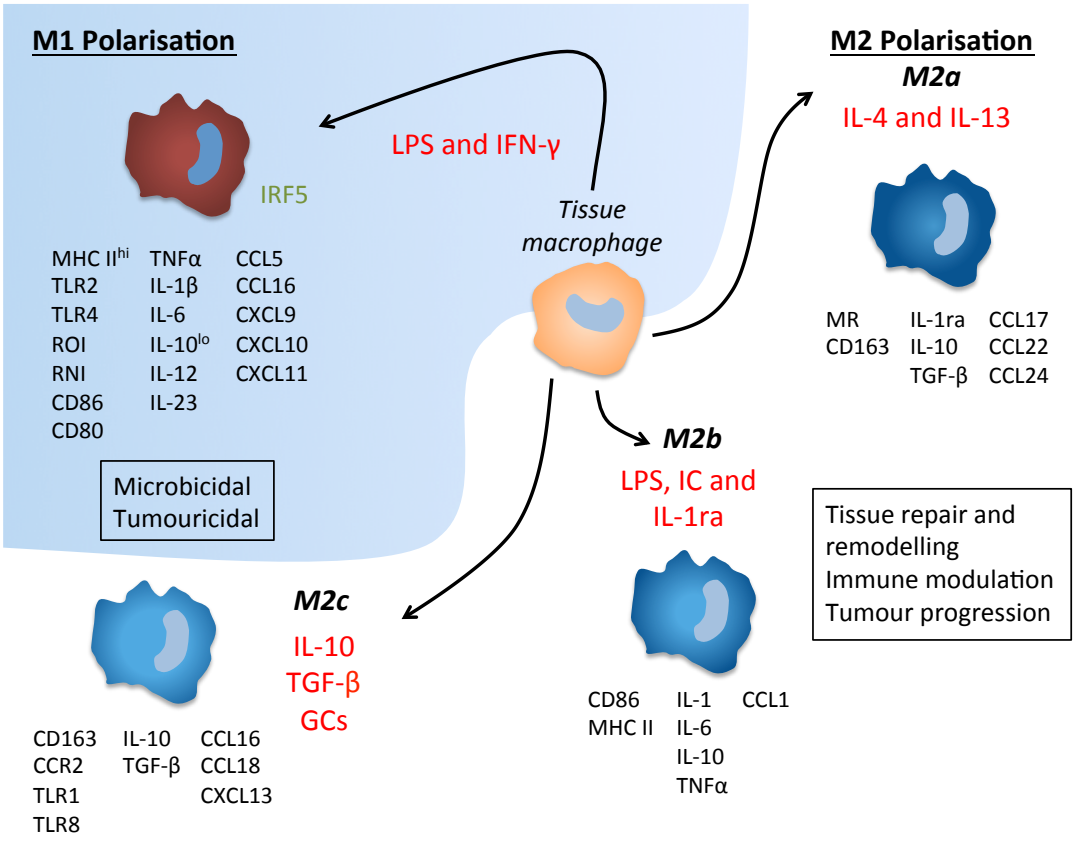

Figure 1.2 Classically and alternatively activated macrophage phenotypes . Classically activated (or M1) macrophages are induced by LPS and IFN-γ and exhibit microbicidal and tumouricidal properties. Alternatively activated (M2) macrophages have contrasting functions, and are involved in tissue remodelling, immunoregulation and aspects of tumour progression. M2 macrophages can be further split into 3 distinct subsets, M2a, b and c. M2a macrophages are induced by IL-4 and IL-13, and M2b macrophages by LPS, IC and IL-1ra, whereas M2c macrophages are conditioned by IL-10, TGF-β and glucocorticoid hormones. However, not all experts in the field believe M2a, b and c to be genuine subsets, arguing that these are just M2 cells. Abbreviations: GC, glucocorticoid; IC, immune complexes; IFN, interferon; IL, interleukin; IRF, interferon regulatory factor; LPS, lipopolysaccharide; MHC, major histocompatibility complex; MR, mannose receptor; ra, receptor antagonist; RNI, reactive nitrogen intermediates; ROI, reactive oxygen intermediates; TGF, transforming growth factor; TLR, Toll-like receptor; TNF, tumour necrosis factor. Image adapted from [104] and [110].

recruitment factor for eosinophils, Th2 cells, and regulatory T cells, through which they promote a Th2 response [112].

Finally, the third population of M2 macrophages are governed by IL-10, TGF-β, and glucocorticoid (GC) hormones [112], and are named M2c macrophages. These macrophages are characterised by CCL16, CCL18 and CXCL13 production in humans [113-115], which are known to chemoattract T lymphocytes, B lymphocytes and monocytes. M2c macrophages also express the scavenger receptor, CD163, and CCR2, which are important for macrophage scavenging and recruitment/migration respectively, and TLRs 1 and 8 [112], which bind bacterial triacyl lipopeptides and single stranded viral RNA, respectively [116]. It is also believed that M2c macrophages, in response to the presence of both LPS and IL-10, are capable of shedding cytokine receptors to act as functional decoys for chemokines, thus dampening inflammation. However, it is worth noting that not all experts in the field believe M2a, b and c to be true subsets, regarding M1 and M2 as the only true macrophage classifications, and so further experimental proof of macrophage subsets is needed. Furthermore, not all described M1 and M2 features are shared between mice and human macrophages; for example, production of arginase and nitric oxide (NO) is a key feature of murine M1 macrophages but is absent in human macrophages [117].

1.6.2 Plasticity of Neutrophils

Neutrophils also display considerable phenotypic plasticity. For example, the stimulation of neutrophils occurs upon interaction with activated endothelial cells and their infiltration into inflamed tissues. This activation has been shown to:

- Upregulate the transcription of such pro-inflammatory genes as IL-8, CCL3, CXCL2, VEGF and IL-1β, which further recruit inflammatory cells and activate their anti-microbial functions, also leading to communication with the adaptive immune system for a full immune response.
- Cause the release of cytoplasmic granules via exocytosis.
- Induce a respiratory burst.

Together these functions help eliminate pathogenic infection [118] via phagocytosis, the release of anti-microbial factors, and the attack by cytotoxic T lymphocytes (CTL) and natural killer (NK) cells.

As mentioned, neutrophils are typically the first responders of the host defence against pathogens. The soluble mediators released locally in the inflammatory milieu include cytokines and chemokines, which activate and induce changes in leukocytes, leading to their sequestration and adhesion to the vascular endothelium, as reviewed previously [11].

Neutrophils bind to the vascular endothelium, a process that involves adhesion mediated by selectin and integrin surface proteins [119-121]. Endothelial cells at inflammatory sites increase their expression of such selectin proteins as E-selectin and P-selectin, which interact with heavily glycosylated proteins on the surface of neutrophils, including P-selectin glycoprotein ligand-1 (PSGL-1), CD44 and ICAM-1 [122]. In regions of inflammation, endothelial cells can express IL-8, which stays bound to their cell surface and triggers activation of CXCR1 and CXCR2 on neutrophils. This activation also stimulates the formation of high affinity interactions with intercellular adhesion molecules (ICAMs) on the surface of inflamed endothelial cells, and a cytoskeletal re-arrangement that facilitates transendothelial migration [123]. In this way, chemokine signalling and selectin signalling co-operate in the recruitment of neutrophils into tissues. Neutrophils undergo extravasation at sites of inflammation, whereupon they are polarised and primed for antimicrobial action. Neutrophil activation triggers the release of such inflammatory oxidants ROS and RNS, alongside an array of cytotoxic factors, during their short lifespan of approximately 1-2 days. Release of these factors by large numbers of neutrophils at sites of infection and inflammation are crucial for fighting invading pathogens. However, the uncontrolled release of these compounds can also lead to severe host tissue damage, which is why under normal homeostatic conditions this process is tightly regulated [121].

Neutrophil plasticity acts as a key negative regulator of inflammation; under certain conditions, the pro-inflammatory nature of tissue neutrophils can

be reversed. For example, the effects of serum amyloid A1 (SAA1) on neutrophil phenotype and differentiation were recently described [124]. SAA1 is a major acute phase protein whose expression and plasma concentration increases substantially during inflammation and tissue injury. This protein was shown to induce the release of anti-inflammatory cytokine, interleukin 10, from healthy neutrophils, acting as a negative regulator to control the magnitude of the neutrophil response.

Additionally, SAA1 promoted the interaction between neutrophils and invariant natural killer T (*i*NKT) cells [124]. In line with the effects *i*NKT cells have on other immune cell subsets [125], the interaction between neutrophils and *i*NKT cells suppressed neutrophil-derived IL-10 and increased pro-inflammatory cytokine IL-12 expression. In this way, a new mechanism for the modulation of inflammatory processes was revealed, initially by the anti-inflammatory skewing effects of SAA1, then the downmodulation of this by crosstalk of neutrophils with *i*NKT cells [124]. The fine balance of these mediatory loops is necessary to control inflammation and subsequent resolution, maintaining homeostatic conditions.

1.7 THE IMMUNE SYSTEM AND CANCER

Tumours can occur in many sites of the body, but the surrounding tissue – or tumour microenvironment – usually comprises of common cellular components including immune cells, blood and lymphatic vessels, and fibroblasts, as well as non-cellular components such as extracellular matrix. Tumour cells are known to release factors that can directly or indirectly reorganise their microenvironment, for example, the recruitment of inflammatory cells [126, 127] and orchestration of angiogenesis and metastasis [128-130]. The cells of the immune system and the molecules they secrete are fundamental elements of the tumour microenvironment. Immune cells that localise to the tumour include macrophages, dendritic cells, neutrophils, natural killer cells, mast cells, effector T cells, and myeloid progenitors [131-133], in response to inflammatory signals.

1.7.1 TUMOUR-PROMOTING INFLAMMATION

The presence of inflammatory cells in tumours is not a recent discovery. In 1863, Rudolf Virchow observed leukocyte infiltrates in human neoplastic tissues and hypothesized a link between inflammation and cancer. Furthermore, Virchow proposed that this 'lymphoreticular infiltrate' might indicate cancer initiation at sites of chronic inflammation.

In the late 19th century a surgical oncologist, William Coley, noted a link between inflammation and cancer regression, which he published in 1891 [134]. 'Coley's toxins' were generated from killed bacterial species, which he used to treat sarcoma patients with a deliberate bacterial infection, and in some patients tumour regression was achieved. In those cases where the cancer did regress it is now believed to be because of a successful activation of cytotoxic immune cells, thus demonstrating the ability of the immune system to eradicate cancer when appropriately activated. Coley's work, however, remains controversial and not readily reproducible [135, 136].

Further key observations were made by Harold Dvorak, discoverer of vascular endothelial growth factor (VEGF). He first postulated that tumours were 'wounds that do not heal' [137] after noting that cancers share tissue-infiltrating cells with inflammation, but failed to resolve unlike healing wounds. In accordance with this, chronic inflammation without resolution will eventually lead to tissue damage and a barrage of genetic errors that will inevitably cause a cell to become cancerous [138, 139].

1.7.2 MACROPHAGES IN CANCER

1.7.2.1 MACROPHAGE RECRUITMENT

Monocytes are recruited to the tumour by such tumour-derived chemokines as CCL2 [140], CCL5 [141], colony stimulating factor-1 (CSF-1) [142], VEGF [143] and Angiopoietin-2 [144]. In humans, CCL2 and CCL5 have been most heavily implicated in monocyte recruitment to tumours, produced by tumour cells, endothelial cells, neutrophils, fibroblasts, and even by infiltrated TAMs themselves [145, 146]. Higher expression of CCL2 and CCL5 has been shown to correlate with increased TAMs in tumours and forced CCL2 expression

in B16 melanoma cells – accomplished via gene transfer – led to increased levels of macrophage infiltration [140], implicating CC cytokines as effective monocyte chemoattractants.

Not only do CCL2 and CCL5 have monocyte chemotactic properties, but CCL5 is also capable of stimulating monocytes to express a variety of genes including IL-1β, CCL2 and CCR1, and genes involved in matrix remodelling and angiogenesis, MMP9, MMP19 and urokinase-type plasminogen activator receptor (uPAR) [147] (**Fig 1.3**), suggestive of a mechanism through which monocytes are recruited and polarised in tumours.

The potent chemoattractant CXCL12 (SDF-1) also recruits monocytes into tumours, more specifically, TIE2-expressing monocytes (TEMs; see **section 1.7.2.3**). Within the tumour, both tumour cells and stromal cells are capable of secreting CXCL12 (identified on the basis of cellular morphology), and increases following treatment with combretastatin A4 phosphate (CA4P), a vascular-disrupting agent [148]. The importance of CXCL12 in monocyte localisation to tumours was demonstrated through the use of AMD-3100 – an inhibitor of the CXCL12 receptor, CXCR4. Tumour-bearing mice treated with combined CA4P and AMD-3100 had fewer TEMs in tumours than mice treated with CA4P alone [148], demonstrating the importance of the CXCL12/CXCR4 axis for (TIE2-expressing) monocyte recruitment.

1.7.2.2 TAM FUNCTIONS IN TUMOURS

High levels of tumour-associated macrophages (TAMs) correlate with poor prognosis in the majority of human tumour types including breast cancer [149], non-small cell lung carcinoma [150], prostate cancer [151], bladder cancer [152], endometrial cancer [153], thyroid cancer [154] and glioma [155].

Similarly, murine TAMs have also been shown to be capable of promoting tumour progression and vascularisation in Lewis lung carcinoma [156], and tumour progression and metastasis in spontaneous PyMT breast tumours [157]. These findings – in both human and mice – suggest that macrophages act mainly in a pro-tumour fashion in the tumour environment, aiding various aspects of tumour survival and metastasis (**Fig 1.3**). However, this is not true of all

tumours, since increased TAM infiltration has also correlated with good patient prognosis in some studies of human gastric carcinoma and prostate cancer [158, 159].

1.7.2.2.1 TAM Modulation of Angiogenesis

TAMs in tumours have been shown to promote angiogenesis in pre-clinical models. Human breast tumour (T47D) spheroids implanted into the dorsal skinfold chamber in nude mice, with or without infiltrated TAMs, demonstrated a TAM-dependent increase in angiogenesis [130]. A 3-fold upregulation of VEGF release by macrophage-infiltrated spheroids was noted *in vitro* as compared with un-infiltrated tumour spheroids. This correlated with *in vivo* measures of new vessel formation at 3 days post implantation, including an increase in the number of vessels and junctions [130], thus suggesting that

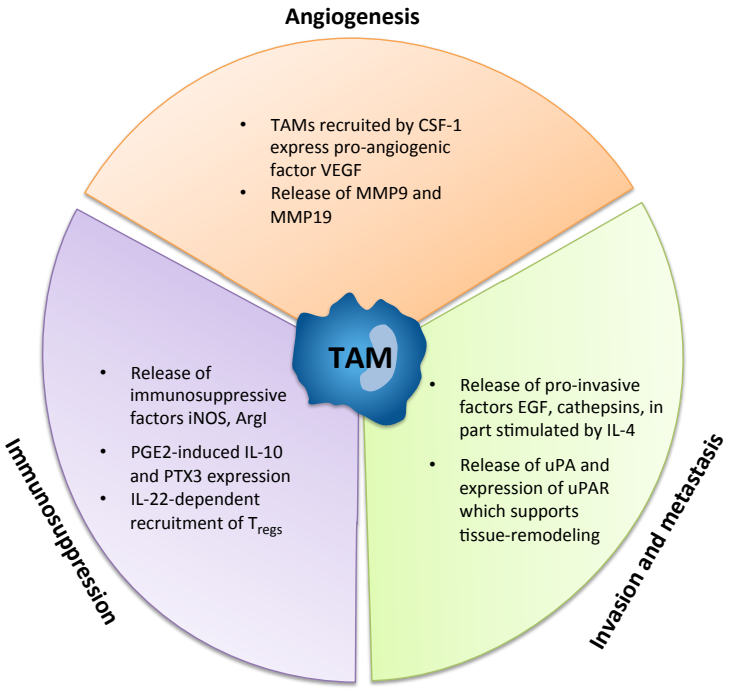

Figure 1.3 TAM pro-tumour functions. Tumour-associated macrophages (TAMs) are capable of supporting a variety of tumour-supporting mechanisms, some of which are summarised here. The release of pro-angiogenic, immunosuppressive, and pro-metastatic factors by TAMs in a variety of tumour types has been shown. The therapeutic targeting TAM recruitment, or re-educating them towards an M1-like phenotype, has been suggested. ArgI, arginase I; CSF-1, colony-stimulating factor-1; EGF, epidermal growth factor; IL, interleukin; iNOS, inducible nitric oxide synthase; MMP, matrix metalloprotease; PTX3, pentraxin 3; T_{reg}, regulatory T cell; uPA(R), urokinase-type plasminogen activator (receptor); VEGF, vascular endothelial growth factor.

macrophages in solid tumours significantly enhance the process of angiogenesis.

Additionally, a study of macrophage infiltration – using the spontaneous PyMT murine breast tumour model – also showed that TAMs encourage angiogenesis and malignancy in tumours [160]. In this model, macrophage migration into tumours was found to precede vascular remodelling and angiogenesis. Furthermore, homozygous *Csf1*^{op} mice that lack wild-type CSF-1 were used to reduce macrophage migration into tumours, and this reduction was shown to impede angiogenesis and the transition to malignancy. Furthermore, manipulating early macrophage infiltration by forced over-expression of CSF-1, prompted vessel network formation in premalignant lesions. This demonstrates that macrophages can have a direct angiogenic effect, irrespective of the progression to malignancy [160].

1.7.2.2.2 TAM CONTRIBUTION TO IMMUNOSUPPRESSION

As TAMs display an M2-like phenotype, their phagocytic and antigen-presenting abilities are then suppressed and they can exhibit pronounced immunosuppressive effects (**Fig 1.3**). In hypoxic areas of tumours, TAMs have been shown to upregulate the immunosuppressive enzymes inducible nitric oxide synthase (iNOS) and the M2 marker arginase I (ArgI) under the control of hypoxia-inducible factor-1α (HIF-1α) [161]. These enzymes profoundly affect T-cell proliferative capacity and their sensitivity to stimulation and explain why inhibition of macrophage infiltration with a CSF-1 receptor/cKIT inhibitor (PLX3397) enhanced anti-tumour immunity mediated by cytotoxic T-cells following chemotherapy [162].

TAMs and tumour cells have been shown to secrete chemokine CCL22, which helps to recruit regulatory T-cells (T_{regs}) into tumours. In line with their known role in suppressing immune responses of other cells, recruited T_{regs} dampened tumour-specific T-cell immunity [163]. Additionally, the immunosuppressive molecule prostaglandin E2 (PGE2) stimulated macrophages to produce IL-10 and pentraxin 3 (PTX3). Autocrine actions of these factors suppressed macrophage phagocytosis of tumour cells [164], demonstrating another mechanism by which TAM aid tumour immune escape.

1.7.2.2.3 TAM MODULATION OF INVASION AND METASTASIS

Tumour invasion and metastasis can also be encouraged by M2-like macrophages in the tumour (**Fig 1.3**). By crossing a transgenic mouse that is prone to the development of mammary tumours (PyMT mouse) with a mouse bearing a CSF-1 null recessive mutation (*Csf1*^{op}), researchers developed a mouse susceptible to cancer but also in the absence of CSF-1 [157]. In these mice, CSF-1 deficiency correlated with reduced numbers of TAMs in tumours and deceleration of the late stages of cancer and slower progression to metastasis, suggesting that TAMs – recruited by CSF-1 – are important for tumour invasion and metastasis. Further support and clarification, again using the PyMT murine mammary tumour model, came from a study showing that TAM expression of EGF increased tumour cell invasion and the number of circulating malignant cells in the blood [165]. Notably, $CD4^+$ T-cell-derived IL-4 induced TAM expression of EGF, which is suggestive of a pro-tumour phenotype. Therefore, $CD4^+$ T-cells appear to stimulate TAMs to encourage tumour cell invasion and metastasis from primary tumours.

However, IL-4 stimulates more than just EGF expression by macrophages; cathepsin protease release by TAMs is also induced by IL-4 in PyMT tumours, and at different stages of malignant progression, including pancreatic islet cancers, mammary tumours, and lung metastases [166]. In particular, TAM-derived cathepsin B and S supported pancreatic tumour growth, angiogenesis and tumour cell invasion *in vivo*. This confirmed an earlier report showing that macrophage- and tumour-derived cathepsin B is important in metastasis of PyMT tumours to the lung [167].

TAMs may also support tumour invasion and metastasis via the expression of urokinase plasminogen activator (uPA) [168], a serine protease that generates active plasmin. It is also involved in many physiological tissue-remodelling processes, making it well suited to supporting invasion and metastasis.

1.7.2.3 TIE2-EXPRESSING MONOCYTES

Over the last ten years a subset of heavily M2-skewed monocytes/macrophages has been identified. These cells express the receptor TIE2, and as such, were called TIE2-expressing monocytes or TEMs. Within tumours, TEMs are distinct lineage of pro-angiogenic monocytes that are recruited predominantly by angiopoietin-2 – a ligand of TIE2 – released by activated endothelial cells and angiogenic vessels [144, 169]. In contrast, tumour-associated macrophages (TAMs) are recruited to tumours through such factors as colony-stimulating factor (CSF)-1 [170], CCL2 [140], CCL5 [171] and VEGF [172], and orchestrate aspects of cancer growth and progression including angiogenesis, immunosuppression and metastasis [173].

TEMs are highly pro-angiogenic [174], stimulated in part by angiopoietin-2 in the tumour microenvironment, but notably, they're also pro-angiogenic in circulation, suggesting this is an innate feature of TEMs [175]. In comparison with $TIE2^-$ monocytes, TEMs were found to express higher levels of pro-angiogenic genes MMP9, VEGF, COX-2 and WNT5A in the circulation, and increased expression of thymidine phosphorylase and cathepsin B upon stimulation with angiopoietin-2, commonly present in tumours [175]. Currently identified mechanisms behind their pro-angiogenic effects, and potential for TEM-targeted therapy, have been extensively reviewed [176-178], and their contribution to tumour angiogenesis has been shown to be non-redundant in a murine glioma model [174].

The gene signature of murine TEMs was compared and contrasted by gene array with that of murine TAMs, splenic $CD11b^+Gr1^+$ cells, circulating inflammatory monocytes, circulating resident monocytes and tumour-derived endothelial cells in PyMT tumours [26]. TEMs and TAMs were identified as $CD11b^+CD31^{low/-}$ cells after showing that the majority of $CD11b^+$ cells were also $F4/80^+$, and distinction between TEMs and TAMs was made based upon a GFP reporter, since the mice received bone marrow transplants from Tie2-GFP mice (GFP expression under the control of the TIE2 promotor). TEMs and TAMs were unsurprisingly shown to express similar gene expression profiles, although some genes were expressed at different levels in line with TEMs being more pro-

angiogenic, and less pro-inflammatory than their $Tie2^-$ counterparts from the same tumours. Interestingly, it was also found that TEMs shared similar expression patterns with the resident monocyte population, suggesting that some may become TEMs. Additionally, inflammatory monocytes may be set to become TAMs in the context of a tumour.

Macrophages in tumours clearly play an important role in several aspects of tumour progression and metastasis. Reducing macrophage infiltration, or 're-educating' macrophages back to an M1-like phenotype [179], may prove to be therapeutically beneficial.

1.7.3 Neutrophils in Cancer

Neutrophils and their myeloid precursors – although less well described than their close relative, the macrophage – also contribute towards many aspects of tumour progression, as will now be discussed.

1.7.3.1 TAN Recruitment

Neutrophils are recruited by such tumour-derived factors as CXCL1, CXCL2 [180] and CXCL8 [181], and can count for a significant fraction of intratumoural inflammatory cells in several human and murine cancers [181-184]. Accordingly, in a murine lung cancer xenograft model, blocking CXCR2 – the receptor for these chemokines – with a small molecule inhibitor (AZ10397767; AstraZeneca) [185] resulted in reduced neutrophil intratumoural TAN accumulation. This verifies the importance of these chemokines in the *in vivo* tumour setting. In addition to CXC cytokines, tumour-derived MIF (macrophage migration inhibitory factor) may also recruit neutrophils into tumours and activate them [186].

In the context of a tumour, polarisation of $CD11b^+Ly6G^+$ cells, or tumour-associated neutrophils (TANs), can be altered by tumour-related inflammation from an N1 phenotype (similar to macrophage M1) to an N2 phenotype (similar to M2) [146]. Furthermore, the addition of a TGF-β receptor inhibitor successfully re-programmed TANs from N2 to N1. Likewise, tumour-infiltrating monocytic MDSCs showed M1- and M2-like polarisations, regulated by (autocrine-acting) TGF-β [187]. Blockade of TGF-β signalling via an anti-TGF-β

antibody was successful at restoring monocytic MDSC ability to express nitric oxide (NO), indicative of a more M1-like phenotype.

As mentioned previously (see **section 1.4.1**), neutrophils can release chromatin bound to granular proteins to form neutrophil extracellular traps (NETs). There is gathering evidence to support a role of NETs in tumour progression also, including the trapping of circulating tumour cells to support the formation of metastases [188]. NETosis is also thought to be a key contributor to cancer-associated thrombosis [189].

1.7.4 Myeloid-derived Suppressor Cells

A myeloid progenitor cell population, named myeloid-derived suppressor cells or MDSCs, play an important part in resolution of inflammation, tumour immune escape, transplantation and trauma [190]. Under normal physiological conditions haematopoietic stem cells (HSCs) differentiate into immature myeloid cells (iMCs) in the bone marrow, which typically migrate to peripheral tissues and further differentiate into macrophages, dendritic cells and granulocytes (**Fig 1.1**) under the direction of soluble factors.

However, the inflammatory milieu contains growth factors that promote iMC expansion and can also hinder their more regular course of differentiation, leading to the development of a subpopulation of iMCs known as MDSCs. The molecular mechanisms responsible for MDSC development are not well understood, but a recent poster and review aptly summarise the current understanding of MDSC polarisation and reprogramming [191, 192]. Murine MDSCs have been divided into two major groups: monocytic ($Ly6G^{-}Ly6C^{high}$) MDSC and granulocytic ($Ly6G^{+}Ly6C^{low}$) MDSC, both with immunosuppressive capabilities [193, 194]. Similar classifications have also been broadly described in humans [195]. Analogous to macrophage M1 and M2 phenotypes, granulocytic MDSCs/neutrophilic cells have also been described to have two opposing polarisations, predominantly mediated by TGF-β.

1.7.4.1 Contribution of MDSCs to Tumour Progression

Due to their initial discovery in tumours, the bulk of the information available on MDSCs relates to their role in cancer; they have, however, been

implicated in autoimmunity and transplantation success as well. Avoiding immune destruction is one of the ten hallmarks of cancer recently described by Hanahan and Weinberg [196], and therefore, tumours survival and progression relies on the suppression of anti-tumour immune responses. Production of TGF-β by MDSCs suppresses the activity of tumour-inhibiting cytolytic $CD8^+$ T lymphocytes, which can be stimulated by the cytokine IL-13 through the binding of receptor IL-13Rα_2 on MDSCs. In line with the finding that tumour necrosis factor alpha (TNFα) is partially responsible for MDSC IL-13Rα_2 expression, neutralisation of TNFα was shown to restore the cytolytic activities of $CD8^+$ T cells and reduce metastatic nodule formation in a murine colon cancer model [197]. These findings support the idea that TGF-β and TGF-βR are potential targets for the manipulation of MDSCs in cancer and other diseases [191].

Several lines of evidence suggest that within the tumour microenvironment, MDSCs act in an M2-like, pro-tumour manner [198]. The adoptive transfer of MDSCs in murine tumour models was linked to an increase in tumour growth and angiogenesis [199, 200]. Notably, the administration of an anti-Gr-1 antibody to deplete Gr-1^+ cells in mice bearing tumours caused a significant inhibition of tumour growth and metastasis, and an increase in survival [201-203]. Similarly, depletion of MDSCs in tumour-bearing mice using gemcitabine, all-trans-retinoic acid, and inhibitors of phosphodiesterase-5, increased overall survival, impeded tumour progression and resistance to anti-cancer therapies [204-206].

MDSCs exert their immunosuppressive effects in part through cross communication with T cells, reducing their ability to mount an immune response against presented antigens. They produce ROS, RNS and arginase 1 (ARG1), which act independently or together to reduce the association of CD3-ζ (zeta) chain with the rest of the T cell receptor (TCR) complex, inhibit the proliferation of T cells, and increase T cell apoptosis [207-209]. In doing so, MDSCs are key regulators of inflammation, bringing about resolution and preventing autoimmunity. However, their ability to suppress immune responses also makes them useful allies of tumours, allowing tumours to remain effectively 'invisible' to the immune system. In a clinical study, circulating MDSCs were more

abundant in cancer patients at all stages, relative to the healthy control group [210]. There was a significant relationship between increased numbers of circulating MDSCs and increasing clinical cancer stage. Observations in stage IV patients revealed that individuals with extensive metastatic tumour burden had significantly higher numbers of MDSCs than patients with limited tumour burden, measured both as a percentage and as an absolute number of MDSCs [210].

As previously mentioned, inflammatory conditions promote the differentiation of MDSC from iMCs. Interestingly, treatment with doxorubicin–cyclophosphamide chemotherapy, which induces further inflammation, was shown to cause an induction in circulating MDSCs in patients with early stage breast cancer [210]. This was also associated with increased metastatic burden, indicating that chemotherapy-induced inflammation may be a contributing factor to tumour metastasis in patients with cancer, with a potential role for MDSCs in this process. Therefore, understanding the mechanisms behind MDSC-driven tumour progression and subversion of the immune system is imperative. Given the propensity of MDSCs to aid tumour progression and immune escape, the presence of increased numbers of MDSCs following chemotherapy is undesirable, and they may also reduce the effectiveness of concurrent immunotherapies.

Further studies on the recruitment of the different populations of myeloid cells into tumours may lead to new therapies that aim to block their accumulation, or to re-educate these cells towards an anti-tumour phenotype in the tumour environment, overcoming the tumours immunomodulating defence mechanisms. Such therapies could be used alone, or in combination with existing treatments such as chemotherapy.

1.8 Chemotherapy Treatment of Cancer

Common treatments for cancer include surgery, chemotherapy, radiotherapy, hormonal therapy, biological therapy, stem cell and bone marrow transplants (depending on the type of cancer) [211], of which, chemotherapy and its effects on the immune system will be the focus here due to the results

described in later chapters. Chemotherapy drugs travel through the bloodstream and damage highly proliferative cells. Tumours are known for their rapid, uncontrolled cellular replication, and as such are more affected by chemotherapeutic agents than most other cells of the body. In many cases, chemotherapy treatment causes an increase in tumour cell death together with the decrease in cells seeding the tumour, which overall cause tumour shrinkage. However, some tumours, especially metastatic tumours, have the capacity to protect themselves against the cytotoxic effects of chemotherapy; using complex mechanisms, tumours can become chemoresistant and refractory to chemotherapy [126, 212].

Additionally, chemotherapy only 'targets' tumour cells by having a greater killing effect on cells that rapidly divide. This crude specificity leads to off-target damage, affecting other rapidly dividing cells such as hair follicles, bone marrow cells and cells of the digestive tract (leading to hair loss, myelosuppression and mucositis, respectively) [211, 213]. Chemotherapies can be grouped according to their mechanism of action; the five main groups are:

- Alkylating agents
- Topoisomerase inhibitors
- Plant alkaloids
- Anti-metabolites
- Anti-tumour antibiotics

In brief, alkylating agents (for example, cyclophosphamide and cisplatin) add alkyl groups to guanine bases. The alkyl groups cause irregular base pairing and generate cross-links between the strands of DNA, which inevitably disrupts cellular division [214]. Topoisomerase inhibitors (for example, etoposide and doxorubicin) cause damage to the DNA; they prevent the proper regulation of DNA by topoisomerases, which are crucial for the binding of DNA back together after it has been cut. Therefore, cells affected by these inhibitors accumulate breaks in one or both strands of DNA, eventually leading to cell death [215].

Anti-metabolites, however, exert their effects by mimicking DNA bases and other necessary metabolites, incorporating themselves into molecules and

disrupting their proper function. For example, fluorouracil's (5-FU) primary mode of action is as a pyrimidine antagonist that blocks the synthesis of pyrimidine-containing nucleotides in DNA and RNA [216]. Similarly, this disruption of proper DNA synthesis during cell replication ultimately leads to cell death.

As the name suggests, plant alkaloids are a type of treatment that derive from various plants, and are also cell-cycle specific. The taxanes, paclitaxel and docetaxel, are semisynthetic molecules derived from the bark and needles of yew trees. Their mode of action is to inhibit mitosis by stabilising microtubules, preventing them from depolymerising – a process which is required during normal cell division. Both compounds are used routinely for the treatment of breast, ovarian, and lung cancer, as well as for metastatic disease and in combination with other anti-cancer therapies [217].

As mentioned above, treatment with chemotherapy causes significant necrotic cell death in tumours [218], which can further contribute towards inflammatory conditions in the tumour. Myeloid cells are recruited to tumours by a variety of inflammatory chemokines, including CCL2 [140], CCL5 [141], CXCL1 and CXCL2 [180] and CXCL8 [181]. Due to the results described in later chapters, the CXC motif chemokines will now be focussed on here.

1.9 CXC CHEMOKINES

The CXC chemokines were first identified as a secretory product of a human malignant melanoma cell line, Hs0294, which had autocrine mitogenic effects [219]. CXCL8/IL8 was the first CXC cytokine to be identified, following which, growth-related oncogene (GRO) α, GROβ and GROγ were identified and later changed for the nomenclature CXCL1, CXCL2 and CXCL3, respectively. This naming reflects their characteristic two N-terminal cysteines (C) separated by another amino acid (X), forming a cysteine-X-cysteine motif, as shown in **Fig 1.4 B and C**. Other important CXC molecules, with regards to neutrophil chemoattraction and activation, include CXCL5 (epithelial-derived neutrophil-activating peptide 78, or ENA-78) and CXCL8 (IL-8). There are a total of 17 described CXC molecules in mammals - they can be split into two groups: those

with the amino acid sequence glutamic acid-leucine-arginine (ELR$^+$) prefacing the CXC motif, and those without (ELR$^-$). The ELR$^+$ cytokines hCXCL1, 2, 3, 5, 6, 7 and 8, have between 40-90% homology in their amino acid sequence in humans.

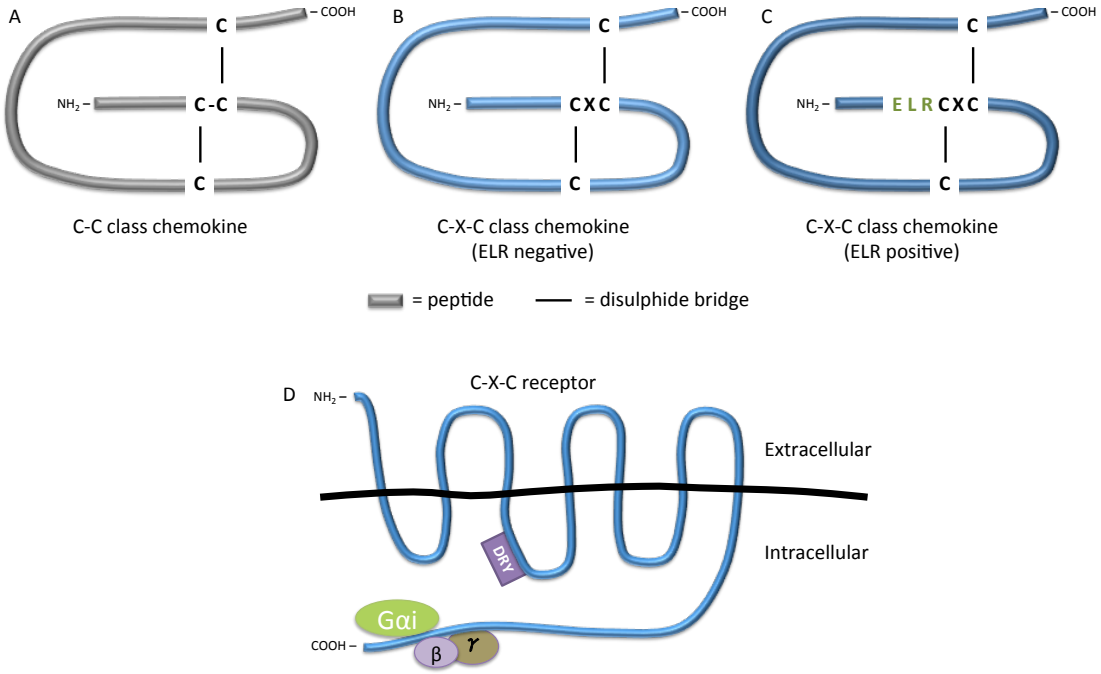

Figure 1.4 Schematic representations of CC and CXC cytokine structure, and of CXC receptors. The structure of CC class cytokines (A), showing the two adjacent cysteine amino acid motif. Similarly, the structure of ELR negative (B) and ELR positive (C) CXC cytokines are shown, where X represents a variety of possible amino acids. The basic structure of G protein-linked, 7-transmembrane CXC chemokine receptors (D) is also shown, including the conserved ELR and DRY motifs. Interchain disulphide bonds are shown as black lines. Adapted from [213].

ELR$^+$ CXC cytokines bind to the receptors CXCR1 and CXCR2, and have potent chemotactic and activatory effects on neutrophilic granulocytes. CXCR1 and CXCR2 are most abundant and co-expressed on neutrophils. However, CXCR1 and CXCR2 are also present on monocytes/macrophages and endothelial cells [222], and one or both of the receptors present on cytokine-activated dendritic cells [223], basophils, T lymphocytes, NK cells [224], mast cells [225], and more recently shown expressed on some non-immune cells [226].

By measuring calcium flux in human embryonic kidney cells transfected with the genes encoding CXCR1 or CXCR2, the binding of ELR$^+$ CXC molecules to the two receptors was analysed [227, 228]. Importantly, the studies showed that

the ligand CXCL1 induced calcium influx more efficiently in CXCR2- than CXCR1-transfected cells, suggesting the CXCR2 is more sensitive to the ligand CXCL1. The same was also found to be true for cytokines CXCL2 and CXCL5. In addition, CXCR1 showed equal or greater responsiveness to other ELR$^+$ cytokines CXCL8 and CXCL6, whereas CXCR2 was more responsive to the ligand CXCL7 [227, 228].

1.9.1 CXC CHEMOKINES IN CANCER

Chronic exposure of cells to a cytokine-rich milieu has been implicated in several aspects of tumour formation and progression, through the recruitment of macrophages and T cells and their extended activation, atypical angiogenesis, and damage to DNA caused by locally produced ROS [229, 230]. In fact, many roles for chemokines and their receptors have been described in different types of cancer [231].

Proteomic analysis of a weakly invasive (RT112) and a highly invasive (T24) bladder carcinoma cell line identified CXCL1 as regulating the invasion of bladder cancer cells [232]. *In vitro*, CXCL1 was able to enhance cell invasion and modulated the expression of pro-invasive MMP13, and *in vivo*, CXCL1 correlated with higher pathologic stages in bladder cancer and levels of the chemokine in urine samples were significantly higher in patients with invasive bladder cancer than non-invasive cancer. CXCL1 was found to be an independent predictive marker of invasive phenotype in bladder cancer [232].

Similarly, CXC cytokines can modulate tumour angiogenesis. In general, CXC cytokines with an ELR motif are potent angiogenic factors, and those lacking the motif have angiostatic effects in the presence of ELR$^+$ cytokines or basic fibroblast growth factor (bFGF) [233, 234]. Therefore, the ELR motif appears to promote angiogenesis – confirmed by the finding that removal of the ELR sequence in CXCL8 inhibited its normal angiogenic effects – and showed that the different classes of CXC cytokines have antagonistic effects. Angiogenesis is also indirectly induced by CXCL1, via the recruitment of VEGF-A-expressing neutrophils in mice [235].

Chemokine analysis of human gastric tumours showed that CXCL5 is overexpressed in late stage disease, and that strong CXCL5 expression

corresponded with increased microvascular density [236]. Similarly, CXCL5 overexpression is indicative of poor prognosis in patients with pancreatic cancer, and is possibly due to its activation of extracellular signal-regulated kinase (ERK), protein kinase B (Akt), and signal transducer and activator of transcription (STAT) in human endothelial cells, stimulating angiogenesis [237]. In hepatocellular carcinoma, CXCL5 expression was increased in more highly metastatic HCC cell lines *in vitro* and in tumour samples from patients with recurrent HCC versus controls [238]. Animal studies showed that increased CXCL5 in HCC cells enhanced tumour growth, lung metastasis, and accumulation of neutrophils in tumours. The overexpression of CXCL5 alone, or given in combination with intra-tumoural neutrophils, was found by multivariate analysis to be an independent indicator of overall survival and cumulative recurrence [238].

These findings, and others [231], demonstrate the importance of chemokine signalling in tumour progression, and suggest that inhibition of chemokines or their receptors concurrent with chemotherapy may benefit therapy.

1.9.2 CXCR2 INHIBITORS

Inhibitors of both CXCR1 and CXCR2 have been developed by several companies, and a selection of the better characterised inhibitors are shown in **Table 1.3.** Some of the inhibitors are currently under investigation in clinical trials for treatment of such inflammation-associated diseases as diabetes, chronic obstructive pulmonary disease (COPD), bronchiectasis, asthma, ozone-induced airway inflammation and neutrophilia, cystic fibrosis and ulcerative colitis, as well as for breast cancer.

Reparixin (Dompé), a small molecule inhibitor, prevents CXCR1 and CXCR2 receptor activation and is in early clinical trials for treatment of breast cancer patients (www.clinicaltrials.gov, study number NCT01861054). A related compound, DF 2162 (Dompé), has since been developed and shows better pharmacokinetic characteristics in pre-clinical studies, including an extended *in vivo* halflife in rats and enhanced oral bioavailability [239]. The CXCR2

Inhibitor	Company	Specificity	Pre-clinical studies	Clinical trials c = current	Refs and clinical trial study numbers*
Reparixin	Dompé S.P.A	CXCR1/CXCR1	Breast cancer xenografts	Diabetes (islet cell transplantation)	[235, 236, 237]
DF 2162	Dompé S.P.A	CXCR1/CXCR2	Adjuvant-induced polyarthritis, bleomycin-induced pulmonary inflammation and fibrosis	Breast cancer [c]	[232, 238, 239, 240]
AZD5069	AstraZeneca	CXCR2		COPD, Bronchiectasis, Asthma [c]	NCT01233232, NCT01255592, NCT01704495
AZ10397767	AstraZeneca	CXCR2	Lung adenocarcinoma xenografts, prostate cancer xenografts		[182, 235
SCH-527123	Schering-Plough	CXCR1/CXCR2	Colorectal cancer xenografts	Ozone-induced neutrophilia, COPD, Asthma	[233, 234, 241, 242, 243, 244]
SB 225002	GlaxoSmithKline	CXCR2	Colitis, nasopharyngeal carcinoma		[245, 246, 247, 248]
SB 656933	GlaxoSmithKline	CXCR2		Ozone-induced airway inflammation, cystic fibrosis, COPD, Ulcerative colitis [c]	[249, 250, 251] NCT00748410
SB 265610	GlaxoSmithKline	CXCR2	Transgenic breast cancer transplants, chemical burn wound healing		[124, 252, 255]

Table 1.3 CXCR2 small molecule antagonists. CXCR2 and CXCR1/CXCR2 small molecule inhibitors have been developed by several pharmaceutical companies, due to their therapeutic potential in a wide range of inflammatory disorders and cancer. This table shows a summary of pre-clinical studies and clinical trials that are reported for some of the better-characterised CXCR2 inhibitors. COPD, Chronic obstructive pulmonary disease; [c] denotes currently recruiting/running clinical trials; * Clinical trail study numbers according to http://clinicaltrials.gov/.

antagonist AZ10397767 (AstraZeneca) was used in a murine lung carcinoma xenograft model to study the effects of neutrophil function in tumours [185]. Inhibition of CXCR2 with AZ10397767 was sufficient to significantly reduce neutrophil infiltration and was associated with a reduction in tumour growth, suggesting that this inhibitor may have potential as an anti-cancer therapy.

The CXCR2 inhibitor SCH-527123 (Schering-Plough) inhibits both CXCR1 and CXCR2. However, it has a much higher affinity for CXCR2 and is therefore therapeutically CXCR2-selective. Using human colorectal cancer cells, SCH-527123 was shown to reduce IL-8-dependent proliferation of cancer cells, as well as reducing cell migration and invasion, and increasing malignant cell apoptosis *in vitro* [240]. Furthermore, study of this inhibitor *in vivo* in murine colorectal cancer xenograft models confirmed that SCH-527123 treatment could reduce tumour growth as well as microvessel density in comparison with vehicle-treated mice. Similar results were shown in another colorectal cancer xenograft model where SCH-527123 enhanced cancer cell apoptosis and inhibited angiogenesis, leading to reduced metastasis [241].

1.9.2.1 Combined chemotherapy and CXCR2 inhibition

The use of CXCR2 inhibitors in combination with chemotherapy has also been investigated in pre-clinical trials (**Table 1.3**). A CXCL8-CXCR2 autocrine network that reduces sensitivity of prostate cancer cells to apoptosis-inducing therapy [261] was inhibited by the CXCR2 antagonist AZ10397767. Inhibition of CXCR2 signalling led to increased cancer cell apoptosis by re-sensitising these cells to therapy. Additionally, CXCR2 inhibition has also been investigated in combination with docetaxel chemotherapy for the treatment of breast cancer [242], where combined docetaxel and reparixin significantly reduced tumour growth in comparison with docetaxel alone.

Notably, Acharyya and colleagues [126] used the inhibitor to disrupt a newly described, pro-tumoural paracrine network, where tumour cell-derived CXCLs 1 and 2 enhanced S100A8/9 production by $CD11b^{+}Gr\text{-}1^{+}$ MDSCs. In tumour-bearing mice, blocking the activation of CXCR2 and the ensuing S100A8/9 expression by MDSCs increased the effectiveness of chemotherapy

and reduced metastatic burden. Therefore, the therapeutic benefits of treating cancer patients with combined chemotherapy and CXCR2 inhibition are being increasingly realised. Benefits include reduced tumour growth, angiogenesis, immune escape, tumour cell invasion and metastasis, and enhanced responsiveness to doxorubicin, cyclophosphamide and paclitaxel chemotherapy [126, 262, 263].

1.10 TUMOUR NECROSIS FACTOR ALPHA

The cytokine, TNFα, is a key modulator of inflammation. Predominantly produced and released by monocytes, macrophages and neutrophils of M1/N1 polarisation, TNFα can also be generated by such cells as endothelial cells, T lymphocytes and mast cells. At the time it was named 'tumour necrosis factor', this molecule was identified as a macrophage-secreted product that caused necrosis of tumours [264]. However, it has since been shown that, at different concentrations and in certain environments, this molecule can have very diverse functions. In the process of host defence against infection, TNFα expression plays a protective role by recruiting phagocytes, stimulating their oxidative respiratory burst and release of lysosomal enzymes [265]. However, it has also been proven to be harmful to the body – in autoimmunity, cancer and toxic shock – when its expression becomes deregulated [266, 267].

TNFα binds to the receptors TNFRI and TNFRII, which have very different expression; whereas TNFRI is thought to be expressed on all cell types except erythrocytes, TNFRII is more restricted to haematopoietic cells and endothelial cells. Although both receptors can be activated by membrane-integrated TNFα, the TNFRI receptor can also be triggered by soluble TNFα. As a negative regulator, both TNFα receptors can be shed from the cell surface and compete for free ligands.

1.10.1 TUMOUR NECROSIS FACTOR ALPHA IN THE TUMOUR ENVIRONMENT

1.10.1.1 TUMOUR CELL-DERIVED TNF ALPHA

The fact that plasma levels of TNFα were higher in patients with poorer prognosis in pancreatic cancer [268], renal cell carcinoma [269], chronic

lymphocytic leukaemia [270] and in metastatic breast cancer [271], and that malignant cells can produce TNFα themselves [272], are strong indicators that TNFα has functions that are beneficial to tumour survival and progression.

With the development of a TNFα-knockout mouse, tumour growth in the absence of TNFα could be studied. Treatment of mice with a carcinogen to induce skin tumours showed that TNFα$^{-/-}$ mice were resistant to the development of both benign and malignant tumours [273], supporting the connection between inflammation and carcinogenesis. Interestingly, in this model of skin cancer, lack of TNFα did not affect the time to malignant progression, implying that TNFα may be required for early stages of carcinogenesis but not the later stages of tumour progression.

Indeed, constitutive expression of TNFα is also a feature of epithelial ovarian cancer cells, where it supports the expression of other factors important for peritoneal cancer proliferation and metastasis, such as the chemokines CCL2 and CXCL12, the cytokines IL-6 and macrophage migration-inhibitory factor (MIF), and pro-angiogenic molecule VEGF [274].

1.10.1.2 TNFA PRODUCTION BY OTHER CELLS

As mentioned above, TNFα is also released by monocytes, macrophages and neutrophils. Production of TNFα by epithelial and inflammatory cells activates nuclear factor kappa B (NF-kB) – a key signalling molecule and hallmark of inflammation – in hepatocytes, contributing to inflammation-associated liver cancer [275]. Similar findings were reported using a transgenic mouse model of gastric cancer [276] and a chemically-induced colorectal cancer model [277], where myeloid cell-derived TNFα promoted tumourigenic signalling in cancer and mucosal cells. Prolonged expression of high levels of TNFα may also explain the link between chronic inflammation and cancer, as it has been shown to cause DNA damage in *Trp53*$^{-/-}$ malignant cells [278] and in normal lung epithelial cells [279], in part via the upregulation of ROS.

Another aspect of tumour progression modulated by TNFα is the induction of epithelial-mesenchymal transition (EMT) – which is linked to the induction of an invasive phenotype – in colon cancer spheroids [280]. In EMT,

epithelial cells lose polarity and break contact with adjacent cells and extracellular matrix (ECM), undergoing cytoskeletal remodelling to enable their characteristic migratory phenotype [281]. Cells undergoing EMT gain such mesenchymal markers as fibronectin, vimentin, smooth muscle actin and N-cadherin, and lose such markers as E-cadherin and α- and γ-catenin that are associated with epithelial cells [282]. In the context of cancer, tumour cell EMT is associated with cancer progression and is a key mechanism behind tumour cell invasion and metastasis [281], and macrophage secretion of TNFα led to an acceleration of TGF-β-induced EMT, implicating macrophages and TNFα in supporting tumour cell invasion and metastasis [280].

1.10.2 TNFα-based Anti-cancer Therapy

Initially, when TNFα was identified as having anti-tumour functions and much less was known about its pro-tumour roles, human recombinant TNF (rTNF) was injected systemically as a form of cancer therapy, with the hopes of inducing haemorrhagic tumour necrosis. However, higher doses of rTNF were associated with severe side effects, including headache, rigors, hypotension and pulmonary oedema, and in several cases, tumour progression [283]. Notably, however, lower doses of rTNF were better tolerated and showed partial anti-cancer effect [284].

With increasing evidence that implicates TNFα in the promotion of tumour development rather than their destruction, the focus of TNFα-based cancer therapies shifted towards blocking TNFα in cancer. Anti-TNFα antibodies were effective in reducing tumour metastasis in a murine fibrosarcoma metastasis model [285], not only demonstrating the role of TNFα in controlling metastasis, but that TNFα inhibition had therapeutic effect, at least in murine cancer.

To determine the effects of TNFα on human pancreatic ductal adenocarcinoma (PDAC) cells, the invasive growth of three cell lines following treatment with TNFα was assessed, and was shown to be significantly increased both *in vitro* and *in vivo* [286]. Furthermore, TNFα treatment of orthotopically xenotransplanted PDAC tumours in mice significantly increased tumour cell

growth and the number of metastatic events. Inhibition of TNFα *in vivo* using infliximab (chimeric monoclonal antibody against TNFα) and etanercept (TNFα antagonist) reduced pancreatic adenocarcinoma growth, and infliximab reduced the number of metastases, supporting the use of TNFα inhibitors to treat cancer [286].

However, in humans, systemic inhibition of TNFα comes with the major drawback that it often leaves the body susceptible to infection, due to a compromised host defence system. The actions of TNFα are crucially important in the coordination and execution of immune responses, and inhibiting TNFα systemically can lead to such major repercussions as tuberculosis infection and cancer, as reviewed elsewhere [287, 288].

Still, TNFα antagonists offer the possibility of inhibiting processes that are crucial to cancers [289] including:

- Cell activation and proliferation
- Production of cytokines and chemokines
- Accumulation of inflammatory cells and inflammation
- Immunosuppression
- Angiogenesis
- Degradation of the extracellular matrix

The general consensus of most experts in the field of TNFα biology is that TNFα antagonist therapy is effective and safe, and a useful addition to the arsenal of anti-cancer therapies [288, 289], but requires more understanding of the relative importance of tumour cell and stromal TNFα contributions in human cancers, and the identification of the subgroups of cancer patients for which TNFα antagonism will be most beneficial.

1.11 MACROPHAGES AND NEUTROPHILS IN THE CHEMOTHERAPY-TREATED TUMOUR ENVIRONMENT

Evidence is accumulating for the function of tumour-associated immune cells being altered during chemotherapy treatment [126, 162, 212, 290, 291], as shown in **Fig 1.5**.

1.11.1 MYELOID CELLS AFFECT RESPONSE TO CHEMOTHERAPY

In vitro, cervical and ovarian cancer cell lines treated with cisplatin and carboplatin were able to induce an M2 phenotype in co-cultured monocytes, as seen by their increased expression of IL-10 and activation of STAT3 signalling [291]. The mechanism of the response involved tumour cell NF-κB signalling and tumour cell-derived IL-6 and PGE_2, suggesting that use of COX-inhibitors or IL-6R inhibitors simultaneously with chemotherapy may impede the development of chemoresistance. Evidence that myeloid cells can adopt a pro-tumour phenotype particularly after chemotherapy is also supported *in vivo*.

In a mouse mammary (MMTV-PyMT) tumour implant model, the effects of paclitaxel (PTX) treatment were investigated. This resulted in mammary epithelial cells upregulating CSF-1 and IL-34, ligands of the CSF-1 receptor CSF1R [162]. Consequently, increased macrophage infiltration into the tumour was observed and inhibition of CSF1R-signalling reduced PTX-induced macrophage accumulation, slowed primary tumour growth, decreased angiogenesis and metastasis, and an initiation of anti-tumour $CD8^+$ T-cell responses.

Similarly, myeloid cells accumulated in PyMT tumours in response to doxorubicin therapy, but regulated by the chemokine receptor CCR2 [212]. A comparison of PyMT tumours grown in *Ccr2*$^{+/-}$ or *Ccr2*$^{-/-}$ mice that lack host CCR2, showed that its absence was associated with a significantly improved response. Tumours relapsed significantly later in *Ccr2*$^{-/-}$ mice when treated with either doxorubicin or cisplatin chemotherapy, and were of a lower histological grade than controls.

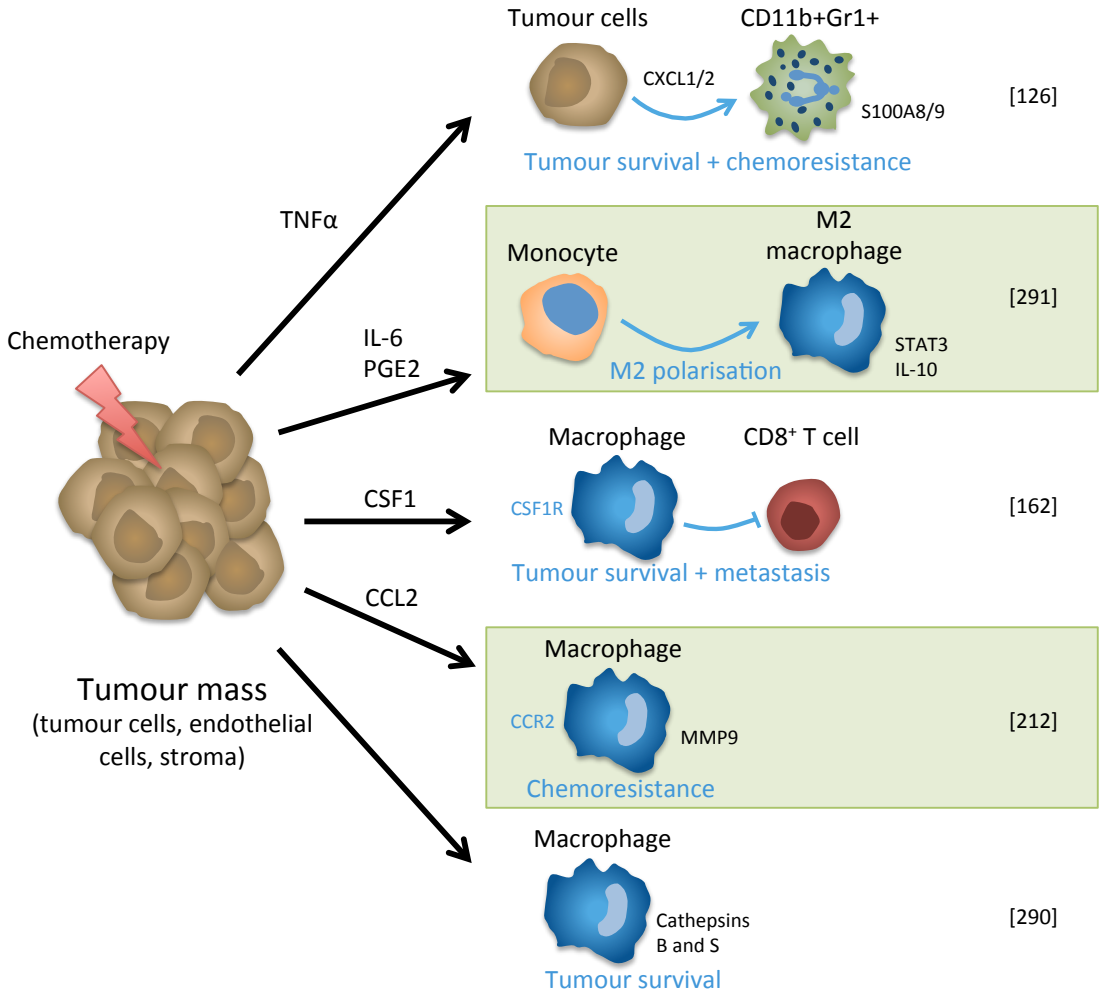

Figure 1.5 Chemotherapy-induced changes in myeloid cell function. Chemotherapy-treatment of the tumour environment can lead to the induction of a variety of myeloid cell-dependent mechanisms that support tumour growth, chemoresistance and metastasis. Inhibition of these mechanisms could help improve efficacy of chemotherapy.

Further support of the chemotherapy-induced macrophage pro-tumour phenotype, also in the PyMT model, came from another study confirming that PTX-induced accumulation of macrophages in tumours, and that macrophage release of cathepsin proteases protected the tumour against PTX, etoposide and doxorubicin [290]. As expected, concurrent cathepsin inhibition with PTX *in vivo* made both primary and metastatic tumours more susceptible to treatment. A summary of these findings can be seen in **Fig 1.5**.

1.11.2 A Paracrine Network Between Tumour and Myeloid Cells Promotes Tumour Growth and Metastasis

A recent study in a mouse mammary tumour model has shown that communication between tumour cells, neutrophils and endothelial cells supports

tumour chemoresistance and metastasis (**Fig 1.6**) [126]. Hyperactivation of the 4q21 region in some breast tumours [292], which leads to excessive transcription of CXCLs 1 and 2 (as well as CXCLs 3-8), was shown to recruit $CD11b^{+}Gr1^{+}$ myeloid cells (possibly neutrophils) into the tumour. PyMT tumour cells and LM2 cells (metastatic breast cancer cells derived from the MDA-MB-231 parental line) were treated with shRNA hairpins to knockdown CXCL1 and CXCL2. When injected into mice, CXCL1/2 knockdown specifically in tumour cells was shown to significantly reduce $CD11b^{+}Gr1^{+}$ cell infiltration, which correlated with the finding that CXCR2 receptor expression was highest in the $CD11b^{+}Ly6G^{+}$ population (Ly6G is together with Ly6C a component of the myeloid differentiation antigen Gr-1) in PyMT tumours [126].

Gene expression analysis showed that genes upregulated in human breast tumours and metastases in association with CXCL1, include the survival factors, S100A8 and S100A9. These proteins – associated with chronic inflammation and cancer – were highly expressed by $CD11b^{+}Gr1^{+}$ cells, and the growth and metastasis of mammary tumours were significantly reduced in mice

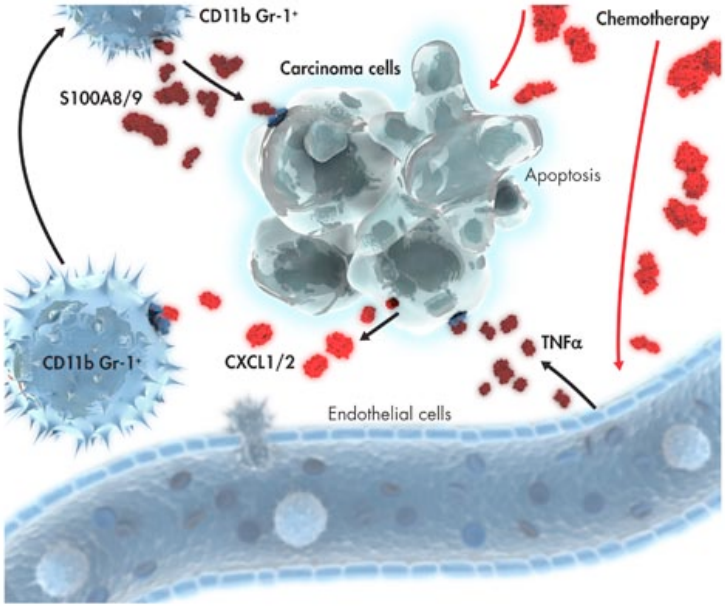

Figure 1.6 Tumour-derived CXCL1/2 recruits S100A8/9-expressing granulocytic cells to the tumour and promotes metastasis. Murine breast cancer cells express CXCL1 and CXCL2 that recruit $CD11b^{+}Gr1^{+}$ cells to the tumour. Subsequently, $CD11b^{+}Gr1^{+}$ cells release S100A8 and S100A9 in the tumour environment, thereby supporting tumour growth and metastasis. Treatment with chemotherapy upregulates TNFα release by endothelial cells which further amplifies CXCL1 expression by tumour cells. Adapted from [287].

transplanted with S100A9$^{-/-}$ bone marrow, in comparison with their S100A9$^{+/+}$ counterpart [126].

Notably, the paracrine loop between tumour cell secretion of chemokines CXCL1 and CXCL2, their recruitment of myeloid cells to the tumour, and their subsequent expression of S100A8/9 to support tumour growth and metastasis, was present in control tumour-bearing mice. Treating these mice with doxorubicin and cyclophosphamide chemotherapy caused a significant upregulation of CXCL1/2 in tumours, as well as an increase in S100A9-expressing cells. The mechanism behind the amplification of the paracrine loop by chemotherapy was discovered to be due to an upregulation of TNFα by stromal cells – including endothelial cells, unidentified bone marrow-derived cells, and smooth muscle cells – as a direct effect of chemotherapy.

Such findings led to the hypothesis that inhibition of CXC chemokine signalling alongside chemotherapy may have a synergistic effect, preventing recruitment of CD11b^{+}Gr1^{+} cell accumulation in the tumour after therapy and their subsequent support of tumour growth and metastasis. Indeed, inhibition of the CXCR2 receptor using the antagonist SB 265610 (Tocris Bioscience) that binds the ligands CXCL1 and CXCL2, concurrent with doxorubicin and cyclophosphamide therapy, significantly reduced both tumour growth and metastasis, as summarised in **Fig 1.6**.

These studies clearly show that myeloid cells dominate tumour responsiveness to chemotherapy since they can blunt the chemotherapeutic response. The evidence discussed here – in mammary tumour models and with different chemotherapies – indicates that combined targeting of the tumour and its microenvironment is important.

1.12 CONCLUSION

Tumour-infiltrating myeloid cells are an important component of most solid tumours. They accumulate in tumours in response to the release of chemokines by tumour cells and other myeloid cells present in the tumour. Myeloid cells display great phenotypic plasticity in response to changes to the

local environment, which has implications in a wide range of inflammation-associated disorders and cancers. Extra layers of complexity are continually added to the classical view that macrophages and neutrophils are host-protecting cells that combat disease, demonstrating that within the macrophage and neutrophil cell types exist phenotypically distinct subsets.

Since chemotherapy can cause changes in the tumour microenvironment – including cell death by apoptosis/necrosis, and in some cases exacerbating tumour inflammation [210] – this is likely to have an effect on the polarisation of intratumoural macrophages and neutrophils. Although the polarisation and function of myeloid cells in chemotherapy-treated tumours is becoming a topic of interest (**Fig 1.5**), few studies have investigated macrophage gene expression specifically in the chemotherapy-treated tumour environment. Similarly, although some studies have investigated tumour-associated neutrophil, and N1/N2 neutrophil gene expression [75, 146, 294, 295], very little is known about human neutrophil gene expression in the chemotherapy-treated tumour environment, or their crosstalk with macrophages.

1.13 HYPOTHESIS

My hypothesis is that following chemotherapy, the harsh conditions in the tumour microenvironment will lead to an alteration of myeloid cell activation and/or polarisation, such that these cells accumulate in the tumour and increase their tumour promoting activity.

1.14 AIMS

The aims of this thesis were to:

- Investigate what effects chemotherapy-treatment of the tumour environment has on macrophage gene expression using microarray technology
- Study the crosstalk between macrophages and neutrophils via cytokine release, and how this affects neutrophil gene expression and function within spheroid-based model of a chemotherapy-treated tumour microenvironment.

- Use a variety of tumour models and types of chemotherapy to observe general features of neutrophil migration and function following treatment, with a view to combining chemotherapy with an inhibitor of neutrophil accumulation and/or function.

CHAPTER 2: MATERIALS AND METHODS

2.1 MATERIALS

2.1.1. REAGENTS

Reagent	Supplier
4-Hydroxy Cyclophosphamide (Cyclophosphamide)	Santa Cruz Biotechnology Inc, Heidelberg, Germany; Santa Cruz Biotechnology (Shanghai) Co. Ltd, Shanghai, China
AB serum (human)	Sigma-Aldrich Inc, Poole, Dorset, UK; Sigma-Aldrich Pte Ltd, Singapore
Acetic acid	BDH Ltd, Poole, Dorset, UK; Fisher General Scientific (SEA) Pte Ltd, Singapore
Agarose type V	Sigma-Aldrich Co. Ltd, Poole, Dorset, UK
Bovine serum albumin (BSA)	Sigma-Aldrich Co. Ltd, UK; Sigma-Aldrich Pte Ltd, Singapore
Cell Tracker™	Life Technologies Ltd, Paisley, UK; Life Technologies Holdings Pte Ltd, Singapore
Cyclophosphamide	*See 4-Hydroxy Cyclophosphamide*
DAPI	Molecular Probes, Life Technologies, Paisley, UK
Dimethylsulphoxide (DMSO)	Sigma-Aldrich Inc, Poole, Dorset, UK; Sigma-Aldrich Pte Ltd, Singapore
DMEM	BioWhittaker UK Ltd, Wokingham, UK; Life Technologies Holdings Pte Ltd, Singapore
Docetaxel (Taxotere®)	Sigma-Aldrich Co. Ltd, UK; Singlab Technologies Pte Ltd, Tocris Biosciences, Singapore
Ethanol	Fisher Scientific Ltd, Leicestershire, UK; Fisher General Scientific (SEA) Pte Ltd, Singapore
Ficoll-Paque™ PLUS	Amersham Biosciences, Buckinghamshire, UK; Amersham Biosciences, Singapore

Foetal calf serum (FCS)	BioWhittaker UK Ltd, Poole, Dorset, UK
Gram's crystal violet solution	Merck Biosciences, Hull, UK; Merck Millipore Pte Ltd, Singapore
Growth factor reduced Matrigel™	Corning Singapore Holdings Pte Ltd, Singapore
Hanks balanced salt solution (HBSS) with Ca^{2+} and Mg^{2+}, without phenol red	BioWhittaker UK Ltd, Wokingham, UK
Hanks balanced salt solution (HBSS) without Ca^{2+} and Mg^{2+}, without phenol red	BioWhittaker UK Ltd, Wokingham, UK
HetaSep™	STEMCELL Singapore Pte Ltd, Singapore
Iscove's Modified Dulbecco's Medium (IMDM)	BioWhittaker UK Ltd, Wokingham, UK; Life Technologies Holdings Pte Ltd, Singapore
L-Glutamine	BioWhittaker UK Ltd, Poole, Dorset, UK; Life Technologies Holdings Pte Ltd, Singapore
Methanol	Fisher Scientific Ltd, Leicestershire, UK; Fisher General Scientific (SEA) Pte Ltd, Singapore
Paclitaxel (Taxol®)	Sigma-Aldrich Co. Ltd, UK
Paraformaldehyde	Sigma-Aldrich Co. Ltd, Poole, Dorset, UK; Fisher General Scientific (SEA) Pte Ltd, Singapore
Phosphate-buffered saline (PBS)	Sigma-Aldrich Co. Ltd, Poole, Dorset, UK; Sigma-Aldrich Inc, Singapore
Power SYBR® Master Mix	Life Technologies Holdings Pte Ltd, Singapore
Prolong Gold Anti-fade reagent	Molecular Probes, Life Technologies, Paisley, UK
Propidium iodide	Sigma-Aldrich Co. Ltd, Poole, Dorset, UK
ToPRO®-3	Life Technologies Holdings Pte Ltd, Singapore
Triton x100	Sigma-Aldrich Co. Ltd, Poole, Dorset, UK

TRIzol®	Life Technologies Holdings Pte Ltd, Singapore
Trypsin/EDTA (0.04%/0.03%)	BioWhittaker UK Ltd, Wokingham, UK; Life Technologies Holdings Pte Ltd, Singapore
Tween-20	BDH Laboratories Suppliers, Poole, Dorset, UK
Vacutainer® tubes	BD Biosciences, Singapore

2.1.2 MATERIALS

Material	**Supplier**
25cm^2 and 75cm^2 tissue culture flasks	Greiner Bio-One Ltd, Gloucestershire, UK; Corning Singapore Holdings Pte Ltd, Singapore
6-well, 12-well and 24-well tissue culture plate	Greiner Bio-One Ltd, Gloucestershire, UK; Corning Singapore Holdings Pte Ltd, Singapore
Cover slips	BDH Ltd, Poole, Dorset, UK
Glass microscopic slides	BDH Ltd, Poole, Dorset, UK
iQ™ 96-Well PCR Plates	Bio-Rad Laboratories Pte Ltd, Singapore
Transwell® Permeable Supports	Corning Holding GmbH, Wiesbaden, Germany; Corning Singapore Holdings Pte Ltd, Singapore

2.1.3 MONOCLONAL (M) AND POLYCLONAL (P) ANTIBODIES AND ANTISERA

Antibody (clone)	**Supplier**
Rat m anti-CD11b	BioLegend UK Ltd, London, UK
Rat m anti-mouse F4/80	Serotec, Oxford, UK
Rat m anti-mouse Ly6G (1A8)	BioLegend UK Ltd, London, UK
Rat m anti-mouse TNFα FITC (LEAF™ purified)	BioLegend UK Ltd, London, UK
Rabbit p anti-active Caspase 3	Abcam Plc, Cambridge, Cambridgeshire, UK
Rabbit p anti-CD31	BD Biosciences, Erembodegem, Belgium
Rabbit p anti-GRO alpha	Abcam Plc, Cambridge, Cambridgeshire, UK
FcR Blocking Reagent	Miltenyi Biotec, Surrey, UK
Mouse m anti-CXCR2	Abcam Plc, Cambridge, Cambridgeshire, UK
Mouse m anti-human TNFα	Abcam Plc, Cambridge, Cambridgeshire, UK

(LEAF™ purified)	
Goat m anti-rat AlexaFluor® 555	Molecular Probes, Life Technologies, Paisley, UK
Goat m anti-rat AlexaFluor® 633	Molecular Probes, Life Technologies, Paisley, UK
Goat m anti-rabbit APC	R&D Systems Europe Ltd, Abingdon, UK

2.1.4 COMMERCIAL KITS

Kit	**Supplier**
CD16 Microbeads, Human	Miltenyi Biotec Asia Pacific Pte Ltd, Singapore
HumanHT-12 v4 Expression BeadChip Kit	Illumina Singapore Pte Ltd, Singapore
Human CXCL1/GRO alpha Quantikine ELISA Kit	Singlab Technologies Pte Ltd, R&D Systems Inc, Singapore
RNeasy Mini and Rneasy Micro Kits	QIAGEN Singapore Pte Ltd, Singapore
RNase-free DNase Set	QIAGEN Singapore Pte Ltd, Singapore
Superscript II	Life Technologies Holdings Pte Ltd, Singapore
TaqMan® Reverse Transcription Reagents	Life Technologies Holdings Pte Ltd, Singapore
TargetAmp Nano-g Biotin-aRNA Labelling kit	Illumina Singapore Pte Ltd, Singapore

2.1.5 INSTRUMENTATION

Instrument	**Supplier**
2100 Bioanalyzer	Agilent technologies
Bead Array Scanner 500 GTX	Illumina
CFX96 Touch™ Real-Time PCR Detection System	Bio-Rad Laboratories Pte Ltd, Singapore
Confocal Microscope Zeiss LSM 510	Zeiss, Hertfordshire, UK

FACSAria II 4-laser	BD Biosciences, Singapore
FACSCalibur Flow Cytometer	BD Biosciences, Cowley, Oxford, UK
FACSCanto II Flow Cytometer	BD Biosciences, Singapore
Infinite® 200 PRO series	Tecan Asia Pte Ltd, Singapore
NanoDrop	Thermo Scientific, Wilminton, USA; Fisher
Spectrophotometer2000	Scientific Pte Ltd, Singapore
Spectrophotometric plate reader	Anthos Labtec Instruments, GmbH, Wals, Austria

2.1.6 SOLUTIONS

Phosphate buffered saline (PBS)

Add 5 PBS tablets to 1L dH_2O (0.01 M phosphate buffer, 0,0027 M potassium chloride and 0.137 M sodium chloride), pH to 7.4 and store at room temperature.

Phosphate buffered saline with tween 20 (PBST)

Add 500µL tween 20 to 1L PBS.

Blocking buffer

Make a 1% BSA, 10% goat serum solution in PBS, and add 1µg Fc block per 100µL.

FACS buffer

Make a 1% BSA solution, diluted in PBS.

Cryopreservation media

Ninety percent FCS and 10% DMSO solution.

Red blood cell lysis solution

Add 8.99g NH_4Cl, 1g $KHCO_3$, 37mg tetrasodium EDTA in 1L H_20 and adjust to pH 7.3

2.1.7 PRIMERS

Primers were validated by members of the research group, or were published already in the literature; validation included the construction of a standard curve from experiments using varying template concentrations, as well as specificity verification by melt curve and gel analysis.

Primer		Sequence
CCL2	F	5'-CAGCCAGATGCAATCAATGCC-3'
	R	5'-TGGAATCCTGAACCCACTTCT-3'
CCL3	F	5'-AGTTCTCTGCATCACTTGCTG-3'
	R	5'-CGGCTTCGCTTGGTTAGGAA-3'
CXCL1	F	5'-AACCGAAGTCATAGCCACAC-3'
	R	5'-GTTGGATTTGTCACTGTTCAGC-3'
CXCL2	F	5'-TCCTCAATGCTGTACTGGTCC-3'
	R	5'-ATGTTCTTCCTTTCCAGGTC-3'
CXCL5	F	5'-AGCTGCGTTGCGTTTGTTTAC-3'
	R	5'-TGGCGAACACTTGCAGATTAC-3'
CXCR4	F	5'-ACTACACCGAGGAAATGGGCT-3'
	R	5'-CCCACAATGCCAGTTAAGAAGA-3'
FAS	F	5'-TCTGGTTCTTACGTCTGTTGC-3'
	R	5'-CTGTGCAGTCCCTAGCTTTCC-3'
HGF	F	5'-GCTATCGGGGTAAAGACCTACA-3'
	R	5'-CGTAGCGTACCTCTGGATTGC-3'
ICAM-1	F	5'-ATGCCCAGACATCTGTGTCC-3'
	R	5'-GGGGTCTCTATGCCCAACAA-3'
MMP9	F	5'-TGTACCGCTATGGTTACACTCG-3'
	R	5'-GGCAGGGACAGTTGCTTCT-3'
STAT3	F	5'-CAGCAGCTTGACACACGGTA-3'
	R	5'-AAACACCAAAGTGGCATGTGA-3'
TNFα	F	5'-GGAGAAGGGTGACCGACTCA-3'
	R	5'-CTGCCCAGACTCGGCAA-3'
TGFβ	F	5'-GGCCAGATCCTGTCCAAGC-3'
	R	5'-GTGGGTTTCCACCATTAGCAC-3'
VEGF	F	5'-AGGGCAGAATCATCACGAAGT-3'
	R	5'-AGGGTCTCGATTGGATGGCA-3'

2.2 METHODS

2.2.1 CELL CULTURE

2.2.1.1 MAINTAINING CELL LINES

Adherent A549 human lung adenocarcinoma cells (ATCC) were cultured in 75cm^2 culture flasks in DMEM (10% FCS and 2mM L-Glutamine). When passaging cells, DMEM was removed and the cells were washed with HBSS (without $Ca2^+$ and $Mg2^+$). Subsequently, 3mL of trypsin/EDTA solution were added to each flask and kept at 37^{o}C until cells could be detached with gentle agitation. Five millilitres of DMEM (with 10% FCS) were then added to neutralise the trypsin/EDTA solution. Cells were pelleted by centrifuging at 400 x *g* for 5 minutes, resuspended in fresh DMEM and counted using a C-Chip haemocytometer (Neubauer improved). For standard culture, cells were seeded at a density of 1 x 10^6 per flask and passaged when approximately 80% confluent.

2.2.1.2 CRYOPRESERVATION OF CELL LINES

Cells were stored in cryopreservation vials, each aliquot containing 2 x 10^6 cells resuspended in 1mL cryopreservation medium. Vials were kept on ice and quickly moved to a freezing container to control the cooling of cells to -80^{o}C overnight. Vials were subsequently kept in liquid nitrogen for storage. To thaw cells, vials were placed in a 37^{o}C waterbath until almost fully defrosted, before being added to 9mL DMEM (containing 10% FCS, 2mM L-Glutamine and pre-warmed to 37^{o}C). The cells were then pelleted by centrifugation at 400 x *g* for 5 minutes, resuspended in 10mL DMEM (containing FCS and L-Glutamine and pre-warmed to 37^{o}C) and transferred to a 75cm^2 tissue culture flask. The culture medium was replaced after 2 hours to remove debris and cells that had not attached.

2.2.1.3 ISOLATION OF HUMAN MONOCYTES FROM PERIPHERAL BLOOD

Peripheral blood monocytes were isolated from waste Buffy coats provided by the National Blood Service, Sheffield, or from blood cones, Singapore. Blood was diluted 1:1 with HBSS (without Ca^{2+} or Mg^{2+}) and 30mL diluted blood were layered on top of 20mL Ficoll-Paque. This was then

centrifuged at 1200 x *g* for 20 minutes with brake set to 0. The monocyte-rich layer was collected and placed into a 50mL centrifuge tube, which was pre-coated with HBSS (without Ca^{2+} or Mg^{2+}) and pre-chilled on ice. Cells were pelleted by centrifuging at 400 x *g* for 5 minutes and then washed by resuspending in HBSS (without Ca^{2+} or Mg^{2+}) and centrifuging again. The remaining erythrocyte contamination was then removed by resuspending the cell pellet in 5mL red blood cell lysis solution for 5 minutes. At which point, 45mL of HBSS (without Ca^{2+} or Mg^{2+}) were added and centrifuged at 400 x *g* for 5 minutes. For gene expression studies, the monocytes were further purified by magnetically isolating $CD14^{+}$ cells using CD14 MicroBeads, according to the manufacturer's instructions. Monocytes were resuspended in 5mL IMDM (with 10% human serum and 2mM L-Glutamine) and counted. Monocyte purity has been tested previously by members of this research group by measuring the number of CD14-expressing cells by flow cytometry, and was determined to be 95-98%.

2.2.1.4 Generating monocyte-derived macrophages

Freshly-isolated monocytes were seeded into tissue culture plates at a density of 2 x 10^6 per well of a 6-well plate, or the equivalent for 12- and 24-well plates, in IMDM (with 10% human serum and 2mM L-Glutamine). After allowing monocytes to adhere for 1 hour, medium and unattached cells were removed and replaced with fresh IMDM. Monocytes were differentiated into monocyte-derived macrophages (MDMs) by their adherence to culture plates and culture for 7 days. Medium was changed for fresh IMDM every 2 days.

2.2.1.5 Isolation of human neutrophils from peripheral blood

Human neutrophils were isolated from peripheral blood by diluting the blood 1:1 with wash buffer and layering on an equal volume of Ficoll, before centrifugation at 1200 x *g* for 20 minutes with brake set to 0 and temperature set to 4^{o}C. Subsequently, plasma and mononuclear cell layers were removed and the erythrocyte-rich pellet was collected. Erythrocytes were cross-linked using HetaSep to enhance sedimentation, where 1 part HetaSep was added to 5 parts blood and mixed gently. The blood/HetaSep mixture was then left at room temperature until the plasma:RBC interface was at approximately 50% of the

total volume, according to the manufacturer's instructions. The leukocyte-rich supernatant was then collected and washed in wash buffer, before pelleting the cells by centrifugation at 120 x *g* for 10 minutes. A CD16 Microbead Kit was then used, according to the manufacturers instructions, to select for neutrophils and remove eosinophil contamination. Neutrophils were >95% pure, as determined by cytospin and/or flow cytometry. Freshly isolated neutrophils are shown in **Fig 2.1**.

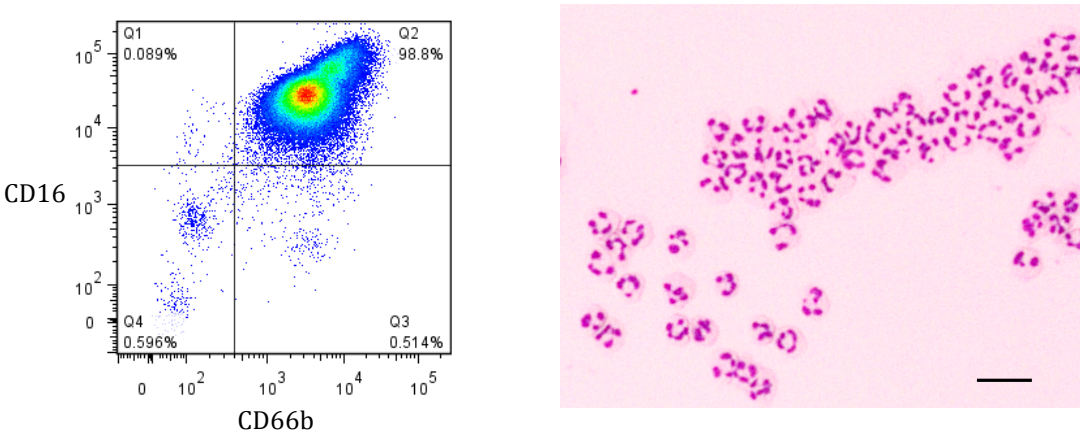

Figure 2.1 Purity of neutrophils freshly isolated from human peripheral blood. Greater than 95% of isolated cells were neutrophils, as measured by flow cytometric analysis (left), using the human neutrophil markers CD16 and CD66b. This was confirmed by cytospin (right). Data shown from one representative donor. Scale bar = 20µm.

2.2.2 Co-culture of MDMs and chemotherapy-treated tumour cells

A549 cells were treated with 10µM paclitaxel or docetaxel for 96 hours in 75cm^2 culture flasks in IMDM. As a control, an equal volume of the vehicle (DMSO) was also used. The media and soluble factors were collected (including dead/detached cells) and adherent cells were detached with Trypsin/EDTA, diluted in IMDM, and pelleted by centrifugation at 400 x *g* for 5 minutes. Tumour cells were then resuspended to a concentration of 1 x 10^6 per mL in the collected conditioned media with tumour-secreted factors. A total of 2 x 10^6 cells were either placed directly on top of MDMs in 6 well plates, or for Transwell experiments, were added to the upper chamber of a Transwell plate (pore size 0.3µm) where MDMs were in the lower chamber. Cells were then co-cultured for 5 hours. For direct co-cultures (**Figs 3.2** and **3.3**) a short treatment (5 minutes) with Trypsin/EDTA was used to detach the tumour cells so that they could be

washed off, and the MDMs could be collected since they remain attached after this short treatment – this method was shown in **Fig 2.2** to produce a >95% pure population of macrophages, and has been reported previously [296].

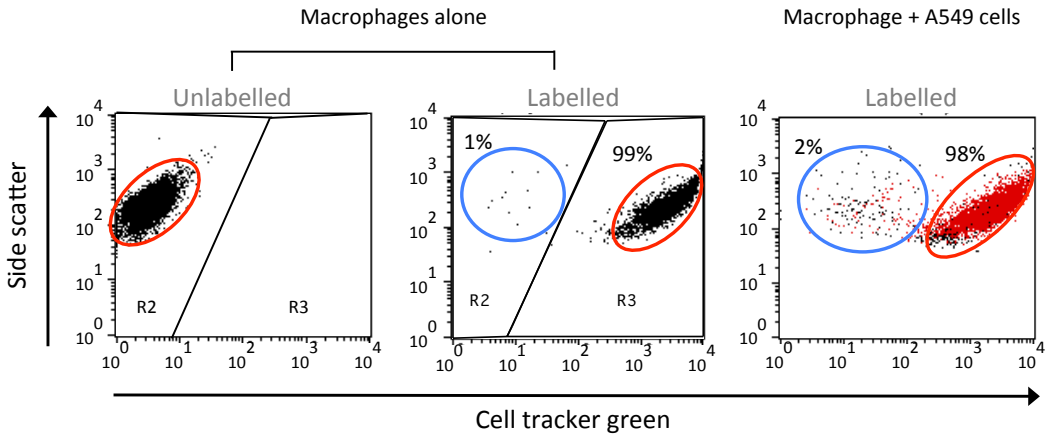

Figure 2.2 A 5-minute trypsin treatment is sufficient to detach A549 cells following co-culture with monocyte-derived macrophages. Seven-day monocyte derived macrophages (MDMs) were labelled with CellTracker green dye, then co-cultured with A549 cells that had been treated with docetaxel (10μM) for 96 hours. A 5-minute treatment with trypsin/EDTA solution at 37°C was sufficient to remove A549 cells, leaving a (>95%) pure population of conditioned MDMs, as determined by flow cytometry based on CellTracker labelling. (A) Unlabelled macrophages (red circle) are negative for CellTracker. (B) CellTracker efficiently labels 99% of MDMs (red circle) with only 1% of MDMs not labelling (blue circle). (C) A549 cells (unlabelled; blue circle) can be selectively detached by a 5-minute trypsin treatment and discarded, leaving a 98% pure population of labelled MDMs (red circle).

2.2.3 Culture of neutrophils for 16 hours in conditioned media from macrophage-infiltrated spheroids

For the analysis of neutrophil gene expression, freshly-isolated neutrophils were seeded at a density of 5 x 10^6 per well of a 6-well plate in 2mL of conditioned media. Neutrophils were then kept at 37°C for 16 hours to allow changes in their gene expression. Subsequently, neutrophils and media were collected and centrifuged to pellet the cells. The supernatant was removed, and neutrophils were resuspended and lysed in 500μL TRIzol, before proceeding to RNA extraction steps.

2.2.4 TUMOUR SPHEROIDS

2.2.4.1 CULTURING TUMOUR SPHEROIDS

To make tumour spheroids, 100µL of a 1.5% agarose solution (in DMEM without serum or L-Glutamine) were added to each well of a flat-bottomed 96-well plate using a multichannel pipette. After allowing agarose solution to set at room temperature, 1.5 x 10^4 cells were added to each well in IMDM (with 10% human serum and 2mM L-Glutamine) in a volume of 200µL. IMDM was used to accommodate the human monocytes that were to be added later, and the agarose coating of wells provided a non-adherent, curved surface (due to the meniscus), on which spheroids could form. The cells were then kept at 37^{o}C and monitored for the formation of spheroids and a necrotic core (see **Fig 2.3**). Half of the medium was removed and replaced with fresh medium every 2-3 days.

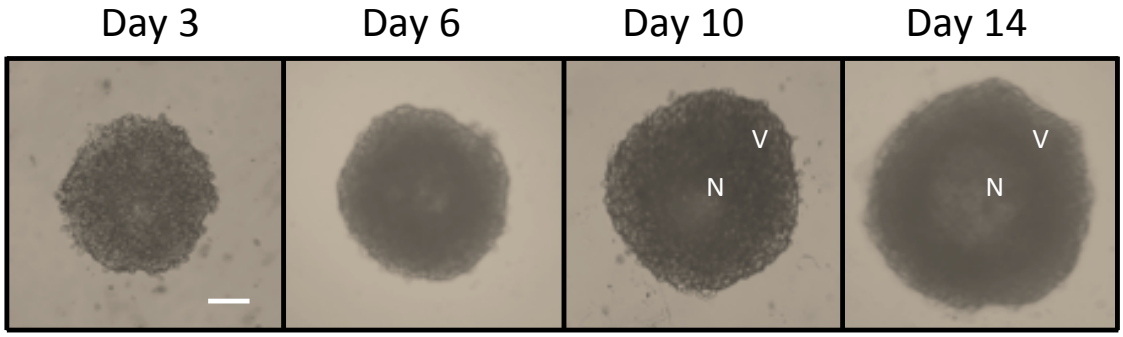

Figure 2.3 A549 human lung adenocarcinoma spheroids: Light microscopic images. A549 spheroids at 3, 6, 10 and 14 days. N, necrosis; V, viable rim. Scale bar = 100µm. Figure provided by Dr. Simon Tazzyman in Professor Lewis's group, Sheffield.

2.2.4.2 MONOCYTE INFILTRATION AND CHEMOTHERAPY TREATMENT OF TUMOUR SPHEROIDS

Spheroids were grown for 8-12 days, at which point almost all had developed a necrotic core, which were visible when using a 10x bright field microscope. To each spheroid, 1 x 10^5 freshly-isolated peripheral blood monocytes were added, which had been labelled with CellTracker Green, according to the manufacturer's instructions, detailed in brief in **section 2.2.10.1**. At the same time, chemotherapy groups received docetaxel such that the final concentration in each well was 10µM. It should be noted that the *in vitro* spheroid assays conducted here could be adapted to investigate the response of

existing, resident TAMs to chemotherapy-treated tumour cells in the context of a 3D tumour mass. For this, monocytes would be allowed to first infiltrate into A549 spheroids (and differentiate into TAMs - if, indeed, this occurs in tumour spheroids) before the spheroids were exposed to docetaxel. Additionally, spheroids could be treated with docetaxel first, and then co-cultured with monocytes – in order to model the possible effects of a docetaxel treated tumour microevironment on gene expression by new, tumour-infiltrating monocytes. This is discussed further in **section 3.5**.

2.2.4.3 COLLECTION OF CONDITIONED MEDIA FROM CHEMOTHERAPY-TREATED TUMOUR SPHEROIDS INFILTRATED WITH MONOCYTES

Monocytes were allowed to infiltrate and differentiate for 48 hours, after which, spheroids and media were collected using a P1000 pipette with a cut tip, and placed in 15mL centrifuge tube. Throughout the process tubes were kept cool on ice. Once spheroids had settled to the bottom of the tube, all the medium was removed and placed in a new 15mL centrifuge tube. Any remaining cells were removed by centrifugation at 500 x *g* for 10 minutes, and filtration through a 0.22μm pore size syringe filter.

2.2.5 RNA EXTRACTION

2.2.5.1 RNA EXTRACTION FROM MONOLAYER-CULTURED MACROPHAGES AND NEUTROPHILS

Macrophage and neutrophil total RNA was isolated using TRIzol and RNA was purified using the RNeasy Mini kit, according to the manufacturers' instructions. Throughout the RNA extraction and cDNA synthesis procedures, samples were kept on ice, RNase-free pipette tips, RNase-free water, and nuclease microtubes were used. Briefly, macrophages and neutrophils were placed on ice and lysed and scraped with TRIzol. The cell lysate was transferred to microtubes and homogenised by adding chloroform and inverting several times to mix. Samples were centrifuged and the RNA-containing aqueous phase collected. Seventy percent ethanol was added to the solution and then pipetted into RNeasy spin columns and centrifuged to collect the RNA in the columns. A DNase step was included at this point to eliminate DNA contamination

(according to the manufacturer's instructions). Columns were then washed with buffer RW1 and RPE and purified RNA was collected in new 2mL microtubes by centrifugation, eluting in 40µL of RNase-free water. Isolated RNA was stored at -80°C.

2.2.5.2 RNA EXTRACTION FROM SORTED MYELOID CELLS

For gene expression analysis of FACS sorted myeloid cells the same procedure was used as described above with the following changes:

- An RNeasy Micro kit was used to isolate total RNA from sorted myeloid cells, according to the manufacturer's instructions.
- Cell numbers between experimental groups were normalised before isolating total RNA.
- RNA was eluted in 14µL RNase-free water.

2.2.6 SYNTHESIS OF CDNA AND REAL-TIME PCR ANALYSIS

2.2.6.1 CDNA SYNTHESIS

For cDNA synthesis, 0.5-1.0µg RNA were used to reverse transcribe into cDNA using the TaqMan Reverse Transcription Reagents, according to the manufacturer's instructions. Sample concentration was estimated by measuring the A260/280 ratio using a Nanodrop 1000. In brief, RNA was diluted in RNase-free water to a volume of 15.4µL in nuclease-free microtubes and added to a mixture containing the following reagents:

Reagents	**Per sample**
10x Buffer	4µL
25mM $MgCl_2$	8.8µL
dNTPs	8µL
Oligo dT primers	2µL
RNase Inhibitors	0.8µL
Reverse Transcriptase	1µL
Total:	**24.6µL**

Samples were then heated in a thermocycler as instructed in the TaqMan Reverse Transcription Reagents kit, and cDNA stored at -20°C. In the case of RNA from FACS sorted macrophages where RNA yield was low, all RNA was used in a reverse transcription reaction, using the Superscript II kit according to manufacturer's instructions.

2.2.6.2 Real-time PCR

Real-time PCR was done using the SYBR Green detection method and using a CFX96 real-time PCR detection system. Primer concentrations were determined experimentally and were used at a concentration of 100 – 350nM. In each well of a 96-well PCR plate, 2µL cDNA were added, and 8µL of the following mixture of reagents:

Reagents	**Per well**
Primer	3µL
Distilled water	5µL
SYBR Green	10µL
Total:	**18µL**

Once all the reagents were added, PCR plates were centrifuged to collect samples at the bottom of the well. A CFX96 real-time PCR detection system was then used with the following thermocycler settings:

Initial hold	**45 cycles of...**			**Melt curve**
95°C for 5 min	95°C for 15s	55°C for 30s	72°C for 45s	55°C to 95°C in increments of 0.5°C every 10s

The $2^{-\Delta\Delta_{Ct}}$ method was then used to calculate fold-change in gene expression, normalised to endogenous controls, and the primer melt curves were consulted to confirm proper primer binding.

2.2.7 Microarray analysis

Analysis of macrophage gene expression was carried out using the HumanHT-12 v4 Expression BeadChip Kit on the Illumina array platform by the Bioinformatics Core Facility at Singapore Immunology Network, A*STAR, Singapore. See **section 3.3** for more information.

2.2.8 ELISA

A CXCL1 (Gro-alpha) ELISA was used to measure levels of CXCL1 in conditioned media collected from various spheroid-based co-cultures. This was carried out according to the manufacturer's instructions, using conditioned media that had been diluted 1:2 or 1:3 in fresh IMDM.

2.2.9 FUNCTIONAL ASSAYS

2.2.9.1 NEUTROPHIL MIGRATION ASSAY

To observe neutrophil migration freshly-isolated neutrophils were added to the upper well of a Transwell plate. Into the lower well, conditioned medium was added and plates were incubated at 37^{o}C for 3 hours. Following this, the numbers of migrated neutrophils (in the lower wells) were counted.

2.2.9.2 INVASION ASSAY

A549 human lung adenocarcinoma cells were added to the upper chamber of a Transwell plate that had been pre-coated with a thin layer of Matrigel to represent the extracellular matrix. Conditioned media were then placed in the lower chamber and the plate was kept at 37^{o}C for 18 hours to allow tumour cells to actively invade through the Matrigel. Subsequently, all medium was removed from the upper and lower chambers and un-infiltrated tumour cells were also removed using a cotton bud to scrape the upper surface of the Matrigel. The invaded tumour cells, on the lower face of the Transwell insert, were fixed in ice-cold methanol and stained using crystal violet. Cells were then lysed in acetic acid and the absorbance (595nm) of this solution was measured in triplicate using a spectrophotometer.

2.2.10 FLOW CYTOMETRY

2.2.10.1 CELLTRACKER LABELLING

Freshly-isolated monocytes were labelled with CellTracker Green before adding to tumour spheroids to facilitate their re-isolation by FACS sorting. Monocytes were incubated in 2.5μM CellTracker Green in pre-warmed IMDM for 30 minutes at 37^{o}C. Following this, monocytes were pelleted by centrifugation at 400 x *g* for 5 minutes and resuspended in fresh, pre-warmed IMDM and

incubated for a further 30 minutes at 37°C. Monocytes were washed one more time in IMDM to ensure complete removal of excess CellTracker Green fluorescent probe.

2.2.10.2 Analysis of necrosis and apoptosis

Flow cytometry was used to investigate the induction of apoptosis and necrosis in tumour cells by the chemotherapeutic docetaxel. The media from chemotherapy-treated tumour cells were collected (to collect any dead/detached cells) and the remaining adherent cells were detached using a 5-minute treatment with trypsin/EDTA solution. The collected conditioned media were used to neutralise the trypsin/EDTA solution, and cells were pelleted by centrifugation at 400 x *g* for 10 minutes. The tumour cells were then resuspended in 100µL FACS buffer and 5µL of FITC-conjugated anti-Annexin V antibody were added for 15 minutes in the dark at room temperature. Cells were subsequently washed in wash buffer and resuspended in 300µL FACS buffer. Immediately before analysis, 5µL propidium iodide (PI) were added and vortexed thoroughly. Tumour cell apoptosis and necrosis was recorded using a FACSCalibur flow cytometer and data were analysed in CellQuest Pro.

2.2.11 Fluorescence activated cell sorting of macrophages from tumour spheroids

Macrophage-infiltrated tumour spheroids were washed thoroughly in HBSS (without Ca^{2+} or Mg^{2+}). Spheroids were then pipetted dynamically several times in order to remove non-infiltrated myeloid cells, which was done in a volume of 1mL HBSS using a P1000 with a cut tip. The total volume was made up to 10mL with HBSS and spheroids were left briefly to settle to the bottom of the tube. HBSS (containing non-infiltrated cells) was removed carefully leaving only macrophage-infiltrated spheroids in the bottom of the tube, and this washing process repeated a further 2 times.

Spheroids were then resuspended in 3mL trypsin/EDTA solution for 5 minutes and pipetted until they formed a single cell suspension. The trypsin/EDTA solution was then neutralised with IMDM (with 10% human serum and 2mM L-Glutamine), centrifuged at 400 x *g* for 5 minutes and

resuspended in FACS buffer. A viability dye (ToPRO-3) was added and the sample filtered through a 35µm filter to remove aggregated cells. Samples were kept on ice and viable, CellTracker Green-positive macrophages were sorted and collected in IMDM (with 10% heat-inactivated human serum and 2mM L-Glycine). The macrophages were then centrifuged at 450 x *g* for 10 minutes and resuspended in TRIzol for RNA analysis.

2.2.12 IMMUNOFLUORESCENCE

2.2.12.1 MURINE TUMOUR MODELS

Four murine tumour models were used to investigate the *in vitro* findings discussed in **Chapter 3** and **Chapter 4** in an *in vivo* setting. Control tumours were not size-matched, except for LLC tumours, and all tumours were fixed in 4% paraformaldehyde for 5 min once thawed, with the exception PyMT tumours that were fixed at time of collection. In brief, the four tumour models that were used were (for more information see **section 5.3**):

PyMT

Transgenic PyMT (FVB) murine breast tumours, grown as orthotopic transplants, were kindly provided by Dr. Joan Massagué (Memorial Sloan-Kettering Cancer Center, USA). This included mice that were treated with dual doxorubicin and cyclophosphamide chemotherapy, mice receiving the SB 265610 compound (CXCR2-specific inhibitor) in combination with chemotherapy, and relevant controls.

LLC

Mice were implanted with LLC1 murine Lewis lung carcinoma tumours by Dr. Hughes in the lab of Prof. Claire Lewis. Mice were treated with cyclophosphamide (150mg/kg) every 48 hours for a total of 3 injections, and culled 48 hours after the last dose of chemotherapy. Control tumours were size-matched.

4T1

Mice were injected with syngeneic 4T1 metastatic breast cancer tumours, and treated with paclitaxel. Frozen sections of tumours from these mice, and control 4T1 tumours, were provided by Prof. De Palma (École Polytechnique Fédérale de Lausanne, Switzerland) for other studies, and were used here to investigate intratumoural neutrophils in paclitaxel treated murine breast cancer.

ASV-B

ASV-B transgenic mice that develop spontaneous hepatocellular carcinoma were given either vehicle or the chemotherapeutic agent etoposide, and tumours were removed and frozen. These studies were also done by Dr. Russell Hughes in the laboratory of Prof. Claire Lewis.

Tumour biopsies were cut into pieces and tissue was snap-frozen by placing into labelled microfuge tubes and immersed for at least 1 minute in liquid nitrogen. Samples were then transferred to -80^{o}C for storage. For sectioning, frozen tumour samples were placed on plastic disposable mounts and covered in optimum cutting temperature compound (OCT), and then returned to -80^{o}C.

2.2.12.2 Immunofluorescent staining of frozen tumour sections

Frozen tumours were cut into 10μm thick sections using a cryotome and then placed on microscope slides before being stored at -80^{o}C. Slides were allowed to warm up to room temperature and then flooded with 4% paraformaldehyde (PFA) for 5 minutes to fix the sections, except for PyMT tumours since these tumours had been fixed in PFA previously. Following this, PFA was removed and slides were washed for 5 minutes with 30mM glycine in PBS at pH 7.5, to quench PFA fixation. Subsequently, slides were washed in PBST for 5 minutes before marking a ring around the tumour section with a PAP pen (Sigma-Aldrich Inc, Poole, Dorset, UK) and flooding with blocking buffer for 20 minutes. Blocking buffer was then tapped off and primary and secondary antibodies were applied (in the dark) according to the times and concentrations

detailed in **sections 4.3** and **5.3**. A list of antibodies used can be found in **section 2.1.3**.

After each antibody application slides were washed thoroughly for 15 minutes in PBST in slide staining racks and agitated gently on a rocker, which was important for removing background signal of some antibodies. After the final wash slides were counterstained with 300nM DAPI for 2 minutes, washed in PBST, and then protected with Prolong Gold Anti-fade reagent and a coverslip. Samples were then analysed on a Zeiss LSM 510 confocal microscope.

2.2.12.3 Semi-quantitative analysis by Z-stack

Z-stack images of tumour sections were taken in order to determine a semi-quantitative measure of protein expression. For each group 11 images were taken throughout the sample at 40x magnification in 4 regions/fields-of-view (FOV) of the tumour, and the mean and SEM calculated from 4 different tumours. Images were then analysed in ImageJ software, and the fluorescence intensity throughout the tumour section (i.e. all 11 images in the z axis) of the particular channel-of-interest was quantified and added together, using a method based on a previously reported analysis [148], to provide a value of overall fluorescence intensity in that FOV. To achieve this, the following macro was used in ImageJ software:

Macro

```
run("8-bit");
run("Invert LUT");
run("Enhance Contrast...", "saturated=0.4");
setAutoThreshold("Default");
//run("Threshold...");
setThreshold(4, 255);
run("Convert to Mask");
```

The Measure function was used to obtain a semi-quantitative measurement of signal fluorescence intensity, which was then recorded for the

comparison of expression between different treatment groups. The 4 FOV were averaged and the mean and SEM of these values from 4 donors are presented.

2.2.13 DATA REPRESENTATION AND STATISTICAL ANALYSIS

All experiments were repeated a minimum of 3 times and data are represented as mean value ± standard error of the mean (SEM) unless otherwise stated. GraphPad Prism 6 software was used to carry out statistical tests, one or two-tailed Mann-Whitney U test or parametric unpaired t test where appropriate, and $p<0.05$ considered statistically significant.

CHAPTER 3: EARLY CHANGES IN MACROPHAGE GENE EXPRESSION FOLLOWING EXPOSURE TO TAXANE-TREATED TUMOUR CELLS IN VITRO

3.1 INTRODUCTION

Considerable evidence exists for tumour-associated macrophages (TAMs) playing an important role in tumour progression, from the promotion of tumour initiation, growth and metastatic spread [149, 297, 298]. The tumour-promoting functions of TAMs include their secretion of a wide array of cytokines and chemokines within the tumour environment, for crosstalk with other cell types.

The chemokines CSF-1, CCL2, CXCL12 (SDF-1) and angiopoietin-2 (Ang-2) are important for monocyte recruitment in multiple types of tumour, and modulation of these proteins and their receptors in mouse models not only changes TAM intratumoural accumulation, but often affects tumour progression [127, 140, 162, 175, 299-303]. Furthermore, in cancer patients, high levels of these chemokines also correlate with increased TAM numbers and poor prognosis [304-307]. This is, in part, because TAMs contribute significantly to:

- Immunosuppression, through their secretion of such factors as IL-10 [164], TGF-β [308], PGE2[309] and the Treg chemoattractant CCL22 [163].
- Angiogenesis, via their release of a wide array of factors including VEGF [310], MMP-9 [303] and PlGF [311] expression.
- Invasion and metastasis, via the release of such factors as cathepsins [166, 167], and urokinase/plasminogen activator (uPA) [168].

As mentioned previously (see **section 1.11.1**), the involvement of macrophages in tumour responsiveness to chemotherapy has also become a focus of study. A number of studies have shown that TAMs are chemoprotective in some mouse tumour models [162, 212, 290, 291, 298] (see **Fig 1.5**). These have proposed a variety of mechanisms by which TAMs help to protect tumour cells from the toxicity of chemotherapy, including the inhibition of T cell

recruitment and activation [162], the secretion of MMP9 [212], IL-10 [291], and cathepsins B and S [290]. Notably, the exact role of TAMs in chemotherapy-treated tumours varies between different types of tumour as well as with different modes of chemotherapy [312]. However, the chemoprotective roles of TAMs in spontaneous MMTV-PyMT murine breast cancers have been reported in mice treated with paclitaxel [162, 290] or doxorubicin [212, 290]. It has therefore been suggested that agents which block TAM accumulation [162, 313, 314] or re-educate them towards a 'classical', or M1, anti-tumour macrophage phenotype [315] may prove to be therapeutically beneficial.

In addition, macrophages may modulate the tumour microenvironment by regulating the recruitment of other inflammatory cells, such as neutrophils [300], which is known to occur at sites of inflammation. For example, macrophages stimulated with LPS, or LPS plus PHA, release CXCL1, CXCL2 [93], and CXCL8 [96], which attract and activate neutrophils. Likewise, neutrophils can also signal the recruitment of monocytes and macrophages to sites of inflammation [87, 89], which together lead to the rapid accumulation of such innate immune effector cells as cytotoxic T cells, B cells and natural killer cells at these sites.

Chemotherapy can also cause the release of inflammatory chemokines by cancer cells. For example, docetaxel can activate NF-κB signalling in human prostate cancer cells *in vitro* [316], and paclitaxel treatment of the PyMT cell line can increase messenger RNA (mRNA) levels of colony-stimulating factor (CSF)-1 [162]. Similarly, chemotherapy induces upregulation of inflammatory molecules from non-tumour cells; combined treatment with doxorubicin and cyclophosphamide induced the release of inflammatory cytokine, TNFα, from endothelial cells, bone marrow-derived cells and smooth muscle cells [126].

In this chapter, the early *in vitro* responses of macrophages following exposure to docetaxel-treated lung carcinoma cells were explored. Microarray analysis and real-time polymerase chain reaction (RT-PCR) identified various important changes in chemokine gene expression that were then confirmed in different co-culture models, and also by RT-PCR.

For *in vitro* studies, A549 lung adenocarcinoma cells were used. Lung cancer is the most common cause of cancer death in the UK in 2010 [317], accounting for almost 35,000 deaths in 2010 alone. The vast majority (87%) of lung cancers are non-small cell lung cancer (NSCLC) [317], and so A549 cells, which derive from the tumour of a patient with NSCLC, were selected for use in the experiments described in **Chapter 3** and **Chapter 4**. Additionally, these cells were selected based on their ability to form 3D spheroids, which has been reported in previous publications [185, 300]. One of the most commonly used chemotherapies for the treatment NSCLC in patients is the taxane drug, docetaxel (Taxotere®) [318], which is used clinically either as a single agent or in combination with other such drugs as cisplatin or carboplatin. Docetaxel was selected for the treatment of A549 cells to emulate the chemotherapy-treatment of lung tumours, albeit in a basic and simplified model.

3.2 AIMS

To characterise changes in gene expression in macrophages following their exposure to chemotherapy-treated tumour cells *in vitro*.

3.3 METHODS

Human A549 non-small cell lung cancer cells were cultured as described in **section 2.2.1.1**. Human monocytes were isolated from waste Buffy coats from healthy blood donors, according to the protocol detailed in **section 2.2.1.3**. To generate monocyte-derived macrophages, monocytes were cultured in tissue culture plates for 7 days in IMDM, supplemented with 10% human serum and 2mM L-Glutamine, as described in and **section 2.2.1.4**. Additionally, A549 tumour spheroids were grown in IMDM in agarose-coated 96-well plates, as described in **section 2.2.4**. To induce cell death, A549 cells were treated with docetaxel, for which the vehicle was dimethyl sulphoxide (DMSO). Docetaxel-treated A549 cells were then co-cultured with macrophages in three different co-culture systems to address three different experimental questions:

1. Direct co-culture – where docetaxel-treated A549 tumour cells were added to wells of MDMs cultured in 6-well plates (see **section 2.2.2**). This

was to observe changes in the levels of macrophage messenger RNA (mRNA) when they encounter docetaxel-treated A549 cells. This setup was also used for the initial microarray analysis of the most highly regulated genes in co-cultured macrophages.

2. Transwell co-culture – whereby macrophages and docetaxel-treated tumour cells were physically separated by a porous membrane (see **section 2.2.2**). MDMs were cultured in the lower wells, and docetaxel-treated A549 cells were added to upper wells. This allowed the investigation of the proportion of the macrophage response that was due to paracrine signalling via soluble factors.
3. Spheroid co-culture – where freshly-isolated monocytes were added to 8-12 day A549 spheroids, and co-cultured for 48 hours to allow monocyte infiltration. Docetaxel, or its vehicle DMSO, were also added to the A549 spheroids at the same time. Re-isolation of monocytes/myeloid cells by fluorescence-activated cell sorting (see **section 2.2.11**) allowed the investigation of myeloid cell gene expression in docetaxel-treated A549 spheroids, in comparison with DMSO-treated spheroids, to confirm the gene expression changes identified by microarray and the first two co-cultures in a more complex, 3D model.

More specifically, for direct co-culture, 2 x 10^6 docetaxel-treated (10μM, 96 hours in IMDM) A549 cells, including their secreted factors, were placed onto 7-day MDMs (initial starting number 2 x 10^6 per well) in 6-well plates. For control, A549 cells were treated with an equivalent volume of the docetaxel vehicle DMSO and all other parameters were kept the same. These tumour cells and MDMs were co-cultured for 5 hours at 37^{o}C, following which all media and detached cells (mainly tumour cells) were removed, and 1mL trypsin/EDTA was added to each well. A 5-minute treatment with trypsin/EDTA at 37^{o}C was sufficient to detach the docetaxel-treated tumour cells but still leave MDMs attached (see **Fig 2.2**), as suggested previously [296]. Conditioned MDMs were then lysed in 1mL TRIzol, scraped with a cell scraper and collected on ice in microtubes for RNA extraction. The same conditions were used for Transwell co-culture experiments, with the exceptions that MDMs were cultured in the lower

well of a 6-well Transwell plate (pore size 0.3μm), and docetaxel-treated A549 cells and their conditioned media were added to the upper well. Following co-culture for 5 hours, the upper wells (containing tumour cells) were removed and the media in the lower wells were also removed. As before, 1mL TRIzol was added, conditioned MDMs were scraped and collected on ice in microtubes for RNA extraction.

For spheroid-based studies (see **section 2.2.4**), A549 tumour spheroids were grown for 8-12 days until a necrotic core was visible under the light microscope. Freshly-isolated human monocytes were labelled with CellTracker green dye (see **section 2.2.10.1**) and then washed several times in fresh IMDM to remove all CellTracker dye from the medium. Subsequently, 1 x 10^5 labelled monocytes were then added to each spheroid. Docetaxel was also added so that the concentration in the cell media was 10μM, or an equivalent volume of the docetaxel vehicle DMSO was added to control groups. Monocyte and A549 spheroids were then cultured at 37°C for 48 hours to allow the monocytes to infiltrate the tumour spheroids. These myeloid cells were re-isolated from spheroids by FACS for gene expression analysis (see **sections 2.2.5.2**, **2.2.10.1** and **2.2.11**).

More specifically, un-infiltrated myeloid cells were removed from spheroids by placing spheroids into a new centrifuge tube, topping up to 15mL with fresh IMDM, allowing spheroids to settle to the bottom of the tube and then removing as much of the media as possible using a stripettor (Corning) and a P1000 pipette. The spheroids were re-suspended in 1mL IMDM and, using a P1000 pipette with a cut tip, the spheroids were pipetted firmly up and down repeatedly to dislodge remaining myeloid cells sticking to the spheroid. Following this, 14mL IMDM was added to the 1mL IMDM, and then all media and suspended cells were removed, leaving just the myeloid cell-infiltrated spheroids in the bottom of the tube. To dissociate the spheroids, 1mL pre-warmed trypsin/EDTA solution was added, and the cells were kept at 37°C for 5 minutes. A P1000 pipette was used to pipette the cells up and down repeatedly and get the A549 cells and myeloid cells into a single cell suspension. The cells were then pelleted by centrifugation at 400 x *g* for 5 minutes and re-suspended in FACS

buffer. Subsequently, 5µL of the viability dye 7-AAD was added and incubated on ice for 15 minutes. The samples were then taken immediately for FACS to collect the viable, CellTracker dye-labelled myeloid cells. The gating strategy involved:

1. Gating out the debris in the sample based on forward scatter (FSC) and side scatter (SSC) profiles.
2. Using SSC-width against SSC-height, as well as FSC-width against FSC-height, to eliminate doublets.
3. Selecting viable cells by gating around the 7-AAD-APC negative cells.
4. Selecting myeloid cells by gating around the CellTracker green-FITC positive cell population (originally monocytes).

Cell sorting was done using FACSAria II 4-laser (BD), run by the FACS core facility at Singapore Immunology Network (SIgN, Singapore). The sorted cells were collected in 15mL centrifuge tubes kept at 4°C. Cells were pelleted by centrifugation at 500 x *g* for 10 minutes, before removing the FACS buffer and re-suspending in 500µL TRIzol for RNA extraction.

The purpose of this spheroid-based myeloid cell gene expression experiment was to observe whether the identified changes in macrophage mRNA levels are also replicated in tumour-infiltrating myeloid cells in a 3D tumour spheroid model. The benefit of using this model is that spheroids contain certain characteristics that are more representative of *in vivo* conditions, including hypoxic core regions, drug diffusion gradients and 3D structure that facilitates infiltration of immune cells [319, 320]. However, this model lacks the full complexities of *in vivo* tumours such as the presence of vasculature.

As stated above, monocytes were added to A549 spheroids for 48 hours in the spheroid co-culture model. It is likely that they will start to differentiate into macrophages as they encounter the tumour mass, the spheroid-derived factors in the media, and as they infiltrate into the A549 spheroids. However, monocyte-derived macrophages are generally considered to differentiate *in vitro* over a period of 5-7 days [321, 322], and thus at 48 hours these cells are unlikely to be fully differentiated macrophages. Therefore, they will be referred to in this thesis as 'myeloid cells'. These cells could be isolated and compared to freshly-

isolated monocytes and 7-day cultured macrophages to determine whether they share more characteristics with monocytes or with differentiated macrophages. Such characteristics as increased cytoplasmic-to-nuclear ratio and greater numbers of mitochondria and lysosomes – measured using MitoTracker and LysoTracker dyes – could be analysed, as reported previously [323]. Additionally, the expression of carboxypeptidase M could be measured by flow cytometry, which is associated with monocyte to macrophage differentiation [324].

Following co-culture of docetaxel-treated A549 cells and monocytes/macrophages in these three co-culture systems, an enzyme-linked immunosorbent assay (ELISA) was used to observe whether the changes in macrophage mRNA were also seen at the protein level for the CXCL1 gene. Conditioned media from the myeloid cell and A549 spheroid co-cultures described above were collected and used in an ELISA for CXCL1 (see **section 2.2.8**), according to the manufacturer's instructions.

Gene expression using total RNA isolated from monocyte-derived macrophages from co-culture experiments, and of myeloid cells from tumour spheroids, was done using RNeasy Mini Kit (Qiagen) and the RNeasy Micro Kit (Qiagen) respectively, according to the manufacturer's instructions (summarised in **section 2.2.5**). The quality and quantity of isolated RNA were assessed with a Nanodrop 1000 using the absorbance readings at 260nm and 280nm. Between 0.5-1.0μg RNA were used for a reverse transcription reaction, with the exception of FACS-sorted myeloid cells from tumour cells, where all of the isolated RNA from at least 1 x 10^5 cells was used in a reverse transcription reaction. Although the concentration and purity of RNA in these FACS-sorted samples were not checked, subsequent RT-PCR reactions were examined for correct primer binding according to the generated meltcurves, and that β-actin had a threshold cycle (Ct) value of fewer than 22 cycles.

Extracted RNA was used to scan the transcriptional profile of MDMs exposed to docetaxel-treated A549 cells by microarray (see **section 2.2.7**). This was done with the Human HT-12_V4 Expression BeadChip kit (Illumina), which

was used here to investigate the expression of over 47,000 transcripts by human macrophages. The array identified a list of differentially expressed genes (DEGs) between macrophages exposed to docetaxel-treated A549 cells and unconditioned macrophages cultured in media alone, based on 5 identical experiments.

More specifically, 7-day MDMs were co-cultured with docetaxel-treated A549 cells, and macrophage RNA was isolated as described in detail above. The RNA was then given to the Bioinformatics Facility (SIgN, Singapore) for processing, starting with determining the RNA quality and quantity using a 2100 Bioanalyzer (Agilent). The RNA integrity number (RIN) was calculated using the ratio of 18s/28s – as well as any peaks present between 18s and 28s and between 5s and 18s – to check how degraded the RNA was, and returned a RIN value of 8. The RNA was amplified and biotinylated using the TargetAmp Nano-g Biotin-aRNA Labelling kit (Epicentre, Illumina) to generate biotinylated cRNA, as per the manufacturer's instructions, and a Direct Hybridization Assay was done according to the protocol provided by Illumina [325]. Subsequently, the microarray chip was scanned using a Beadarray Scanner 500GX (Illumina). The expression values were then extracted (without background subtraction) in GenomeStudio with Illumina annotation Human HT-12_V4_0_R2_15002873_B.bgx. These values were then quantile-normalized to give samples an even distribution, and then $\log_2$-transformed. An analysis of differentially expressed genes (DEGs) was done using Limma (Bioconductor) [326], an open source package for R software. DEG analysis was done with normalized and $\log_2$-transformed data, and identified 2,466 DEGs. The software MultiExperiment Viewer (TM4) was used for the generation of heatmaps. Since primary cells were used (human monocyte-derived macrophages), the variation between donors was quite high; therefore, the heatmap in **Fig 3.2** shows fold change in expression between treatment groups.

Extracted RNA was also used to study the expression of co-cultured macrophages, and expression of myeloid cells isolated from tumour spheroids, by real-time PCR; RNA was isolated as described above. For MDM and chemotherapy-treated tumour cell co-cultures (direct co-culture and Transwell

co-culture), TaqMan Reverse Transcription Reagents were used to reverse transcribe macrophage RNA into cDNA, according to the manufacturer's instructions, and summarised in **section 2.2.6.1.** For RNA isolated from FACS-sorted myeloid cells using the RNeasy Micro Kit (in a volume of 14µL), the Superscript II kit (Life Technologies) was used, according to manufacturer's instructions, as it delivers a higher cDNA yield than the TaqMan Reverse Transcription Reagents kit (determined previously in-house). All cDNA was stored at -20^{o}C.

For Real-time PCR, cDNA samples were analysed by SYBR® green (Applied Biosystems)-based quantitative PCR, as described in **section 2.2.6.2**. Primer concentrations were determined experimentally and used at between 100 and 300nM, and meltcurves were analysed to check proper primer binding. Gene expression was normalised to a β-actin housekeeping gene using the $2^{-\Delta\Delta Ct}$ method. Samples were run in duplicate (i.e. 2 wells for each sample/gene combination), and the data from a minimum of 3 experimental repeats were collected.

3.4 RESULTS

3.4.1 OPTIMISING THE INDUCTION OF TUMOUR CELL DEATH BY DOCETAXEL

A549 human lung carcinoma cells were exposed to various concentrations of the taxane chemotherapy, docetaxel, for 24, 48, 72 and 96h *in vitro*. The cells, both attached and in suspension, were then analysed by flow cytometry for markers of apoptosis and necrosis, using an anti-Annexin V antibody to detect apoptotic cells, and propidium iodide (PI) to detect necrotic cells. The percentage of apoptotic and necrotic cells were compared between docetaxel-treated and vehicle (DMSO)-treated A549 cells, shown in **Fig 3.1**.

The cell death by apoptosis and necrosis were highest at the 96-hour time-point. Differences in the drug concentration used had negligible effect on A549 apoptosis and necrosis, especially at the 24-72 hour time-points (see **Fig 3.1**), but an increase in the percentage of necrotic cells was observed between 5µm and 10µm at the 96 hour time-point, and so a treatment of 10µm for 96

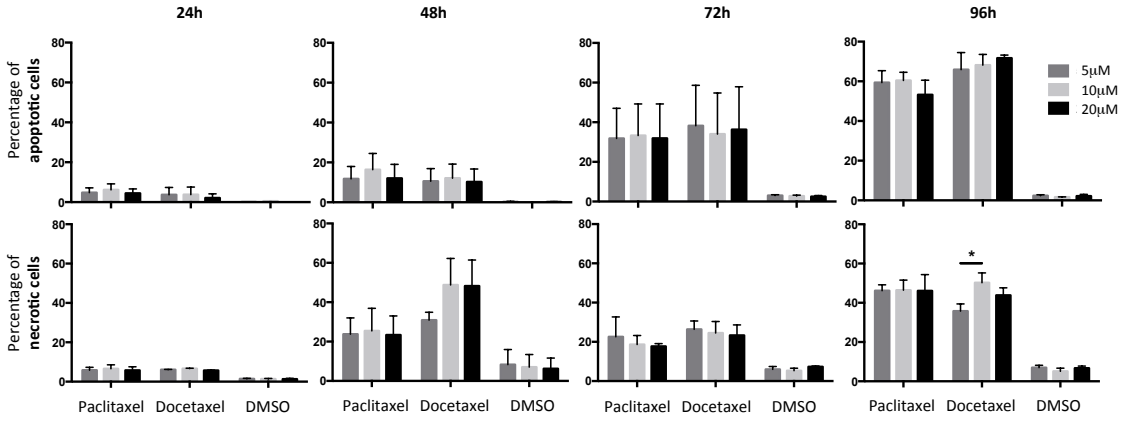

Figure 3.1 Induction of apoptosis and necrosis in A549 cells by exposure to docetaxel in vitro. Adherent A549 cells (between 50-70% confluent) were treated with docetaxel or its vehicle, dimethyl sulfoxide (DMSO), at concentrations of 5μM, 10μM or 20μM, for 24h, 48h, 72h and 96h. DMSO was given at a volume equivalent to the chemotherapy dose (20μM). Levels of apoptosis and necrosis were measured using an anti-Annexin V antibody and propidium iodide viability dye using flow cytometry at the given time points. The mean ± SEM from 3 identical experiments are shown. Data are expressed as percentage of apoptotic or non-viable cells following culture with docetaxel or its vehicle DMSO, Mann-Whitney U test, * $p < 0.05$ w.r.t. DMSO control, ^ $p < 0.05$.

hours was selected for future experiments. This treatment induced approximately 70% apoptosis and 50% necrosis in A549 tumour cells.

3.4.2 EARLY RESPONSE OF MACROPHAGES TO DOCETAXEL-TREATED TUMOUR CELLS

Following chemotherapy, monocytes recruited into tumours may be activated to change their gene expression by tumour-derived factors. Possible early changes in macrophage expression following exposure to docetaxel-induced apoptotic or necrotic A549 cells (i.e. within 5h) were first investigated using a Human HT-12 v4 microarray (Illumina). A list of the top 100 upregulated and 100 downregulated differentially expressed genes (DEGs, i.e. those genes that show a statistically significant increase or decrease) between macrophages exposed to docetaxel-treated A549 cells, and unconditioned macrophage controls in fresh IMDM, is shown in **Supplementary Table 1**. This analysis identified 2,466 DEGs in macrophages exposed to docetaxel-treated A549 cells, of which 1,385 genes were upregulated and 1,081 were downregulated. Many of these genes coded for cytokines, chemokines, surface molecules and miscellaneous molecules involved in tumour promotion. Since studying all these

genes is out of scope of this work, the cytokine/chemokine genes were focussed on because this group of molecules has been implicated in the recruitment of stromal cells into tumours [126, 145, 185], which are important regulators of tumour growth, angiogenesis, immune escape and metastasis. The ELR⁺ CXC cytokines, CXCL1, CXCL2 and CXCL5, were found to be highly upregulated in macrophages conditioned by docetaxel-treated A549 cells (**Fig 3.2**). These chemokines are known to be major chemoattractants and/or activators of neutrophils. Additionally, three other chemokine genes, CCL2, CCL7 and CCL8, were downregulated in conditioned macrophages.

The upregulation of CXCL1, CXCL2 and CXCL5 mRNA was confirmed in the identical co-culture experiments, by real-time polymerase chain reaction (RT-PCR) (**Fig 3.3** and **3.4**). These experiments also included a comparison of

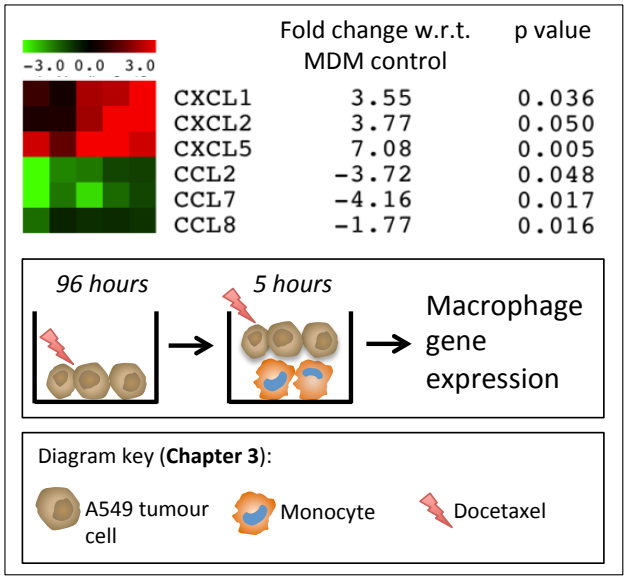

Figure 3.2 Macrophages regulation of cytokine mRNA following co-culture with docetaxel-treated tumour cells. The early response of 7-day monocyte-derived macrophages (MDMs) to a 5-hour co-culture with docetaxel-treated (10μM for 96 hours) A549 cells was analysed by gene array to identify significantly regulated genes. Unconditioned, 7-day MDMs co-cultured in IMDM were used as a control in this experiment. MDMs plus vehicle (DMSO), and MDMs plus viable A549 cell controls were included in later real-time PCR experiments, shown in **Fig 3.3** and **3.4**. Macrophages and docetaxel-treated tumour cells were directly co-cultured and separated after 5 hours by a short (5 minute) trypsin treatment that was sufficient for detaching tumour cells (see **Fig 2.2**). Data show fold change in gene expression w.r.t. unconditioned MDM controls in IMDM, fold change and Mann-Whitney U test p-values based on 5 identical experiments.

gene expression in MDMs cultured for 5 hours in the docetaxel vehicle DMSO, as well as MDMs exposed for 5 hours with viable tumour cells (i.e. A549 cells that were cultured for 96 hours in IMDM containing an equivalent volume of DMSO). These results demonstrated that the induction of these genes is not just a response to chemotherapy, since docetaxel alone was not sufficient to upregulate macrophage mRNA levels greater than 2-fold above control macrophages (MDMs that were cultured for 5 hours in IMDM and the docetaxel vehicle DMSO). Similarly, MDMs exposed to viable tumour cells (A549 cells treated with DMSO for 96 hours) did not upregulate CXCL1, CXCL2 or CXCL5 gene expression very highly (less than 4-fold) in comparison with control macrophages. **Fig 3.3** shows that MDMs upregulated these chemokine genes significantly ($p < 0.05$) higher

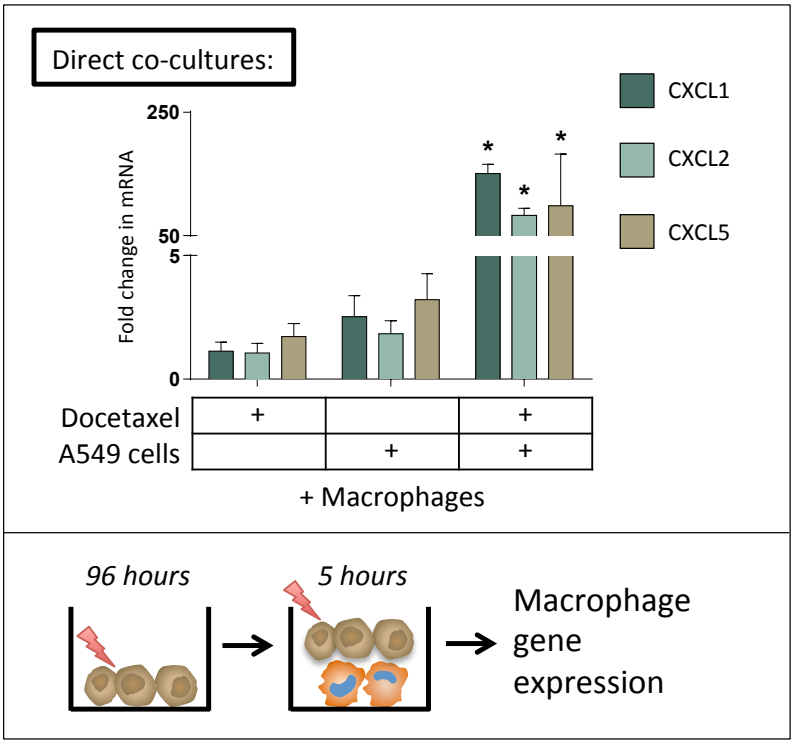

Figure 3.3 Real-time PCR confirms an upregulation of CXCL1, CXCL2 and CXCL5 mRNA by macrophages following co-culture with docetaxel-treated tumour cells. Real-time PCR (RT-PCR) confirmed an upregulation of CXC chemokines by macrophages co-cultured with docetaxel-treated A549 cells, which was not observed in macrophages exposed to viable tumour cells (cultured for 96 hours with the drug vehicle DMSO). Viable A549 cells were collected using the same method - i.e. viable cells including cell supernatant/DMSO added to macrophages for 5 hours. The mean ± SEM from 3 identical experiments are shown. Data show fold change in mRNA levels w.r.t. macrophages cultured for 5 hours in DMSO, Mann-Whitney U test, * $p < 0.05$ w.r.t. macrophages plus viable A549 cells.

following exposure to docetaxel-treated A549 cells, as compared to macrophages exposed to viable (DMSO-treated) A549 cells. These *in vitro* data suggest that when human lung tumours are exposed to docetaxel, macrophage expression of CXCL1, CXCL2 and CXCL5 may be upregulated.

The differences between the data in **Fig 3.3** and **3.4** could be due to the fact that, in the latter experiments, macrophages and docetaxel-treated tumour cells were physically separated in a Transwell system, thereby limiting interaction between the cell types to soluble factors only and no physical interaction. Therefore, it appears that macrophage upregulation of CXCL1 and, to an extent CXCL2, may be heavily dependent on interaction via soluble factors, whereas CXCL5 induction involves cell-cell contact as well as soluble factor stimulation for increased induction.

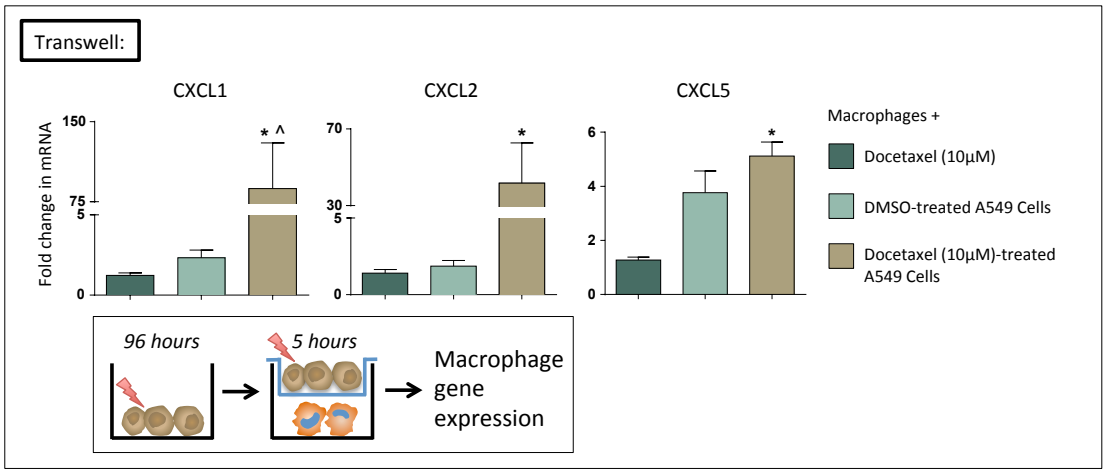

Figure 3.4 Macrophages upregulate CXCL1, CXCL2 and CXCL5 mRNA in response to soluble factors, although macrophage upregulation of CXCL5 mRNA is reduced, as compared to direct co-cultures. In Transwell plates, where docetaxel-treated A549 cells in the upper chamber are physically separated from MDMs by a porous membrane, macrophages respond to soluble factors and upregulate CXCL1, CXCL2, and to a much less extent, CXCL5. A significant increase in CXCL1 upregulation was observed between macrophages co-cultured for 5 hours with docetaxel-treated A549 cells, and those co-cultured with DMSO-treated A549 cells. The mean ± SEM 3 identical experiments are shown. Data show fold change in mRNA levels w.r.t. macrophages cultured for 5 hours in DMSO, Mann-Whitney U test, * $p < 0.05$ w.r.t. macrophages plus viable A549 cells, ^ $p < 0.05$ w.r.t. macrophages plus viable A549 cells.

3.4.3 MYELOID CELLS FROM DOCETAXEL-TREATED TUMOUR SPHEROIDS UPREGULATE CXCL1, 2 AND 5 MRNA

Macrophage gene expression of CXCL1, CXCL2 and CXCL5 was then investigated using a 3D spheroid co-culture system. As mentioned previously in **section 3.3**, monocytes were added to A549 spheroids for 48 hours in the spheroid co-culture model. Monocytes differentiate into macrophages as they infiltrate into tissue *in vivo* [23], or by adherence to plastic culture plates *in vitro* for 5-7 days in media [321, 322], often supplemented with GM-CSF or M-CSF. Therefore, it is likely that monocytes will begin to differentiate as they infiltrate tumour spheroids and respond to A549-derived factors in the media, but may require longer than 48 hours culture to become fully differentiated macrophages. These cells will be referred to here as 'myeloid cells', but ideally would be isolated and analysed for such characteristics as increased cytoplasmic to nuclear ratio, and increased numbers of mitochondria and lysosomes, indicative of macrophage differentiation [323].

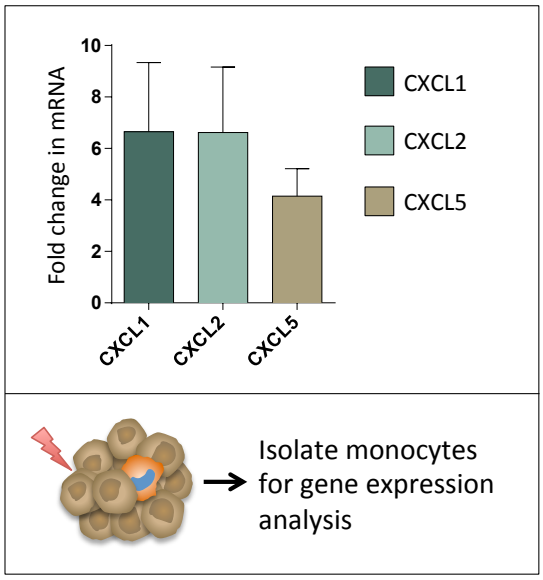

Figure 3.5 Myeloid cells isolated from docetaxel-treated A549 spheroids show increased expression of CXC chemokines. Freshly-isolated human monocytes labelled with a CellTracker probe were added to tumour spheroids for 48 hours, with docetaxel or medium containing the equivalent amount of DMSO. Infiltrated myeloid cells were then isolated by FACS and analysed by RT-PCR for the expression of CXCL1, CXCL2 and CXCL5 mRNA. All three were upregulated in the docetaxel-treated group, compared to spheroids infiltrated with myeloid cells but exposed to medium containing DMSO. The mean ± SEM 3 identical experiments are shown. Data show fold change in mRNA levels w.r.t. myeloid cells isolated from spheroids treated with DMSO for 48 hours.

An increase of approximately 6-fold was observed in expression of CXCL1 and CXCL2 mRNA in myeloid cells with the addition of docetaxel treatment (**Fig 3.5**). The chemokine CXCL5 was upregulated by approximately 4-fold. Upregulation of these CXC cytokines by macrophages confirms earlier microarray and RT-PCR findings from cells in monolayer systems, shown in **Fig 3.3** and **3.4**.

3.4.4 Myeloid cells from docetaxel-treated tumour spheroids upregulate their release of CXCL1

In order to investigate whether changes in CXC chemokine expression at mRNA level could also be seen at the protein level, an enzyme-linked immunosorbent assay (ELISA) was used. Ideally, all three chemokines would have been investigated, but because of budget restrictions an ELISA for one gene was chosen. Of the three chemokines, the most is known about CXCL1 (also called GRO-α, homolog of KC in mice and CINC-1 in rats). It was determined to be a more potent chemoattractant of human neutrophils than CXCL2 and CXCL5, using neutrophils isolated from neonates and adults [327]. The chemoattraction of neutrophils/granulocytic cells by CXCL1 has also been established in a murine breast cancer model [126], whereby recruited $CD11b^{+}Gr1^{+}$ cells supported tumour growth and metastasis, particularly in chemotherapy-treated tumours. Therefore, CXCL1 was selected for investigation by ELISA. The levels of CXCL1 protein in the supernatants of non-infiltrated spheroids, and myeloid cell-infiltrated spheroids exposed to either DMSO or docetaxel, were assessed (**Fig 3.6**).

The production of CXCL1 protein by tumour spheroids incubated with DMSO or docetaxel for 48 hours was significantly ($p < 0.05$) lower than when spheroids were infiltrated by myeloid cells. Docetaxel treatment of tumour spheroids in the absence of myeloid cells did not increase CXCL1 production by tumour cells. Therefore, it is likely that the increase in CXCL1 seen for docetaxel treatment of myeloid cell-infiltrated tumour spheroids is due to CXCL1 secretion by myeloid cells. However, the possibility that the presence of myeloid cells in spheroids may have stimulated the tumour cells to upregulate CXCL1 cannot be excluded.

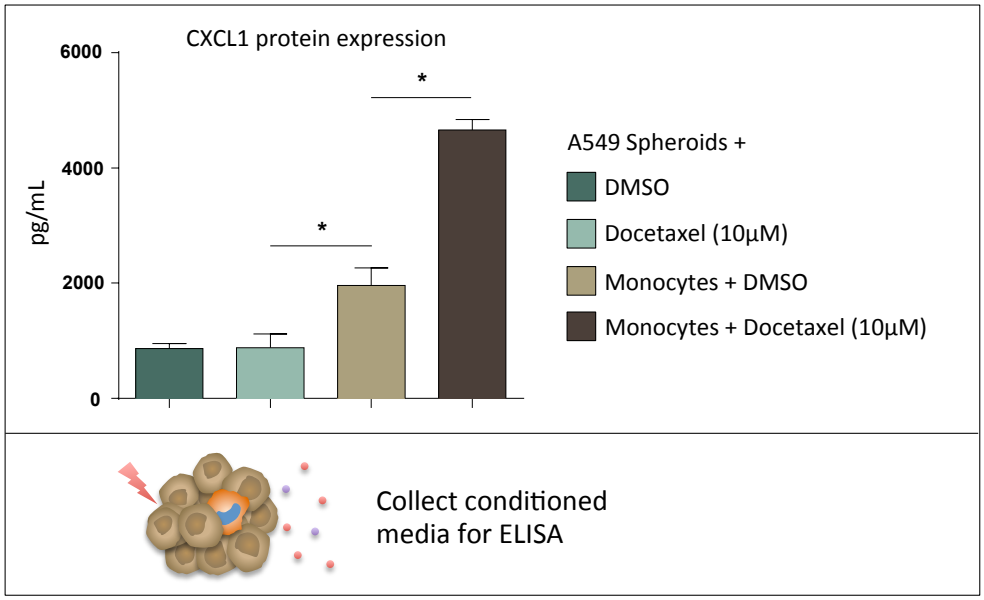

Figure 3.6 Effect of myeloid cell infiltration and docetaxel treatment on CXCL1 released by A549 spheroids over 48 hours. Spheroid supernatants were analysed by ELISA for CXCL1 protein. A549 tumour spheroids released detectable CXCL1 in the absence of monocytes, but this was significantly increased following their infiltration (with DMSO) – and yet further when exposed to docetaxel. The mean ± SEM from 4 experiments are shown. Data show the level of detected CXCL1 protein in spheroid supernatants in picograms per millilitre, Mann-Whitney U test, * $p < 0.05$.

3.5 Discussion

Monocytes and macrophages are constantly recruited to tumours by tumour and stromal cell-secreted factors [127, 140, 162, 299-303], and in some instances recruitment of macrophages increases following chemotherapy [162, 212, 290]. Recruited monocytes subsequently differentiate into TAMs as they cross the tumour vasculature where they then respond to local stimuli and signals, including those induced by exposure to chemotherapeutic agents. Upon such treatments, pronounced changes occur in tumour metabolic activity [328] and also in gene expression of breast cancer tumours (measured 3 weeks after treatment with doxorubicin or docetaxel chemotherapy) [329]. Chemotherapeutic agents can also directly or indirectly alter stromal cell gene expression and polarisation, as summarised in **Fig 1.5**.

In summary, the data in this chapter show that treatment with docetaxel for 96 hours *in vitro* is sufficient to induce approximately 70% apoptosis and 50% necrosis in A549 non-small cell lung cancer cells. Co-culture of docetaxel-treated A549 cells with MDMs resulted in an upregulation of neutrophil chemokines CXCL1, CXCL2 and CXCL5 at the mRNA level in macrophages, which was not observed in response to DMSO-treated (viable) tumour cells. All three chemokines were also upregulated in myeloid cells isolated from A549 spheroids treated with docetaxel, in comparison with DMSO-treated controls. Furthermore, this expression was confirmed at protein level at least for CXCL1, which was higher in conditioned media from myeloid cell-infiltrated spheroids than A549 spheroids treated with DMSO or docetaxel, and was increased ($p = 0.0143$) further still when myeloid cell-infiltrated spheroids were also treated with docetaxel.

Timepoints from 24 to 96 hours were selected based upon previously reported findings [330]. Prolonged exposure (72h, 96h) of A549 human lung adenocarcinoma cells to docetaxel is required to elicit cell death in A549 human lung carcinoma cells by apoptosis and necrosis. This slow effect of docetaxel on inducing cell death is supported by a previous report using paclitaxel [330] (a taxane chemotherapeutic from which docetaxel was derived). Paclitaxel induction of tumour cell death was duration-dependent, rather than concentration-dependent, as was shown by the treatment of 5 different tumour cell lines (including A549 lung carcinoma cells) with paclitaxel *in vitro* at different concentrations and for different durations. This slow induction of cell death is most likely to be a product of the replication-halting mechanism of taxane-induced cell death, which inhibits microtubule dynamics by binding to β-tubulin subunits. An increased dose may not disrupt microtubule dynamics further, but prolonging the cell cycle-inhibitory effects may cause higher levels of necrotic and apoptotic cell death.

The percentage of apoptotic and necrotic cells varies in in the tumours with tumour type and the chemotherapeutic agent used. Such variability in tumour responsiveness to these agents is important clinically, as it is as a predictor of both progression-free and overall survival in many forms of cancer

[218, 331, 332]. Ideally, treatment with chemotherapy would induce apoptosis/necrosis in 100% of tumour cells, followed by a controlled clearance of cell debris by phagocytes. However, viable residual masses often remain, partly due to intrinsic chemo-resistive mechanisms of tumour cells and partly to extrinsic factors like the chemoprotective effects of stromal cells/factors [162]. Several clinical studies have investigated cell death in the tumour following chemotherapy. Partially or completely excised residual tumour masses from patients with disseminated non-seminomatous germ-cell tumours and post-chemotherapy surgery were analysed for the percentage of necrotic cells [331]. Analysis of these samples showed that half of the patients had <10% viable cells in residual masses from tumours. However, other studies have found that levels of necrosis following chemotherapy vary greatly; primary tumours surgically resected from patients with hepatoblastoma and treated with neo-adjuvant chemotherapy had levels of necrosis ranging from 5–99%, where 10 of 32 patients had $\geq$90% tumour necrosis, and the median was 70% [218]. Similar studies have investigated the percentage of apoptotic tumour cells following chemotherapy. For example, TUNEL staining of cancer patient biopsies revealed that the percentage of apoptotic cells within a tumour at 24h was between 0.06% and 12%, reaching 37% by 48h [332].

Taken together, these studies show that chemotherapy-treated tumours can vary greatly in their post-therapy viability, and so for the purposes the experiments reported here, a concentration was selected which induced the highest levels of apoptosis and necrosis. A treatment of 10μM docetaxel for 96h was selected, resulting in approximately 60–70% apoptosis and 50% necrosis. Notably, apoptosis was measured using Annexin V, which binds to exposed phosphatidylserine on cell surfaces. As such, Annexin V also binds cells undergoing secondary necrosis as well as apoptosis. In secondary necrosis, otherwise known as type 2 necrosis, a cell undergoing apoptosis activates self-hydrolytic enzymes, but also swells and potentially releases its contents, rather than being engulfed by phagocytes. The value for the percentage of cells undergoing apoptosis (as measured by Annexin V) will also include these cells, leading to an over-representation of the number of cells undergoing apoptosis.

Additionally, these cells will also be counted as necrotic cells based on propidium iodide (PI) viability dye staining.

Time permitting, other methods for analysing apoptosis would also have been used to confirm the above findings with Annexin V. Such apoptotic stains as cleaved caspase 3 or TUNEL staining could have been used. One advantage of the caspase 3 marker would have been that it is activated early in the process of apoptosis [333], and is a key executor of apoptosis in somatic cells. Additionally, the half maximal inhibitory concentration (IC50) of docetaxel on A549 tumour cell growth should also have been calculated, thus allowing for a better understanding of the effectiveness of this drug on these cells in culture.

In monolayer co-cultures, the dead and dying A549 cells (or factors they release) stimulate human macrophages to upregulate transcription of the CXC chemokines CXCL1, CXCL2 and CXCL5. Furthermore, myeloid cells isolated from docetaxel-treated A549 spheroids showed a similar upregulation of mRNA for these CXC molecules compared to those from DMSO-treated spheroids. These data were supported by the finding that CXCL1-release by myeloid cell-infiltrated spheroids was increased following their exposure to docetaxel. Changes in gene expression between macrophages exposed to docetaxel-treated tumour cells for 5 hours, and unconditioned macrophages cultured in IMDM, were analysed for differentially expressed genes (DEGs), i.e. those genes that showed a statistically significant increase or decrease in gene array analysis. Given the importance of macrophage cytokine production in inflammation and cancer [106, 266, 334], differentially expressed cytokines were focussed on. The results from the gene array, as well as later confirmation by RT-PCR, showed a clear upregulation of cytokines CXCL1, CXCL2 and CXCL5 in docetaxel-treated macrophages. These ELR^+ CXC chemokines are expressed by macrophages and are mainly involved in recruitment and activation of neutrophils [93, 335, 336]. All three chemokines are ligands of CXCR2, a receptor expressed by neutrophils and endothelial cells in tumours [337-339], and elevated CXCL1 and CXCL2 levels have been correlated with increased numbers of $CD11b^+Gr1^+$ granulocytic cells in murine metastatic lung (LM2) tumours [126]. Furthermore, CXCL1 directly enhances tumour growth and transformation [340], as well as acting on

endothelial cells to promote angiogenesis [233, 341]. CXCL1 expression by human monocyte-derived macrophages has also been shown previously, in response to exposure to human immunodeficiency virus type 1 (HIV-1) *in vitro* [342], and production of CXCL1 and CXCL2 by tissue macrophages is crucial for neutrophil recruitment into inflamed tissue [93]. Therefore, the upregulation of such ELR^+ CXC chemokines by macrophages during/after chemotherapy may have a significant role in neutrophil recruitment and aspects of tumour promotion. Importantly, CXC chemokines – including CXCL1, CXCL2 – are also expressed highly by tumour cells [126], including A549 lung carcinoma cells [185]. Although gene expression analysis clearly demonstrates that macrophages upregulate CXCL1, CXCL2 and CXCL5, similar analysis of A549 tumour cell expression should also have been done to assess the importance of tumour-derived CXC chemokines in the pre- and post-chemotherapy environment.

Conversely, the microarray used here showed that expression of CCL2, CCL7 and CCL8 were downregulated significantly by macrophages following their exposure to docetaxel-treated A549 cells. These chemokines are ligands of the CCR2 receptor, and individually can bind additional receptors CCR1, CCR3, CCR4, CCR5, decoy and viral receptors [30]. CCR2 is most highly expressed on monocytes/macrophages, and it plays a central role in monocytes/macrophage chemotaxis [13, 30]. The observed downregulation of CCL2, CCL7 and CCL8 by macrophages suggests that they might be less likely to recruit other monocytes into tumours following docetaxel treatment. These results are in opposition to previous findings that undefined stromal cells express more CCL2 following chemotherapy [212]. These stromal cells may not have been macrophages (later findings in **Chapter 4** suggest they may have been neutrophils), and a different type of chemotherapy (doxorubicin) was used. It is also possible that different forms of cytotoxic agent elicit different forms of tumour cell death, and this triggers different patterns of gene expression in macrophages. Some agents may also have direct effects on tumour cells.

Ideally, the microarray analysis would have included more treatment groups, and the expression of macrophages co-cultured with docetaxel-treated tumour cells could have been compared with:

- Macrophages co-cultured with the drug vehicle DMSO to see whether this alone induced changes in expression.
- Macrophages co-cultured with DMSO-treated A549 cells, so that the gene expression profile of macrophages responding to viable A549 cells could be compared with that of macrophages exposed to doxetaxel-treated A549 cells.
- Macrophages co-cultured with docetaxel-treated, non-malignant epithelial cells, to study whether the cross-talk is specifically between macrophages and malignant lung adenocarcinoma cells.

Despite not being included in the microarray, the first two of these experimental groups were included as controls in later RT-PCR experiments, and are discussed below. These data, however, lack a non-malignant cell control that has been used by previous macrophage and tumour cell co-culture experiments [343]. This control group would help identify whether the upregulation of CXCL1, CXCL2 and CXCL5 is specifically in response to docetaxel-treated A549 cells, or whether docetaxel-treated, non-malignant lung epithelial cells also induce this response in macrophages. It would also have been beneficial to use additional malignant cell lines in order to confirm these findings.

To determine the extent to which upregulation of CXCL1, CXCL2 and CXCL5 is mediated by direct physical contact, a transwell co-culture assay was used, and macrophage gene expression analysed by RT-PCR. This also ensured purity of macrophage mRNA, since the two cell types were separated in culture by a 0.3μm pore size nylon mesh. Any genetic material (mRNA/DNA) in the docetaxel-induced A549 cell debris that might have been able to pass through the membrane during co-culture would most likely have been discarded with the removal of media from macrophages after co-culture, such that any tumour cell contamination would be negligible. The results showed a similar (but slightly reduced) induction in cytokines CXCL1 and CXCL2, and a lower induction of CXCL5 than in directly co-cultured macrophages, indicating cell-to-cell contact may play a part in CXCL5 upregulation by macrophages in response to docetaxel-treated tumour cells. Recently, the physical interaction between macrophages and tumour cells has been shown to occur between MDA-MB-231 human breast

cancer cells and murine macrophages, both *in vitro* and *in vivo* [344]. Physical interaction between these two cell types was shown to encourage tumour cell intravasation, an important step in the metastatic cascade, although the molecules responsible for their interaction were not known. Another study, however, identified an interaction between macrophages and breast cancer cells via vascular cell adhesion molecule-1 (VCAM-1) and α4 integrins, which supported tumour cell survival by protecting them from pro-apoptotic cytokines [345]. VCAM-1 expressed on the surface of tumour cells interacted with macrophages via the leukocyte α4 integrins, as demonstrated by the use of an anti-α4 integrin-blocking antibody. This highlights a possible mechanism through which macrophage and tumour cell interactions may occur in the direct co-cultures used here in **Figs 3.3** and **3.5**, which could be investigated in a similar experiment using an anti-α4 integrin-blocking antibody. Physical interaction between macrophages and A549 cells in this way may instigate intracellular signalling in macrophages, contributing to their increased expression of CXCL1, CXCL2 and CXCL5. Importantly, the macrophage response was demonstrated to be specific for docetaxel-treated A549 cells (or dead/dying A549 tumour cells), as exposure of macrophages to docetaxel alone or the co-culture of macrophages with live, non-docetaxel-treated A549 tumour cells failed to induce CXC cytokine gene expression.

A criticism of the experimental technique used here is that RT-PCR samples were run in duplicate (two technical replicates), i.e. two identical repeats were run in two adjacent wells on a RT-PCR plate for each donor, and were used to calculate the relative expression of that particular gene in that particular sample. Instead, the samples should have been run in triplicate, so that three values were obtained per sample/gene combination; this would help to control for pipetting error and provide more accurate results.

The spheroid model offers several advantages over more conventional 2D monolayer or Transwell co-cultures. Spheroids are more representative of a 3D tumour mass (albeit a more simple, non-vascularised one) and generate something of the drug and oxygen diffusion gradients known to exist in tumours [319, 320]. Oxygen consumption and diffusion gradients lead to hypoxic cores,

which are also challenged by reduced nutrient availability. This can lead to altered gene expression, proliferation rate (slower proliferation reduces effectiveness of chemotherapy) and cell death. Drug diffusion gradients also lead to differing drug concentrations through the spheroid, as is the case in patient tumours [43]. In spheroids, myeloid cells were also found to express higher levels of CXCL1, CXCL2 and CXCL5 mRNA following exposure to docetaxel than in DMSO-treated spheroids. If this occurs in human tumours after docetaxel treatment, it could result in the recruitment of increased numbers of neutrophils from the circulation into the tumour residue. This could impact on tumour progression after the conclusion of chemotherapy as tumour-associated neutrophils have been shown to promote tumour growth [185], angiogenesis [346] and metastasis [347]. Of course, this would only be relevant where tumours are inaccessible and cannot be surgically removed – as is the case with some forms of lung tumour [348]**.** Further studies are now warranted to see whether such neutrophil chemoattractants are upregulated by monocytes/macrophages in response to tumour cells treated with docetaxel, or indeed other chemotherapeutic agents.

Given the aforementioned benefits of the tumour spheroid model, it would have been interesting to conduct arrays not only from macrophages in monolayers but also from myeloid cells isolated from docetaxel- and DMSO-treated spheroids. The DEGs in these may have been different if myeloid cells had been exposed to docetaxel-treated A549 cells in such a 3D microenvironment as a tumour spheroid. Monocytes and macrophages are capable of forming strong attachments to other cells, including tumour cells and other monocytes/macrophages; thus a potential criticism of the spheroid model used here is that when the spheroids were washed (to remove uninfiltrated myeloid cells) it is possible that not all of the cells were successfully removed. Light microscopy confirmed that the majority of uninfiltrated myeloid cells were removed (80–95%), but confocal microscopy could be used to identify whether all uninfiltrated myeloid cells were washed off, since the myeloid cells were labelled with a CellTracker dye and could be distinguished from A549 cells in this way. Additionally, an investigation of A549 cell death (similar to **Fig 3.1**)

should have been done using docetaxel-treated spheroids to observe the number of apoptotic and necrotic cells at various time-points, particularly since drug diffusion gradients are affected by the 3D shape and cell replication is reduced in hypoxic core regions (making chemotherapy less effective).

In this experiment (and when conditioned media were generated and used in **Chapter 4**), monocytes and docetaxel were added simultaneously to A549 spheroids. This could be seen as modelling a subset of monocytes that infiltrate tumours at the time the patient is being treated with chemotherapy. These would differentiate into TAMs as tumour cells are responding to docetaxel. However, as mentioned in **section 2.2.4.2**, further studies could use an adapted version of such *in vitro* spheroid assays to also investigate: (i) the response of existing TAMs in tumours to docetaxel treatment, or (ii) the response of newly infiltrating monocytes to tumour cells recently exposed to the cytotoxic agent. This could be done by simply adding monocytes to A549 spheroids first before the latter were exposed to docetaxel, or by adding the docetaxel to spheroids first before the monocytes were allowed to infiltrate them. It is possible that monocytes/macrophages in these two scenarios may have responded differently to monocytes infiltrating spheroids while both were exposed to docetaxel (**Fig 3.5**). Therefore, ideally all three scenarios would have been applied in the spheroid model, as suggested in **section 2.2.4.2**. It is possible that docetaxel treatment increased monocyte infiltration into docetaxel-treated spheroids, as compared with DMSO, and that the increased presence of infiltrated myeloid cells in spheroids had an effect on myeloid cell expression in **Fig 3.5** and conditioned media used in **Chapter 4**. However, this is unlikely since a FACS experiment suggested that there were similar numbers of myeloid cells present in tumour spheroids treated with docetaxel and DMSO (**Table 3.1**).

The supernatants conditioned by the various tumour spheroid groups shown in **Fig 3.4** were used in a CXCL1 ELISA, to check whether upregulation of CXCL1 occurs at the protein level. Since spheroids were grown in 96-well plates in small volumes of media, protein concentrations were relatively high. Conditioned media from tumour spheroids alone contained CXCL1 protein at a

Sample	No. infiltrated monocytes
DMSO-treated spheroids	965,806
Docetaxel-treated spheroids	963,490

Table 3.1 Monocyte infiltration into A549 spheroid treated with docetaxel or DMSO. Analysis of the number of CellTracker labelled monocytes that had infiltrated into A549 spheroids either treated with docetaxel or its vehicle DMSO, showed that docetaxel/DMSO treatment may have little effect on monocyte infiltration (0.24% increase in monocyte infiltration in DMSO-treated spheroids). However, these data are from one experiment and so further confirmation is necessary before any conclusions can be made. This could potentially involve an experiment where both monocytes and neutrophils are added to A549 spheroids, and treated with docetaxel or DMSO, as suggested in **section 4.5**. Data show the number of viable, labelled monocytes that had infiltrated into a total of 120 spheroids for each sample, as analysed by FACS.

concentration of approximately 1μg/mL. Tumour cells have been shown previously to upregulate immunodetectable CXCL1 upon exposure to some forms of chemotherapeutic agent, such as combined doxorubicin and cyclophosphamide (DOX/CTX) chemotherapy in mammary MMTV-PyMT tumours [126]. However, **Fig 3.5** shows that tumour spheroids did not upregulate CXCL1 in response to docetaxel in the absence of myeloid cells. The reason for this difference could be because the mechanism of CXCL1 upregulation by tumours cells reported for DOX/CTX was via endothelial cell-derived TNFα [126], whereas the spheroid model used here does not include endothelial cells. Another reason could be the differences in chemotherapy. Their mechanism of action is very different, since docetaxel inhibits microtubule dynamics, whereas doxorubicin intercalates into DNA and disrupts transcription and cyclophosphamide crosslinks DNA strands irreversibly.

Importantly, several cell types are known to be capable of expressing CXC chemokines in human tumours; aside from monocytes/macrophages, CXCL1 can also be expressed by mast cells [349], tumour cells [126, 232], neutrophils [350],

eosinophils [351] and endothelial cells [350]. The presence of myeloid cells in tumour spheroids led to an increase in CXCL1 protein release into conditioned media, and this was upregulated further in the presence of docetaxel. Infiltration into a 3D tumour mass could increase CXCL1 expression by macrophages. Previous RT-PCR analysis showed that CXCL1 was upregulated approximately 85-fold in Transwell co-cultures, but approximately 150-fold in direct co-cultures, demonstrating that cell-to-cell contact enhances the upregulation of CXCL1 by macrophages. Myeloid cells infiltrated into A549 spheroids also physically interact with tumour cells. The fact that CXC chemokines were still upregulated by 4- to 7-fold in myeloid cells from docetaxel-treated spheroids after longer co-culture time (48 hours as opposed to 5 hours co-cultures used previously) suggests that this might be a sustained response of monocytes/macrophages in docetaxel-treated lung tumours. It would be interesting to observe later time-points, such as 72 hours and 96 hours, to see whether myeloid cells were still viable and expressing higher levels of CXC chemokines in docetaxel-treated A549 spheroids.

Given that monocytes/macrophages were seen to increase their CXCL1, CXCL2 and CXCL5 mRNA levels substantially in both a Transwell system and in spheroids – and that tumour spheroids alone do not produce as much CXCL1 protein as when myeloid cells are also present – it follows that CXCL1 protein present in the conditioned media from myeloid cell-infiltrated spheroids is predominantly released by myeloid cells. However, it is possible that tumour cells become a major source of CXCL1 only after co-culture with myeloid cells, and so as an additional experiment, myeloid cells from the spheroid co-culture model could be isolated and conditioned media generated from myeloid cells alone (no tumour cells) for ELISA analysis of CXC chemokines. Likewise, tumour cells could also be collected and used to generate conditioned media, and the relative contributions of both tumour cells and myeloid cells could be assessed.

Interestingly, signalling via Toll-like receptors like TLR2, TLR3 and TLR4 has been shown to control macrophage expression of CXCL1 and CXCL2 mRNA [92]. For example, TLR4 signalling can increase CXC expression via MyD88-dependent or TRIF-dependent signalling pathways and increase neutrophil

recruitment [92]. Since TLR4 is known to bind damage-associated molecular patterns, or DAMPS, which derive from stressed or injured tissues, monocyte/macrophage TLR4 signalling could be involved in the upregulation seen here for CXCLs 1, 2 and/or 5 after docetaxel treatment. Further studies could explore this by investigating the ability of macrophages to upregulate these CXC chemokines in response to docetaxel-treated tumour cells in the presence of such TLR4 antagonists as presented by Eritoran [352]. If inhibition of TLR4 blocked macrophage CXC chemokine induction, this would suggest that DAMPs and/or other TLR4 ligands released by tumour cells after chemotherapy could bind TLR4 and are responsible for macrophage chemokine expression. Should this be the case, it would add further evidence for the importance of macrophage TLR4 signalling in the chemotherapy-treated tumour environment. As discussed previously (see **section 1.5**), neutrophils are usually the first responders to the inflammatory signals that can be released by endothelial cells or resident tissue macrophages at the inflammatory site. The data in this chapter suggest that TAMs resident in the tumour, or monocytes infiltrating the tumour, may respond to docetaxel-induced changes in A549 cells, in part by recruiting neutrophils. This is in accordance with the understanding that resident macrophages directly control the synthesis of neutrophil-attracting chemokines in response to bacterial infection, which are crucial for the earliest recruitment step in initiating an innate immune response to microbial challenge [92].

Had time permitted, it would have been interesting to look into other highly expressed DEGs from the same arrays. For example, the alpha and gamma chains of fibrinogen were within the top 20 upregulated genes following chemotherapy, shown in **Supplementary Table 1**, increasing approximately 25-fold in comparison with macrophages from non-chemotherapy-treated spheroids. Fibrinogen is classically known for its importance in the coagulation cascade, responsible for regulating blood clotting at sites of injury. However, it has more recently been suggested also to play a role in metastasis via the coating and protection of tumour cells in the circulation [353], and inhibition of coagulation has been shown to limit metastasis. It is thought that this 'cloaking' of metastasising tumour cells may protect them from the effects of NK cells and

other cytotoxic cells, and it would be interesting to see if this is another chemotherapy-enhanced and macrophage-dependent process. Additionally upregulated in the top 20 genes was SERPINE2, a potent serine protease inhibitor and regulator of blood coagulation, indicating that a controlled set of coagulation genes is being modulated here in macrophages. Given more time, it would be interesting to identify the mechanism behind coagulation-related gene expression specifically after chemotherapy, since tumour cells [354] and stromal cells, including macrophages [355], are already known to play a role in coagulation-assisted metastasis. The connections between metastasis and coagulation are being increasingly recognised and may prove to become an important area of study [356].

In conclusion, the findings from this chapter show that monocytes and macrophages exposed to docetaxel-treated A549 human lung tumour cells increase the expression of CXCL1, CXCL2 and CXCL5 at the transcription level, both in monolayer (macrophage) and spheroid-based (monocyte) co-culture systems. Ideally, key experiments would have been confirmed using a second human non-small cell lung cancer cell line, such as Calu-3 or H157 cell lines, to identify whether the upregulation of CXC chemokines by macrophages is just a response to docetaxel-treated A549 cells, or whether it is a more general phenomenon. The findings in **Figs 3.3, 3.4** and **3.6** showed that this is not just a response to DMSO-treated (viable) A549 cells, but instead is induced by the presence of docetaxel. Conditioned media from tumour spheroids and myeloid cells contains CXCL1 protein, which was increased in conditioned media collected from spheroids exposed to docetaxel, rather than its vehicle DMSO. The fact that the concentration of CXCL1 is much lower in conditioned media from tumour spheroids alone, together with the transcription expression results, suggests that myeloid cells may be the dominant source of CXC chemokines in this context. Therefore, in patients with non-small cell lung cancer, treatment with docetaxel may lead to the expression of CXC chemokines by TAMs or monocytes infiltrating into the tumour. This could then lead to the recruitment of neutrophils and impact on tumour responses to subsequent rounds of chemotherapy and/or tumour regrowth after the cessation of chemotherapy.

This is investigated further in the *in vitro* experiments that will be described in **Chapter 4**.

CHAPTER 4: MYELOID CELLS IN SPHEROIDS RECRUIT AND STIMULATE A PRO-INVASIVE PHENOTYPE IN NEUTROPHILS AFTER EXPOSURE TO DOCETAXEL: ROLE OF TNF ALPHA

4.1 INTRODUCTION

Neutrophils are generally believed to be the first innate effectors to infiltrate sites from the circulation during initial stages of infection and inflammation. However, there is now evidence that show resident macrophages at such sites play an important role in mediating this [93]. The chemokines, CXCL1 and CXCL2, control the initial stages of neutrophil recruitment during acute inflammation – first secreted by mast cells in close proximity to vasculature, then shifting towards macrophage production as they infiltrate further into the tissue [92, 93]. Both of these chemokines signal through the CXCR2 receptor, which is expressed highly on neutrophils [16, 126, 357]. Other producer cells include epithelial cells [358] and neutrophils themselves [294]. As mentioned previously (see **section 1.2.1**), other chemokines, including CXCL8 (IL-8) [18], TNFα, leukotriene B4 (LTB4) and complement 5a (C5a) [19] have also been shown to recruit neutrophils during inflammation, and CXCL8 signals through both CXCR2 and CXCR1 receptors [243]. Although CXCR1 and CXCR2 are both very highly expressed on neutrophils, they are also present on monocytes/macrophages and endothelial cells [222], and one or both of the receptors are present on cytokine-activated dendritic cells [223], basophils, T lymphocytes, NK cells [224], mast cells [225], and on some non-immune cells [226].

Interestingly, high levels of circulating neutrophils are associated with poor prognosis in several types of human cancer, including metastatic melanoma [359], bronchoalveolar carcinoma [360] and renal carcinoma [361], suggesting that neutrophils do not always exhibit anti-tumour functions to kill tumour cells. Murine neutrophils have been shown to be capable of expressing the polarized activation states, N1 and N2, in tumours [146], as summarised in **Fig 4.1**.

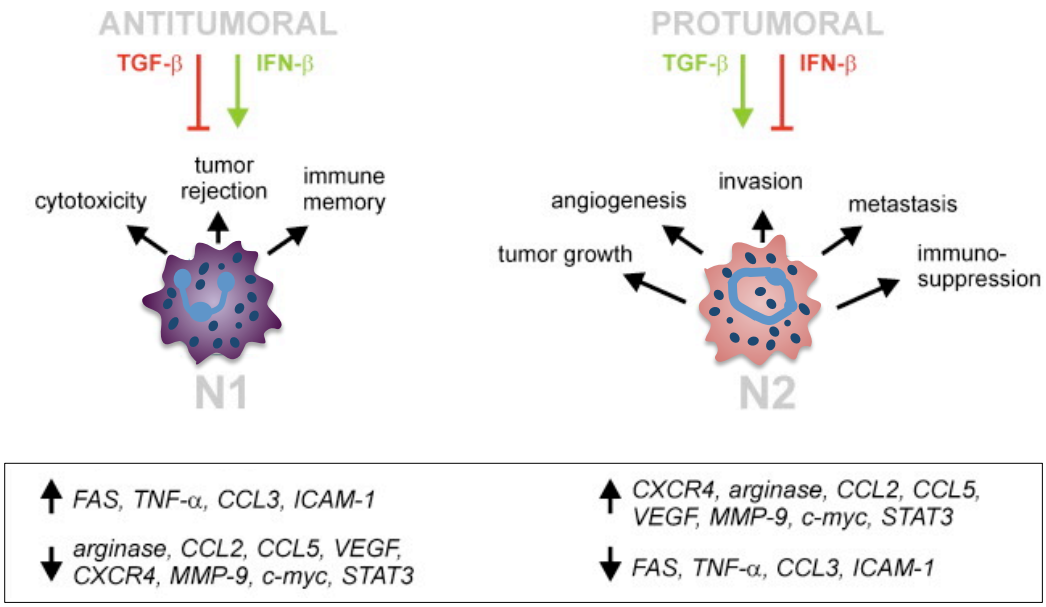

Figure 4.1 N1 and N2 polarisation of tumour-associated neutrophils (TANs) in mice. TGF-β and IFN-β in the tumour environment can stimulate N1 and N2 phenotypes in neutrophils. N1 neutrophils are associated with tumour cell cytotoxicity, the rejection of tumours and immune memory, and with upregulation of FAS, TNFα, CCL3 and ICAM-1 mRNA. Conversely, N2 neutrophils can promote several aspects of tumour progression, including tumour growth, angiogenesis, invasion, metastasis and immunosuppression, and upregulate expression of CXCR4, arginase, CCL2, CCL5, VEGF, MMP9, c-myc and STAT3 mRNA. Image adapted from [289].

N1 tumour-associated neutrophils (TANs) are cytotoxic for tumour cells and can also promote tumour rejection by activating $CD8^+$ cytotoxic T cells, under the stimulation of IFN-β in the tumour [362]. Alternatively, N2 TANs, promote tumour cell invasion and metastasis, stimulated by such tumour-derived cytokines as TGF-β [146, 295].

Neutrophils are a known source of TNFα in tissues, including tumours [146]. Other TNFα-expressing cells in the tumour include macrophages, lymphocytes [266], tumour cells [272, 363], mast cells [93] and endothelial cells [126, 364]. As mentioned previously (see **section 1.10**), TNFα is a key pro-inflammatory cytokine that signals through two distinct receptors, TNFRI and TNFRII. Signalling via these receptors, this multifunctional molecule can mediate the expression of cytokines, growth factors, proteases, genes involved in cell cycle and immune cell receptors [365, 366]. The most important physiological functions of TNFα relate to its regulation of such processes as inflammation,

apoptosis, and angiogenesis: TNFα can facilitate neutrophil chemoattraction [367]; adhesion of leukocytes to endothelial cells in regions of inflammation [368] (see **section 1.6.2**); regulate coagulation during inflammation [369]; facilitate the production of reactive oxygen species by immune cells and endothelial cells [279]; regulate cell death by apoptosis (including virally infected host cells) [370]; stimulate angiogenesis [371, 372].

Furthermore, TNFα plays a complex role in tumour onset. It contributes towards DNA damage by inducing oxidative stress and nucleotide damage [278]. It also promotes tumour growth and supports a metastatic tumour cell phenotype. For example, when Chinese hamster ovary cells were transfected with the human TNFα gene and implanted into nude mice, they showed an increased ability to invade peritoneal surfaces and metastasise, compared to cells transfected with a control vector [373]. This could be blocked by inhibition of TNFα with a neutralising antibody, showing the importance of TNFα in these processes. Similarly, TNFα also induces epithelial-mesenchymal transition (EMT), an indicator of an invasive phenotype, in colon cancer spheroids [280]. Activated macrophages are known to express TNFα in tumours, which accelerate TGF-β-induced EMT in tumour cells (see **section 1.10**).

4.2 AIMS

The *in vitro* results discussed in **Chapter 3** suggest that monocytes/macrophages upregulate ELR^+ CXC chemokines CXCL1, CXCL2 and CXCL5 when they come into contact with docetaxel-treated tumour cells. The aim of the work in this chapter was to investigate what effects this might have on neutrophil chemotaxis and gene expression.

4.3 METHODS

In summary, in this chapter an *in vitro* cell migration assay was used to investigate whether media conditioned by myeloid cell-infiltrated A549 spheroids, following exposure to docetaxel or its vehicle DMSO, was chemotactic towards freshly-isolated human neutrophils. This assay was then used to study whether this was dependent upon CXCR2 ligands by inhibiting neutrophil CXCR2

signalling. To examine gene expression by neutrophils (i.e. their N1/N2 polarization state), they were exposed to medium conditioned by A549 spheroid and myeloid cells, in the presence/absence of docetaxel, and expression of N1 and N2 genes [295] analysed by RT-PCR. Finally, the ability of factors secreted by neutrophils after their exposure to docetaxel-treated tumour cells to stimulate tumour invasiveness was investigated using an *in vitro* invasion assay. Monocytes and neutrophils were freshly-isolated from human Buffy coats or freshly-sampled human peripheral blood, respectively (see **sections 2.2.1.3** and **2.2.1.5**), and subsequently cultured in IMDM supplemented with 10% human serum and 2mM L-Glutamine.

To make A549 (human lung adenocarcinoma) spheroids, 100µL of a 1.5% agarose solution (in DMEM without serum or L-Glutamine) was added to each well of a flat-bottomed 96-well plate using a multichannel pipette. After allowing agarose solution to set at room temperature, 1.5 x 10^4 A549 cells were added to each well in IMDM (with 10% human serum and 2mM L-Glutamine) in a volume of 200µL. The cells were then kept at 37^{o}C and monitored for the formation of spheroids and a necrotic core. Half of the medium was removed and replaced with fresh medium every 2-3 days. Tumour spheroids were expanded in culture for 8-12 days, at which point they had developed a necrotic core that was visible when using a 10x bright field microscope. One x 10^5 freshly-isolated peripheral blood monocytes labelled with CellTracker Green (according to the manufacturer's instructions and detailed in brief in **section 2.2.10.1**) were added to each spheroid. At the same time, some groups received docetaxel at a final concentration of 10µM in each well or an equivalent volume of its vehicle DMSO. Monocytes were allowed to infiltrate and differentiate for 48 hours, after which spheroids and media were collected using a P1000 pipette with a cut tip and placed in 15mL centrifuge tube. Throughout the process tubes were kept cool on ice. Once spheroids had settled to the bottom of the tube, all of the conditioned media was removed and collected in a new 15mL centrifuge tube. Any remaining cells were removed by centrifugation at 500 x *g* for 10 minutes and filtration through a 0.22µm pore size syringe filter.

Neutrophil migration towards media conditioned by myeloid cell-infiltrated A549 spheroids, in the presence of docetaxel or its DMSO control, was assessed using a migration assay (as described in **section 2.2.9.1**). One x 10^5 fresh neutrophils in 500µL IMDM without human serum were placed in the upper chamber of a 24-well Transwell plate, with a pore size of 3µm. At the same time 400µL of conditioned media generated from myeloid cell-infiltrated tumour spheroids treated with docetaxel or DMSO, were diluted 1 in 5 and added to the lower chamber. All conditioned media had been previously filtered through a 0.22µm pore size syringe filter to ensure no cells were present in the media before use in the assay. The Transwell plates were then incubated at 37°C for 3 hours to allow neutrophil migration across the filters. The number of viable (trypan blue negative) neutrophils that had migrated into the media in the lower chamber was then counted using C-Chip disposable hemocytometers (Neubauer Improved).

The above experiment was then repeated with neutrophils that had been pre-incubated for 30 minutes at 37°C with either a CXCR2-blocking antibody (used at a concentration of 1.5 µg/mL) or an IgG isotype-matched control antibody at the same concentration. Neutrophils were then washed to remove excess, un-bound antibodies. Finally, the experiment was repeated again using an antibody to neutralise soluble TNFα in the conditioned media. An anti-human TNFα antibody, or IgG isotype-matched control, were added to conditioned media at a concentration of 1µg/mL for 30 minutes at 37°C immediately before use in assays. For a list of antibodies, see **section 2.1.3**.

To study the response of neutrophils to media conditioned by tumour spheroids, freshly-isolated neutrophils were cultured for 16 hours in conditioned media and then collected for RNA isolation. Neutrophil viability was found to be between 86-97% by trypan blue staining following 16-hour culture in IMDM (with human serum and L-Glutamine) (**Table 4.1**).

Neutrophil total messenger RNA was isolated using an RNeasy Mini Kit, followed by reverse transcription to cDNA using TaqMan Reverse Transcription Reagents and SYBR green-based real-time (RT)-PCR (see **section 2.2.5**). Genes

	Donor 1	Donor 2	Donor 3	Donor 4	Donor 5
Percentage viable neutrophils	92	97	86	92	87

Table 4.1 Percentage viability of neutrophils following 16 hour culture in conditioned media. Neutrophils were freshly isolated from healthy donors before culture in IMDM for 16 hours. Neutrophil viability, as measured by trypan blue staining, was between 86-97%.

were selected based on their reported expression by neutrophils of N1/N2 polarisation [146, 294, 295] (**Fig 4.1**), to identify whether neutrophils in these *in vitro* studies were N1 or N2 polarised. The following primers were used for RT-PCR:

Primer	**Sequence**	
	Forward	Reverse
CCL2	5'-CAGCCAGATGCAATCAATGCC-3'	5'-TGGAATCCTGAACCCACTTCT-3'
CCL3	5'-AGTTCTCTGCATCACTTGCTG-3'	5'-CGGCTTCGCTTGGTTAGGAA-3'
CXCR4	5'-ACTACACCGAGGAAATGGGCT-3'	5'-CCCACAATGCCAGTTAAGAAGA-3'
FAS	5'-TCTGGTTCTTACGTCTGTTGC-3'	5'-CTGTGCAGTCCCTAGCTTTCC-3'
HGF	5'-GCTATCGGGGTAAAGACCTACA-3'	5'-CGTAGCGTACCTCTGGATTGC-3'
ICAM-1	5'-ATGCCCAGACATCTGTGTCC-3'	5'-GGGGTCTCTATGCCCAACAA-3'
MMP9	5'-TGTACCGCTATGGTTACACTCG-3'	5'-GGCAGGGACAGTTGCTTCT-3'
STAT3	5'-CAGCAGCTTGACACACGGTA-3'	5'-AAACACCAAAGTGGCATGTGA-3'
TNFα	5'-GGAGAAGGGTGACCGACTCA-3'	5'-CTGCCCAGACTCGGCAA-3'
TGF-β	5'-GGCCAGATCCTGTCCAAGC-3'	5'-GTGGGTTTCCACCATTAGCAC-3'
VEGF	5'-AGGGCAGAATCATCACGAAGT-3'	5'-AGGGTCTCGATTGGATGGCA-3'

Conditioned media were collected from cultures of A549 spheroids and myeloid cells, as well as neutrophils, according to **Fig 4.2**. Only the media (and soluble factors) were collected - contaminating cells or debris were removed by filtering them through a 0.22µm pore size syringe filter. For the *in vitro* invasion assay (see **section 2.2.9.2**), Matrigel was diluted 1:4 with phosphate buffered saline (PBS), and 100µL pipetted into the insert of an 8µm pore size, 24-well Transwell plate. After leaving for 2 hours at 37°C to allow the Matrigel to polymerise and form a gel, PBS was removed and the plate was air dried for 30 minutes. Conditioned media were filtered to remove any cells/debris and were diluted 1:4. Subsequently, 400µL was pipetted into the lower chamber of the

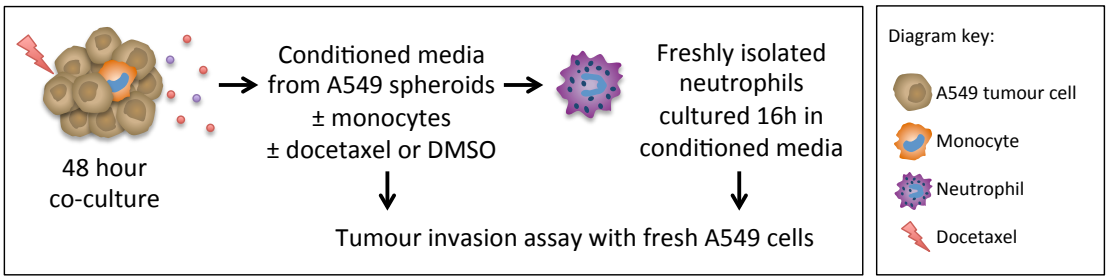

Figure 4.2 Collection of conditioned media from A549 spheroids, monocytes and neutrophils. The conditioned media were collected from A549 spheroids following the addition of monocytes for 48 hours to allow their infiltration. Docetaxel, or its vehicle DMSO were also added simultaneously. In later experiments this conditioned media from monocyte-infiltrated A549 spheroids were then used for 16-hour culture with neutrophils, before collecting the conditioned media again, this time with added neutrophil-derived factors. For some experiments, neutrophils were pre-incubated with an anti-CXCR2 antibody to block CXCR2 signalling prior to, and during, the 16-hour culture.

Transwell plate, before carefully adding 3 x 10^5 A549 cells in 500µL serum-free DMEM to the upper chamber on top of the Matrigel layer. The Transwell plate was kept at 37°C for 18 hours to allow tumour cells to invade through the Matrigel. Following this, media were removed from both the insert and the lower well, and a cotton bud used to scrape the surface of the Matrigel gently but thoroughly to remove any non-infiltrated tumour cells. The upper chamber Transwell inserts, which contained the infiltrated tumour cells on the *lower* surface of the 8µm pore size membrane, were placed into a new plate with 750µL ice-cold MeOH for 5 minutes to fix the invaded tumour cells, before aspirating and air drying. To stain the cells, Transwell inserts were placed in 750µL 0.1% crystal violet solution for 20 minutes, and then washed 3 times for 2 minutes with PBS. The stained cells were then lysed in 500µL acetic acid for 5 minutes, and 100µL of this solution was then added into each well of a 96-well plate for absorbance measurement at 595nm in triplicate. Control groups received an equal amount of DMSO vehicle (i.e. to the amount present in the volume of docetaxel added).

Additionally, key experiments were repeated with a second chemotherapeutic, cyclophosphamide. Cyclophosphamide is a pro-drug that is hydroxylated *in vivo* by cytochrome P450 enzymes in the liver [374]. Therefore, in these *in vitro* experiments in **Chapter 4**, cyclophosphamide was used in its active form 4-hydroxy cyclophosphamide (Santa Cruz Biotechnology). Cell death

induction by 4-hydroxy cyclophosphamide (referred to in **chapter 4** as cyclophosphamide) was determined previously by members of our research group, shown in **Fig 4.3**. A concentration of 100μM for 24 hours was used to induce cell death in A549 cells (or DMSO vehicle control), which were then co-cultured with MDMs for 5 hours to induce gene expression, as done previously using docetaxel. Similarly, A549 spheroids were grown and freshly-isolated monocytes were added for 48 hours to infiltrate. At the same time, cyclophosphamide was added at 100μM for 48 hours, or an equivalent of the vehicle DMSO, and conditioned media were collected as before. Freshly-isolated neutrophils were then cultured in this cyclophosphamide-induced conditioned media for 16 hours and the conditioned media collected again (see **Fig 4.2**). Using the same experimental setup as detailed previously with docetaxel, A549 cell invasiveness was determined using an invasion assay with this cyclophosphamide-induced conditioned media, and the dependency on TNFα was investigated using an anti-TNFα neutralising antibody.

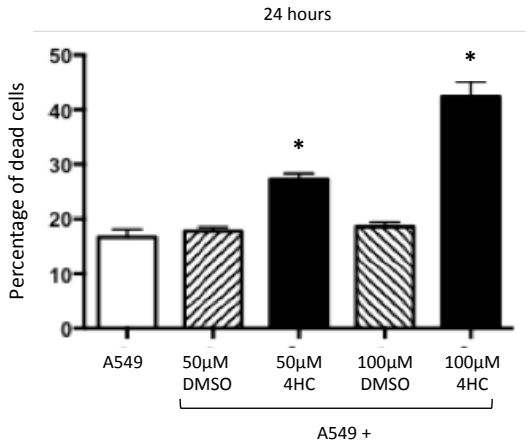

Figure 4.3 Induction of cell death by 4-hydroxy cyclophosphamide. Cell death induced in A549 human non-small cell lung carcinoma cells by 4-hydroxy cyclophosphamide (active product of cyclophosphamide), as measured by propidium iodide staining using a flow cytometer. One-hundred μM cyclophosphamide for 24 hours induces approximately 45% cell death. 4HC, 4-hydroxy cyclophosphamide; DMSO, dimethyl sulphoxide. Pooled data from 3 identical experiments are shown, * $p < 0.05$ w.r.t. A549 cells treated with DMSO. Data collected by Jonathan Borland and Jade Hawson.

4.4 RESULTS

4.4.1 CONDITIONED MEDIUM FROM TUMOUR SPHEROIDS AND MYELOID CELLS IS CHEMOTACTIC FOR NEUTROPHILS

As shown in **Chapter 3**, monocytes/macrophages increase their expression of neutrophil chemokines CXCL1, CXCL2 and CXCL5 at mRNA level upon culture with docetaxel-treated A549 cells. This suggests that macrophages may help to recruit neutrophils into lung tumours following treatment with docetaxel. In this chapter, monocytes were added to tumour spheroids and co-cultured for 48 hours to allow monocyte infiltration and differentiation into monocyte-derived macrophages. At the same time, docetaxel was added to chemotherapy groups at a concentration of 10μM. Conditioned media from myeloid cell-infiltrated and non-infiltrated tumour spheroids, after exposure to docetaxel or DMSO, were assessed for their ability to cause the migration of human neutrophils (**Fig 4.4**).

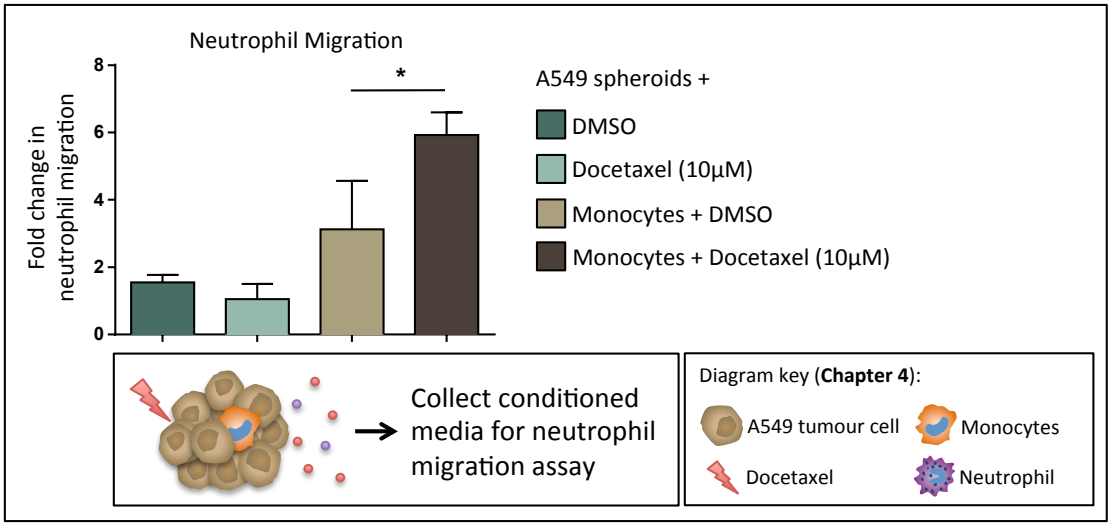

Figure 4.4 Release of neutrophil chemoattractants by A549 spheroids *in vitro*: effect of exposure to docetaxel (or its vehicle DMSO) in the presence or absence of infiltrating monocytes. Media conditioned by non-myeloid cell-infiltrated spheroids, whether exposed to docetaxel or its vehicle DMSO, did not induce neutrophil chemotaxis. Similarly, no induction of neutrophil chemotaxis was seen with media from monocyte–infiltrated spheroids exposed to DMSO alone. Media conditioned by myeloid cell-infiltrated spheroids treated with docetaxel, however, induced neutrophil chemotaxis. The mean ± SEM from 4 identical experiments are shown. Data are expressed as fold change in neutrophil migration w.r.t. unconditioned medium, Mann-Whitney U test, * $p < 0.05$.

Co-culture of spheroids with myeloid cells led to slight, non-significant increase in neutrophil migration. However, the highest neutrophil migration was observed with the conditioned media from myeloid cell-infiltrated tumour spheroids exposed to docetaxel, showing approximately 6-fold induction of neutrophil chemotaxis above unconditioned media, and an increase above spheroids co-incubated with myeloid cells and DMSO. It should be noted that such increases in neutrophil migration could also simply be due to increased neutrophil mobility, rather than their migration along a chemoattractant gradient emanating from the conditioned media. The possibility, therefore, exists that neutrophils may simply be induced to be more mobile, and so more of them would cross the membrane into the lower Transwell chamber.

To test whether the above movement of neutrophils was dependent upon CXCR2 ligands (such as CXCL1, CXCL2 and CXCL5) an anti-CXCR2 blocking antibody was used. Untreated neutrophils, or neutrophils treated with anti-CXCR2 antibody or isotype control, were used in a migration assay using conditioned media from myeloid cell-infiltrated, docetaxel-treated spheroids. The results shown in **Fig 4.5** suggest that although the migration-promoting factors released by macrophages in docetaxel-treated spheroids appear to work mainly via CXCR2, this was not the only signalling pathway involved. There was still a doubling of neutrophil migration in the presence of the CXCR2 antibody.

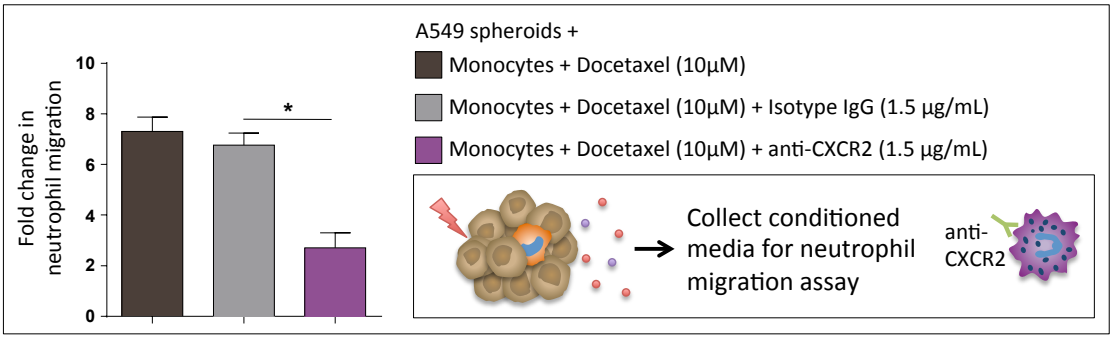

Figure 4.5 Neutrophil migration induced by docetaxel-treated, myeloid cell-infiltrated spheroids *in vitro* is markedly reduced by addition of a specific CXCR2-neutralising antibody. Neutrophils were treated with the anti-CXCR2-blocking antibody or isotype control, prior to being used in a migration assay. Addition of an isotype-matched control had no effect on neutrophil migration. The mean ± SEM from 4 identical experiments are shown. Data are expressed as fold change in neutrophil migration w.r.t. fresh, unconditioned medium, Mann-Whitney U test, * $p < 0.05$.

Alternatively, the dose of the antibody used may not have been sufficient to block completely the binding of ligands to this receptor on neutrophils.

4.4.2 Effect of factors released by myeloid cell-infiltrated A549 spheroids on mRNA levels of N1 and N2 genes in neutrophils *in vitro*.

To investigate the possible phenotype of neutrophils recruited into docetaxel-treated tumours, mRNA levels for various N1 and N2 genes were assessed by real-time PCR, as described in **Fig 4.1** [295]. The gene expression profile is shown in **Fig 4.6**. In general, neutrophils exposed to conditioned media both in the presence and absence of docetaxel expressed a mixed profile of N1 and N2 gene mRNAs. However, the levels of TNFα, CCL2, and CCL3 mRNA were markedly increased in both groups. Additionally, STAT3 and TGF-β were significantly upregulated ($p < 0.05$) by neutrophils cultured in docetaxel-containing conditioned media, by comparison with medium conditioned by DMSO-treated A549 spheroids.

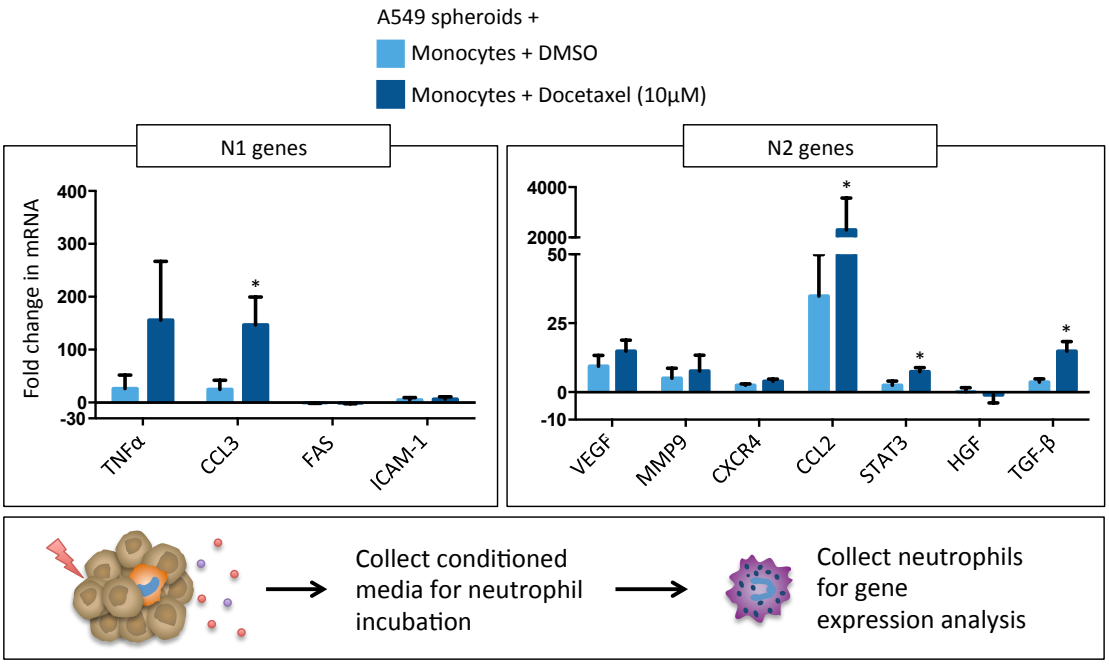

Figure 4.6 Effect of spheroid-conditioned media on mRNA levels for N1 and N2 genes in neutrophils *in vitro*. Neutrophils exhibit neither an N1 nor N2 phenotype. The mean ± SEM from 3 identical experiments are shown. Data are expressed as fold change in neutrophil gene expression w.r.t. neutrophils cultured in spheroid-unconditioned medium containing DMSO, Mann-Whitney U test, * $p < 0.05$.

4.4.3 FUNCTIONAL ASSAYS

4.4.3.1 INVASION ASSAY

Previously, TNFα has been implicated in the process of tumour invasion. As mentioned in **section 1.10.1**, macrophage-derived TNFα was shown to enhance epithelial-to-mesenchymal cell transition (EMT) in colon cancer spheroids [280], which is associated with a more invasive phenotype. Additionally, intraperitoneal injection of mice with TNFα enhanced the number of lung metastases when the mice were subsequently injected with murine fibrosarcoma cells [285] (**Table 4.2**). Although a marked trend towards increased TNFα gene expression by neutrophils exposed to docetaxel-treated, myeloid cell-infiltrated A549 spheroids (compared to those exposed to DMSO alone), this failed to reach significance due to the high variability within these groups (**Fig 4.6**). As TNFα is known to stimulate the invasiveness of tumour cells *in vitro* [375], it was decided to investigate the potential of media conditioned by such neutrophils in an *in vitro* assay of A549 invasiveness. Had time permitted, it would also have been good to use a number of other tumour cell lines in such invasion assays.

Conditioned media from these cells were added to an *in vitro* tumour cell invasion assay in which A549 cells invade through a layer of Matrigel in a Transwell system (**Fig 4.7**). Conditioned media from myeloid cell-infiltrated A549 spheroids induced tumour cell invasion approximately 2-fold above the control, which has fresh unconditioned media (IMDM) in the lower well. However, when factors released by neutrophils are included, to model the recruitment of neutrophils to docetaxel-treated tumours, pro-invasive factors dominate and induce a significant ($p = 0.0198$) increase in tumour cell invasion.

Since CXC chemokines not only chemoattract neutrophils but also modulate and active them [235, 376], it is possible that CXCL1, CXCL2 and CXCL5 released by macrophages in a docetaxel-treated tumour environment may also be responsible for neutrophil promotion of invasion. As shown in **Fig 4.8**, the exposure of neutrophils to a neutralising anti-CXCR2 antibody showed that blocking CXCR2 signalling markedly reduced their ability to promote tumour cell

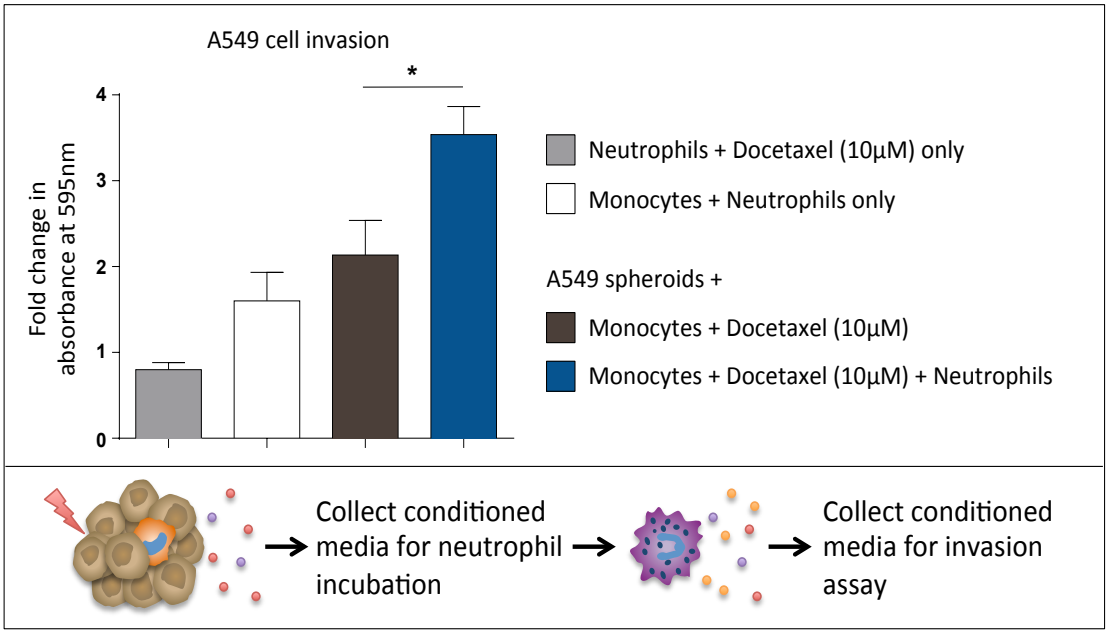

Figure 4.7 Release of pro-invasive factors by neutrophils. Conditioned media from myeloid cell-infiltrated A549 spheroids, treated with docetaxel or DMSO control, induce significantly more A549 tumour invasion when neutrophil-derived factors are included. The mean ± SEM from 4 identical experiments or 12 identical experiments (A549 spheroids + monocytes + Docetaxel + Neutrophils) are shown. Data are expressed as fold change in tumour cell invasion w.r.t. fresh, unconditioned medium, Mann-Whitney U test, * $p < 0.05$.

invasion in response to spheroid-conditioned medium tumour cell invasion. This suggests that either CXCR2 ligands released by myeloid cells in docetaxel-treated spheroids trigger this in neutrophils, or that CXCR2 ligands are required for neutrophil survival, and blocking these leads to neutrophil death. Therefore, lower amounts of pro-invasive factors are present in the conditioned media. Such CXCR2 ligands could include CXCL1, CXCL2 and CXCL5 released by myeloid cells as suggested by **Chapter 3**, but could also be A549 cell-, myeloid cell- or neutrophil-derived CXCR2 ligands CXCL1, 2, 3, 5, 6, 7 and/or 8 [30].

4.4.4 Neutrophils enhance tumour invasion through expression of TNFα

Given that TNFα mRNA was upregulated by neutrophils following exposure to conditioned media from myeloid cell-infiltrated spheroids treated with either docetaxel or DMSO (Fig 4.6), and that this cytokine is known to stimulate the invasiveness of tumour cells [280], a neutralising antibody to TNFα was used to see if the increased invasive activity reported in **Fig 4.7** was

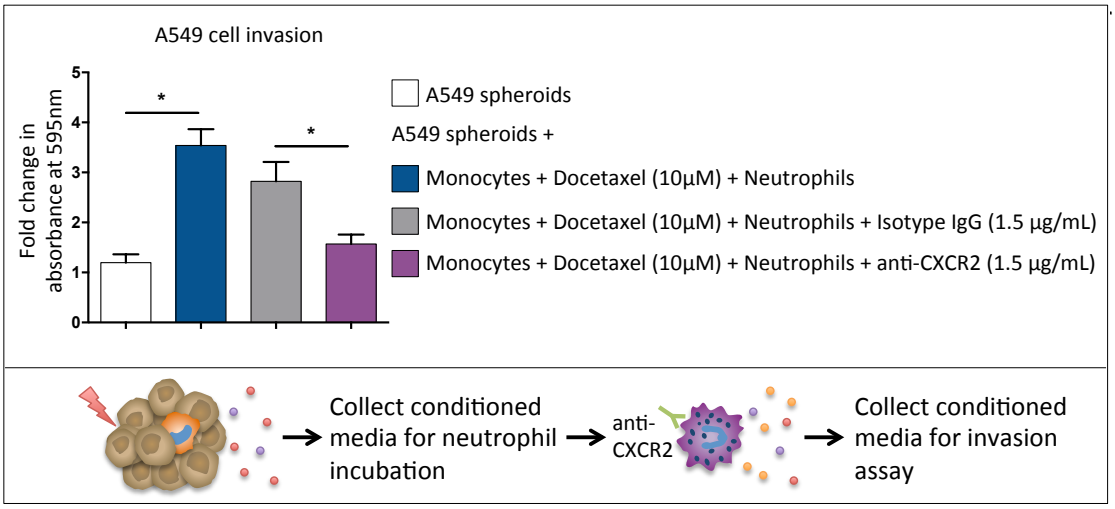

Figure 4.8 The pro-invasive effects of spheroid/neutrophil-conditioned medium was ablated by a CXCR2-neutralising antibody. Neutrophil CXCR2 signalling was inhibited by addition of an anti-CXCR2 antibody to the spheroid-conditioned media before it was added to neutrophils. This reduced tumour invasion, in comparison with an isotype control. The mean ± SEM from 5 identical experiments or 12 identical experiments (A549 spheroids + monocytes + Docetaxel + Neutrophils) are shown. Data are expressed as fold change in tumour cell invasion w.r.t. fresh, unconditioned medium, Mann-Whitney U test, * $p < 0.05$.

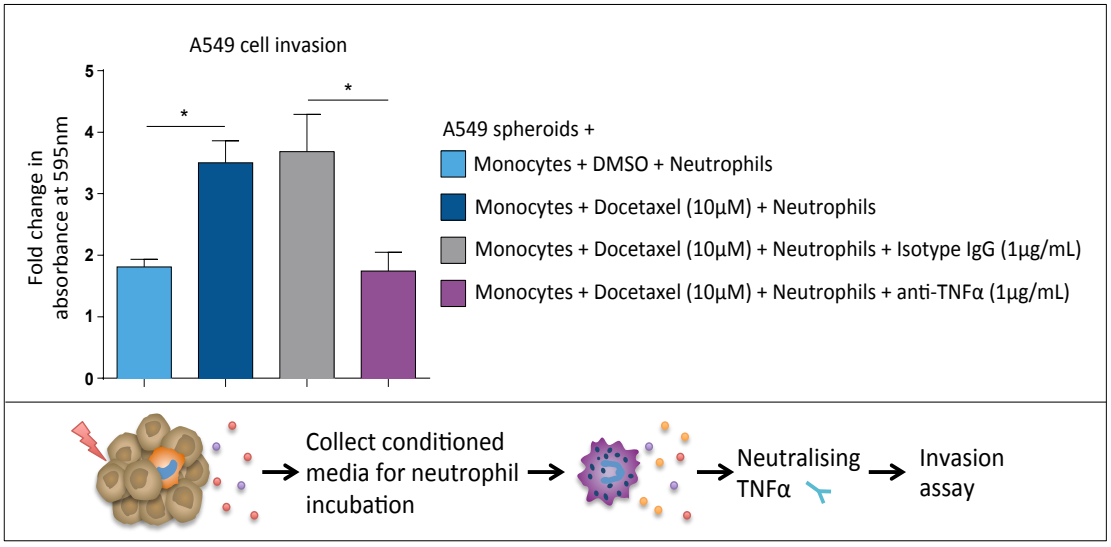

Figure 4.9 TNFα released by neutrophils (after their exposure to medium conditioned by docetaxel–treated A549 spheroids containing monocytes) stimulates tumour cell invasiveness *in vitro*. Neutrophils exposed to medium conditioned by myeloid cell-infiltrated A549 spheroids significantly increased tumour invasion when treated with docetaxel, in comparison with the DMSO control. This induction in tumour invasion is significantly reduced when TNFα is neutralised using an anti-TNFα neutralising antibody. The mean ± SEM from 4 identical experiments are shown. Data are expressed as fold change in tumour cell invasion w.r.t. unconditioned medium, Mann-Whitney U test, * $p < 0.05$.

predominantly driven by neutrophil-derived TNFα (**Fig. 4.9**). In the absence of TNFα, neutrophil induction of tumour cell invasion was significantly ($p = 0.0286$) reduced, suggesting that TNFα was a crucial factor in this induction.

Since monocytes/macrophages and tumour cells are also known to release this factor, the effect of neutralising TNFα in conditioned media from docetaxel-treated tumour spheroids and myeloid cells (no neutrophils) was also investigated, as shown in **Fig 4.10**. Tumour invasion was marginally reduced when TNFα was neutralised, suggesting that tumour cells and macrophages contribute to the overall TNFα production, but to a much lesser extent than when neutrophils are present.

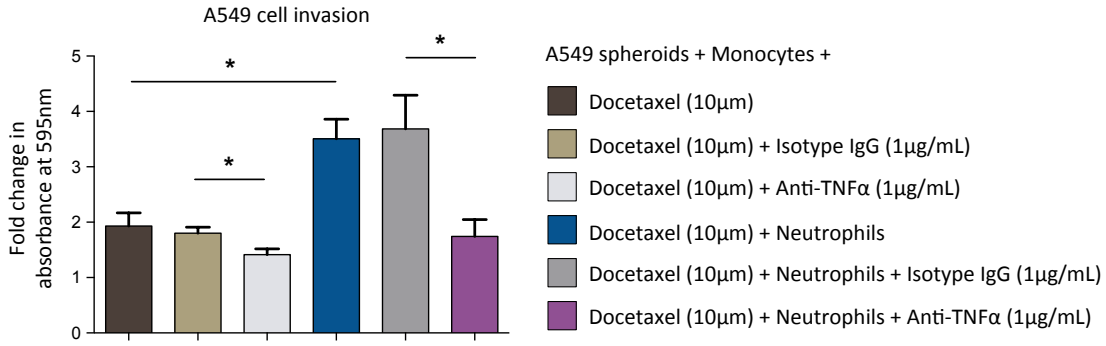

Figure 4.10 Neutralising TNFα in conditioned media from spheroids reduces tumour invasion *in vitro*. As shown in **Fig 4.9**, neutralising TNFα in conditioned media from myeloid cell-infiltrated A549 spheroids treated with docetaxel, with added neutrophil-derived factors, significantly reduces A549 cell invasion, in comparison with an isotype antibody control. In the absence of neutrophil-derived factors, tumour cell invasion is reduced, and although neutralising TNFα significantly reduces tumour invasion in comparison with an isotype antibody control, this change is much less. This suggests that there is more TNFα released when neutrophils are present, and that TNFα enhances A549 cell invasion. Pooled data from 4 identical experiments are shown. Data are expressed as fold change in tumour cell invasion w.r.t. fresh, unconditioned medium, * $p < 0.05$ w.r.t. A549 cells treated with DMSO.

4.4.5 Myeloid cells also upregulate CXC chemokines in A549 spheroids exposed to another chemotherapeutic agent, cyclophosphamide.

In order to understand whether the experiments described in **Chapter 3** and **Chapter 4** is specific to docetaxel, or may also occur with other forms of chemotherapeutic agent, the key experiments described in this chapter and **Chapter 3** were repeated using cyclophosphamide. Unlike docetaxel that kills

cells by stabilising microtubules, cyclophosphamide is an alkylating agent that induces cell death by causing irregular base pairing and generating crosslinks between the strands of DNA. This leads to disrupted cell division and, ultimately, to cell death [377]. However, in order for this to occur, cyclophosphamide must first be converted into the active component 4-hydroxy cyclophosphamide, by P450 enzymes in the liver. The name 'cyclophosphamide' will be used here to describe the active compound 4-hydroxy cyclophosphamide, as well as to describe the unprocessed pro-drug used in the *in vivo* experiments in **Chapter 5**.

As before with docetaxel, A549 cells were exposed to cyclophosphamide (100μM) or DMSO for 24h (as determined previously by members of this research group, see **Fig 4.3**). Then the cyclophosphamide-treated cells and supernatants from this were co-cultured with macrophages for 5h in a Transwell assay (see **sections 2.2.9.2** and **4.3**). Macrophage expression of CXCL1, CXCL2 and CXCL5 is shown in **Fig 4.11**. As can be seen, CXCL1 and CXCL2 were slightly, but not significantly, upregulated compared to vehicle-treated macrophages, whereas CXCL5 was markedly upregulated. Exposure to cyclophosphamide alone did not induce macrophage expression of CXC chemokines.

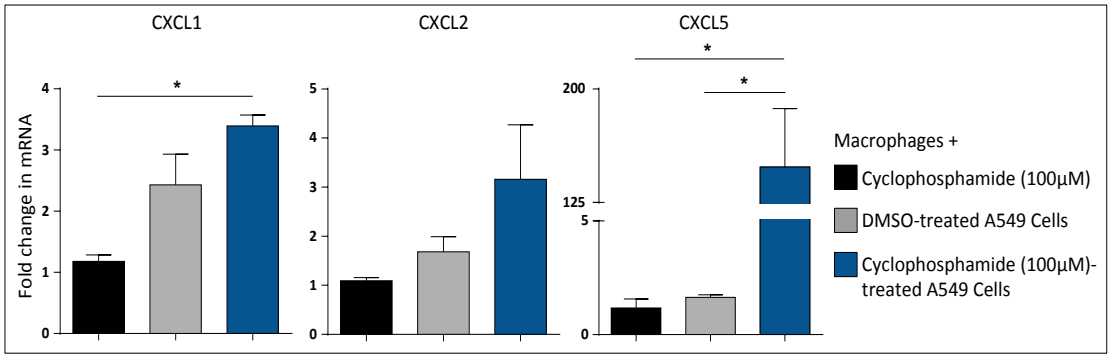

Figure 4.11 Macrophage levels of CXL1, CXCL2, CXCL5 mRNA in response to cyclophosphamide-treated A549 cells. Monocyte-derived macrophages significantly upregulate only CXCL5 mRNA when co-cultured for 5 hours with A549 cells exposed previously to cyclophosphamide (100μM) for 24 hours, in comparison with DMSO-treated A549 cells. Fold change is relative to macrophages co-cultured with A549 cells exposed to the vehicle DMSO. Minor inductions in CXCL1 and CXCL2 were also observed, but were not significantly different between cyclophosphamide- and DMSO-treated A549 groups. The mean ± SEM from 4 identical experiments are shown, Mann-Whitney U test, * $p < 0.05$.

4.4.6 CYCLOPHOSPHAMIDE-TREATED TUMOUR SPHEROIDS, INFILTRATED WITH MYELOID CELLS, ALSO UPREGULATED TNFA EXPRESSION BY NEUTROPHILS.

As before, conditioned media were collected from tumour spheroids infiltrated with myeloid cells, but in the presence of cyclophosphamide or its vehicle DMSO. Neutrophils were incubated for 16 hours in this conditioned media and then the media collected again and added to tumour cell invasion assays. Neutrophil viability following 16 hour incubation was 86–97% as measured by trypan blue staining (see **Section 4.5**). There was a significant ($p = 0.0143$) increase in invasion in the cyclophosphamide-treated group in comparison with its vehicle (**Fig 4.12**).

Interestingly, conditioned media from vehicle-treated, myeloid cell-infiltrated spheroids alone induced tumour invasion approximately 2-fold above the non-spheroid-conditioned media, whereas the corresponding cyclophosphamide-treated group induced invasion almost 6-fold. Neutralisation of TNFα in conditioned media from the latter group significantly ($p = 0.0286$) inhibited tumour invasiveness to less than half of the corresponding isotype control group. Therefore, as seen with docetaxel, myeloid cells in cyclophosphamide-treated A549 spheroids appear to stimulate TNFα release by neutrophils, which promote the invasiveness of A549 cells *in vitro*.

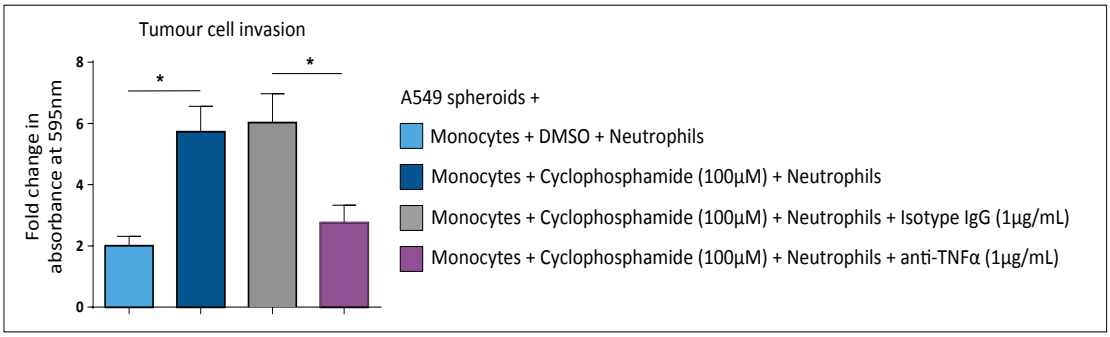

Figure 4.12 Neutrophils exposed to media from cyclophosphamide-treated, myeloid cell-infiltrated A549 spheroids stimulate tumour cell invasion *in vitro*: role of TNFα. Conditioned media from myeloid cell-infiltrated A549 spheroids treated with docetaxel was collected, and then cultured for 16 hours with neutrophils. Conditioned media induced A549 cell invasion, particularly when neutrophil-derived factors were included. This occurred in a TNFα-dependent manner. The mean ± SEM from 4 identical experiments are shown. These data show fold change in tumour cell invasion w.r.t. unconditioned medium, Mann-Whitney U test, * $p < 0.05$.

4.5 DISCUSSION

Initially, it was discovered that myeloid cells upregulate three chemokines for neutrophils, CXCL1, CXCL2 and CXCL5, in docetaxel-treated tumour spheroids. Therefore, it follows that conditioned media from these co-cultures would be chemoattractive for neutrophils *in vitro*. In summary of the results from this chapter, neutrophil migration assays showed that not only did neutrophils increase their migration in conditioned media from myeloid cell-infiltrated, docetaxel-treated tumour spheroids, but also that this was mediated, in part, by CXCR2 signalling. Although no distinct polarisation of neutrophils towards an N1 or N2 phenotype occurred in these experiments, they upregulated their expression of pro-inflammatory chemokines TNFα, CCL3 and CCL2, in comparison with neutrophils exposed to medium containing DMSO. Neutrophil-derived TNFα was shown to stimulate the invasiveness of A549 cells *in vitro*. Essentially similar results were obtained using cyclophosphamide in these assays. Macrophages were shown to upregulate mainly CXCL5, rather than CXCL1 and 2, in response to cyclophosphamide-treated A549 tumours cells. TNFα released by neutrophils following their exposure to factors released by cyclophosphamide-treated, myeloid cell-infiltrated spheroids stimulated A549 cell invasion *in vitro*.

Neutrophil migration induced by conditioned media from tumour spheroids increased less than 2-fold above the unconditioned medium, suggesting that tumour spheroids alone do not secrete significant amounts of neutrophil chemokines. Moreover, the addition of docetaxel to tumour spheroids did not increase the release of chemoattractants, showing that tumour cells are not responsible for a significant release of CXC chemokines or other neutrophil-chemotactic molecules, irrespective of chemotherapy treatment. This is notable because LM2 murine mammary tumour cells have previously been reported to express CXCL1 and CXCL2 following treatment with doxorubicin and cyclophosphamide chemotherapy [126], contrary to the results shown here. This, however, may be explained by the fact that CXCL1- and CXCL2-overexpressing tumour cells were selected in this earlier study, stimulated by a transcriptional hyperactivation of the 4q21 chromosome region occurring in

some breast cancers [292]. This would not be present in the A549 lung carcinoma cells used here. Furthermore, the increase in CXC chemokine expression reported in these mammary tumours after doxorubicin and cyclophosphamide was in part mediated by endothelial cell-derived TNFα release. Endothelial cells were not present in the spheroid studies described in this or the previous chapter.

Neutrophil migration towards conditioned media from myeloid cell-infiltrated tumour spheroids was approximately 3 times that of fresh IMDM, but almost doubled upon docetaxel treatment of myeloid cell-infiltrated spheroids. This shows that under basal conditions, such spheroids release a certain level of neutrophil-chemoattracting factors, which may maintain a steady influx of neutrophils into untreated tumours. The stress and damage induced by chemotherapy may then activate signalling pathways that lead to the recruitment of much higher numbers of neutrophils. The release of neutrophil chemokines appears to be dependent upon the presence of both myeloid cells and docetaxel in this spheroid model. However, it is worth noting that neutrophils may have migrated through the filter in between the upper and lower chambers of the Transwell plate but remained attached to the filter, and thus may have been removed along with the Transwell insert. If so, the number of infiltrated neutrophils would be under-represented, although it may not have an effect on the relative migration of neutrophils between docetaxel- and DMSO-treated groups. The migration assay used here is a simplistic one as it only assesses the movement of neutrophils through pores in a membrane towards conditioned media, which could simply reflect an increase in neutrophil motility rather than a directional chemoattraction. This is a massive oversimplification of the processes involved in neutrophil recruitment into tumours which involves release from the bone marrow, extravasation across the tumour vasculature and infiltration through the tumour mass. Therefore, it is very important to observe whether neutrophils are recruited into chemotherapy-treated tumours *in vivo.* This is investigated in **Chapter 5**.

The data in this chapter also show that CXCR2 on neutrophils mediates the effects of myeloid cells from docetaxel-treated spheroids on their migratory

activity. These results are analogous to earlier findings that neutrophil infiltration into tumours is largely dependent upon CXCR2 [126, 185]. However, it is worth noting that CXCR2 also binds chemokines CXCL3, CXCL6, CXCL7 and CXCL8, and so CXCR2 inhibition will also block signalling by these molecules [30], all of which have neutrophil chemotactic properties [378-380]. The gene array (**Fig 3.2**), however, did not identify any of these chemokines to be upregulated by macrophages conditioned with tumour cells or docetaxel-treated tumour cells. Had time permitted, an experiment to determine the dominant CXC chemokine could have been done. Using individual inhibitors of human CXCL1, CXCL2 and CXCL5 to neutralise protein in the conditioned media, the chemokine most responsible for neutrophil migration would have been identified. The gene array identified CXCL5 as being most highly upregulated CXC chemokine by myeloid cells in the docetaxel-treated tumour environment (**Fig 3.2**); however, subsequent real-time PCR analysis suggested that myeloid cell expression followed the pattern CXCL1 > CXCL2 > CXCL5 (**Figs 3.4**, **3.5** and **3.6**). Additionally, the CXCR2-dependency of neutrophil migration towards conditioned media generated by non-docetaxel-treated spheroids was not tested, since neutrophil migration and infiltration into A549 tumours has already been shown to be largely dependent upon CXCR2 signalling both *in vitro* and *in vivo* [185].

As mentioned previously in **section 4.1** and shown in **Fig 4.1**, two distinct activation states have been identified for TANs, stimulated by transforming growth factor-β (TGF-β) and interferon-β (IFN-β) [146]. N1 neutrophils are described as expressing increased TNFα, CCL3, FAS and ICAM-1 mRNA; in contrast, N2 neutrophils express higher CCL2, CCL5, CXCR4, MMP9, VEGF, arginase, c-myc, and STAT3 [295]. Hepatocyte growth factor (HGF) expression has also been reported as a marker of protumour/N2-like phenotype, since its release by neutrophils has been shown to promote enhanced invasion by human cholangiocellular carcinoma and hepatocellular carcinoma cells *in vitro* [381]. Freshly-isolated, human blood neutrophils were cultured for 16 hours in conditioned media from myeloid cell-infiltrated tumour spheroids, and their gene expression was analysed by RT-PCR for N1 and N2 genes. They were found

to express a mixture of N1 and N2 genes - both in the presence or absence of docetaxel. However, neutrophils isolated from untreated mouse or human lung tumours may have responded differently to medium conditioned by myeloid cell-infiltrated, docetaxel-treated A549 spheroids. The mRNA for CCL3 and CCL2 were upregulated by neutrophils exposed to such conditioned medium. Similarly, STAT3 and TGF-β were also induced, although their expression was much lower than either CCL3 or CCL2. This spheroid-conditioned media had little effect on FAS, ICAM-1, VEGF, MMP9, CXCR4, and HGF mRNA levels in human neutrophils. Although the difference in TNFα expression was not significant between the two groups, a trend towards a large increase was observed.

The results in **Fig 4.6** show that VEGF and MMP-9 were not significantly affected at the mRNA level by spheroid-conditioned medium, although STAT3 was upregulated marginally, which is a signalling factor known to regulate VEGF and MMP-9. It appears that docetaxel does not have a great effect on this particular pathway at this time-point. It would have been interesting to observe neutrophil expression of STAT3 – and the regulated pro-angiogenic and pro-invasive genes MMP9 and VEGF – at earlier time-points, since the data shown here represent a late time-point (16h). Previously it has been reported that early and sustained STAT3 activation in dendritic cells, induced by IL-6 and IL-10 respectively, led to opposing regulation of a panel of inflammatory and anti-inflammatory genes [382]. Therefore, investigating expression at an earlier time-point (e.g. 4h) may have uncovered an early induction of STAT3 in neutrophils that drives a different STAT3-dependent response. It would also have been interesting to investigate the expression of S100A8 and S100A9 by neutrophils had time permitted. Both have been shown to promote the survival and metastasis of tumour cells in the mouse PyMT implant model – and to be stimulated by CXCL1 in $CD11b^{+}Gr1^{+}$ cells (most likely neutrophils) [126]. Importantly, S100A8 and S100A9 were expressed at higher levels by neutrophils after doxorubicin and cyclophosphamide chemotherapy, and they may also have been induced in neutrophils exposed to medium conditioned by docetaxel-treated, myeloid cell-infiltrated tumour spheroids.

Both CCL2 and CCL3 are potent leukocyte chemoattractants, mainly reported to attract monocytes/macrophages, but also known to affect dendritic cells and neutrophil migration [127, 301, 383]. As such, the fact that neutrophil expression of CCL2 and CCL3 increases by 35- and 25-fold respectively (following 16-hour culture in conditioned media from myeloid cell-infiltrated spheroids), and over 100-fold for both CCL2 and CCL3 (in the presence of myeloid cell-infiltrated spheroids after their exposure to docetaxel), shows that neutrophils are highly likely to recruit monocytes, macrophages and other lymphocytes to the tumour. This is in line with their known ability to recruit monocytes/macrophages to sites of inflammation (see **section 1.5**). These results are also in accordance with previous reports of CCL2 being one of the most prevalent cytokines in the tumour environment [384], and the most highly upregulated chemokine in murine mammary tumour lysates following doxorubicin treatment [212]. Tumour- and stromal-derived CCL2 has been shown to contribute towards M2-polarisation, tumour progression, metastasis and chemotherapeutic efficacy via the recruitment of monocytes and macrophages [127, 301, 302, 384], including a chemotherapy-specific recruitment of myeloid cells which leads to decreased chemotherapeutic drug response [212], as discussed in **section 1.11.1**. Neutrophil-derived CCL2 induction was not confirmed at protein level, and CCL2 expression (specifically after chemotherapy) was not explored further.

Although there was a marked trend towards increased TNFα gene expression by neutrophils exposed to docetaxel-treated, myeloid cell-infiltrated A549 spheroids (compared to those exposed to DMSO alone), this failed to reach significance due to the high variance within these groups. Human neutrophils were isolated from blood samples taken from healthy volunteers, and such primary cells are particularly susceptible to the natural variations that occur between human donors. This experiment might have benefited from the inclusion of more donors/repeat experiments and also a neutrophils plus docetaxel control group. However, the finding that neutrophils in chemotherapy-treated, murine tumours upregulate their expression of immunoreactive TNFα support the *in vitro* data presented here (see **Chapter 5**).

Rather than investigating neutrophil migration and activation/gene expression separately, as detailed above in **Figs 4.3** and **4.5**, this could have been done jointly using the spheroid model. Freshly-isolated monocytes, labelled with CellTracker dye, could have been added to A549 spheroids and treated with docetaxel or DMSO (see **section 3.5** for a discussion on exactly when docetaxel should be added, to model TAM response or tumour-infiltrating monocyte response). Then, freshly-isolated neutrophils could have been labelled with a different CellTracker dye and also added to tumour spheroids. After washing off un-infiltrated cells, CellTracker labelled monocytes and neutrophils could be re-isolated by fluorescence-activated cell sorting, as well as unlabelled A549 cells, for the analysis of gene expression by RT-PCR of these 3 cell types. The percentage of cells that are neutrophils could be compared between samples treated with docetaxel, and those treated with DMSO, as an indication of recruitment of neutrophils into tumours. Technically, this experiment would not be much more difficult than the experiment used to isolate myeloid cells from A549 spheroids. It could be used to confirm/identify the expression of CXC chemokines by myeloid cells (as well as tumour cells and neutrophils), and the expression of TNFα, CCL2 and CCL3 by neutrophils (as well as tumour cells and myeloid cells). The differences between the gene expression of neutrophils cultured in docetaxel-generated spheroid media and DMSO-generated spheroid media shown in **Fig 4.6** highlight the effects that docetaxel may have on TAN gene expression in patients with non-small cell lung cancer. However, this experiment lacks a neutrophil plus docetaxel control, which would identify whether neutrophils upregulate any of these genes in response to the chemotherapy itself. It also lacks myeloid cell plus neutrophil controls, to identify whether the co-culture and cross-talk of these two cells (in the presence of docetaxel or DMSO) leads to neutrophil gene expression, in the absence of A549 spheroids.

The experimental setup used to investigate neutrophil gene expression was then used to study the possible biological significance of such neutrophil secreted factors in tumours. Rather than collecting neutrophils for expression analysis, the conditioned media was collected – including neutrophil secretory products –

and used in two *in vitro* functional assays. The invasiveness of tumour cells is known to be induced by TNFα (see **Table 4.2**) directly [280, 373] and indirectly by stimulating pro-invasive functions of $CD11b^{+}Ly6G^{+}$ cells [126] or macrophages [375, 385]. The ability of factors in the conditioned media, including TNFα, to enhance invasiveness of tumour cells was assayed using an *in vitro* invasion assay. The A549 human lung carcinoma cells were used in an invasion assay to assess their ability to actively degrade extracellular matrix (Matrigel) and migrate towards conditioned media from myeloid cell-infiltrated tumour spheroids, treated with docetaxel or DMSO, and cultured with neutrophils. Neither conditioned media from neutrophils and docetaxel-treated spheroids, nor from monocytes and neutrophils (freshly-isolated monocytes cultured with neutrophils for 16 hours), induced tumour invasion greater than 2-fold above unconditioned medium alone. These controls show that neutrophils do not simply release pro-invasive factors in response to docetaxel, and that these factors are not released just because of monocyte and neutrophil co-culture in the absence of tumour cells or their secretory factors.

Conditioned media from myeloid cell-infiltrated spheroids treated with docetaxel induced tumour invasion 2.4-fold above the control (myeloid cell-infiltrated spheroids exposed to DMSO), showing that even conditioned media collected in the absence of neutrophils contains pro-invasive factors that encourage tumour invasiveness. This may represent a production of TNFα by monocytes/macrophages or by tumour cells themselves [272, 288, 363], or the production of other pro-invasive factors by macrophages induced by tumour cells, such as MMPs 1 and 9 and COX2 [386], especially since macrophages have been shown to accumulate at the invasive front of mammary tumours and promote invasion [387]. It is worth noting, however, that no major pro-inflammatory cytokines were identified as being upregulated by tumour-conditioned macrophages in the gene array shown in **Fig 3.2**.

Tumour invasiveness, however, was found to be most highly induced by conditioned media collected from myeloid cell-infiltrated spheroids and neutrophils, following treatment with docetaxel. Tumour invasion increased significantly ($p = 0.0198$) with the addition of neutrophil-derived factors to 3.5-

Pro-tumour characteristic	Details	Ref.
Genetic damage to tumour cells	Chronic exposure of murine haematopoietic stem cells (with the Fanconi anaemia mutation) to TNFα-induced ROS-dependent genetic instability.	[388]
	High doses of TNFα-induced ROS-dependent DNA damage in human $p53^{-/-}$ colon carcinoma cells.	[278]
	TNFα-stimulated ectopic production of activation-induced cytidine deaminase (AID), an important RNA/DNA editing enzyme that can lead to mutations in p53 and c-myc, in human colorectal cancer cell lines.	[389]
Tumour growth	Human colon cancer cells release TNFα, which induced murine macrophages to upregulate CSF-1, VEGF and MMP2 *in vitro* and support tumour growth.	[363]
EMT	Epithelial-to-mesenchymal transition of human colon cancer spheroids is stimulated by macrophage-derived TNFα.	[280]
Tumour invasion and metastasis	TNFα-dependent MMP induction in macrophages is capable of stimulating the invasion of human breast tumour cell lines *in vitro.*	[375]
	Intraperitoneal injection of recombinant murine TNFα into mice prior to injection of murine fibrosarcoma cells enhanced the number of metastases in the lungs.	[285]
	Chinese hamster ovary (CHO) cells transfected with the human gene for TNFα demonstrated increased invasion of peritoneal surfaces and metastasis	[373]
	Co-culture of human urothelial bladder cancer cells and macrophages caused a release of TNFα by macrophages, which in turn enhanced tumour cell invasiveness.	[385]
	Chemotherapy induced endothelial cells to release TNFα, which stimulated mammary tumour cell recruitment of $CD11b^{+}Gr1^{+}$ cells to the tumour. The release of pro-invasive factors, S100A8 and S100A9, by $CD11b^{+}Gr1^{+}$ cells enhanced metastasis.	[126]
Tumour angiogenesis	TNFα stimulated murine lung adenocarcinoma cells to produce TNFα and VEGF, which enhanced angiogenesis.	[390]

Table 4.2 The role of TNFα in tumour progression and metastasis. Some of the pro-tumour functions of TNFα include inducing genetic instability, supporting tumour growth, enhancing EMT, invasion and metastasis, and promoting tumour angiogenesis. CSF-1, colony-stimulating factor-1; EMT, epithelial-to-mesenchymal transition; MMP, matrix metalloprotease; p53, tumour protein 53; TNFα, tumour necrosis factor alpha; VEGF, vascular endothelial growth factor.

fold above the fresh, unconditioned media control group, adding to the effect of tumour spheroids and myeloid cells. Notably, the effects of any neutrophil-derived factors on tumour invasion could not be mediated indirectly via the stimulation of myeloid cells or tumour cells, as reported elsewhere [301], since conditioned media was collected in a linear manner, where only the secreted factors of tumour cells and myeloid cells were incubated with neutrophils (see experimental design diagram in **Fig 4.7**). The *in vitro* data presented in this and

in the previous chapter suggest that neutrophils in docetaxel-treated tumours may contribute towards the production of pro-invasive factors. Thus treatment of lung cancer patients with docetaxel therapy could potentially cause a release of CXC chemokines by TAMs and the recruitment of neutrophils and their release of pro-invasive factors. This might be a mechanism by which tumours support invasion following chemotherapy. Enhanced invasion is an indicator that more tumour cells are being induced to disassemble their connections with adjacent cells (although these may not have had time to form in this invasion assay), degrade extracellular matrix, and increase their motility. Such motile cells may invade other tissues or migrate into blood vessels, where it is possible they will be transported to distant sites and form metastases. Although the process of tumour cells metastasising to other sites requires many steps, including avoiding immune destruction and the establishment of a pre-metastatic niche [391, 392], an increase in tumour cell invasiveness would still increase the likelihood of a successful metastatic event. Therefore, it is important to understand mechanisms through which chemotherapy may enhance metastasis [126, 162], so that novel therapies can be used to target such mechanisms.

An additional group, however, is needed to identify whether the induction of pro-invasive factors by neutrophils is unique to the docetaxel-treated tumour environment, or whether this occurs in the absence of docetaxel also. Therefore, a similar invasion assay should be done using conditioned media collected from myeloid cell-infiltrated spheroids (in the absence of docetaxel), and again after culture with neutrophils for 16 hours. Notably, since neutrophils are reported to survive for only hours in culture *in vitro* [99], this might suggest that the majority of neutrophils in the cultures used here may have died by 16 hours, and that it might be the cellular content of dead neutrophils which affects tumour invasion. However, the growth factors G-CSF and GM-CSF have been shown to prolong the survival of TANs in patients with lung adenocarcinoma [393]. Furthermore, using the same human lung adenocarcinoma cell line (A549 cells) as used in **Chapters 3** and **4**, G-CSF and GM-CSF were shown to originate in A549 cells *in vitro* and promote neutrophil survival; this inhibition of neutrophil death was only observed following exposure of A549 cells to cell-free

supernatants from peripheral blood mononuclear cells (PBMCs) or alveolar macrophages.

These findings are highly significant for this thesis since the neutrophils in this experiment were cultured for 16 hours in conditioned media from human myeloid cells and A549 spheroids, and their viability was between 86–97%, suggesting that myeloid cell-stimulated A549 cells may promote neutrophil survival in this *in vitro* co-culture system as well. Measuring the concentration of G-CSF and GM-CSF by ELISA in conditioned media from A549 spheroids, and comparing with myeloid cell-infiltrated A549 spheroids, could be used to investigate this. It would also be interesting to observe any effects the addition of docetaxel chemotherapy has on this mechanism, and whether it is important for TAN viability in a chemotherapy-treated tumour.

Furthermore, the conditioned media used in this assay have been incubated with tumour spheroids and myeloid cells for 48 hours, and then with neutrophils for 16 hours, and so the level of nutrients remaining may be low in the conditioned media by the time they are used in invasion assays. It is possible that docetaxel treatment of spheroids slowed their proliferation during the 48-hour co-culture with myeloid cells, such that they used up a lesser amount of the nutrients in the media. Subsequently, when used in invasion assays, docetaxel-generated conditioned media may have had a higher concentration of nutrients than the DMSO-generated conditioned media control, thereby affecting A549 cell invasion. The docetaxel still remaining in conditioned media (not taken up by A549 cells, myeloid cells and neutrophils) could similarly have an effect on the invasiveness of A549 cells in the invasion assay; however, it might be expected to reduce tumour cell invasion rather than to enhance it.

The reduction in tumour cell invasion observed when neutrophil CXCR2 signalling is blocked, as shown in **Fig 4.8**, demonstrates a dependency on this receptor for the promotion of tumour cell invasiveness by neutrophils. Blocking CXCR2 signalling on neutrophils significantly ($p = 0.0159$) reduced tumour invasion to less than 2-fold above controls, indicating that not only do CXCL1, CXCL2 and CXCL5 chemoattract neutrophils, they – or other such CXCR2 ligands

as CXCL3, CXCL6, CXCL7 and CXCL8 – also stimulate neutrophils to release pro-invasive molecules. As before, it is possible that one, or a combination of these CXC chemokines, is accountable for this response, and so further studies are now needed to dissect this – possibly by depleting CXCL1, CXCL2 and CXCL5 individually from the conditioned media using neutralising antibodies. In this way, it would be possible to identify the key factor(s) responsible for causing neutrophil pro-invasive response.

As mentioned previously, both TNFα and CCL2 were upregulated by neutrophils after exposure to spheroid-conditioned medium. Interestingly, both factors have been shown to regulate tumour invasion and so could contribute to the neutrophil stimulation of tumour invasiveness reported here; however, due to time and budget constraints, only TNFα was explored here in this thesis. To investigate the importance of TNFα in this mechanism, a TNFα-neutralising antibody was used to deplete conditioned media of this cytokine. Neutralising TNFα in the media led to a significant reduction, approximately halving the number of successfully invading tumour cells, thereby demonstrating a central role for TNFα in stimulating A549 human lung carcinoma cell invasiveness. Notably, in the absence of docetaxel, conditioned media from myeloid cell-infiltrated tumour spheroids (treated with DMSO) and neutrophils did not induce tumour invasion as highly; the stimulation of an invasive tumour cell phenotype is primarily induced by factors secreted in the docetaxel-challenged tumour environment. Enhanced neutrophil activation and recruitment to the docetaxel-treated tumour, orchestrated by resident TAM-derived CXCL chemokines, may lead to the release of TNFα and more invasive tumour cells. Since monocytes/macrophages are a major source of TNFα, including in the tumour environment, and that tumour cells themselves can release TNFα [288], the relative contribution of these cells types and neutrophils needed to be investigated. As shown in **Fig 4.9**, not only was tumour invasion reduced in the absence of neutrophil-derived factors, but the dependence upon TNFα was much less, proving that neutrophils are required for the maximum production of TNFα and TNFα-dependent tumour cell invasion. The induction of invasiveness by tumour cells and myeloid cells is dependent on other factors as well as TNFα,

which could include MMPs 1, 9 and COX2 [386]. One criticism, however, is that the neutralising efficiency of anti-TNFα and anti-CXCR2 antibodies were not investigated in the context of this assay. This could have been done using dose response experiments (observe the reduction in gene expression with increasing concentrations of antibody), or with a Ca^{2+} mobilisation assay to demonstrate blocking of TNFα in media or the CXCR2 receptor.

Conditioned media from tumour cells treated with docetaxel induced a less than 1.5-fold increase in tumour cell invasiveness. This suggests tumour cells are not directly enhancing the invasiveness of other tumour cells, whereby docetaxel-challenged tumour cells signal the invasion and escape of local tumour cells. With more time, further experiments to gain more understanding of this mechanism would include infiltrating monocytes and neutrophils into tumour spheroids simultaneously, followed by the addition of docetaxel. This would allow crosstalk and physical interaction between all 3 cell types. The different cell types could be isolated using fluorescence-activated cell sorting (FACS), and individually analysed for gene expression by RT-PCR, and by ELISA or cytometric bead array from cell supernatants. This mixed co-culture would be more representative of the true *in vivo* conditions. Instead, the conditioned media here were collected following co-cultures of tumour spheroids and myeloid cells, and then these conditioned media were used for neutrophil 16-hour culture to collect neutrophil-derived factors. This more linear approach followed a progression of unfolding events, and provided information as to which cell produced each factor, also allowing easier manipulation of cells with blocking antibodies.

As shown in **Fig 4.11** and **Fig 4.12**, the docetaxel-responsive upregulation of CXC chemokines by monocytes/macrophages, and the promotion of tumour invasion were not unique to docetaxel – similar results were obtained using 4-hydroxy cyclophosphamide (the active, metabolised form of cyclophosphamide). However, whereas CXCL1 was highly induced in monocytes/macrophages by docetaxel (**Fig 3.4**), when cyclophosphamide was used the most highly upregulated chemokine analysed was CXCL5. CXCL1 and CXCL2 mRNA were expressed at much lower levels than with docetaxel. Nonetheless, cyclophosphamide still induced an upregulation of CXCL5, which is important for

neutrophil activation and recruitment [238]. Future experiments should include investigating expression of all three CXCL chemokines at the protein level in media conditioned by docetaxel versus cyclophosphamide-treated, myeloid cell-infiltrated and non-infiltrated tumour spheroids.

As with docetaxel, the tumour invasion assay showed an almost identical ability of cyclophosphamide to induce the pro-invasive function of neutrophils via their secreted TNFα. The tumour invasion induced by conditioned media from myeloid cell-infiltrated A549 spheroids treated with docetaxel was significantly increased ($p = 0.0143$) by the addition of neutrophil-derived factors. However, conditioned media from just neutrophils plus cyclophosphamide alone was not investigated, and so this should be included to observe whether it is simply that cyclophosphamide induces the secretion of pro-invasive factors by neutrophils. It would have been interesting to observe how general this mechanism of inducing tumour invasiveness is, using a panel of chemotherapeutics, and different tumour cell lines *in vitro*. It is possible that this TNFα-dependent invasion of tumour cells is unique to A549 cells, and so it is important to use other cell lines *in vitro*, which could include MCF-7 human breast cancer cells and HT-29 human colorectal carcinoma cells. However, intratumoural TNFα is explored in four different tumour models later *in vivo* in **Chapter 5**.

Additionally, neutrophils were found to upregulate TGF-β mRNA (approximately 15-fold) upon exposure to medium conditioned by docetaxel-treated, macrophage-infiltrated spheroids. Since this growth factor has been shown to polarise tumour-associated neutrophils towards a pro-tumour phenotype [146], as well as inducing epithelial-mesenchymal transition (EMT) in colon carcinoma in concert with TNFα [280], its expression by neutrophils in docetaxel-treated tumours may drive neutrophils towards an N2 phenotype (although this was not seen in the 16h co-cultures used here, which induced a mixed N1/N2 phenotype) and tumour cells towards invasion and metastasis. A similar confirmation of TGF-β expression at the protein level by ELISA or cytometric bead array is now warranted, before pursuing neutrophil-derived

TGF-β as a potentially important modulator of neutrophil phenotype and tumour metastasis.

Despite the advantages of using a spheroid-based model over traditional monolayer co-cultures (including the presence of drug diffusion gradients and hypoxic cores as in tumours), this model still lacks many features of human tumours. The biggest drawback is the simplification in terms of cell types, since tumours are comprised of tumour cells and a multitude of stromal cells including monocytes/macrophages, neutrophils, endothelial cells, fibroblasts, lymphocytes, and mast cells, of which only two are represented in the model used here. Therefore, intricate crosstalk between the array of cell types, as well as subsets within cell types, is not present. Additionally, extracellular matrix and tissue structure are not fully formed, in part because the spheroids form over a short period of time and often remain below $1mm^3$ in volume [319]. Endothelial cells and vasculature do not exist in this model, and so the many tumour-driven processes that modulate their supply of oxygen and nutrients, vital to their progression, are not present. Therefore, it is very important to test and validate such *in vitro* spheroid-based findings using *in vivo* models, as is done here in **Chapter 5**.

In summary, the data in this chapter suggest that myeloid cells in chemotherapy-treated tumour spheroids produce CXCL chemokines that are chemotactic towards neutrophils. These factors (and potentially others) released by macrophage-infiltrated, docetaxel-treated spheroids failed to polarise neutrophils towards an N1 or N2 phenotype. However, the upregulation of TNFα, CCL2 and CCL3 may be important for the regrowth and invasion/metastasis of tumours after such forms of chemotherapy. Moreover, this effect was not just limited to docetaxel, as cyclophosphamide also triggers a similar interplay between macrophages and neutrophils. It remains to be seen whether this constitutes a general response to chemotherapy treatment. Attempts have been made to explore this further in the *in vivo* studies described in **Chapter 5**. If this also occurs in patients with lung cancer after treatment with docetaxel or cyclophosphamide (or other forms of chemotherapy), it might be a method

through which tumour cell invasion/metastasis is increased post-therapy and may highlight new therapeutic targets.

CHAPTER 5: CERTAIN CHEMOTHERAPEUTIC AGENTS INCREASE CXCL1 EXPRESSION AND THE NUMBER OF TNF ALPHA-EXPRESSING NEUTROPHILS IN MURINE TUMOURS

5.1 INTRODUCTION

The involvement of innate immune cells in tumour responses to chemotherapy has been shown in a number of recent studies [126, 162, 212, 290, 291], as summarised in **Fig 1.5**. The findings in **Chapters 3** and **4** describe a possible collaboration between chemotherapy-treated A549 lung tumour cells and human myeloid cells to increase neutrophil chemotaxis *in vitro*. This collaboration also stimulated neutrophils to release factors that enhance the invasiveness of A549 cells *in vitro* via a mechanism involving the cytokine TNFα and neutrophil CXCR2 signalling. This mechanism was triggered by A549 cells exposed to different chemotherapeutic agents docetaxel and cyclophosphamide (**Fig 4.11** and **Fig 4.12**). Therefore, in this chapter the response of myeloid cells was investigated *in vivo* using various mouse tumour models.

A very common side effect and limiting factor of chemotherapy treatment is neutropenia, the presence of abnormally low numbers of neutrophils in the blood (less than 2×10^6 neutrophils per millilitre), which is not only caused by the suppression of neutrophil production by chemotherapy, but also its direct cytotoxic effects [394]. A patient's chemotherapy treatment regimen will be stopped or changed to a reduced dose if a patient becomes neutropenic, since this condition is associated with increased chance of potentially life-threatening infections, such as Streptococcal infections [395]. Many forms of chemotherapy are known to cause this decrease in the number of circulating neutrophils (i.e. neutropenia), and so it is feasible that chemotherapy may also reduce the number of neutrophils infiltrating into tumours, causing a decrease in the numbers of TANs.

However, the *in vitro* studies described in **Chapters 3** and **4** suggest that docetaxel chemotherapy is likely to cause an increase in expression of CXC

chemokines by TAMs, and thus neutrophil recruitment. If this were found to be true *in vivo*, such neutrophil recruitment might overcome the general neutropenic state of the patient, and lead to a local increase in TANs. Additionally, other such factors as G-CSF and GM-CSF have been shown to prolong the survival of TANs in patients with lung adenocarcinoma [393], as mentioned previously in **section 4.5.** If present in tumours after chemotherapy, such factors might promote TAN survival despite chemotherapy-induced neutropenia. Interestingly, TANs accumulate in orthotopic mouse mammary tumour (PyMT) transplants following combined treatment with cyclophosphamide and doxorubicin [126].

The markers CD11b and Ly6G are commonly used to identify murine TANs [146, 396, 397]. The CD11b integrin – a differentiation marker of the myelomonocytic lineage – is transcriptionally upregulated in precursor cells as they mature, but decreases again as monocytes differentiate into macrophages [398]. CD11b is the integrin alpha M chain, which forms a dimer with the integrin beta 2 subunit (CD18) to form macrophage-1 antigen (Mac-1), an important adhesion receptor and regulator of inflammation. Ly6G is a small GPI-linked protein that, together with Ly6C, forms the complex known as the myeloid differentiation antigen, or Gr1, in mice. Flow cytometry analysis using a monoclonal antibody to Ly6G (1A8) has shown that Ly6G is predominantly expressed in murine bone marrow, and to a much lesser extent in other lymphoid tissues that contained activated T and B lymphocytes [399]. The Ly6G antibody predominantly bound to the surface of mouse neutrophils, whereas Ly6C is present on bone marrow cells, subsets of monocytes/macrophages, neutrophils, endothelial cells, plasma cells and subsets of T cells [84, 400]. Antibodies to the entire Gr1 complex are also used to identify neutrophils. However, as mentioned previously (see **Table 1.1**), Gr1 is not just expressed by murine neutrophils and granulocytic MDSCs, but also by inflammatory ($CX_3CR1^{lo}CCR2^{+}Gr1^{+}$) monocytes [22]. Similarly, both anti-Gr1 [401, 402] and anti-Ly6G [403-405] antibodies have been used to deplete neutrophils in mice, but the anti-Ly6G antibody is favoured due to the preservation of non-neutrophil $Gr1^{+}$ cells, which are depleted by the anti-Gr1 antibody [405]. The anti-Ly6G

monoclonal antibody 1A8 specifically depletes blood neutrophils and does not affect $Gr1^+$ blood monocytes. Additionally, murine neutrophils can also be identified by the marker Ly6B.2 (7/4), but again, this marker is also expressed on some bone marrow progenitors and monocytes as well. Ly6G has, therefore, been proposed to be a more specific marker for neutrophils.

In Acharyya et al. (2012) [126], cell populations from LM2 mouse mammary tumours were analysed by flow cytometry using antibodies for the markers Ly6G and Gr1, as well as F4/80, CD31 and CD11b antibodies. Cells were separated into the following populations: $CD11b^+Gr1^+$ cells, $CD11b^+Ly6G^+$ cells, $CD11b^+Ly6C^+$ cells (predominantly monocytes), $F4/80^+$ cells (macrophages), $CD31^+$ cells (endothelial cells), and unsorted cells (predominantly tumour cells). Sorted cells were used to investigate the expression of *Cxcr2* gene by each population, as shown in **Fig 5.1** (taken from [126]). The results showed that $CD11b^+Gr1^+$ cells, and specifically the $CD11b^+Ly6G^+$ neutrophil population (since $Gr1^+$ cells also include such non-neutrophil cells as granulocytic MDSC and inflammatory monocytes), had the highest *Cxcr2* mRNA levels. The other cell populations had only low levels of this gene.

As mentioned in previous chapters, the chemokines CXCL1, CXCL2,

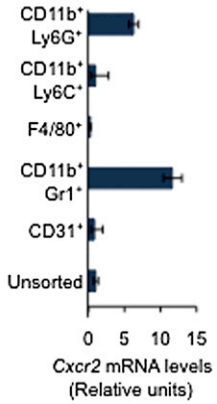

Figure 5.1 The levels of CXCR2 mRNA are highest in granulocytic cell populations LM2 murine breast tumours. Sorted subpopulations of murine metastatic breast (LM2) tumours were used to analyse messenger RNA expression of the Cxcr2 gene. The $CD11b^+Gr1^+$ and $CD11b^+Ly6G^+$ granulocytic populations showed highest expression of the receptor, with much lower expression by $CD11b^+Ly6C^+$ (predominantly monocytes), $F4/80^+$ (macrophages), $CD31^+$ (endothelial cells), and unsorted cell populations. Image adapted from [126].

CXCL3, CXCL5 and CXCL8 all signal through the CXCR2 receptor and are potent neutrophil chemotactic and activating factors [30, 93, 228]. Several reports have suggested that blockade of CXCR2 signalling may be therapeutically beneficial where excessive neutrophil infiltration causes progressive damage; this has been suggested in such inflammatory disorders as colitis, type 1 diabetes, cystic fibrosis and reperfusion injury [244, 258, 406, 407], as well as murine lung, skin and gastrointestinal cancers [126, 337]. Several CXCR2-inhibiting molecules have been developed, some of which are currently in clinical trials (see **Table 1.3**).

The CXCR2 inhibitor SB 265610 shows specificity towards CXCR2 and inhibits CXCL8 binding this receptor with an IC_{50} of 10nM in humans. In a rat model, SB 265610 antagonises CXCL1 (CINC-1)-induced neutrophil chemotaxis in a concentration-dependent manner [260]. Furthermore, in two orthotopic xenograft murine breast cancer models (MDA231-LM2 and CN34-LM1), combined treatment with cyclophosphamide and doxorubicin triggered not only CXCL1 upregulation by tumour cells but also increased stromal expression of TNFα (largely described as being by endothelial and other, unidentified stromal cells) which also augments CXCL1 expression by tumour cells. It was suggested that CXCL1/2-induced S100A8/9 expression by recruited $CD11b^{+}Gr1^{+}$ cells leads to chemoresistance [126].

Given the findings reported in **Chapters 3** and **4** – that A549 cells and certain chemotherapeutic agents stimulate myeloid cells to upregulate CXCLs 1, 2 and/or 5, leading to increased tumour cell invasiveness via neutrophil-derived TNFα – further *in vivo* studies were undertaken to investigate the effects of chemotherapy on neutrophil recruitment and TNFα expression in mouse tumours, and the possible role of CXCL1 expression by TAMs in this.

5.2 AIMS

The aim of the work in this chapter was to test the relevance of the *in vitro* findings discussed in **Chapters 3** and **4** to mouse tumours, using a variety of mouse tumour models and chemotherapeutic agents. This includes investigating the upregulation of CXCL1 expression by TAMs, and the number of

TNFα-expressing TANs in chemotherapy-treated tumour. The hypothesis that blocking CXC chemokine signalling through systemic inhibition of CXCR2 will reduce neutrophil infiltration into tumours, as well as their production of TNFα, was tested *in vivo*. Finally, in the same way as reported previously in xenograft MDA231-LM2 and CN34-LM1 tumours [126], this work aimed to assess the effect of doxorubicin and cyclophosphamide chemotherapy, combined with SB 265610 treatment, on the growth of primary PyMT transplants and their lung metastases.

5.3 METHODS

In summary, mice bearing subcutaneous LLC (syngeneic lung) tumours, orthotopic PyMT (transgenic murine mammary) tumour transplants, orthotopic ASV-B (transgenic murine liver) tumours, or orthotopic 4T1 (syngeneic murine mammary) tumours were used for immunofluorescence analysis of TANs using a Ly6G antibody, in combination with a CD11b antibody where stated. These tumour-bearing mice were treated with cyclophosphamide (LLC), doxorubicin plus cyclophosphamide (PyMT), etoposide (ASV-B), paclitaxel (4T1) or the appropriate vehicles for these agents. The numbers of $Ly6G^+$ neutrophils, $Ly6G^+TNF\alpha^+$ neutrophils, and TAMs expressing CXCL1 were then assessed, as described in **section 2.2.12.2**. In the PyMT transplant model, the effects of combining chemotherapy with CXCR2 inhibition (i.e. treatment with SB 265610) on the above parameters (and tumour levels of the apoptosis marker, caspase 3) were examined.

Frozen sections of chemotherapy or vehicle-treated LLC, 4T1 and ASV-B mouse tumours were generated during previous studies by other scientists in Professor Lewis's group in Sheffield (LLCs and ASV-B), or in the laboratory of a collaborator (the 4T1 tumours by Dr. Michele De Palma at the Swiss Federal Institute of Technology Lausanne in Lausanne) (see **section 2.2.12.1**). While the *in vivo* studies using the PyMT transplants were conducted by scientists in the laboratory of Dr. Joan Massagué (Memorial Sloane Kettering Centre in New York), they were designed jointly by the Lewis and Massagué labs (with input from this PhD project).

5.3.1 LEWIS LUNG CARCINOMA (LLC1) EXPERIMENTS

Mice (FVB) were implanted with mouse LLC1 lung tumour cells by Dr. Hughes in Professor Lewis's group in Sheffield. LLC1 cells (1 x 10^6 cells) were injected subcutaneously into the mouse hind flank. When tumours reached a volume of 100mm^3 they were given intraperitoneal injections of cyclophosphamide (150mg/kg) every 48 hours for a total of 3 injections. These mice were then culled 48 hours after the last dose of cyclophosphamide and the tumours were removed and snap frozen (as described in **section 2.2.12.1**).

5.3.2 ASV-B

ASV-B mice are transgenic mice that carry the Simian vacuolating virus 40 (SV40) oncogene under the control of the liver-specific albumin promoter [408]. These mice develop spontaneous hepatocellular carcinoma from 12 weeks of age. At 16 weeks of age, ASV-B mice were given either vehicle or the chemotherapeutic agent etoposide (10 mg/kg), in a sequence of daily intraperitoneal injections for 5 days, then rested for 2 days, and given another 5 days of the same treatment. Mice were culled 48 hours after the last dose of etoposide or vehicle, tumours removed and frozen as described in **section 2.2.12.1**. These studies were conducted by Dr. Munitta Muthana and Dr. Russell Hughes in the laboratory of Professor Claire Lewis.

5.3.3 4T1

Frozen sections of 4T1 tumours were kindly provided by Dr. De Palma in Switzerland. One million cells in 100µL of PBS were injected into the mammary fat pad of 7-week old BALB/c mice and then given 3 intraperitoneal injections of paclitaxel (10mg/kg) separated by 5 days. These mice were then culled 72 hours after their last injection and tumours removed and frozen.

5.3.4 PYMT

Mice (FVB) were injected with the FVB.MMTV-PyMT cell line, 1 x 10^5 cells per mouse in 50µL, in a 1:1, Matrigel:cell suspension (in PBS) mix. When tumours reached approximately 150mm^3, mice were randomised into treatment groups. Doxorubicin was given at 2mg/kg once a week, and cyclophosphamide was given at 45mg/kg once a week. For mice given the CXCR2 inhibitor, SB

265610, this was given at 2mg/kg, 5 times per week. For vehicle-treated control mice an equivalent volume of PBS (chemotherapy vehicle) and PEG400 (SB 265610 vehicle) were used. Mice were culled after two rounds of this combined chemotherapy (15 days) due to the large size of control tumours. At this point, tumours and lung tissues were removed and fixed overnight in 4% paraformaldehyde.

5.3.5 IMMUNOFLUORESCENT STAINING OF FROZEN TISSUE SECTIONS

Frozen tumours were cut on a cryotome into 10µm-thick sections, fixed with 4% PFA (except PyMT sections which were already fixed) and immunofluorescently labelled according to the methods described in **section 2.2.12.2**, using the antibodies from suppliers listed in **section 2.1.3**. For the analysis of CXCL1 (Gro-alpha), TNFα, Ly6G, F4/80, CD31, CD11b and cleaved (i.e. active form of) caspase 3, the following antibody concentrations and durations were used (in PBST buffer, see **section 2.1.6**):

Primary/conjugated Antibodies	**Application of antibody to sections**
Rat m anti-CD11b	4µg/mL for 2 hours at RT
Rat m anti-mouse F4/80	4µg/mL for 16 hours at 4°C
Rat m anti-mouse Ly6G (1A8) FITC	20µg/mL for 2 hours at RT
Rat m anti-mouse TNFα (LEAF™ purified)	20µg/mL for 6 hours at RT
Rabbit p anti-active Caspase 3	4µg/mL for 2 hours at RT
Rabbit p anti-CD31	2µg/mL for 1 hour at RT
Rabbit p anti-GRO alpha (murine CXCL1)	4µg/mL for 2 hours at RT
Secondary antibodies	
Goat m anti-rat AlexaFluor® 555	10µg/mL for 1 hour at RT
Goat m anti-rat AlexaFluor® 633	10µg/mL for 1 hour at RT
Goat m anti-rabbit APC	10µg/mL for 1 hour at RT

The use of CD11b/Ly6G (dual immunofluorescent staining) and Ly6G (single staining) for the labelling of neutrophils was compared (**Table 5.1**), and this showed that less than 6% of $Ly6G^+$ cells were not $CD11b^+$ in that particular tumour, suggesting that Ly6G can be used alone to label TANs. A Ly6G single stain was used to label neutrophils in PyMT, LLC and 4T1 tumours.

Tumour	No. $Ly6G^+$ cells	No. $CD11b^+Ly6G^+$ cells	% $Ly6G^+$ cells also $CD11b^+$
Vehicle	24	23	**95.83%**
Etoposide	35	33	**94.29%**

Table 5.1 Comparison of immunofluorescent staining of TANs using CD11b and Ly6G antibodies, or Ly6G antibody alone. Neutrophils in transgenic ASV-B murine liver tumours were labelled using CD11b and Ly6G antibodies. The sum of $CD11b^+Ly6G^+$ (dual positive) cells and $Ly6G^+$ cells in 5 field-of-view from one vehicle-treated and one etoposide-treated ASV-B tumour were counted, and used to calculate the percentage of $Ly6G^+$ cells that were also $CD11b^+$. Very few (<6%) $Ly6G^+$ cells were not $CD11b^+$.

Slides were washed thoroughly for 15 minutes in PBST after exposure to each of the primary antibodies listed above. Where applicable, secondary antibodies were added, and the slides washed. After the final wash, tissue sections were counterstained with 300nM DAPI for 2 minutes, washed in PBST, and covered with Prolong Gold Anti-fade reagent and a coverslip. Confocal microscopy was done using a Zeiss LSM 510 confocal microscope and LSM 510 software to capture between 5 and 8 images of randomly selected fields-of-view (FOV) at x25 or x40, as stated. All the cells in each FOV were counted manually and the images were counted blind. Isotype antibody controls were used to ensure background staining was low/absent for each staining experiment, and each time the confocal microscope settings were changed.

A semi-quantitative method using Z-stack images of tumour sections was also applied in order to assess changes in immunofluorescence per cell (e.g. TNFα in neutrophils) in the different treatment groups. The levels of immunodetectable protein were determined by taking 11 images of each stained tumour section at different focal depths in each sample. This was done at 40x

magnification in 4 randomly selected regions of each tumour. Images were then analysed in ImageJ software, where the channel-of-interest was isolated and the Z-stack images displayed as individual images (rather than stacked). A macro (see **section 2.2.12.3**) based on a previously reported analysis [148] was then run to set thresholds and transform the image into a format that could be quantified. To get a semi-quantitative measurement of signal fluorescence intensity the Measure function (ImageJ) was then used. A total value was calculated for each Z-stack by summation of these fluorescence intensity values, which was done for 4 FOV/Z-stacks in each tumour. The average and SEM of these 4 tumours/donors is shown.

5.3.6 IMMUNOHISTOCHEMISTRY (FOR TISSUES EMBEDDED IN PARAFFIN WAX)

This method was only applied to detect and quantify the number of PyMT antigen-expressing metastatic cells in the lungs of PyMT transplant-bearing mice, as these were embedded in paraffin wax upon removal from mice. This part of the study was performed by Dan Macalinao in Dr. Joan Massagué's group as part of a collaborative study between the Lewis and Massagué groups using the PyMT transplant model. As outlined in **Supplementary Method 1**, lung tissue sections were deparaffinised using xylene/histoclear and rehydrated using a series of ethanol washes. Heat-induced epitope retrieval was done using a steamer in combination with citrate-based antigen retrieval solution. Slides were blocked with 2.5% normal goat serum and a rat anti-PyMT antibody was used at a dilution of 1:200 overnight (in 2.5% normal goat serum). ImmPRESS reagent (anti-rat, mouse adsorbed) was used to detect the primary anti-PyMT antibody, and the peroxidase substrate DAB (3, 3'-diaminobenzidine) was used to detect signal. Slides were then counterstained using haematoxylin, dehydrated and mounted with Cytoseal XYL (Richard-Allen Scientific).

5.4 RESULTS

5.4.1 EFFECT OF COMBINED DOXORUBICIN AND CYCLOPHOSPHAMIDE TREATMENT ON THE NUMBER OF CXCL1$^+$ MACROPHAGES (AND OTHER CELL TYPES) IN MOUSE PYMT MAMMARY TUMOUR TRANSPLANTS

Immunofluorescent analysis was used to enumerate the number of CXCL1$^+$ TAMs and 'other' (non-TAM) cells in PyMT tumours treated with doxorubicin and cyclophosphamide, in the presence or absence of the CXCR2 inhibitor, SB 265610 (**Fig 5.2**).

The inhibitor SB 265610 is a CXCR2-specific antagonist. It has been shown to inhibit CXCR2 and prevent neutrophil accumulation in hyperoxia-exposed newborn rats, and antagonises rat CXCL1 (CINC-1)-induced calcium mobilisation in rat neutrophils *in vitro* with a half maximal inhibitory concentration (IC_{50}) of 3.7nM [260]. The affinity of SB 265610 was investigated by observing the binding of radiolabelled CXCL8 (IL-8) to Chinese hamster ovary (CHO) membranes stably expressing CXCR1 or CXCR2, in the presence or absence of SB 265610 [409]. The inhibitor SB 265610 was found to block CXCL8 binding CXCR2, IC_{50} = 39.1 ± 11.0nM, whereas it blocked CXCL8 binding to CXCR1, IC_{50} = 7,400 ± 2,400nM, thus demonstrating considerable specificity towards CXCR2. Similarly, SB 265610 inhibited calcium mobilisation in human neutrophils in response to CXCL1 (which binds CXCR2, not CXCR1), IC_{50} = 5.2 ± 1.5nM, whereas it inhibited calcium mobilisation in response to CXCL8 (which binds both CXCR1 and CXCR2), IC_{50} 426 nM [409]. However, only two experimental repeats of CXCL8 binding were done.

Increases in both the number F4/80$^+$CXCL1$^+$ TAMs in tumours, and the proportion of TAMs expressing CXCL1 following treatment with doxorubicin and cyclophosphamide, were seen (**Fig 5.2 B** and **C**). Combining this chemotherapy with SB 265610 failed significantly to alter either. Interestingly, however, the number of 'other' (i.e. F4/80$^-$) cells expressing CXCL1 increased in chemotherapy-treated tumours (**Fig 5.2 D**), and increased further in the chemotherapy plus SB 265610-treated tumours. These non-TAM cells that express CXCL1 could be tumour cells, based on their larger nuclear morphology.

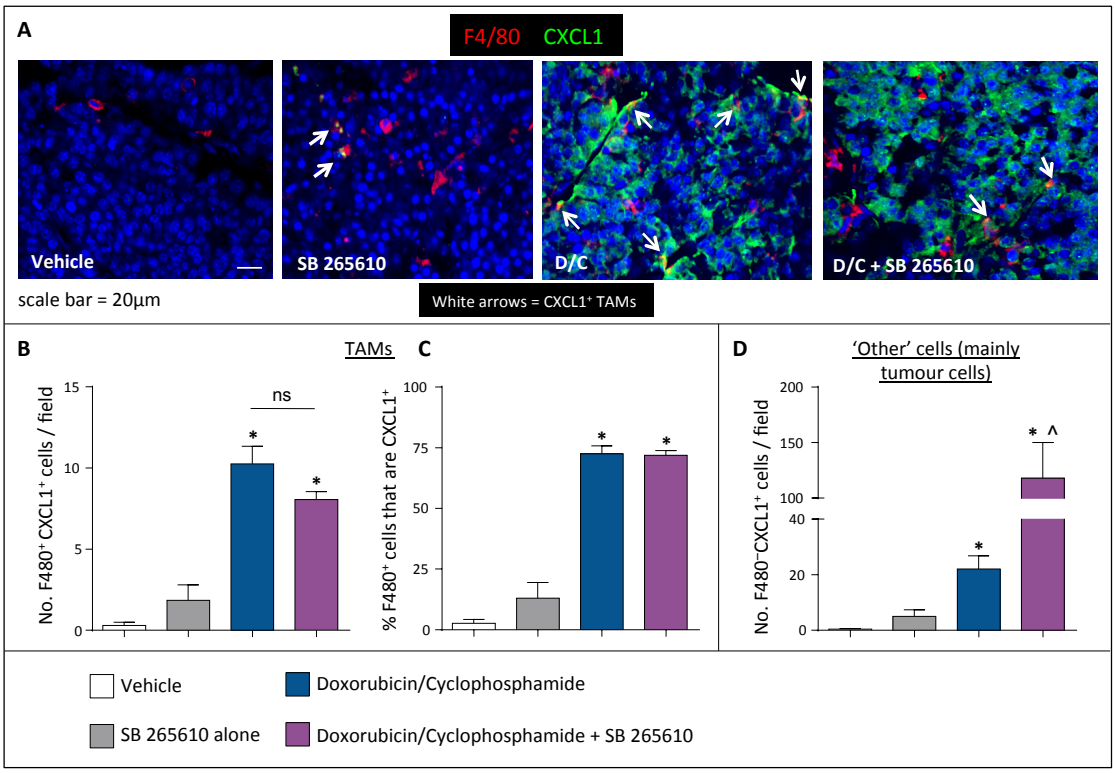

Figure 5.2 Effect of doxorubicin and cyclophosphamide on CXCL1 expression by F4/80⁺ TAMs (and other unidentified cell types) in PyMT tumour transplants. Mice bearing PyMT transplants were treated with doxorubicin and cyclophosphamide (D/C) and/or the CXCR2 inhibitor, SB 265610. (A) Representative images of F4/80⁺ macrophages (red), CXCL1 (green), and CXCL1⁺ TAMs (white arrows) in tumour sections. Magnification bar =20µm. (B) The number of F4/80⁺CXCL1⁺ cells in tumours (C) The percentage of F4/80⁺ cells that are CXCL1⁺, and (D) The number of F4/80⁻CXCL1⁺ cells (which appeared to be mostly tumour cells on the basis of morphology). Images were taken at x25 magnification. The mean ± SEM from 4 identical experiments are shown, Mann-Whitney U test, * $p < 0.05$ w.r.t. vehicle-treated PyMT-bearing mice, ^ $p < 0.05$ w.r.t. doxorubicin- and cyclophosphamide-treated PyMT-bearing mice.

However, time permitting, it would have been interesting to use a panel of cell markers to identify these other CXCL1-producer cell types.

5.4.2 Chemotherapy increases tumour recruitment of Ly6G⁺TNFα⁺ cells in four murine tumour models

The role of myeloid cells in tumours following chemotherapy varies with type of treatment and tumour model, as has been recently reviewed [312]. Therefore, 4 different murine tumour models were used to investigate the presence of Ly6G⁺TNFα⁺ cells in tumours following chemotherapy, and to see

whether TANs respond in a general way to a range of chemotherapeutics in these different models.

Frozen sections of tumours from four murine models (given different

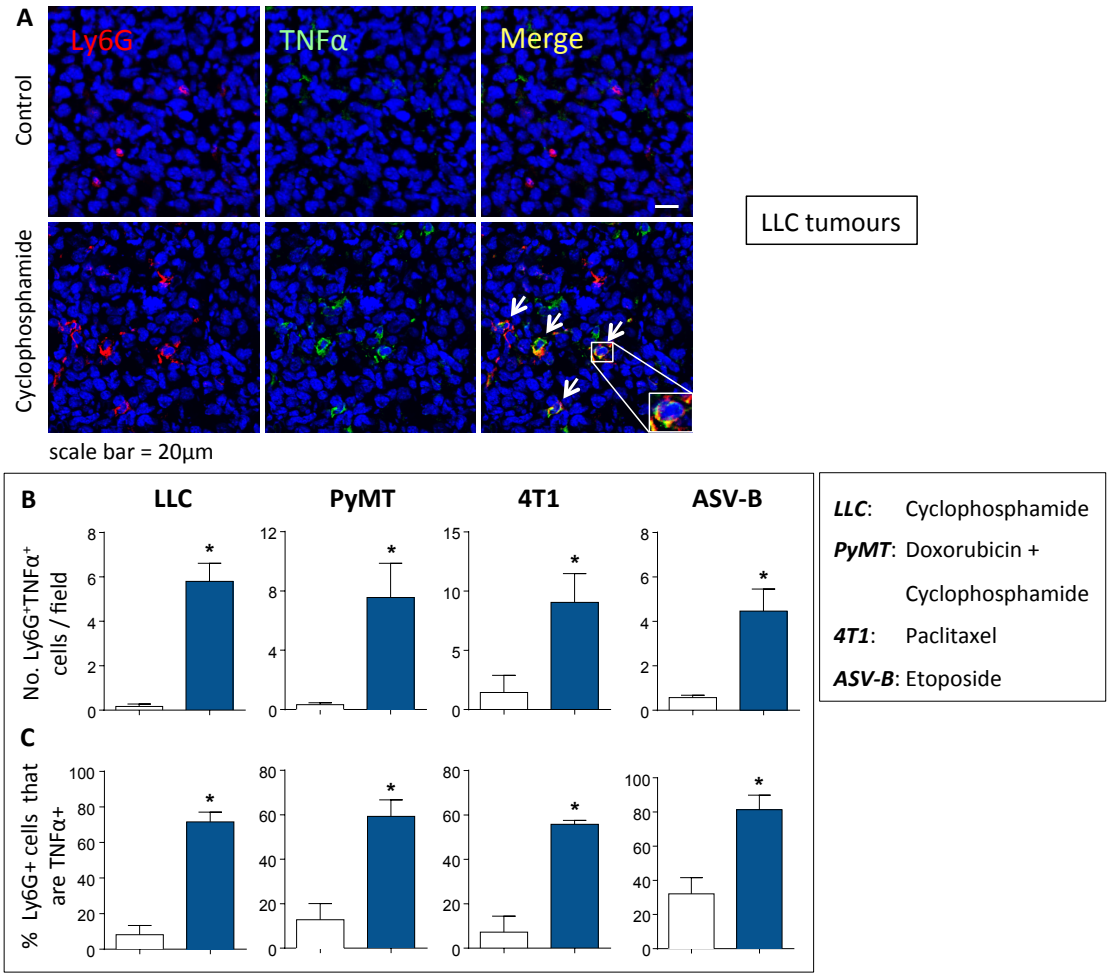

Figure 5.3 The number of Ly6G⁺TNFα⁺ cells, and the proportion of Ly6G cells that are TNFα⁺, increases in tumours from 4 different tumour models given different types of chemotherapy. Mice bearing LLC (syngeneic lung tumour), PyMT (transgenic breast tumour transplant), ASV-B (spontaneous transgenic liver tumour), or 4T1 (syngeneic breast tumour) were treated with cyclophosphamide, doxorubicin plus cyclophosphamide, etoposide, or paclitaxel chemotherapy, respectively. (A) Representative images of control or chemotherapy-treated LLC tumours stained with Ly6G (red), TNFα (green) antibodies and DAPI (blue), as well as merged images. Scale bar = 20μm (B) Numbers of Ly6G⁺TNFα⁺ cells increased significantly following chemotherapy. Additionally, (C) the number of Ly6G⁺ cells that were also TNFα⁺ increased significantly across all tumour models. Data from ASV-B tumours show double stained CD11b⁺Ly6G⁺ cells, and CD11b⁺Ly6G⁺TNFα⁺ cells. Images were taken at x25 magnification. The mean ± SEM from 5 identical experiments (LLC, PyMT), 4 identical experiments (ASV-B) or 3 identical experiments (4T1) are shown, Mann-Whitney U test, * $p < 0.05$.

chemotherapeutic agents) were immunofluorescently stained for Ly6G and TNFα (**Fig 5.3**). In the LLC model treated with cyclophosphamide, PyMT model treated with doxorubicin and cyclophosphamide, and ASV-B model treated with etoposide, the numbers of Ly6G$^+$ cells (or CD11b$^+$Ly6G$^+$ cells for ASV-B model) increased significantly ($p < 0.05$) after chemotherapy, as shown in **Fig 5.4**. Therefore, despite any potential neutropenic effects induced by chemotherapy, it is clear that neutrophil accumulation in tumours is increased in 3 out of 4 tumour models and chemotherapy types. Moreover, all four tumour types also showed a significant ($p < 0.05$) increase in the number of Ly6G$^+$TNFα$^+$ cells after chemotherapy, as seen in **Fig 5.3 B**. The percentage of Ly6G$^+$ cells that were TNFα$^+$ also increased in all 4 tumour types (**Fig 5.3 C**).

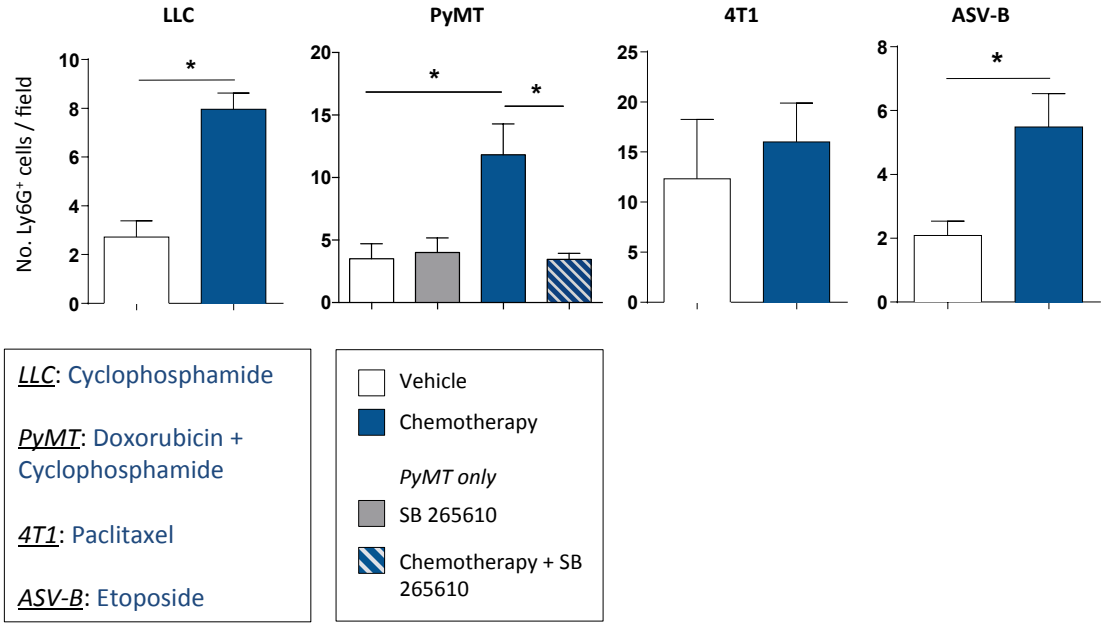

Figure 5.4 The number of Ly6G$^+$ cells increases in tumours in 3 out of 4 different tumour models given different types of chemotherapy. Significantly increased numbers of Ly6G$^+$ TANs were observed in LLC, PyMT and ASV-B tumours treated with cyclophosphamide, doxorubicin plus cyclophosphamide and etoposide, respectively. Treatment of PyMT-bearing mice with both chemotherapy and SB 265610 successfully blocked this recruitment of neutrophils to tumours post-chemotherapy. Data from ASV-B tumours shows double stained CD11b+Ly6G+ cells, and CD11b+Ly6G+TNFα+ cells. Images were taken at x25 magnification. Pooled data from 5 identical experiments (LLC, PyMT), 4 identical experiments (ASV-B) or 3 identical experiments (4T1) are shown, * $p < 0.05$.

5.4.3 TUMOUR LEVELS OF TNFA PROTEIN ARE INCREASED FOLLOWING CHEMOTHERAPY TREATMENT IN THE SYNGENEIC LLC MURINE LUNG CANCER MODEL AND TRANSPLANTED PYMT MURINE MAMMARY TUMOUR MODEL

Overall TNFα protein levels in Lewis lung carcinoma (LLC) tumours, treated with/without cyclophosphamide chemotherapy, were measured by confocal microscopy. The fluorescence intensity of TNFα staining was measured in Z-stacks from these tumours to get a semi-quantitative measurement, based on a previously described method [148].

Levels of TNFα in chemotherapy-treated tumours were increased above size-matched controls, as shown in **Fig 5.5 B**, which supports the findings in **Chapters 3** and **4**. Additionally, the number of TNFα⁺ cells (**Fig 5.5 C**) showed an increasing trend between control and chemotherapy-treated tumours,

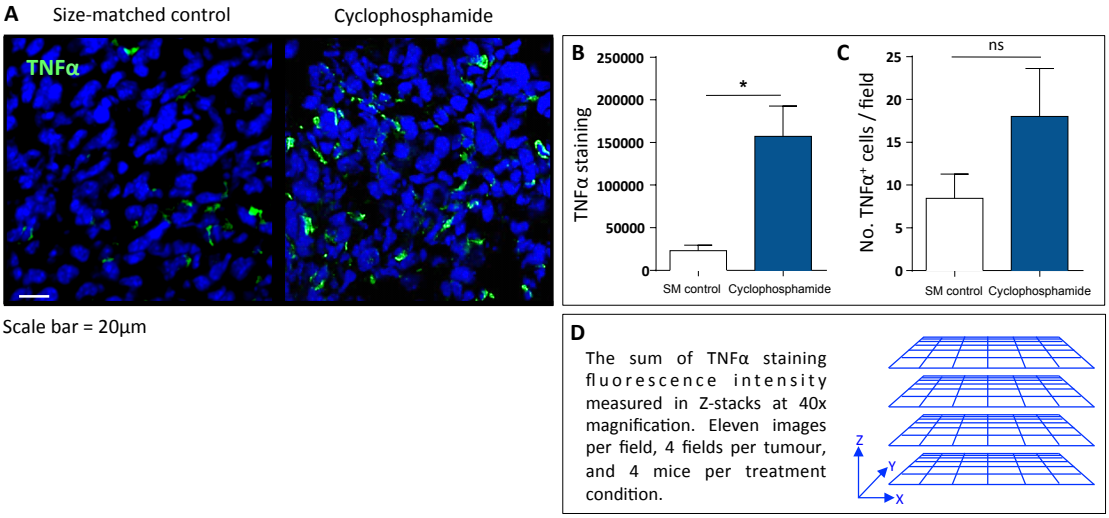

Figure 5.5 TNFα protein levels generally increase in LLCs in following treatment with cyclophosphamide although the number of TNFα⁺ cells was not significantly increased. (A) Representative images of TNFα staining (green) and DAPI (blue) in LLCs. Tumour-bearing mice were treated with cyclophosphamide chemotherapy (150mg/kg), and (B) the level of TNFα was significantly increased in tumours excised from cyclophosphamide-treated mice, by comparison with size-matched tumours from control mice injected with vehicle only. (C) The number of all TNFα-expressing cells did not significantly increase, but a clear trend towards an increase was observed. Therefore, significant increase in TNFα staining (B) must be due to an increase in mean fluorescence per cell. (D) TNFα levels were determined using a semi-quantitative analysis of TNFα immunofluorescent staining in Z-stack images (see **section 2.2.12.3**). Images were taken at x40 magnification. The mean ± SEM from 4 experiments are shown, Mann-Whitney U test, * $p < 0.05$. Scale bar = 20μm.

however the difference was not significant. Importantly, similar experiments using the PyMT transplant model showed a similar significant TNFα protein induction in chemotherapy-treated tumours, as compared to control tumours (**Fig 5.6 C**). Furthermore, a marked and significant (p = 0.0143) increase in the number of TNFα⁺ cells was seen in this model (**Fig 5.6 D**).

5.4.4 TNFA UPREGULATION IN CHEMOTHERAPY-TREATED TUMOURS CAN BE DIMINISHED BY SYSTEMIC INHIBITION OF THE CXCR2 RECEPTOR IN A PYMT TRANSPLANT MODEL

The increase in the levels of TNFα in the tumour post-chemotherapy (**Fig 5.6 C**), measured by a semi-quantitative method, was matched by an increase in the number of TNFα⁺ cells (**Fig 5.6 D**). Notably, both changes were prevented by

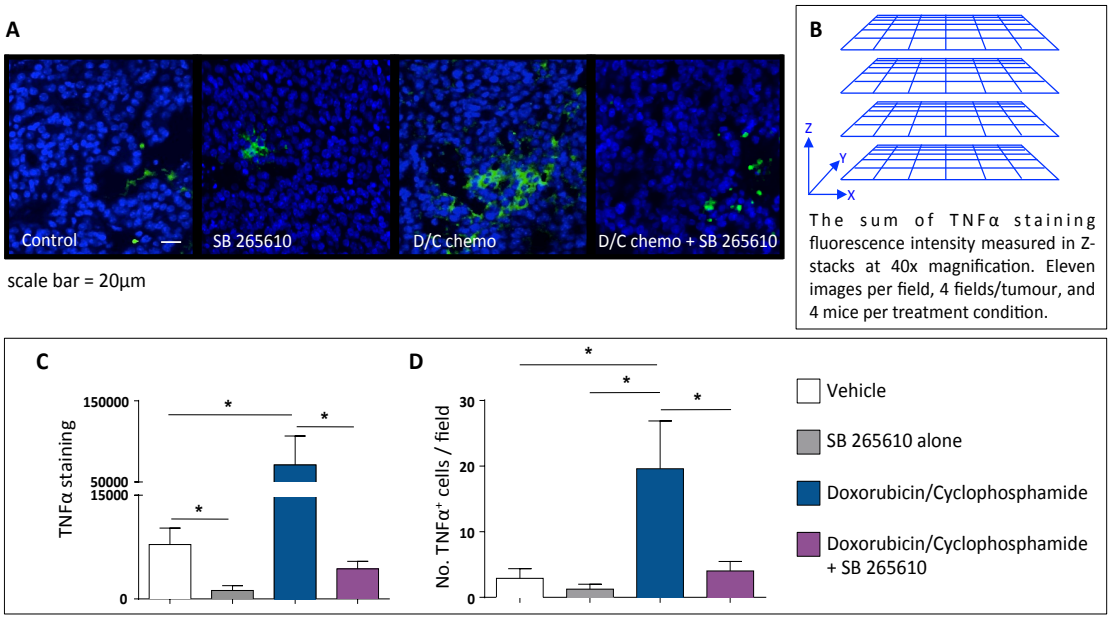

Figure 5.6 Overall TNFα levels in PyMT transplants significantly increase following doxorubicin and cyclophosphamide treatment: blockade by systemic CXCR2 inhibition. Mice injected with PyMT tumors were treated with chemotherapy and SB 265610, a CXCR2-specific inhibitor. (A) Representative images of control, chemotherapy- and SB 265610-treated PyMT tumours showing TNFα (green) and DAPI (blue) and (B) schematic diagram of Z-stack imaging. Images were taken at x40 magnification. Scale bar = 20μm. (C) Semi-quantitative analysis of TNFα staining showed that intratumoural TNFα levels increase significantly in chemotherapy-treated tumours, but that combining chemotherapy with SB 265610 treatment significantly reduced this upregulation. (D) A similar pattern was observed in the number of TNFα⁺ cells. The mean ± SEM from 4 identical experiments (vehicle, Dox/Cyc) or 3 identical experiments (SB 265610, Dox/Cyc plus SB265610) are shown, Mann-Whitney U test, * $p < 0.05$.

inhibition of CXCR2 receptor using SB 265610. This suggests that signalling through CXCR2 (expressed most highly on granulocytic cells, at least in LM2 murine breast tumours, **Fig. 5.1**) is central to TNFα upregulation by chemotherapy. The CXCR2 inhibitor-alone group trended towards a decrease in TNFα$^+$ cells, and a significant ($p = 0.0286$) decrease in immunodetectable TNFα was observed in tumours from SB 265610-treated mice, in comparison with control tumours.

5.4.5 Neutrophils are not the only TNFα-expressing cells in PyMT and LLC tumours that respond to CXCR2 inhibition

During imaging of tumour sections it was noted that not all TNFα$^+$ cells were Ly6G$^+$ neutrophils. Many other cell types are known to express TNFα in tumours, including macrophages [266], endothelial cells [126], T lymphocytes, B lymphocytes, NK cells [410], mast cells, and tumour cells [288]. Given that endothelial cell production of TNFα has been previously implicated in tumour growth, metastasis and response to chemotherapy [126], and the general importance of TAMs as major TNFα-producing cells [288], tumours were co-stained for TNFα and either the endothelial cell marker CD31, or the pan mouse macrophage marker F4/80. In addition, pericytes are capable of expressing TNFα [411], and so TNFα$^+$ perivascular cells (i.e. possible pericytes) were also counted in these tumour sections to assess their relative contribution. Had time permitted, it would have been good to use a pericyte marker, like alpha-smooth muscle actin (αSMA) or NG2 proteoglycan, to identify these cells in frozen sections. Similarly, tumour cells are also capable of expressing TNFα [272, 412], and given that markers for macrophages, neutrophils, endothelial cells and pericytes were used to stain for these cells, the remaining 'other' TNFα$^+$ cells are likely to be predominantly tumour cells. In addition, most of these 'other' TNFα$^+$ cells have larger nuclei, also suggesting that they might be tumour cells.

As seen in **Fig 5.7 A**, the largest increases in TNFα⁺ cells were seen in Ly6G⁺TNFα⁺ population and the 'other' population; however, significant increases ($p < 0.05$) were also observed in the number of F4/80⁺TNFα⁺ cells and CD31⁺TNFα⁺ vessels. The CXCR2 inhibitor SB 265610 alone did not significantly alter the number of TNFα⁺ cells of any cell population in comparison with control

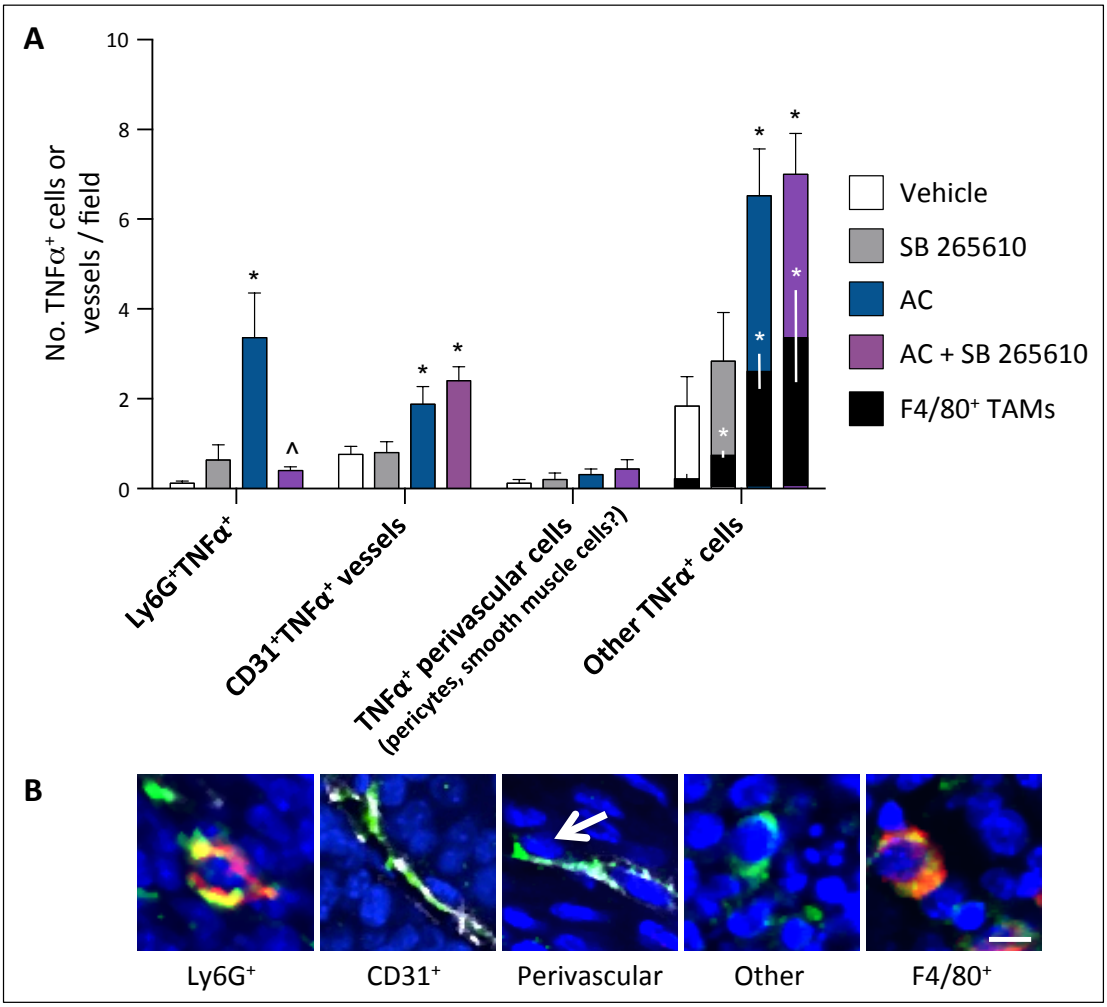

Figure 5.7 Identification of some of the TNFα-expressing cell types in PyMT tumours: effect of D/C therapy treatment in the presence or absence of CXCR2 inhibition. To identify TNFα⁺ cells other than Ly6G⁺ neutrophils, tumour sections were stained for the markers CD31 (endothelial cells) and F4/80 (macrophage), in conjunction with an anti-TNFα antibody. (A) The number of cells or vessels per field of view in control, CXCR2 inhibitor-treated, chemotherapy-treated and chemotherapy plus CXCR2 inhibitor-treated tumours. (B) Representative images of the different TNFα⁺ cell types in the tumour, showing TNFα (green), Ly6G (red; far left panel), CD31 (white) and F4/80 (red; far right panel). The mean ± SEM from 5 identical experiments are shown, or 4 identical experiments (F4/80⁺ TAMs). Differences in Ly6G⁺ cell numbers in PyMT tumours between this figure and **Fig 5.4** are due to different image magnifications. Images were taken at x40, Mann-Whitney U test, * $p < 0.05$ w.r.t. control, ^ $p < 0.05$ w.r.t. chemotherapy-treated group. Scale bar = 10μm.

tumours, except for F4/80$^+$TNFα$^+$ cells, which showed a small but significant (p = 0.0286) increase.

Importantly, combination of chemotherapy and CXCR2 inhibitor had very little effect on the number of TNFα$^+$ cells of all cell types – macrophages, endothelial vessels, perivascular cells, and 'other' cells – except for neutrophils; the number of Ly6G$^+$TNFα$^+$ cells reduced with the application of the CXCR2 inhibitor (**Fig 5.7 A**). Significantly, LLCs treated with cyclophosphamide (**Fig 5.8**) confirmed the findings of the PyMT model (with the exception of the CXCR2 inhibitor-treated groups). Increased TNFα$^+$ cells following chemotherapy treatment of tumours were noted in this model as well, with similar increases in Ly6G$^+$TNFα$^+$ cells and 'other' TNFα$^+$ cells. However, the number of CD31$^+$TNFα$^+$ vessels did not change, and a small but significant (p = 0.0176) increase in TNFα$^+$ perivascular cells was observed.

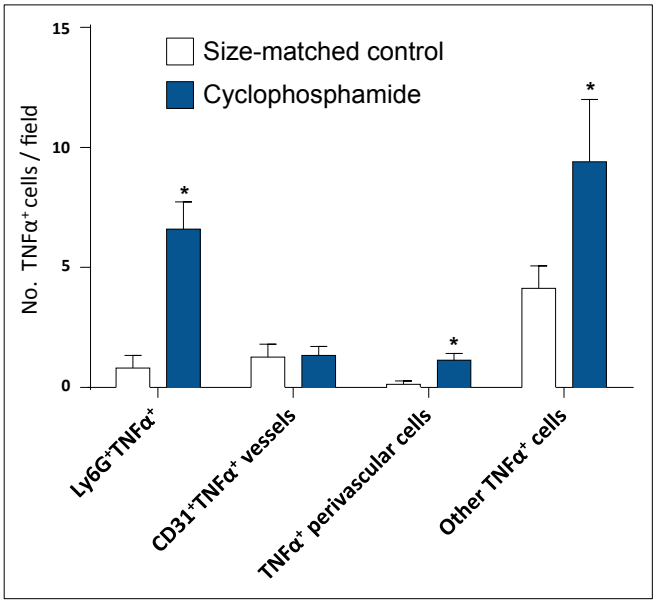

Figure 5.8 Identification of the TNFα$^+$ cell types in LLC tumours. To confirm the results in **Fig 5.7** using PyMT tumours, LLC tumours were also analysed by immunoflourescent staining for the number of TNFα$^+$ neutrophils, macrophages, endothelial cells, perivascular cells and 'other' (possibly tumour) cells. Similarly, the numbers of TNFα$^+$ neutrophils and 'other' cells increased significantly after treatment with chemotherapy, in comparison with size-matched controls. In contrast, however, the number of TNFα$^+$ endothelial cells did not change significantly, and the number of TNFα$^+$ perivascular cells increased, although numbers were still low. The mean ± SEM from 3 identical experiments are shown. Images were taken at x25. Mann-Whitney U test, * $p < 0.05$ w.r.t. size-matched controls.

5.4.6 DOXORUBICIN AND CYCLOPHOSPHAMIDE TREATMENT REDUCES TUMOUR VOLUME, AND COMBINED CHEMOTHERAPY AND CXCR2 INHIBITION LEADS TO A FURTHER, NON-SIGNIFICANT TREND

Tumour measurements were taken twice weekly during treatment and used to calculate tumour volume (provided by Dr. Joan Massagué; Memorial Sloan-Kettering Cancer Center, USA). The final tumour volumes measured at day 36 post partum are shown in **Fig 5.9**. Doxorubicin and cyclophosphamide chemotherapy treatment, as well as treatment with SB 265610, were initiated when tumour volume reached approximately 150mm^3 (see **section 5.3.4**). In comparison with control tumours, chemotherapy treatment reduced tumour volume. Chemotherapy plus SB 25610 also led to a significant ($p < 0.05$)

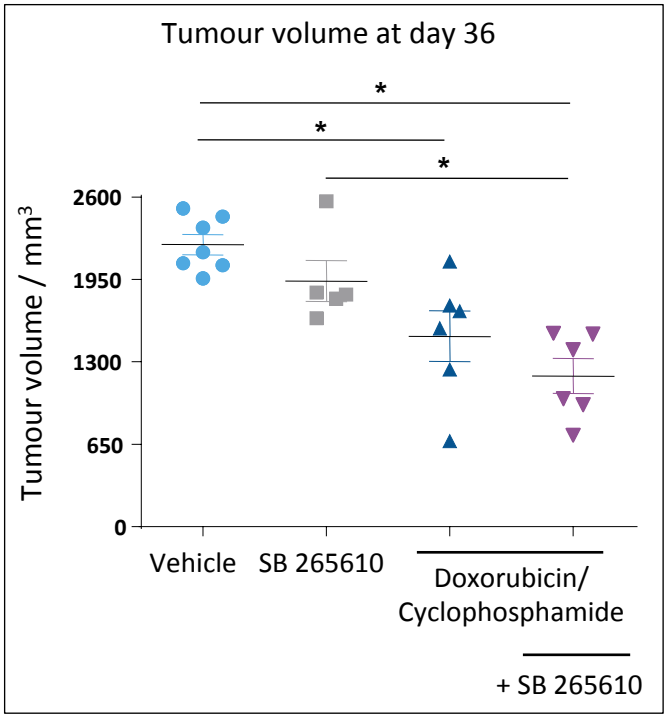

Figure 5.9 The size of PyMT tumour transplants was significantly reduced by doxorubicin and cyclophosphamide chemotherapy. These measurements of PyMT transplant size were recorded and kindly provided by Dr Massagué's group (Memorial Sloan-Kettering Cancer Center, USA). Tumour volumes taken before the mice were sacrificed showed a significant reduction in tumour volume after chemotherapy by comparison with control mice. The combination of chemotherapy and SB 265610 also reduced tumour volume, and a decreasing trend was seen between chemotherapy and chemotherapy plus SB 265610, but was not significant. The mean ± SEM 7 tumours (vehicle), 6 tumours (DOX/CYC and DOX/CYC plus SB 265610) or 5 tumours (SB 265610) are shown. Mann-Whitney U test, * $p < 0.05$.

decrease in tumour volume, as compared with both control tumours and SB 265610-only treated tumours. However, despite this group showing lower tumour volumes on average, the difference between chemotherapy-treated and chemotherapy plus SB 265610-treated tumours, was not significant. Tumour volumes in SB 265610-only treated mice were lower than control mice, but the difference was not significant.

5.4.7 Treatment with doxorubicin/cyclophosphamide and the CXCR2 inhibitor, SB 265610, results in an increase in tumour apoptosis in PyMT tumour transplants

Tumours were analysed by immunofluorescence microscopy for changes in the number of apoptotic cells between different treatment groups. To identify apoptotic cells, an anti-active caspase 3 antibody was used. Caspase 3 is cleaved early in apoptosis and it cleaves other apoptosis-related caspases, including caspases 6, 7 and 9 [413]. However, it is worth noting that caspase 3 is not required for apoptosis of all cells.

There was a trend towards increased numbers of active caspase 3^+ cells in tumours exposed to the CXCR2 inhibitor alone in comparison with control tumours (**Fig 5.10**). Surprisingly, a significant increase in the number of caspase 3^+ cells was not observed between control tumours and chemotherapy treated tumours, suggesting that chemotherapy did not induce apoptotic cell death (or at least a form of this which resulted in the generation of active caspase 3). These tumours were smaller (**Fig 5.9**) and so it is possible that doxorubicin and cyclophosphamide chemotherapy induce necrotic, rather than apoptotic, cell death. A comparison of chemotherapy-treated, and chemotherapy plus SB 265610-treated tumours, showed a significant ($p = 0.0286$) increase in apoptotic cells (**Fig 510**), suggesting that CXCR2 inhibition may prevent anti-apoptotic mechanisms required for cell survival after chemotherapy.

5.4.8 On-going metastasis study

The lungs from all of the PyMT transplant-bearing mice mentioned in the previous section were collected, fixed in formalin and embedded in paraffin wax, sectioned, and then stained for the PyMT antigen to identify metastatic foci in

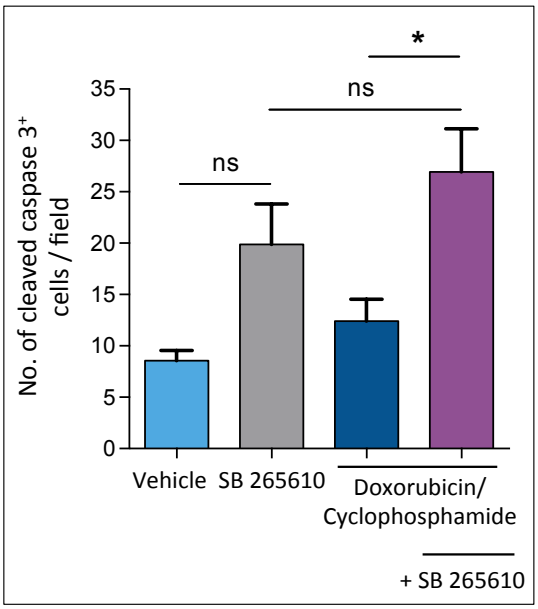

Figure 5.10 Cleaved (active) caspase 3 immunostaining shows that blocking CXCR2 with SB 265610 in combination with chemotherapy increases apoptosis in the tumour environment (compared to chemotherapy alone). PyMT tumour samples were stained by immunofluorescence for detectable levels of cellular active caspase 3. A non-significant increase in the number of apoptotic cells was seen in the SB 265610-only treated group in comparison with control tumours. No discernable increase was observed after chemotherapy but a significant increase was observed between chemotherapy (or vehicle) and the chemotherapy plus CXCR2 inhibitor groups. The mean ± SEM from 4 identical experiments (vehicle and DOX/CYC) or 3 identical experiments (SB 265610 and DOX/CYC plus SB265610) are shown, Mann-Whitney U test, * $p < 0.05$.

this tissue (as described in **section 5.3.6** and **Supplementary Method 1**). In summary, tissue sections were deparaffinised with xylene and histoclear and rehydrated using a series of ethanol washes. The sections were then subjected to heat-induced epitope retrieval in combination with citrate-based antigen retrieval solution. Slides were blocked with 2.5% normal goat serum and a rat anti-PyMT antibody was used (dilution 1:200) overnight in 2.5% normal goat serum. ImmPRESS reagent (anti-rat, mouse adsorbed) was used to detect the primary anti-PyMT antibody, and the peroxidase substrate DAB (3, 3'-diaminobenzidine) was used to detect signal. The lung tissue sections were then counterstained using haematoxylin, dehydrated and mounted with Cytoseal XYL (Richard-Allen Scientific). This work was done by Dan Macalinao in Dr. Joan Massagué's group (Memorial Sloan-Kettering Cancer Center, USA). Although the

staining for lung metastases has been optimised and metastases can be clearly seen in paraffin-embedded lung sections (**Fig 5.11**), the number of micrometastases was low and they were very small, and so were not were not suitable for analysing the effects of chemotherapy and SB 265610 on metastasis. The low numbers of metastatic cells is likely due to the short duration of the treatment, which lasted just 15 days before the mice were culled. This experiment is currently being repeated with longer treatment duration to allow larger metastases to form.

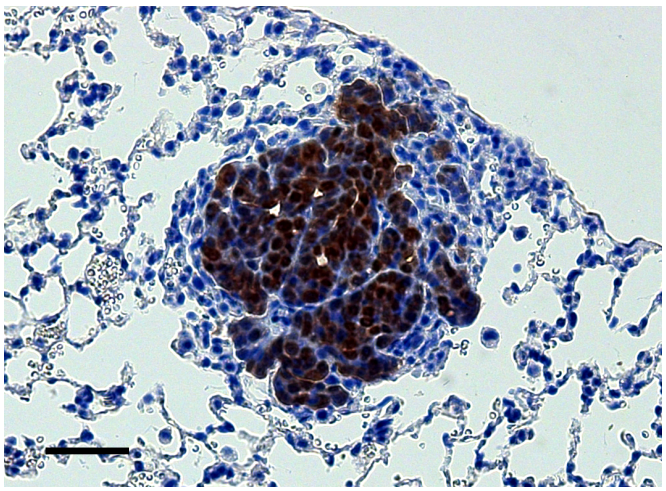

Figure 5.11 Immunohistochemical identification of lung micrometastases in mice with orthotopic PyMT transplanted tumours. Five µM sections lungs from PyMT tumour-bearing mice were immunostained for PyMT antigen. Small metastatic foci were detected but the numbers of these were low. This experiment is, therefore, currently being repeated in the Massagué lab, using a longer treatment duration (to allow the metastases to grow to a larger size). Scale bar = 100µm

5.5 DISCUSSION

In summary, this chapter investigated the *in vitro* findings from **Chapter 3** and **Chapter 4** in an *in vivo* setting, using various tumour models in which mice were administered different forms of chemotherapeutic agent. Immunofluorescent analysis of F4/80 and CXCL1 in PyMT tumours showed that the number of $CXCL1^{+}$ macrophages increased after chemotherapy. However, large numbers of $F4/80^{-}$ cells were also $CXCL1^{+}$, suggesting CXCL1 upregulation

is a more general feature of tumour response to chemotherapy, and increased further in tumours treated with combined chemotherapy and CXCR2 inhibition. Four tumour models treated with different chemotherapies were used to investigate neutrophil accumulation and TNFα expression. In all 4 models, $Ly6G^{+}TNF\alpha^{+}$ cells were significantly ($p < 0.05$) increased following chemotherapy treatment. A semi-quantitative analysis of overall TNFα protein levels in LLC and PyMT tumours suggested a similar chemotherapy-specific upregulation, and importantly, this was inhibited in PyMT tumours when chemotherapy was given with CXCR2 blockade. Not all $TNF\alpha^{+}$ cells were neutrophils, and immunofluorescent analysis of different cell populations showed that numbers of $TNF\alpha^{+}$ neutrophils and 'other' cells, including macrophages and presumably tumour cells, increase in chemotherapy-treated PyMT and/or LLC tumours. Smaller increases in $TNF\alpha^{+}$ endothelial cells and perivascular cells were seen in PyMT and in LLC tumours, respectively. Nonetheless, as expected, only the number of chemotherapy-induced $TNF\alpha^{+}$ neutrophils decreased in PyMT tumours upon CXCR2 blockade. Although tumour volume trended towards a decrease in combined chemotherapy and SB 265610-treated mice, the difference between this group and chemotherapy alone was not significant. Analysis of the number of apoptotic cells did, however, show increased induction of apoptotic cell death with combined therapy, suggesting that SB 265610 treatment can improve tumour responsiveness to chemotherapy.

Macrophage expression of CXCL1 is known to be important for the recruitment of neutrophils in tissue inflammation [93]. The data in this chapter show that inhibition of CXCR2 did not significantly reduce the effect of chemotherapy on $CXCL1^{+}$ TAM accumulation, and therefore, this and possibly $CXCL1^{+}$ TAM survival may not be dependent on CXCL/CXCR2 signalling. It remains to be seen what the factors are that either recruit $CXCL1^{+}$ TAMs or activate $CXCL1^{-}$ TAMs to express CXCL1 (and possibly other CXCLs). With further experimentation, it might be possible to determine whether TAMs accumulate and express CXCL1 after chemotherapy via activation of TLR4 signalling [92], induced by damage-associated molecular patterns (DAMPS; e.g. HMGB1, HSPs, ATP) that are released by necrotic cells. Although the number of $F4/80^{+}CXCL1^{+}$

cells markedly increased post-chemotherapy, an increase was also seen in F4/80^{-}CXCL1^{+} cells which could have been tumour cells since they were large cells with large nuclei. To investigate whether these cells are tumour cells, an anti-cytokeratin antibody (binds tumour cells) could have been used in combination with CXCL1. As mentioned previously, several different cell types in the tumour are capable of secreting CXCL1 [93, 126, 232, 350]. Therefore it is not possible to guarantee the source of CXCL1 stain in these images. However, only cells with overlapping F4/80 and CXCL1 stain were counted for F4/80^{+}CXCL1^{+} cell counts. Additionally, it is worth noting that the control PyMT tumours were not size-matched to the chemotherapy treated tumours, and that tumour volume has previously been shown to affect TAM phenotype [414]. Therefore, it is possible that the larger size of control tumours affected the expression of CXCL1 by macrophages or other cells. This applies to other findings below, except for LLC tumour data where the controls were size-matched. Interestingly, these *in vivo* results are contrary to the finding that tumour cells in docetaxel-treated tumour spheroids failed to upregulate CXCL1 expression (**Fig 3.6**). This could be due to the use of a different type of chemotherapy (doxorubicin and cyclophosphamide in the PyMT study and docetaxel in the *in vitro* studies), the type of tumour cells used (PyMT transgenic murine mammary tumour cells, and human A549 lung carcinoma cells in *in vitro* studies), or because the *in vitro* spheroid model lacks true *in vivo* complexity (such as the presence of vasculature or lymphocytes, which may be needed for tumour cells to express/upregulate CXCL1). Alternatively, the non-F4/80^{-} cells seen to upregulate CXCL1 in PyMT tumours after doxorubicin and cyclophosphamide treatment may not have been tumour cells, but rather an abundant stromal cell type like fibroblasts [415]. The increase in F4/80^{-}CXCL1^{+} cells shows that this chemotherapy-induced CXCL1 expression is not just a feature of macrophages but is a more general effect. It has not been identified here whether this is a direct or indirect effect of chemotherapy (doxorubicin and cyclophosphamide) on these cells/cell types. Previously, LM2 murine mammary cancer cells have been shown to express higher levels of CXCL1 protein in response to TNFα *in vitro*, and that inhibition of the NF-κB pathway blocked this [126]. Therefore, it is also possible that PyMT murine mammary cancer cells also respond to

doxorubicin- and cyclophosphamide-induced TNFα (**Fig 5.6**) via an NF-κB-dependent mechanism to upregulate CXCL1. Although combining chemotherapy with SB 265610 had no discernable effect on $CXCL1^+$ macrophages, it led to a significant increase in the number of other $CXCL1^+$ cells, possibly because CXCR2 inhibition blocked a negative feedback mechanism that normally limits CXC chemokine production. Cells in the tumour, potentially tumour cells, may have a negative feedback regulatory loop that relies on CXCR2 signalling, such that high levels CXC chemokines (including CXCL1) feedback and inhibit tumour cell production of these chemokines. Blocking this negative feedback by SB 265610 would cause the cells to upregulate CXCL1. It is possible therefore that using combined chemotherapy and SB 265610 in the clinic may lead to higher levels of CXCL1 being expressed by tumours, and possibly released into the bloodstream to recruit tumour-promoting neutrophils.

CXCL1 signals only through the CXCR2 receptor even though it reportedly binds to the non-signalling receptor, Duffy, and two viral receptors [30]. Therefore, the pro-tumour effects of CXCL1, such as the promotion of melanoma and breast tumour growth [126, 340], tumour angiogenesis in colorectal cancer [341], and metastasis in breast cancer [126] could conceivably be blocked by the systemic inhibition of such a CXCR2 inhibitor as SB 265610 (if it is safe to do so in patients). Nevertheless, if tumour/plasma CXCL1 protein levels also increase in cancer patients given chemotherapy and SB 265610 therapy, it might mean that a high concentration of SB 265610 needs to be administered for effective blockade of CXCR2 signalling, and this could be associated with harmful side effects.

Chemotherapy can cause neutropenia, in both humans and mice [394, 416]. Therefore, a neutropenic state associated with fewer circulating neutrophils could lead to lower intratumoural neutrophil counts. However, immunofluorescent staining of four different tumour models and types of chemotherapy suggested the opposite, since 3 out of 4 chemotherapeutic regimes in different tumour models induced a significant ($p < 0.05$) increase in accumulation of $Ly6G^+$ TANs (**Fig 5.4**). Recruitment of neutrophils/granulocytic cells into the tumour by CXC chemokines has been previously described [126,

185], and it has been suggested that chemotherapy encourages this process [126], although the supporting evidence is not definitive. As mentioned previously, PyMT, 4T1 and ASV-B models lacked size-matched controls, and so it is possible that neutrophil infiltration is also affected by tumour size, rather than (or as well as) chemotherapy treatment. Therefore, despite the fact that the results from these non-size-matched models are very similar to those from the LLC model, which did have size-matched controls, these experiments should be repeated using size-matched control tumours for proper comparison. In addition, although Ly6G is a good marker for murine neutrophils [399] and more than 94% of Ly6G cells also stained for CD11b (**Table 5.1**), combined use of anti-$CD11b^+$ and anti-Ly6G antibodies would have allowed the counting of dual stained $CD11b^+Ly6G^+$ cells, which would ensure more accurate counting of neutrophils. This was done with the ASV-B model here, shown in **Fig 5.3**.

A marked upregulation in the overall levels of immunoreactive TNFα was seen in both LLCs and PyMT transplants after chemotherapy, confirming earlier reports that chemotherapy increases TNFα expression by endothelial cells, bone marrow-derived cells and smooth muscle cells in murine mammary tumours [126]. Higher TNFα in tumours correlates with poor prognosis in many types of cancer [268-271], and is known to induce epithelial-mesenchymal transition (EMT) in colon cancer spheroids [280], and so such a chemotherapy-induced increase in TNFα may support tumour invasiveness. This is further supported by the finding that LM2 mammary tumour cells treated with TNFα for two hours showed an upregulation of CXCL1, which correlated with increased $S100A9^+$ cell accumulation in tumours, enhancing tumour survival and metastasis [126].

Crucially, a dramatic reduction of TNFα staining was observed in PyMT tumours following treatment with chemotherapy and SB 265610, demonstrating that chemotherapy-specific TNFα upregulation is dependent upon CXCR2 signalling. The fact that granulocytes/neutrophils are the main *Cxcr2*-expressing cell in LM2 tumours (**Fig 5.1**), are known to be recruited and activated by CXCR2 signalling [93], and are capable of expressing TNFα [146, 295], suggests that SB 265610 may block neutrophil recruitment and TNFα-expression in these tumours. This is, however, based on semi-quantitative fluorescence intensity

values from a Z-stack through 10μm sections of tumour, and ideally would have been confirmed by western blot analysis or ELISA of tumour homogenates from this experiment. However, such tumour samples were not available as the LLC and PyMT studies had already been completed by the time of the immunofluorescent analyses reported in this thesis.

Furthermore, a set focal distance between each Z-stacked image was not used when generating Z-stacks, but instead, just the numbers of images per stack were kept constant. Ideally, both the numbers of images and the depth/distance (in the Z-axis) between images would be kept the same. It is possible that antibodies bind more readily to epitopes on the surface of the (10μm-thick) sections and are less efficient at binding epitopes deeper into the tissue, meaning the staining is not uniform across the section, thus making it important to keep a constant depth between captured images. However, the high number of images taken per stack (11 images) across the 10μm-thick sections meant that despite not using a set Z-axis distance, the distance between Z-stacks did not differ by much and is unlikely to have had a significant effect on the overall results.

TNFα can be expressed on cell surfaces as a membrane-bound protein, secreted into the local environment as a soluble factor, or bound to TNF receptors, TNFRI and TNFRII [288, 417]. Therefore, as with CXCL1, it is possible that staining for each factor may not represent expression by a given cell, but could represent uptake of these factors by the cell. The TNF receptor, TNFRI, is constitutively expressed at low levels on almost all nucleated human cells, and TNFRII is expressed on myeloid cells including macrophages, as well as peripheral T cells and alveolar lymphocytes [418-422]. These receptors can be enzymatically cleaved from the cell surface to form soluble receptors (sTNFRI and sTNFRII), which are able to neutralise TNFα and act as TNFα antagonists, or to stabilise soluble TNFα by binding it and forming a more stable complex [423]. Therefore, TNFα signal detected by immunofluorescence could be due to the detection of membrane-bound TNFα, soluble TNFα, TNFα being taken up by TNFRI/TNFRII-expressing cells, or bound by soluble forms of these receptors in a neutralising or stabilising way, and may have very different effects in the tumour microenvironment. However, since TNFα was detected in these tumour

sections using an antibody that also neutralises TNFα (Rat anti-mouse TNFα FITC; Biolegend, UK), only 'free' TNFα that is not bound to TNF receptors would be stained (since they bind competitively). With more time and access to freshly-excised tumours, cell populations could have been analysed by flow cytometry to see if there is an observable increase in viable $CD11b^{+}Ly6C^{-}Ly6G^{+}$ cells (TANs) in the tumour. FACS could then have been used to separate various cell types (neutrophils, macrophages, endothelial cells, lymphocytes, tumour cells) and their ability to release TNFα or CXCL1 could have been assessed in short-term cultures by ELISA.

Given that cells other than neutrophils are known to express TNFα in the tumour [126, 266, 288, 410], and that not all $TNF\alpha^{+}$ cells were $Ly6G^{+}$, further characterisation of $TNF\alpha^{+}$ cells in the PyMT and LLC was done. Analysis of the number of TNFα-expressing cells of key tumour populations in two different models offers novel insight into the expression of this important cytokine in the vehicle-treated and chemotherapy-treated tumour. Additionally, the PyMT model was used to observe the changes in $TNF\alpha^{+}$ cells of each population following CXCR2 inhibition with SB 265610, for the study of how this inhibitor may alter CXCR2-expressing cell dynamics. In both tumour models, neutrophils and the 'other' cell group showed upregulation of TNFα expression after chemotherapy, as well as macrophages, which were not investigated in the LLC model but should be confirmed in future studies. A smaller but significant ($p = 0.0159$) induction in $CD31^{+}TNF\alpha^{+}$ vessels in the PyMT model was observed, which confirmed previous observations with this chemotherapy regimen and in a breast tumour model [126], but this might not be a general feature since there was no significant difference in LLC tumours. The 'other' cell population is likely to be mostly tumour cells, judging by larger nuclear morphology and by elimination of neutrophils, endothelial cells and perivascular cells. Increasing numbers of $TNF\alpha^{+}$ tumour cells would align with prior reports that tumour cells express TNFα [272, 363] and show that they respond to chemotherapy to upregulate this cytokine. Given the opposing roles that TNFα can have in different concentrations and environments, as evidenced by pro- and anti-tumour functions in cancer [288], the increased expression of TNFα by

(unconfirmed) tumour cells following chemotherapy-induced stress, suggests that this molecule is advantageous for their survival. Such advantages could include recruitment of pro-tumour TAMs to the tumour [363], increased angiogenesis [424] and metastasis [280, 425].

Interestingly, PyMT tumours from mice treated with combined chemotherapy and SB 265610 clearly demonstrated that only the $Ly6G^+$ cell population responded to CXCR2 inhibition, and macrophages, endothelial cells, perivascular cells and 'other' cells did not. These results explicitly demonstrate that, at least in the PyMT murine breast tumour transplant model, SB 265610 at this concentration (2mg/kg) only modulates $Ly6G^+$ cell recruitment and/or production of TNFα. The $Ly6G^-$ cell populations either do not respond to the inhibitor, or compensate between cell recruitment and TNFα expression, such that the number of $TNF\alpha^+$ cells remains unchanged. Given that granulocytes were shown to be the main *Cxcr2*-expressing cells in the LM2 metastatic breast cancer model, it seems likely that SB 265610 is showing specificity for granulocytes/neutrophils in this experiment. Use of this CXCR2 inhibitor was also indirectly associated with $CD11b^+Gr1^+$ cell reduction in tumours from combined chemotherapy and SB 265610-treated mice, in comparison with chemotherapy-treated mice without the inhibitor [126]. Furthermore, the results in **Fig 5.4** show that CXCR2 inhibition decreases both the number of neutrophils, as well as the percentage of neutrophils that are $TNF\alpha^+$. Therefore, CXCR2 inhibition is not just blocking the recruitment of neutrophils by CXC chemokines secreted by macrophages and other cells, but is blocking neutrophil induction of TNFα, potentially also induced by the same CXC chemokines. Previously it has been reported that CXCR2 ligands are able to induce TNFα [426], supporting this hypothesis; however, the induction of TNFα by CXCL1 and CXCL5 was shown to be via macrophages, and could be inhibited by reparixin (CXCR1 and CXCR2 inhibitor), whereas macrophages in the PyMT tumour model did not respond to CXCR2 inhibition. This discrepancy could be because reparixin inhibits both CXCR1 and CXCR2, which are both expressed on macrophages and neutrophils [427], whereas SB 265610 is far more specific for CXCR2 [409].

The fact that SB 265610 specifically reduces the number of $Ly6G^+TNF\alpha^+$ cells, and does not affect other populations, suggests that inhibiting neutrophil contribution to TNFα in the tumour results in the significant decrease seen in overall TNFα levels in the PyMT tumour with the SB 265610 inhibitor. Since $TNF\alpha^+$ neutrophils are outnumbered by $TNF\alpha^+$ 'other' cells and are at a similar level to $TNF\alpha^+$ macrophages, this implies that neutrophil production of TNFα is greater per cell than these other populations. The 'other' cell population will also include such non-tumour CXCR2-expressing cells as lymphocytes, dendritic cells, mast cells, and NK cells, so it is possible that some of these cells may produce TNFα and be responsive to SB 265610, but that the inhibitory effects are masked by other populations in this group. Crucially, however, the suggested use of SB 265610 in combination with chemotherapy aims to reduce pro-tumour effects of recruited myeloid cells, specifically neutrophils. Although combination therapy dramatically decreases the number of $TNF\alpha^+$ neutrophils in comparison with chemotherapy alone, the larger $TNF\alpha^+$ 'other' and considerable $TNF\alpha^+$ macrophage populations appear unchanged by combined therapy, which elicits the question of whether TNFα from these populations will still maintain the pro-tumour and pro-metastatic effects suggested in **Chapter 4**. It seems, however, that inhibition of neutrophil-derived TNFα by SB 265610 treatment does in fact suppress overall TNFα levels, therefore suggesting that other $TNF\alpha^+$ populations cannot maintain the high level of TNFα production in the absence of neutrophils, making combined SB 265610 and chemotherapy very relevant to the clinical setting.

The data on changes in the size of PyMT transplants after chemotherapy in the absence or presence of a CXCR2 inhibitor (provided by Dr. Joan Massagué's lab for the general interest of the reader and to accompany the immunofluorescent staining done here) showed that chemotherapy significantly ($p = 0.0041$) reduced tumour size, compared to control tumours. Chemotherapy is well known to reduce the size and growth of tumours, and to correlate with better prognosis in many types of cancer [428-431]. Similarly, chemotherapy given with SB 265610 also reduced tumour volume in comparison with control tumours, and SB 265610 only-treated tumours. However, the difference between

the volumes of combination therapy-treated tumours and standard chemotherapy-treated tumours failed to reach significance ($p = 0.0898$), unlike previous reports using the LM2 murine mammary tumour model [126]. In the current PyMT tumour study, one tumour was smaller in size than the others in the chemotherapy-treated group, but was not found to be an outlier by Chauvenet's criterion test. Since there is a clear trend, but only 6 mice were included in each group, the Massagué group is currently repeating this PyMT experiment in order to make the analysis more robust.

As mentioned, combining doxorubicin and cyclophosphamide chemotherapy with SB 265610 has also been shown to make LM2 tumours more responsive to chemotherapy [126]. To see whether such combined therapy might increase apoptosis in PyMT transplants (without causing changes in tumour volume), tumours were stained with an anti-active caspase 3 antibody, and the number of cleaved caspase 3^+ cells counted. The fact that SB 265610 alone showed an increasing trend (non-significant) in comparison with control tumours, suggested that blocking CXCR2 signalling even in tumours not undergoing chemotherapy treatment might be beneficial. It will be interesting to see if this achieves significance after the Massagué lab has completed the repeat experiment by the end of December 2013. If so, this would be in line with an earlier report in which AZ10397767 (Astrazeneca), a small molecule CXCR2 inhibitor, reduced neutrophil infiltration into A549 lung carcinoma spheroids *in vitro* and *in vivo*, slowing tumour growth and progression [185]. Remarkably, in the PyMT transplants stained in the current study, chemotherapy treatment failed significantly to increase tumour apoptosis compared to control tumours. Since chemotherapy-treated tumours were significantly smaller, it is possible that the treatment induced cell death by necrosis, not apoptosis, or that it just slowed tumour replication dramatically. However, the main mechanism of tumour cell killing for both doxorubicin and cyclophosphamide reported in the literature is via induction of apoptosis [432, 433], and so higher numbers of cleaved caspase 3^+ cells would be expected in chemotherapy-treated tumours in comparison with control tumours. These data suggest that this chemotherapy regimen may not have been fully effective in these mice, even with the significant

reduction in tumour volume. Future studies could confirm these findings using other apoptosis assays such as TUNEL or annexin-V staining of tumours after chemotherapy treatment.

Previously, combining these chemotherapeutic agents with this CXCR2 inhibitor reduced the formation of lung metastases in mice [126]. However, this was shown using the highly metastatic cell lines MDA231-LM2 and CN34-LM1, selected for their metastatic potential, grown as orthotopic xenografts. It remains to be seen whether this combination is effective in the less metastatic PyMT transplant model.

CHAPTER 6: SUMMARY AND GENERAL DISCUSSION

As outlined in detail in **Chapter 1**, macrophages and neutrophils are major components of the innate immune system. They have a common lineage in their early stages of development and share a number of characteristics as mature cells (see **Table 1.2**). However, at later stages of maturation, these two cell types acquire a number of distinct features which enable them to cooperate in early immune responses to infection and inflammation [56]. In addition to stimulating other cells of the immune system [69, 106], neutrophils can recruit and activate monocytes (and vice versa) in acute inflamed sites via the release of such chemokines as CXCL1, CXCL2, and TNFα, as well as HNP1, HNP3 [87, 93]. Inflammation is a key component of both the onset and progression of many forms of malignant tumour [139], and the extent of tumour infiltration by such cells is an important determinant of disease outcome, as they have the potential to destroy or support tumours depending upon their state of activation [102, 146, 191, 295, 311]. Evidence is also emerging from *in vitro* studies that tumour exposure to cytotoxic agents can also lead to changes in the tumour microenvironment, which in turn lead to immune cell activation [291].

The work described in this thesis investigated the interplay between macrophages and neutrophils in chemotherapy-treated tumours – first in a variety of *in vitro* models and then in chemotherapy-treated mouse tumours. Human monocytes/macrophages were found to upregulate CXCL1, CXCL2 and CXCL5 after exposure to the human non-small cell lung cancer cell line, A549, treated with docetaxel *in vitro*. These findings suggested that monocytes infiltrating into tumours (and then differentiating into TAMs), may upregulate these chemokines in non-small cell lung cancer patients receiving docetaxel chemotherapy, as summarised in **Fig 6.1**. Had time permitted, it would have been interesting to see whether TAMs expressed these CXCL chemokines in resected human non-small cell lung carcinomas (NSCLCs) following their treatment with docetaxel (and possibly other chemotherapeutic agents). Dual immunofluorescent staining for TAMs (using an antibody for the pan macrophage marker, CD68) and CXCL1, CXCL2 or CXCL5, would allow the number of $CD68^{+}CXCL^{+}$ cells to be compared in docetaxel-treated versus

untreated NSCLCs. Ideally, these would be 'matched' samples (i.e. 'before' and 'after' chemotherapy) from the same patients. Furthermore, conditioned media from docetaxel-treated myeloid cells and tumour spheroids were shown to induce neutrophil migration *in vitro*, in a CXCR2-dependent manner. Neutrophils conditioned in this way expressed high levels of TNFα, CCL2 and CCL3, of which CCL2 and CCL3 were upregulated between docetaxel-treated and DMSO-treated groups. Given that CCL2 and CCL3 can recruit macrophages and/or neutrophils [145, 434], TANs in docetaxel-treated NSCLC tumours may contribute towards further recruitment of macrophages and neutrophils, resulting in higher levels of TAMs and TANs. Interestingly, increased numbers of TAMs have already been shown in chemotherapy (doxorubicin)-treated murine tumours as a result of upregulated CCL2 expression by (unidentified) stromal cells [212].

Neutrophil expression of TNFα was investigated further since TNFα can contribute towards genetic instability of tumour cells, tumour growth, epithelial-to-mesenchymal transition and invasiveness of tumour cells, metastasis and tumour angiogenesis (see **Table 4.2**), and was upregulated over 150-fold by neutrophils exposed to conditioned media from docetaxel-treated A549 spheroids and myeloid cells (in comparison with neutrophils cultured in spheroid-unconditioned medium containing DMSO). Notably, however, although a large increasing trend was seen between conditioned media from myeloid cell-infiltrated A549 spheroids treated with either docetaxel or DMSO, this difference was not significant. Nonetheless, media from myeloid cell-infiltrated A549 spheroids, treated with docetaxel and conditioned by neutrophils, induced A549 cells to become more invasive *in vitro*, via a mechanism that was dependent upon TNFα and neutrophil CXCR2-signalling (**Fig 6.1**). The above *in vitro* effects were not confined to docetaxel-treated tumour cells since similar results were obtained using a second chemotherapeutic agent, cyclophosphamide. This suggested that tumour cells exposed to a number of such commonly used therapeutic agents might elicit similar effects on TAMs and TANs.

So, the possible recruitment of TANs and their upregulation of TNFα after chemotherapy were then investigated in four different mouse tumour models (each treated with a different chemotherapeutic agent). These studies showed an increase in TNFα⁺ neutrophils in chemotherapy versus vehicle-treated mouse tumours. Furthermore, a collaborative study with the Massagué group in New York, showed that combining chemotherapy (doxorubicin and cyclophosphamide) with systemic inhibition of CXCR2 (using SB 265610) reduced both the number of TNFα⁺ neutrophils and the overall levels of TNFα in PyMT tumour transplants. However, the possible effect, if any, of this combined treatment on the formation of lung metastases in this mouse model had not been demonstrated at the time of submission of this thesis (and the focus of an ongoing study in the Massagué laboratory).

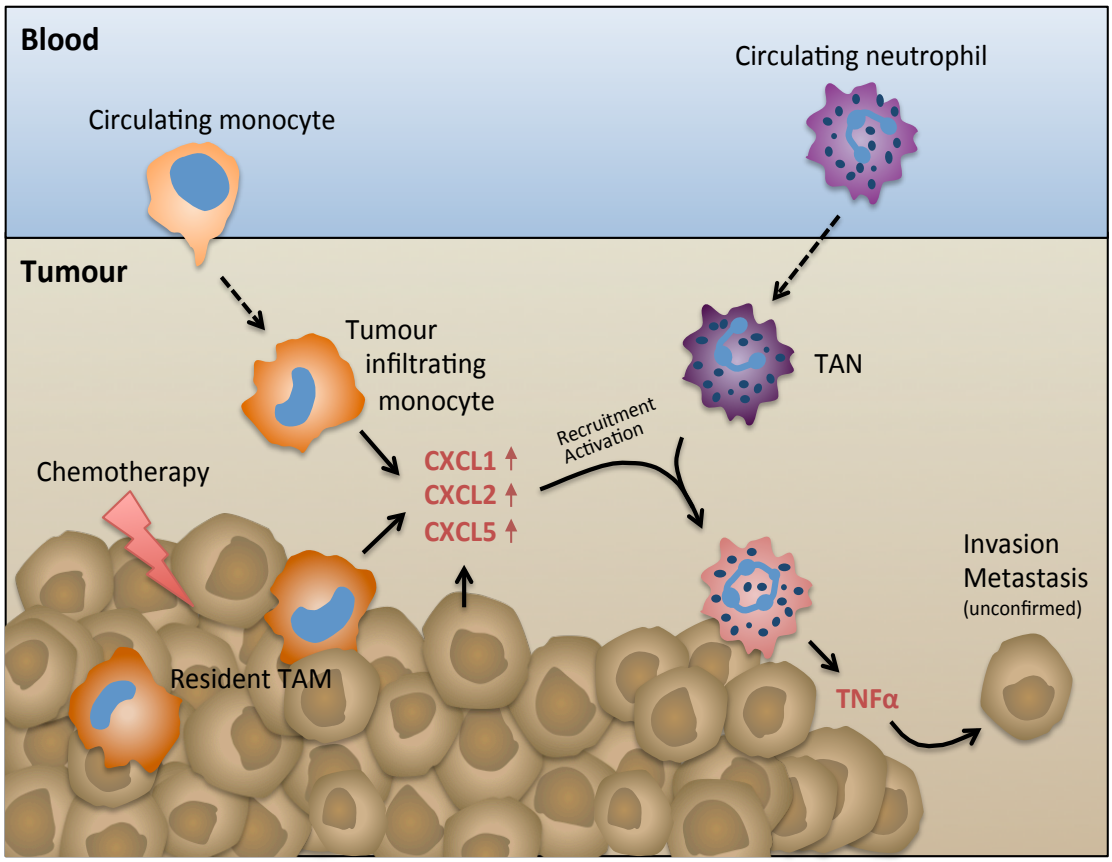

Figure 6.1 TAMs in chemotherapy-treated tumours may stimulate neutrophil recruitment and TNFα expression: possible role in the regulation of invasion/metastasis? Neutrophils also upregulated CCLs 2 and 3 under these conditions, which could have recruited more TAMs and TANs. TAM, tumour-associated macrophage; TAN, tumour-associated neutrophil; TNFα, tumour necrosis factor-alpha.

If combining doxorubicin and cyclophosphamide chemotherapy and the CXCR2 inhibitor does significantly reduce metastasis in the PyMT transplant tumour model, this may potentially have implications for the treatment of breast cancer patients. Doxorubicin and cyclophosphamide (sometimes known as 'AC' chemotherapy), is currently used to treat breast cancer patients [435], so it could perhaps be administered with SB 265610 to such patients as a neoadjuvant therapy to block the accumulation and activation of TANs in both primary and metastatic tumours. It has not been identified yet whether this mechanism of neutrophil accumulation and TNFα expression occurs in lung metastases (or any other form of metastasis) following chemotherapy, and so combining chemotherapy with CXCR2 inhibition may not be beneficial as adjuvant therapy, when the primary tumour has been resected. However, this combined treatment may be beneficial as a neoadjuvant therapy, and may improve the efficacy of chemotherapy and reduce tumour metastasis, as suggested previously in two metastatic mammary cancer mouse models treated with doxorubicin/cyclophosphamide plus SB 265610 [126].

In addition to such small molecular weight CXCR2 antagonists as SB 265610, the use of anti-CXCR2 antibodies could also be investigated in pre-clinical trials using this PyMT murine mammary cancer model. As discussed previously (see **section 1.9**), CXCR2 is expressed most highly on neutrophils, but can also be expressed by monocytes/macrophages, dendritic cells, endothelial cells, mast cells, lymphocytes, as well as such non-immune cells as neurons and glial cells. Therefore, systemic inhibition of CXCR2 is likely to block CXCR2-induced signalling in these cells as well, leading to possible side effects. Since CXCR2 signalling, like TNFα signalling, is important for inflammation and immune responses, it is possible that CXCR2 inhibitors will also leave patients susceptible to bacterial and fungal infection [246], as is sometimes observed with systemic TNFα inhibition (see **section 1.10.2**). The fact that mice deficient in CXCR2 have defects in the wound healing process [259] suggests that systemic CXCR2-inhibition of patients may also impede their wound healing responses. However, a safety and efficacy study of CXCR2 inhibitor SCH527123 (Schering-Plough) used to treat patients with severe asthma reported that SCH527123 was

safe, and was not associated with an increase in adverse events except for a small but significant increase in minor gastrointestinal symptoms [251]. A similar study observed the safety and efficacy of the CXCR2 inhibitor SB 656933 (GlaxoSmithKline), which was used for the treatment of patients with cystic fibrosis [258]. The inhibitor (given at doses of 20mg or 50mg) was generally well tolerated, although 5 of 146 patients were withdrawn from the trial due to adverse effects, and increases in the systemic inflammatory markers fibrinogen, C-reactive protein (CRP) and CXCL8 were found in the blood. SB 656933 was also reported to be safe and well tolerated, even up to 1100mg given as a single dose to healthy patients [257]. Therefore, initial clinical studies of the safety of CXCR2 inhibitors suggest that inhibiting CXCR2 systemically using small molecule CXCR2 antagonists (at biologically relevant doses) is safe in humans.

Follow-on studies are now warranted to investigate the effects of selectively knocking down expression of TNFα in neutrophils on metastasis in various murine tumour models. This could be done by inducing tumour formation in mice previously given a bone marrow transplant where the bone marrow cells had been treated with a lentivirus containing a short hairpin (sh)RNA against TNFα (or a control shRNA) under the control of the Ly6G promoter. Alternatively, murine neutrophils could be isolated from the tumours of $TNF\alpha^{-/-}$ mice and could then be injected into the tumours of wild-type mice. This is likely to increase the proportion of $TNF\alpha^{-/-}$ TANs within the tumours, and the growth and metastasis of these tumours could be compared with tumours injected with an identical number of neutrophils from tumours grown in wild-type (i.e. TNFα-expressing) mice.

Interestingly, the expression of TNFα was investigated in a mouse skin wound healing model by *in situ* hybridisation and immunofluorescence analysis [436], and was shown to be produced by a layer of neutrophils – and to a lesser extent by macrophages – in close proximity to wound clots. Neutrophil-derived TNFα is known to be a crucial part of the wound healing process [437]. So, it is tempting to speculate that tumours, which have been described as 'wounds that do not heal' [137], take advantage of such pre-existing 'wound healing' mechanisms as the upregulation of CXCL chemokines [58, 229] and the

recruitment/activation of TNFα-expressing neutrophils to support angiogenesis, matrix remodelling and tumour growth.

The findings of this thesis suggest that combining chemotherapy with TNFα inhibitors might also be beneficial in the treatment of cancer patients at risk of developing metastasis (i.e. stage 2 breast cancer patients, where the cancer may have spread to the lymph nodes, but has not metastasised yet). However, as discussed in **sections 1.10.2** and **4.1**, systemic inhibition of TNFα can be associated with increased susceptibility to infection.

Notably, combined chemotherapy and G-CSF is commonly used to treat a variety of cancers [438-440] in order to counteract the neutropenic side effects of many chemotherapeutic drugs, and the associated increase in susceptibility to infection. Granulocyte colony-stimulating factor is capable of mobilising peripheral blood progenitor cells, helping to sustain blood neutrophil numbers in chemotherapy-treated patients, which is important for protecting the body against infection. The use of chemotherapy and G-CSF combined therapy has been associated with improved progression-free survival in patients with chronic lymphocytic leukaemia [438]. However, such therapy is not beneficial in all types of cancer patients given chemotherapy, which includes early breast cancers [441] and inflammatory/locally advanced breast cancers [442]. Furthermore, combined chemotherapy and G-CSF therapy has even been identified as a poor prognostic factor in patients with head and neck squamous cell carcinoma when given as adjuvant therapy [443].

The use of combined chemotherapy and G-CSF to treat patients with cancer may appear contradictory to the results discussed here. Increased blood neutrophil levels stimulated by G-CSF, and the increase in CXC chemokine expression by macrophages and other cells in the tumour in response to chemotherapy (**Chapter 5**), would suggest that there would be more intratumoural neutrophils in tumours of these patients. Neutrophils can be polarised in the tumour by such factors as TGF-β, such that their tumour destructive properties are suppressed, and their tumour promoting/N2 phenotype activated [295]. Furthermore, the results in this thesis suggest that

these neutrophils may respond to the chemotherapy-treated tumour environment by upregulating their expression of TNFα, potentially stimulating tumour cell invasiveness, which is an important feature in the process of metastasis [444]. A possible reason why combined chemotherapy and G-CSF can improve patient prognosis is that G-CSF may promote the polarisation of TANs away from an N2 phenotype towards N1, restoring their tumour destructive capabilities (although TNFα has been reported to be expressed by N1-polarised neutrophils [295], but can support tumour progression and metastasis, as mentioned above). In a previous study, murine colon adenocarcinoma (C26) cells were unable to form tumours when injected into syngeneic mice transduced with the G-CSF gene, rather than an unrelated control gene, which correlated with very high numbers of associated neutrophilic granulocytes [445]. Interestingly, G-CSF has been shown to have opposing effects on the expression of TNFα by whole blood (including neutrophils) *in vitro*; G-CSF was found to increase TNFα expression as measured by ELISA, yet pre-treatment of whole blood with G-CSF reduced LPS-induced TNFα secretion [446]. Therefore, it is possible that combined chemotherapy and G-CSF treatment may condition neutrophils and reduce their expression of TNFα in response to stimuli in chemotherapy-treated tumours.

6.1 CONCLUDING REMARKS

The findings in this thesis identify a novel macrophage/neutrophil axis contributing to the upregulation of TNFα in tumours after chemotherapy. Crucially, TNFα has been shown to be upregulated in human primary breast tumours following neoadjuvant doxorubicin and cyclophosphamide chemotherapy [126]. This novel macrophage/neutrophil-dependent mechanism was found to involve the expression of CXC chemokines by TAMs and CXCR2 on neutrophils. If current studies combining chemotherapy with a CXCR2 antagonist in tumour-bearing mice show a reduction in the formation of post-therapy metastasis, this approach could be used in patients to reduce tumour recurrence and increase survival after chemotherapy.

REFERENCES

1. Cortez-Retamozo, V., et al., *Origins of tumor-associated macrophages and neutrophils.* Proc Natl Acad Sci U S A, 2012. **109**(7): p. 2491-6.
2. Akashi, K., et al., *A clonogenic common myeloid progenitor that gives rise to all myeloid lineages.* Nature, 2000. **404**(6774): p. 193-197.
3. Manz, M.G., et al., *Prospective isolation of human clonogenic common myeloid progenitors.* Proceedings of the National Academy of Sciences of the United States of America, 2002. **99**(18): p. 11872-11877.
4. Iwasaki, H. and K. Akashi, *Myeloid lineage commitment from the hematopoietic stem cell.* Immunity, 2007. **26**(6): p. 726-40.
5. Fogg, D.K., et al., *A clonogenic bone marrow progenitor specific for macrophages and dendritic cells.* Science, 2006. **311**(5757): p. 83-7.
6. Wynn, T.A., A. Chawla, and J.W. Pollard, *Macrophage biology in development, homeostasis and disease.* Nature, 2013. **496**(7446): p. 445-55.
7. Chow, A., B.D. Brown, and M. Merad, *Studying the mononuclear phagocyte system in the molecular age.* Nat Rev Immunol, 2011. **11**(11): p. 788-98.
8. Ginhoux, F., et al., *Fate mapping analysis reveals that adult microglia derive from primitive macrophages.* Science, 2010. **330**(6005): p. 841-5.
9. Hoeffel, G., et al., *Adult Langerhans cells derive predominantly from embryonic fetal liver monocytes with a minor contribution of yolk sac-derived macrophages.* J Exp Med, 2012. **209**(6): p. 1167-81.
10. Schulz, C., et al., *A lineage of myeloid cells independent of Myb and hematopoietic stem cells.* Science, 2012. **336**(6077): p. 86-90.
11. Borregaard, N., *Neutrophils, from marrow to microbes.* Immunity, 2010. **33**(5): p. 657-70.
12. Frankenberger, M., et al., *A defect of CD16-positive monocytes can occur without disease.* Immunobiology, 2013. **218**(2): p. 169-74.
13. Tsou, C.L., et al., *Critical roles for CCR2 and MCP-3 in monocyte mobilization from bone marrow and recruitment to inflammatory sites.* J Clin Invest, 2007. **117**(4): p. 902-9.
14. Serbina, N.V. and E.G. Pamer, *Monocyte emigration from bone marrow during bacterial infection requires signals mediated by chemokine receptor CCR2.* Nat Immunol, 2006. **7**(3): p. 311-7.
15. Bugl, S., et al., *Steady-state neutrophil homeostasis is dependent on TLR4/TRIF signaling.* Blood, 2013. **121**(5): p. 723-33.
16. Martin, C., et al., *Chemokines acting via CXCR2 and CXCR4 control the release of neutrophils from the bone marrow and their return following senescence.* Immunity, 2003. **19**(4): p. 583-93.
17. Burdon, P.C., C. Martin, and S.M. Rankin, *The CXC chemokine MIP-2 stimulates neutrophil mobilization from the rat bone marrow in a CD49d-dependent manner.* Blood, 2005. **105**(6): p. 2543-8.
18. Rainger, G.E., A.C. Fisher, and G.B. Nash, *Endothelial-borne platelet-activating factor and interleukin-8 rapidly immobilize rolling neutrophils.* Am J Physiol, 1997. **272**(1 Pt 2): p. H114-22.
19. Jagels, M.A. and T.E. Hugli, *Neutrophil chemotactic factors promote leukocytosis. A common mechanism for cellular recruitment from bone marrow.* J Immunol, 1992. **148**(4): p. 1119-28.

20. Bleul, C.C., et al., *A highly efficacious lymphocyte chemoattractant, stromal cell-derived factor 1 (SDF-1).* J Exp Med, 1996. **184**(3): p. 1101-9.
21. Wang, Y., et al., *CCR2 and CXCR4 regulate peripheral blood monocyte pharmacodynamics and link to efficacy in experimental autoimmune encephalomyelitis.* J Inflamm (Lond), 2009. **6**: p. 32.
22. Geissmann, F., S. Jung, and D.R. Littman, *Blood monocytes consist of two principal subsets with distinct migratory properties.* Immunity, 2003. **19**(1): p. 71-82.
23. Auffray, C., et al., *Monitoring of blood vessels and tissues by a population of monocytes with patrolling behavior.* Science, 2007. **317**(5838): p. 666-70.
24. Serbina, N.V., et al., *Monocyte-mediated defense against microbial pathogens.* Annu Rev Immunol, 2008. **26**: p. 421-52.
25. Barbalat, R., et al., *Toll-like receptor 2 on inflammatory monocytes induces type I interferon in response to viral but not bacterial ligands.* Nat Immunol, 2009. **10**(11): p. 1200-7.
26. Pucci, F., et al., *A distinguishing gene signature shared by tumor-infiltrating Tie2-expressing monocytes, blood "resident" monocytes, and embryonic macrophages suggests common functions and developmental relationships.* Blood, 2009. **114**(4): p. 901-14.
27. Wright, S.D., et al., *CD14, a receptor for complexes of lipopolysaccharide (LPS) and LPS binding protein.* Science, 1990. **249**(4975): p. 1431-3.
28. Passlick, B., D. Flieger, and H.W. Ziegler-Heitbrock, *Identification and characterization of a novel monocyte subpopulation in human peripheral blood.* Blood, 1989. **74**(7): p. 2527-34.
29. Ziegler-Heitbrock, H.W., et al., *The novel subset of CD14+/CD16+ blood monocytes exhibits features of tissue macrophages.* Eur J Immunol, 1993. **23**(9): p. 2053-8.
30. Balkwill, F., *Cancer and the chemokine network.* Nat Rev Cancer, 2004. **4**(7): p. 540-50.
31. Weber, C., et al., *Differential chemokine receptor expression and function in human monocyte subpopulations.* J Leukoc Biol, 2000. **67**(5): p. 699-704.
32. Cros, J., et al., *Human CD14dim monocytes patrol and sense nucleic acids and viruses via TLR7 and TLR8 receptors.* Immunity, 2010. **33**(3): p. 375-86.
33. Amulic, B., et al., *Neutrophil function: from mechanisms to disease.* Annu Rev Immunol, 2012. **30**: p. 459-89.
34. Bainton, D.F., J.L. Ullyot, and M.G. Farquhar, *The development of neutrophilic polymorphonuclear leukocytes in human bone marrow.* J Exp Med, 1971. **134**(4): p. 907-34.
35. Li, Y., et al., *A critical concentration of neutrophils is required for effective bacterial killing in suspension.* Proc Natl Acad Sci U S A, 2002. **99**(12): p. 8289-94.
36. Basu, S., et al., *Evaluation of role of G-CSF in the production, survival, and release of neutrophils from bone marrow into circulation.* Blood, 2002. **100**(3): p. 854-61.
37. Athens, J.W., et al., *Leukokinetic studies. IV. The total blood, circulating and marginal granulocyte pools and the granulocyte turnover rate in normal subjects.* J Clin Invest, 1961. **40**: p. 989-95.

38. Dancey, J.T., et al., *Neutrophil kinetics in man.* J Clin Invest, 1976. **58**(3): p. 705-15.
39. McMillan, R. and J.L. Scott, *Leukocyte labeling with 51-Chromium. I. Technic and results in normal subjects.* Blood, 1968. **32**(5): p. 738-54.
40. Pillay, J., et al., *In vivo labeling with 2H2O reveals a human neutrophil lifespan of 5.4 days.* Blood, 2010. **116**(4): p. 625-7.
41. Tofts, P.S., et al., *Doubts concerning the recently reported human neutrophil lifespan of 5.4 days.* Blood, 2011. **117**(22): p. 6050-2; author reply 6053-4.
42. Cain, D.W., et al., *Inflammation triggers emergency granulopoiesis through a density-dependent feedback mechanism.* PLoS One, 2011. **6**(5): p. e19957.
43. He, R.L., et al., *Serum amyloid A induces G-CSF expression and neutrophilia via Toll-like receptor 2.* Blood, 2009. **113**(2): p. 429-37.
44. Kimura, G., et al., *Toll-like receptor 3 stimulation causes corticosteroid-refractory airway neutrophilia and hyperresponsiveness in mice.* Chest, 2013. **144**(1): p. 99-105.
45. Casadevall, A. and L.A. Pirofski, *Host-pathogen interactions: redefining the basic concepts of virulence and pathogenicity.* Infect Immun, 1999. **67**(8): p. 3703-13.
46. Akira, S., S. Uematsu, and O. Takeuchi, *Pathogen recognition and innate immunity.* Cell, 2006. **124**(4): p. 783-801.
47. Kawai, T. and S. Akira, *The role of pattern-recognition receptors in innate immunity: update on Toll-like receptors.* Nat Immunol, 2010. **11**(5): p. 373-84.
48. Akira, S., K. Takeda, and T. Kaisho, *Toll-like receptors: critical proteins linking innate and acquired immunity.* Nat Immunol, 2001. **2**(8): p. 675-80.
49. Takeuchi, O., et al., *Cellular responses to bacterial cell wall components are mediated through MyD88-dependent signaling cascades.* Int Immunol, 2000. **12**(1): p. 113-7.
50. Kawai, T., et al., *Unresponsiveness of MyD88-deficient mice to endotoxin.* Immunity, 1999. **11**(1): p. 115-22.
51. Hayashi, F., et al., *The innate immune response to bacterial flagellin is mediated by Toll-like receptor 5.* Nature, 2001. **410**(6832): p. 1099-103.
52. Jiang, F., et al., *Structural basis of RNA recognition and activation by innate immune receptor RIG-I.* Nature, 2011. **479**(7373): p. 423-7.
53. Ekman, A.K. and L.O. Cardell, *The expression and function of Nod-like receptors in neutrophils.* Immunology, 2010. **130**(1): p. 55-63.
54. Medzhitov, R. and C. Janeway, Jr., *Innate immune recognition: mechanisms and pathways.* Immunol Rev, 2000. **173**: p. 89-97.
55. *Ilya Mechnikov - Facts*. Updated 4 Dec 2013, Accessed 6 June 2013]; Available from: http://www.nobelprize.org/nobel_prizes/medicine/laureates/1908/mechnikov-facts.html.
56. Silva, M.T., *When two is better than one: macrophages and neutrophils work in concert in innate immunity as complementary and cooperative partners of a myeloid phagocyte system.* J Leukoc Biol, 2010. **87**(1): p. 93-106.
57. Silva, M.T. and M. Correia-Neves, *Neutrophils and macrophages: the main partners of phagocyte cell systems.* Front Immunol, 2012. **3**: p. 174.

58. Mantovani, A., et al., *Macrophage plasticity and polarization in tissue repair and remodelling.* J Pathol, 2013. **229**(2): p. 176-85.
59. Lech, M., et al., *Tissues use resident dendritic cells and macrophages to maintain homeostasis and to regain homeostasis upon tissue injury: the immunoregulatory role of changing tissue environments.* Mediators Inflamm, 2012. **2012**: p. 951390.
60. Ganz, T., *Iron in innate immunity: starve the invaders.* Curr Opin Immunol, 2009. **21**(1): p. 63-7.
61. Nauseef, W.M., *How human neutrophils kill and degrade microbes: an integrated view.* Immunol Rev, 2007. **219**: p. 88-102.
62. Xing, Z., et al., *Cytokine expression by neutrophils and macrophages in vivo: endotoxin induces tumor necrosis factor-alpha, macrophage inflammatory protein-2, interleukin-1 beta, and interleukin-6 but not RANTES or transforming growth factor-beta 1 mRNA expression in acute lung inflammation.* Am J Respir Cell Mol Biol, 1994. **10**(2): p. 148-53.
63. Bassing, C.H., W. Swat, and F.W. Alt, *The mechanism and regulation of chromosomal V(D)J recombination.* Cell, 2002. **109 Suppl**: p. S45-55.
64. Jabbari, A. and J.T. Harty, *The generation and modulation of antigen-specific memory CD8 T cell responses.* J Leukoc Biol, 2006. **80**(1): p. 16-23.
65. Hayashi, F., T.K. Means, and A.D. Luster, *Toll-like receptors stimulate human neutrophil function.* Blood, 2003. **102**(7): p. 2660-9.
66. Hahn, I., et al., *Cathepsin G and neutrophil elastase play critical and nonredundant roles in lung-protective immunity against Streptococcus pneumoniae in mice.* Infect Immun, 2011. **79**(12): p. 4893-901.
67. Faurschou, M. and N. Borregaard, *Neutrophil granules and secretory vesicles in inflammation.* Microbes Infect, 2003. **5**(14): p. 1317-27.
68. Anderson, M.M., et al., *Human neutrophils employ the myeloperoxidase-hydrogen peroxide-chloride system to convert hydroxy-amino acids into glycolaldehyde, 2-hydroxypropanal, and acrolein. A mechanism for the generation of highly reactive alpha-hydroxy and alpha,beta-unsaturated aldehydes by phagocytes at sites of inflammation.* J Clin Invest, 1997. **99**(3): p. 424-32.
69. Mantovani, A., et al., *Neutrophils in the activation and regulation of innate and adaptive immunity.* Nat Rev Immunol, 2011. **11**(8): p. 519-31.
70. Thomas, C.J. and K. Schroder, *Pattern recognition receptor function in neutrophils.* Trends Immunol, 2013. **34**(7): p. 317-28.
71. Soehnlein, O., L. Lindbom, and C. Weber, *Mechanisms underlying neutrophil-mediated monocyte recruitment.* Blood, 2009. **114**(21): p. 4613-23.
72. Soehnlein, O., et al., *Neutrophil secretion products pave the way for inflammatory monocytes.* Blood, 2008. **112**(4): p. 1461-71.
73. Theilgaard-Monch, K., et al., *The transcriptional activation program of human neutrophils in skin lesions supports their important role in wound healing.* J Immunol, 2004. **172**(12): p. 7684-93.
74. Gong, Y. and D.R. Koh, *Neutrophils promote inflammatory angiogenesis via release of preformed VEGF in an in vivo corneal model.* Cell Tissue Res, 2010. **339**(2): p. 437-48.
75. Tazzyman, S., C.E. Lewis, and C. Murdoch, *Neutrophils: key mediators of tumour angiogenesis.* Int J Exp Pathol, 2009. **90**(3): p. 222-31.

76. Brinkmann, V., et al., *Neutrophil extracellular traps kill bacteria.* Science, 2004. **303**(5663): p. 1532-5.
77. Caudrillier, A., et al., *Platelets induce neutrophil extracellular traps in transfusion-related acute lung injury.* J Clin Invest, 2012. **122**(7): p. 2661-71.
78. Urban, C.F., et al., *Neutrophil extracellular traps capture and kill Candida albicans yeast and hyphal forms.* Cell Microbiol, 2006. **8**(4): p. 668-76.
79. Keshari, R.S., et al., *Cytokines induced neutrophil extracellular traps formation: implication for the inflammatory disease condition.* PLoS One, 2012. **7**(10): p. e48111.
80. Fialkow, L., Y. Wang, and G.P. Downey, *Reactive oxygen and nitrogen species as signaling molecules regulating neutrophil function.* Free Radic Biol Med, 2007. **42**(2): p. 153-64.
81. Subbian, S., et al., *A Mycobacterium marinum mel2 mutant is defective for growth in macrophages that produce reactive oxygen and reactive nitrogen species.* Infect Immun, 2007. **75**(1): p. 127-34.
82. Sasmono, R.T., et al., *Mouse neutrophilic granulocytes express mRNA encoding the macrophage colony-stimulating factor receptor (CSF-1R) as well as many other macrophage-specific transcripts and can transdifferentiate into macrophages in vitro in response to CSF-1.* J Leukoc Biol, 2007. **82**(1): p. 111-23.
83. Friedman, A.D., *Transcriptional regulation of granulocyte and monocyte development.* Oncogene, 2002. **21**(21): p. 3377-90.
84. Rose, S., A. Misharin, and H. Perlman, *A novel Ly6C/Ly6G-based strategy to analyze the mouse splenic myeloid compartment.* Cytometry A, 2012. **81**(4): p. 343-50.
85. Scapini, P., et al., *The neutrophil as a cellular source of chemokines.* Immunol Rev, 2000. **177**: p. 195-203.
86. Rydell-Tormanen, K., L. Uller, and J.S. Erjefalt, *Neutrophil cannibalism--a back up when the macrophage clearance system is insufficient.* Respir Res, 2006. **7**: p. 143.
87. Grigat, J., et al., *Chemoattraction of macrophages, T lymphocytes, and mast cells is evolutionarily conserved within the human alpha-defensin family.* J Immunol, 2007. **179**(6): p. 3958-65.
88. Chaly, Y.V., et al., *Neutrophil alpha-defensin human neutrophil peptide modulates cytokine production in human monocytes and adhesion molecule expression in endothelial cells.* Eur Cytokine Netw, 2000. **11**(2): p. 257-66.
89. Gallin, J.I., et al., *Human neutrophil-specific granule deficiency: a model to assess the role of neutrophil-specific granules in the evolution of the inflammatory response.* Blood, 1982. **59**(6): p. 1317-29.
90. Mokart, D., et al., *Monocyte deactivation in neutropenic acute respiratory distress syndrome patients treated with granulocyte colony-stimulating factor.* Crit Care, 2008. **12**(1): p. R17.
91. Soehnlein, O., C. Weber, and L. Lindbom, *Neutrophil granule proteins tune monocytic cell function.* Trends Immunol, 2009. **30**(11): p. 538-46.
92. De Filippo, K., et al., *Neutrophil chemokines KC and macrophage-inflammatory protein-2 are newly synthesized by tissue macrophages using distinct TLR signaling pathways.* J Immunol, 2008. **180**(6): p. 4308-15.

93. De Filippo, K., et al., *Mast cell and macrophage chemokines CXCL1/CXCL2 control the early stage of neutrophil recruitment during tissue inflammation.* Blood, 2013. **121**(24): p. 4930-7.
94. Takahashi, M., et al., *Human monocyte-endothelial cell interaction induces synthesis of granulocyte-macrophage colony-stimulating factor.* Circulation, 1996. **93**(6): p. 1185-93.
95. Takahashi, T., et al., *Activation of human neutrophil by cytokine-activated endothelial cells.* Circ Res, 2001. **88**(4): p. 422-9.
96. Peveri, P., et al., *A novel neutrophil-activating factor produced by human mononuclear phagocytes.* J Exp Med, 1988. **167**(5): p. 1547-59.
97. Fang, H.Y., et al., *Hypoxia-inducible factors 1 and 2 are important transcriptional effectors in primary macrophages experiencing hypoxia.* Blood, 2009. **114**(4): p. 844-59.
98. Bona, E., et al., *Chemokine and inflammatory cell response to hypoxia-ischemia in immature rats.* Pediatr Res, 1999. **45**(4 Pt 1): p. 500-9.
99. Cox, G., J. Crossley, and Z. Xing, *Macrophage engulfment of apoptotic neutrophils contributes to the resolution of acute pulmonary inflammation in vivo.* Am J Respir Cell Mol Biol, 1995. **12**(2): p. 232-7.
100. Michlewska, S., et al., *Macrophage phagocytosis of apoptotic neutrophils is critically regulated by the opposing actions of pro-inflammatory and anti-inflammatory agents: key role for TNF-alpha.* FASEB J, 2009. **23**(3): p. 844-54.
101. Biswas, S.K. and A. Mantovani, *Macrophage plasticity and interaction with lymphocyte subsets: cancer as a paradigm.* Nat Immunol, 2010. **11**(10): p. 889-96.
102. Mantovani, A., et al., *Macrophage polarization: tumor-associated macrophages as a paradigm for polarized M2 mononuclear phagocytes.* Trends Immunol, 2002. **23**(11): p. 549-55.
103. Stein, M., et al., *Interleukin 4 potently enhances murine macrophage mannose receptor activity: a marker of alternative immunologic macrophage activation.* J Exp Med, 1992. **176**(1): p. 287-92.
104. Mosser, D.M., *The many faces of macrophage activation.* J Leukoc Biol, 2003. **73**(2): p. 209-12.
105. Gordon, S. and F.O. Martinez, *Alternative activation of macrophages: mechanism and functions.* Immunity, 2010. **32**(5): p. 593-604.
106. Mantovani, A., et al., *The chemokine system in diverse forms of macrophage activation and polarization.* Trends Immunol, 2004. **25**(12): p. 677-86.
107. Martinez, F.O., et al., *Transcriptional profiling of the human monocyte-to-macrophage differentiation and polarization: new molecules and patterns of gene expression.* J Immunol, 2006. **177**(10): p. 7303-11.
108. Sindrilaru, A., et al., *An unrestrained proinflammatory M1 macrophage population induced by iron impairs wound healing in humans and mice.* J Clin Invest, 2011. **121**(3): p. 985-97.
109. Krausgruber, T., et al., *IRF5 promotes inflammatory macrophage polarization and TH1-TH17 responses.* Nat Immunol, 2011. **12**(3): p. 231-8.
110. Mills, C.D., et al., *M-1/M-2 macrophages and the Th1/Th2 paradigm.* J Immunol, 2000. **164**(12): p. 6166-73.

111. Stout, R.D., et al., *Macrophages sequentially change their functional phenotype in response to changes in microenvironmental influences.* J Immunol, 2005. **175**(1): p. 342-9.
112. Hao, N.B., et al., *Macrophages in tumor microenvironments and the progression of tumors.* Clin Dev Immunol, 2012. **2012**: p. 948098.
113. Hedrick, J.A., et al., *Characterization of a novel CC chemokine, HCC-4, whose expression is increased by interleukin-10.* Blood, 1998. **91**(11): p. 4242-7.
114. Pannellini, T., et al., *The expression of LEC/CCL16, a powerful inflammatory chemokine, is upregulated in ulcerative colitis.* Int J Immunopathol Pharmacol, 2004. **17**(2): p. 171-80.
115. Perrier, P., et al., *Distinct transcriptional programs activated by interleukin-10 with or without lipopolysaccharide in dendritic cells: induction of the B cell-activating chemokine, CXC chemokine ligand 13.* J Immunol, 2004. **172**(11): p. 7031-42.
116. Uematsu, S. and S. Akira, *Toll-Like receptors (TLRs) and their ligands.* Handb Exp Pharmacol, 2008(183): p. 1-20.
117. Schneemann, M. and G. Schoeden, *Macrophage biology and immunology: man is not a mouse.* J Leukoc Biol, 2007. **81**(3): p. 579; discussion 580.
118. Galli, S.J., N. Borregaard, and T.A. Wynn, *Phenotypic and functional plasticity of cells of innate immunity: macrophages, mast cells and neutrophils.* Nat Immunol, 2011. **12**(11): p. 1035-44.
119. Harlan, J.M., *Leukocyte-endothelial interactions.* Blood, 1985. **65**(3): p. 513-25.
120. Carlos, T.M. and J.M. Harlan, *Leukocyte-endothelial adhesion molecules.* Blood, 1994. **84**(7): p. 2068-101.
121. Grommes, J. and O. Soehnlein, *Contribution of neutrophils to acute lung injury.* Mol Med, 2011. **17**(3-4): p. 293-307.
122. Yago, T., et al., *E-selectin engages PSGL-1 and CD44 through a common signaling pathway to induce integrin alphaLbeta2-mediated slow leukocyte rolling.* Blood, 2010. **116**(3): p. 485-94.
123. Yang, L., et al., *ICAM-1 regulates neutrophil adhesion and transcellular migration of TNF-alpha-activated vascular endothelium under flow.* Blood, 2005. **106**(2): p. 584-92.
124. De Santo, C., et al., *Invariant NKT cells modulate the suppressive activity of IL-10-secreting neutrophils differentiated with serum amyloid A.* Nat Immunol, 2010. **11**(11): p. 1039-46.
125. Brennan, P.J., M. Brigl, and M.B. Brenner, *Invariant natural killer T cells: an innate activation scheme linked to diverse effector functions.* Nat Rev Immunol, 2013. **13**(2): p. 101-17.
126. Acharyya, S., et al., *A CXCL1 paracrine network links cancer chemoresistance and metastasis.* Cell, 2012. **150**(1): p. 165-78.
127. Qian, B.Z., et al., *CCL2 recruits inflammatory monocytes to facilitate breast-tumour metastasis.* Nature, 2011. **475**(7355): p. 222-5.
128. Cao, Y., et al., *VEGF exerts an angiogenesis-independent function in cancer cells to promote their malignant progression.* Cancer Res, 2012. **72**(16): p. 3912-8.
129. Wyckoff, J., et al., *A paracrine loop between tumor cells and macrophages is required for tumor cell migration in mammary tumors.* Cancer Res, 2004. **64**(19): p. 7022-9.

130. Bingle, L., et al., *Macrophages promote angiogenesis in human breast tumour spheroids in vivo.* Br J Cancer, 2006. **94**(1): p. 101-7.
131. Gajewski, T.F., H. Schreiber, and Y.X. Fu, *Innate and adaptive immune cells in the tumor microenvironment.* Nat Immunol, 2013. **14**(10): p. 1014-22.
132. Murdoch, C., et al., *The role of myeloid cells in the promotion of tumour angiogenesis.* Nat Rev Cancer, 2008. **8**(8): p. 618-31.
133. Hanahan, D. and L.M. Coussens, *Accessories to the crime: functions of cells recruited to the tumor microenvironment.* Cancer Cell, 2012. **21**(3): p. 309-22.
134. Coley, W.B., *II. Contribution to the Knowledge of Sarcoma.* Ann Surg, 1891. **14**(3): p. 199-220.
135. Hallam, S., et al., *Activated macrophages in the tumour microenvironment-dancing to the tune of TLR and NF-kappaB.* J Pathol, 2009. **219**(2): p. 143-52.
136. Hoption Cann, S.A., J.P. van Netten, and C. van Netten, *Dr William Coley and tumour regression: a place in history or in the future.* Postgrad Med J, 2003. **79**(938): p. 672-80.
137. Dvorak, H.F., *Tumors: wounds that do not heal. Similarities between tumor stroma generation and wound healing.* N Engl J Med, 1986. **315**(26): p. 1650-9.
138. Balkwill, F., K.A. Charles, and A. Mantovani, *Smoldering and polarized inflammation in the initiation and promotion of malignant disease.* Cancer Cell, 2005. **7**(3): p. 211-7.
139. Coussens, L.M. and Z. Werb, *Inflammation and cancer.* Nature, 2002. **420**(6917): p. 860-7.
140. Bottazzi, B., et al., *Monocyte chemotactic cytokine gene transfer modulates macrophage infiltration, growth, and susceptibility to IL-2 therapy of a murine melanoma.* J Immunol, 1992. **148**(4): p. 1280-5.
141. Robinson, S.C., et al., *A chemokine receptor antagonist inhibits experimental breast tumor growth.* Cancer Res, 2003. **63**(23): p. 8360-5.
142. Kawamura, K., et al., *Detection of M2 macrophages and colony-stimulating factor 1 expression in serous and mucinous ovarian epithelial tumors.* Pathol Int, 2009. **59**(5): p. 300-5.
143. Dineen, S.P., et al., *Vascular endothelial growth factor receptor 2 mediates macrophage infiltration into orthotopic pancreatic tumors in mice.* Cancer Res, 2008. **68**(11): p. 4340-6.
144. Murdoch, C., et al., *Expression of Tie-2 by human monocytes and their responses to angiopoietin-2.* J Immunol, 2007. **178**(11): p. 7405-11.
145. Murdoch, C., A. Giannoudis, and C.E. Lewis, *Mechanisms regulating the recruitment of macrophages into hypoxic areas of tumors and other ischemic tissues.* Blood, 2004. **104**(8): p. 2224-34.
146. Fridlender, Z.G., et al., *Polarization of tumor-associated neutrophil phenotype by TGF-beta: "N1" versus "N2" TAN.* Cancer Cell, 2009. **16**(3): p. 183-94.
147. Locati, M., et al., *Analysis of the gene expression profile activated by the CC chemokine ligand 5/RANTES and by lipopolysaccharide in human monocytes.* J Immunol, 2002. **168**(7): p. 3557-62.

148. Welford, A.F., et al., *TIE2-expressing macrophages limit the therapeutic efficacy of the vascular-disrupting agent combretastatin A4 phosphate in mice.* J Clin Invest, 2011. **121**(5): p. 1969-73.
149. Leek, R.D., et al., *Association of macrophage infiltration with angiogenesis and prognosis in invasive breast carcinoma.* Cancer Res, 1996. **56**(20): p. 4625-9.
150. Koukourakis, M.I., et al., *Different patterns of stromal and cancer cell thymidine phosphorylase reactivity in non-small-cell lung cancer: impact on tumour neoangiogenesis and survival.* Br J Cancer, 1998. **77**(10): p. 1696-703.
151. Lissbrant, I.F., et al., *Tumor associated macrophages in human prostate cancer: relation to clinicopathological variables and survival.* Int J Oncol, 2000. **17**(3): p. 445-51.
152. Ajili, F., et al., *Prognostic value of tumor-associated macrophages count in human non-muscle-invasive bladder cancer treated by BCG immunotherapy.* Ultrastruct Pathol, 2013. **37**(1): p. 56-61.
153. Salvesen, H.B. and L.A. Akslen, *Significance of tumour-associated macrophages, vascular endothelial growth factor and thrombospondin-1 expression for tumour angiogenesis and prognosis in endometrial carcinomas.* Int J Cancer, 1999. **84**(5): p. 538-43.
154. Ryder, M., et al., *Increased density of tumor-associated macrophages is associated with decreased survival in advanced thyroid cancer.* Endocr Relat Cancer, 2008. **15**(4): p. 1069-74.
155. Nishie, A., et al., *Macrophage infiltration and heme oxygenase-1 expression correlate with angiogenesis in human gliomas.* Clin Cancer Res, 1999. **5**(5): p. 1107-13.
156. Nowicki, A., et al., *Impaired tumor growth in colony-stimulating factor 1 (CSF-1)-deficient, macrophage-deficient op/op mouse: evidence for a role of CSF-1-dependent macrophages in formation of tumor stroma.* Int J Cancer, 1996. **65**(1): p. 112-9.
157. Lin, E.Y., et al., *Colony-stimulating factor 1 promotes progression of mammary tumors to malignancy.* J Exp Med, 2001. **193**(6): p. 727-40.
158. Migita, T., et al., *Differing expression of MMPs-1 and -9 and urokinase receptor between diffuse- and intestinal-type gastric carcinoma.* Int J Cancer, 1999. **84**(1): p. 74-9.
159. Shimura, S., et al., *Reduced infiltration of tumor-associated macrophages in human prostate cancer: association with cancer progression.* Cancer Res, 2000. **60**(20): p. 5857-61.
160. Lin, E.Y., et al., *Macrophages regulate the angiogenic switch in a mouse model of breast cancer.* Cancer Res, 2006. **66**(23): p. 11238-46.
161. Doedens, A.L., et al., *Macrophage expression of hypoxia-inducible factor-1 alpha suppresses T-cell function and promotes tumor progression.* Cancer Res, 2010. **70**(19): p. 7465-75.
162. DeNardo, D.G., et al., *Leukocyte complexity predicts breast cancer survival and functionally regulates response to chemotherapy.* Cancer Discov, 2011. **1**(1): p. 54-67.
163. Curiel, T.J., et al., *Specific recruitment of regulatory T cells in ovarian carcinoma fosters immune privilege and predicts reduced survival.* Nat Med, 2004. **10**(9): p. 942-9.

164. Hsiao, Y.W., et al., *CCAAT/Enhancer Binding Protein delta in Macrophages Contributes to Immunosuppression and Inhibits Phagocytosis in Nasopharyngeal Carcinoma.* Sci Signal, 2013. **6**(284): p. ra59.
165. DeNardo, D.G., et al., *CD4(+) T cells regulate pulmonary metastasis of mammary carcinomas by enhancing protumor properties of macrophages.* Cancer Cell, 2009. **16**(2): p. 91-102.
166. Gocheva, V., et al., *IL-4 induces cathepsin protease activity in tumor-associated macrophages to promote cancer growth and invasion.* Genes Dev, 2010. **24**(3): p. 241-55.
167. Vasiljeva, O., et al., *Tumor cell-derived and macrophage-derived cathepsin B promotes progression and lung metastasis of mammary cancer.* Cancer Res, 2006. **66**(10): p. 5242-50.
168. Almholt, K., et al., *Reduced metastasis of transgenic mammary cancer in urokinase-deficient mice.* Int J Cancer, 2005. **113**(4): p. 525-32.
169. Venneri, M.A., et al., *Identification of proangiogenic TIE2-expressing monocytes (TEMs) in human peripheral blood and cancer.* Blood, 2007. **109**(12): p. 5276-85.
170. Dorsch, M., et al., *Macrophage colony-stimulating factor gene transfer into tumor cells induces macrophage infiltration but not tumor suppression.* Eur J Immunol, 1993. **23**(1): p. 186-90.
171. Niwa, Y., et al., *Correlation of tissue and plasma RANTES levels with disease course in patients with breast or cervical cancer.* Clin Cancer Res, 2001. **7**(2): p. 285-9.
172. Lewis, J.S., et al., *Expression of vascular endothelial growth factor by macrophages is up-regulated in poorly vascularized areas of breast carcinomas.* J Pathol, 2000. **192**(2): p. 150-8.
173. Qian, B.Z. and J.W. Pollard, *Macrophage diversity enhances tumor progression and metastasis.* Cell, 2010. **141**(1): p. 39-51.
174. De Palma, M., et al., *Tie2 identifies a hematopoietic lineage of proangiogenic monocytes required for tumor vessel formation and a mesenchymal population of pericyte progenitors.* Cancer Cell, 2005. **8**(3): p. 211-26.
175. Coffelt, S.B., et al., *Angiopoietin-2 regulates gene expression in TIE2-expressing monocytes and augments their inherent proangiogenic functions.* Cancer Res, 2010. **70**(13): p. 5270-80.
176. Gerald, D., et al., *Angiopoietin-2: an attractive target for improved antiangiogenic tumor therapy.* Cancer Res, 2013. **73**(6): p. 1649-57.
177. Lewis, C.E., M. De Palma, and L. Naldini, *Tie2-expressing monocytes and tumor angiogenesis: regulation by hypoxia and angiopoietin-2.* Cancer Res, 2007. **67**(18): p. 8429-32.
178. De Palma, M., et al., *Tie2-expressing monocytes: regulation of tumor angiogenesis and therapeutic implications.* Trends Immunol, 2007. **28**(12): p. 519-24.
179. Hagemann, T., et al., *"Re-educating" tumor-associated macrophages by targeting NF-kappaB.* J Exp Med, 2008. **205**(6): p. 1261-8.
180. Ji, H., et al., *K-ras activation generates an inflammatory response in lung tumors.* Oncogene, 2006. **25**(14): p. 2105-12.

181. Bellocq, A., et al., *Neutrophil alveolitis in bronchioloalveolar carcinoma: induction by tumor-derived interleukin-8 and relation to clinical outcome.* Am J Pathol, 1998. **152**(1): p. 83-92.
182. Eck, M., et al., *Pleiotropic effects of CXC chemokines in gastric carcinoma: differences in CXCL8 and CXCL1 expression between diffuse and intestinal types of gastric carcinoma.* Clin Exp Immunol, 2003. **134**(3): p. 508-15.
183. Jensen, H.K., et al., *Presence of intratumoral neutrophils is an independent prognostic factor in localized renal cell carcinoma.* J Clin Oncol, 2009. **27**(28): p. 4709-17.
184. Wislez, M., et al., *Hepatocyte growth factor production by neutrophils infiltrating bronchioloalveolar subtype pulmonary adenocarcinoma: role in tumor progression and death.* Cancer Res, 2003. **63**(6): p. 1405-12.
185. Tazzyman, S., et al., *Inhibition of neutrophil infiltration into A549 lung tumors in vitro and in vivo using a CXCR2-specific antagonist is associated with reduced tumor growth.* Int J Cancer, 2011. **129**(4): p. 847-58.
186. Dumitru, C.A., et al., *AHNAK and inflammatory markers predict poor survival in laryngeal carcinoma.* PLoS One, 2013. **8**(2): p. e56420.
187. Umemura, N., et al., *Tumor-infiltrating myeloid-derived suppressor cells are pleiotropic-inflamed monocytes/macrophages that bear M1- and M2-type characteristics.* Journal of Leukocyte Biology, 2008. **83**(5): p. 1136-1144.
188. Cools-Lartigue, J., et al., *Neutrophil extracellular traps sequester circulating tumor cells and promote metastasis.* J Clin Invest, 2013.
189. Demers, M., et al., *Cancers predispose neutrophils to release extracellular DNA traps that contribute to cancer-associated thrombosis.* Proc Natl Acad Sci U S A, 2012. **109**(32): p. 13076-81.
190. Gabrilovich, D.I. and S. Nagaraj, *Myeloid-derived suppressor cells as regulators of the immune system.* Nat Rev Immunol, 2009. **9**(3): p. 162-74.
191. Yang, W.C., et al., *Polarization and reprogramming of myeloid-derived suppressor cells.* J Mol Cell Biol, 2013. **5**(3): p. 207-9.
192. Bronte, V. and D. Gabrilovich, *Myeloid-derived suppressor cells*, 2010, Macmillan Publishers Ltd.: Nat Rev Immunol.
193. Youn, J.I., et al., *Subsets of myeloid-derived suppressor cells in tumor-bearing mice.* J Immunol, 2008. **181**(8): p. 5791-802.
194. Movahedi, K., et al., *Identification of discrete tumor-induced myeloid-derived suppressor cell subpopulations with distinct T cell-suppressive activity.* Blood, 2008. **111**(8): p. 4233-44.
195. Duffy, A., et al., *Comparative analysis of monocytic and granulocytic myeloid-derived suppressor cell subsets in patients with gastrointestinal malignancies.* Cancer Immunol Immunother, 2013. **62**(2): p. 299-307.
196. Hanahan, D. and R.A. Weinberg, *Hallmarks of cancer: the next generation.* Cell, 2011. **144**(5): p. 646-74.
197. Fichtner-Feigl, S., et al., *Restoration of tumor immunosurveillance via targeting of interleukin-13 receptor-alpha 2.* Cancer Res, 2008. **68**(9): p. 3467-75.
198. Zhi, L., B. Toh, and J. Abastado, *Myeloid Derived Suppressor Cells: Subsets, Expansion, and Role in Cancer Progression* in *Tumor Microenvironment and Myelomonocytic Cells*, S.K. Biswas, Editor 2012, InTech. p. 63-88.

199. Balwit, J.M., et al., *The iSBTc/SITC primer on tumor immunology and biological therapy of cancer: a summary of the 2010 program.* J Transl Med, 2011. **9**: p. 18.
200. Yang, L., et al., *Expansion of myeloid immune suppressor Gr+CD11b+ cells in tumor-bearing host directly promotes tumor angiogenesis.* Cancer Cell, 2004. **6**(4): p. 409-21.
201. Li, H., et al., *Cancer-expanded myeloid-derived suppressor cells induce anergy of NK cells through membrane-bound TGF-beta 1.* J Immunol, 2009. **182**(1): p. 240-9.
202. Pekarek, L.A., et al., *Inhibition of tumor growth by elimination of granulocytes.* J Exp Med, 1995. **181**(1): p. 435-40.
203. Zhang, Y., et al., *Fas signal promotes lung cancer growth by recruiting myeloid-derived suppressor cells via cancer cell-derived PGE2.* J Immunol, 2009. **182**(6): p. 3801-8.
204. Kusmartsev, S., et al., *All-trans-retinoic acid eliminates immature myeloid cells from tumor-bearing mice and improves the effect of vaccination.* Cancer Res, 2003. **63**(15): p. 4441-9.
205. Serafini, P., et al., *Phosphodiesterase-5 inhibition augments endogenous antitumor immunity by reducing myeloid-derived suppressor cell function.* J Exp Med, 2006. **203**(12): p. 2691-702.
206. Suzuki, E., et al., *Gemcitabine selectively eliminates splenic Gr-1+/CD11b+ myeloid suppressor cells in tumor-bearing animals and enhances antitumor immune activity.* Clin Cancer Res, 2005. **11**(18): p. 6713-21.
207. Ezernitchi, A.V., et al., *TCR zeta down-regulation under chronic inflammation is mediated by myeloid suppressor cells differentially distributed between various lymphatic organs.* J Immunol, 2006. **177**(7): p. 4763-72.
208. Nagaraj, S., et al., *Mechanism of T cell tolerance induced by myeloid-derived suppressor cells.* J Immunol, 2010. **184**(6): p. 3106-16.
209. Rodriguez, P.C., et al., *Arginase I production in the tumor microenvironment by mature myeloid cells inhibits T-cell receptor expression and antigen-specific T-cell responses.* Cancer Res, 2004. **64**(16): p. 5839-49.
210. Diaz-Montero, C.M., et al., *Increased circulating myeloid-derived suppressor cells correlate with clinical cancer stage, metastatic tumor burden, and doxorubicin-cyclophosphamide chemotherapy.* Cancer Immunol Immunother, 2009. **58**(1): p. 49-59.
211. *Treatment types*. Updated 1 Sep 2012, Accessed 10 May 2013]; Available from: http://www.macmillan.org.uk/Cancerinformation/Cancertreatment/Treatmenttypes/Treatmenttypes.aspx.
212. Nakasone, E.S., et al., *Imaging tumor-stroma interactions during chemotherapy reveals contributions of the microenvironment to resistance.* Cancer Cell, 2012. **21**(4): p. 488-503.
213. *Cancer Topics*. Accessed 6 June 2013]; Available from: http://www.cancer.gov/cancertopics.
214. Alzeer, J. and O.D. Scharer, *A modified thymine for the synthesis of site-specific thymine-guanine DNA interstrand crosslinks.* Nucleic Acids Research, 2006. **34**(16): p. 4458-4466.

215. Goldwasser, F., et al., *Topoisomerase I-related parameters and camptothecin activity in the colon carcinoma cell lines from the National Cancer Institute anticancer screen.* Cancer Res, 1995. **55**(10): p. 2116-21.
216. Liekens, S., A. Bronckaers, and J. Balzarini, *Improvement of purine and pyrimidine antimetabolite-based anticancer treatment by selective suppression of mycoplasma-encoded catabolic enzymes.* Lancet Oncology, 2009. **10**(6): p. 628-635.
217. Gligorov, J. and J.P. Lotz, *Preclinical pharmacology of the taxanes: implications of the differences.* Oncologist, 2004. **9 Suppl 2**: p. 3-8.
218. Venkatramani, R., et al., *Tumor necrosis predicts survival following neo-adjuvant chemotherapy for hepatoblastoma.* Pediatr Blood Cancer, 2012. **59**(3): p. 493-8.
219. Richmond, A., et al., *Characterization of autostimulatory and transforming growth factors from human melanoma cells.* Cancer Res, 1985. **45**(12 Pt 1): p. 6390-4.
220. Bulysheva AA, Y.W. *CXCL5 (chemokine (C-X-C motif) ligand 5)*. Atlas Genet Cytogenet Oncol Haematol 13 May 2013 20 June 2013]; Available from: http://atlasgeneticsoncology.org/Genes/CXCL5ID40223ch4q13.html.
221. Rossi, D. and A. Zlotnik, *The biology of chemokines and their receptors.* Annual Review of Immunology, 2000. **18**: p. 217-243.
222. Schraufstatter, I.U., J. Chung, and M. Burger, *IL-8 activates endothelial cell CXCR1 and CXCR2 through Rho and Rac signaling pathways.* Am J Physiol Lung Cell Mol Physiol, 2001. **280**(6): p. L1094-103.
223. Sozzani, S., et al., *Receptor expression and responsiveness of human dendritic cells to a defined set of CC and CXC chemokines.* Journal of Immunology, 1997. **159**(4): p. 1993-2000.
224. Morohashi, H., et al., *Expression of Both Types of Human Interleukin-8 Receptors on Mature Neutrophils, Monocytes, and Natural-Killer-Cells.* Journal of Leukocyte Biology, 1995. **57**(1): p. 180-187.
225. Nilsson, G., et al., *Mast cell migratory response to interleukin-8 is mediated through interaction with chemokine receptor CXCR2/interleukin-8RB.* Blood, 1999. **93**(9): p. 2791-2797.
226. Goczalik, I., et al., *Expression of CXCL8, CXCR1, and CXCR2 in neurons and glial cells of the human and rabbit retina.* Invest Ophthalmol Vis Sci, 2008. **49**(10): p. 4578-89.
227. Wuyts, A., et al., *Differential usage of the CXC chemokine receptors 1 and 2 by interleukin-8, granulocyte chemotactic protein-2 and epithelial-cell-derived neutrophil attractant-78.* Eur J Biochem, 1998. **255**(1): p. 67-73.
228. Ahuja, S.K. and P.M. Murphy, *The CXC chemokines growth-regulated oncogene (GRO) alpha, GRObeta, GROgamma, neutrophil-activating peptide-2, and epithelial cell-derived neutrophil-activating peptide-78 are potent agonists for the type B, but not the type A, human interleukin-8 receptor.* J Biol Chem, 1996. **271**(34): p. 20545-50.
229. Gillitzer, R. and M. Goebeler, *Chemokines in cutaneous wound healing.* J Leukoc Biol, 2001. **69**(4): p. 513-21.
230. Hembruff, S.L. and N. Cheng, *Chemokine signaling in cancer: Implications on the tumor microenvironment and therapeutic targeting.* Cancer Ther, 2009. **7**(A): p. 254-267.

231. Vandercappellen, J., J. Van Damme, and S. Struyf, *The role of CXC chemokines and their receptors in cancer.* Cancer Lett, 2008. **267**(2): p. 226-44.
232. Kawanishi, H., et al., *Secreted CXCL1 is a potential mediator and marker of the tumor invasion of bladder cancer.* Clin Cancer Res, 2008. **14**(9): p. 2579-87.
233. Strieter, R.M., et al., *The functional role of the ELR motif in CXC chemokine-mediated angiogenesis.* J Biol Chem, 1995. **270**(45): p. 27348-57.
234. Addison, C.L., et al., *The CXC chemokine receptor 2, CXCR2, is the putative receptor for ELR+ CXC chemokine-induced angiogenic activity.* J Immunol, 2000. **165**(9): p. 5269-77.
235. Scapini, P., et al., *CXCL1/macrophage inflammatory protein-2-induced angiogenesis in vivo is mediated by neutrophil-derived vascular endothelial growth factor-A.* J Immunol, 2004. **172**(8): p. 5034-40.
236. Park, J.Y., et al., *CXCL5 overexpression is associated with late stage gastric cancer.* J Cancer Res Clin Oncol, 2007. **133**(11): p. 835-40.
237. Li, A., et al., *Overexpression of CXCL5 is associated with poor survival in patients with pancreatic cancer.* Am J Pathol, 2011. **178**(3): p. 1340-9.
238. Zhou, S.L., et al., *Overexpression of CXCL5 mediates neutrophil infiltration and indicates poor prognosis for hepatocellular carcinoma.* Hepatology, 2012. **56**(6): p. 2242-54.
239. Barsante, M.M., et al., *Blockade of the chemokine receptor CXCR2 ameliorates adjuvant-induced arthritis in rats.* Br J Pharmacol, 2008. **153**(5): p. 992-1002.
240. Ning, Y., et al., *The CXCR2 antagonist, SCH-527123, shows antitumor activity and sensitizes cells to oxaliplatin in preclinical colon cancer models.* Mol Cancer Ther, 2012. **11**(6): p. 1353-64.
241. Varney, M.L., et al., *Small molecule antagonists for CXCR2 and CXCR1 inhibit human colon cancer liver metastases.* Cancer Lett, 2011. **300**(2): p. 180-8.
242. Ginestier, C., et al., *CXCR1 blockade selectively targets human breast cancer stem cells in vitro and in xenografts.* J Clin Invest, 2010. **120**(2): p. 485-97.
243. Moriconi, A., et al., *Design of noncompetitive interleukin-8 inhibitors acting on CXCR1 and CXCR2.* J Med Chem, 2007. **50**(17): p. 3984-4002.
244. Citro, A., et al., *CXCR1/2 inhibition enhances pancreatic islet survival after transplantation.* J Clin Invest, 2012. **122**(10): p. 3647-51.
245. Cunha, T.M., et al., *Treatment with DF 2162, a non-competitive allosteric inhibitor of CXCR1/2, diminishes neutrophil influx and inflammatory hypernociception in mice.* Br J Pharmacol, 2008. **154**(2): p. 460-70.
246. Chapman, R.W., et al., *CXCR2 antagonists for the treatment of pulmonary disease.* Pharmacol Ther, 2009. **121**(1): p. 55-68.
247. Russo, R.C., et al., *Role of the chemokine receptor CXCR2 in bleomycin-induced pulmonary inflammation and fibrosis.* Am J Respir Cell Mol Biol, 2009. **40**(4): p. 410-21.
248. Salchow, K., et al., *A common intracellular allosteric binding site for antagonists of the CXCR2 receptor.* Br J Pharmacol, 2010. **159**(7): p. 1429-39.

249. Gonsiorek, W., et al., *Pharmacological characterization of Sch527123, a potent allosteric CXCR1/CXCR2 antagonist.* J Pharmacol Exp Ther, 2007. **322**(2): p. 477-85.
250. Holz, O., et al., *SCH527123, a novel CXCR2 antagonist, inhibits ozone-induced neutrophilia in healthy subjects.* Eur Respir J, 2010. **35**(3): p. 564-70.
251. Nair, P., et al., *Safety and efficacy of a CXCR2 antagonist in patients with severe asthma and sputum neutrophils: a randomized, placebo-controlled clinical trial.* Clin Exp Allergy, 2012. **42**(7): p. 1097-103.
252. Lo, M.C., et al., *Role of MIF/CXCL8/CXCR2 signaling in the growth of nasopharyngeal carcinoma tumor spheres.* Cancer Lett, 2013. **335**(1): p. 81-92.
253. White, J.R., et al., *Identification of a potent, selective non-peptide CXCR2 antagonist that inhibits interleukin-8-induced neutrophil migration.* J Biol Chem, 1998. **273**(17): p. 10095-8.
254. Pease, J. and R. Horuk, *Chemokine receptor antagonists.* J Med Chem, 2012. **55**(22): p. 9363-92.
255. Bento, A.F., et al., *The selective nonpeptide CXCR2 antagonist SB225002 ameliorates acute experimental colitis in mice.* J Leukoc Biol, 2008. **84**(4): p. 1213-21.
256. Jin, Q., et al., *Discovery of potent and orally bioavailable N,N'-diarylurea antagonists for the CXCR2 chemokine receptor.* Bioorg Med Chem Lett, 2004. **14**(17): p. 4375-8.
257. Lazaar, A.L., et al., *SB-656933, a novel CXCR2 selective antagonist, inhibits ex vivo neutrophil activation and ozone-induced airway inflammation in humans.* Br J Clin Pharmacol, 2011. **72**(2): p. 282-93.
258. Moss, R.B., et al., *Safety and early treatment effects of the CXCR2 antagonist SB-656933 in patients with cystic fibrosis.* J Cyst Fibros, 2013. **12**(3): p. 241-8.
259. Milatovic, S., et al., *Impaired healing of nitrogen mustard wounds in CXCR2 null mice.* Wound Repair Regen, 2003. **11**(3): p. 213-9.
260. Auten, R.L., et al., *Nonpeptide CXCR2 antagonist prevents neutrophil accumulation in hyperoxia-exposed newborn rats.* J Pharmacol Exp Ther, 2001. **299**(1): p. 90-5.
261. Wilson, C., et al., *Interleukin-8 signaling attenuates TRAIL- and chemotherapy-induced apoptosis through transcriptional regulation of c-FLIP in prostate cancer cells.* Mol Cancer Ther, 2008. **7**(9): p. 2649-61.
262. Sharma, B., et al., *Targeting CXCR2 enhances chemotherapeutic response, inhibits mammary tumor growth, angiogenesis, and lung metastasis.* Mol Cancer Ther, 2013. **12**(5): p. 799-808.
263. Campbell, L.M., P.J. Maxwell, and D.J. Waugh, *Rationale and Means to Target Pro-Inflammatory Interleukin-8 (CXCL8) Signaling in Cancer.* Pharmaceuticals (Basel), 2013. **6**(8): p. 929-959.
264. Carswell, E.A., et al., *An endotoxin-induced serum factor that causes necrosis of tumors.* Proc Natl Acad Sci U S A, 1975. **72**(9): p. 3666-70.
265. Ferrante, A., *Tumor necrosis factor alpha potentiates neutrophil antimicrobial activity: increased fungicidal activity against Torulopsis glabrata and Candida albicans and associated increases in oxygen radical*

production and lysosomal enzyme release. Infect Immun, 1989. **57**(7): p. 2115-22.
266. Grivennikov, S.I., et al., *Distinct and nonredundant in vivo functions of TNF produced by t cells and macrophages/neutrophils: protective and deleterious effects.* Immunity, 2005. **22**(1): p. 93-104.
267. Balkwill, F., *TNF-alpha in promotion and progression of cancer.* Cancer Metastasis Rev, 2006. **25**(3): p. 409-16.
268. Karayiannakis, A.J., et al., *Serum levels of tumor necrosis factor-alpha and nutritional status in pancreatic cancer patients.* Anticancer Res, 2001. **21**(2B): p. 1355-8.
269. Yoshida, N., et al., *Interleukin-6, tumour necrosis factor alpha and interleukin-1beta in patients with renal cell carcinoma.* Br J Cancer, 2002. **86**(9): p. 1396-400.
270. Ferrajoli, A., et al., *The clinical significance of tumor necrosis factor-alpha plasma level in patients having chronic lymphocytic leukemia.* Blood, 2002. **100**(4): p. 1215-9.
271. Bozcuk, H., et al., *Tumour necrosis factor-alpha, interleukin-6, and fasting serum insulin correlate with clinical outcome in metastatic breast cancer patients treated with chemotherapy.* Cytokine, 2004. **27**(2-3): p. 58-65.
272. Galban, S., et al., *von Hippel-Lindau protein-mediated repression of tumor necrosis factor alpha translation revealed through use of cDNA arrays.* Mol Cell Biol, 2003. **23**(7): p. 2316-28.
273. Moore, R.J., et al., *Mice deficient in tumor necrosis factor-alpha are resistant to skin carcinogenesis.* Nat Med, 1999. **5**(7): p. 828-31.
274. Kulbe, H., et al., *The inflammatory cytokine tumor necrosis factor-alpha generates an autocrine tumor-promoting network in epithelial ovarian cancer cells.* Cancer Res, 2007. **67**(2): p. 585-92.
275. Pikarsky, E., et al., *NF-kappaB functions as a tumour promoter in inflammation-associated cancer.* Nature, 2004. **431**(7007): p. 461-6.
276. Oguma, K., et al., *Activated macrophages promote Wnt signalling through tumour necrosis factor-alpha in gastric tumour cells.* EMBO J, 2008. **27**(12): p. 1671-81.
277. Popivanova, B.K., et al., *Blocking TNF-alpha in mice reduces colorectal carcinogenesis associated with chronic colitis.* J Clin Invest, 2008. **118**(2): p. 560-70.
278. Yan, B., et al., *Tumor necrosis factor-alpha is a potent endogenous mutagen that promotes cellular transformation.* Cancer Res, 2006. **66**(24): p. 11565-70.
279. Babbar, N. and R.A. Casero, Jr., *Tumor necrosis factor-alpha increases reactive oxygen species by inducing spermine oxidase in human lung epithelial cells: a potential mechanism for inflammation-induced carcinogenesis.* Cancer Res, 2006. **66**(23): p. 11125-30.
280. Bates, R.C. and A.M. Mercurio, *Tumor necrosis factor-alpha stimulates the epithelial-to-mesenchymal transition of human colonic organoids.* Mol Biol Cell, 2003. **14**(5): p. 1790-800.
281. Kang, Y. and J. Massague, *Epithelial-mesenchymal transitions: twist in development and metastasis.* Cell, 2004. **118**(3): p. 277-9.
282. Yang, J., et al., *Twist, a master regulator of morphogenesis, plays an essential role in tumor metastasis.* Cell, 2004. **117**(7): p. 927-39.

283. Kuei, J.H., D.P. Tashkin, and R.A. Figlin, *Pulmonary toxicity of recombinant human tumor necrosis factor.* Chest, 1989. **96**(2): p. 334-8.
284. Blick, M., et al., *Phase I study of recombinant tumor necrosis factor in cancer patients.* Cancer Res, 1987. **47**(11): p. 2986-9.
285. Orosz, P., et al., *Enhancement of experimental metastasis by tumor necrosis factor.* J Exp Med, 1993. **177**(5): p. 1391-8.
286. Egberts, J.H., et al., *Anti-tumor necrosis factor therapy inhibits pancreatic tumor growth and metastasis.* Cancer Res, 2008. **68**(5): p. 1443-50.
287. Keane, J., *TNF-blocking agents and tuberculosis: new drugs illuminate an old topic.* Rheumatology (Oxford), 2005. **44**(6): p. 714-20.
288. Balkwill, F., *Tumour necrosis factor and cancer.* Nat Rev Cancer, 2009. **9**(5): p. 361-71.
289. Tracey, D., et al., *Tumor necrosis factor antagonist mechanisms of action: a comprehensive review.* Pharmacol Ther, 2008. **117**(2): p. 244-79.
290. Shree, T., et al., *Macrophages and cathepsin proteases blunt chemotherapeutic response in breast cancer.* Genes Dev, 2011. **25**(23): p. 2465-79.
291. Dijkgraaf, E.M., et al., *Chemotherapy alters monocyte differentiation to favor generation of cancer-supporting M2 macrophages in the tumor microenvironment.* Cancer Res, 2013. **73**(8): p. 2480-92.
292. Beroukhim, R., et al., *The landscape of somatic copy-number alteration across human cancers.* Nature, 2010. **463**(7283): p. 899-905.
293. Allison Bierly, K.M. *Chemokines: manipulators of metastasis*. SABiosciences August 17, 2012 8 Nov 2013]; Available from: http://www.sabiosciences.com/pathwaymagazine/minireview/chmkns.php.
294. Fridlender, Z.G. and S.M. Albelda, *Tumor-associated neutrophils: friend or foe?* Carcinogenesis, 2012. **33**(5): p. 949-55.
295. Piccard, H., R.J. Muschel, and G. Opdenakker, *On the dual roles and polarized phenotypes of neutrophils in tumor development and progression.* Crit Rev Oncol Hematol, 2012. **82**(3): p. 296-309.
296. Weigert, A., et al., *Tumor cell apoptosis polarizes macrophages role of sphingosine-1-phosphate.* Mol Biol Cell, 2007. **18**(10): p. 3810-9.
297. Ruffell, B., N.I. Affara, and L.M. Coussens, *Differential macrophage programming in the tumor microenvironment.* Trends Immunol, 2012. **33**(3): p. 119-26.
298. De Palma, M. and C.E. Lewis, *Cancer: Macrophages limit chemotherapy.* Nature, 2011. **472**(7343): p. 303-4.
299. Gazzaniga, S., et al., *Targeting tumor-associated macrophages and inhibition of MCP-1 reduce angiogenesis and tumor growth in a human melanoma xenograft.* J Invest Dermatol, 2007. **127**(8): p. 2031-41.
300. Pahler, J.C., et al., *Plasticity in tumor-promoting inflammation: impairment of macrophage recruitment evokes a compensatory neutrophil response.* Neoplasia, 2008. **10**(4): p. 329-40.
301. Fujimoto, H., et al., *Stromal MCP-1 in mammary tumors induces tumor-associated macrophage infiltration and contributes to tumor progression.* Int J Cancer, 2009. **125**(6): p. 1276-84.

302. Mizutani, K., et al., *The chemokine CCL2 increases prostate tumor growth and bone metastasis through macrophage and osteoclast recruitment.* Neoplasia, 2009. **11**(11): p. 1235-42.
303. Du, R., et al., *HIF1alpha induces the recruitment of bone marrow-derived vascular modulatory cells to regulate tumor angiogenesis and invasion.* Cancer Cell, 2008. **13**(3): p. 206-20.
304. Chambers, S.K., et al., *Overexpression of epithelial macrophage colony-stimulating factor (CSF-1) and CSF-1 receptor: a poor prognostic factor in epithelial ovarian cancer, contrasted with a protective effect of stromal CSF-1.* Clin Cancer Res, 1997. **3**(6): p. 999-1007.
305. Lu, X., et al., *Serum CCL2 and serum TNF-alpha--two new biomarkers predict bone invasion, post-treatment distant metastasis and poor overall survival in nasopharyngeal carcinoma.* Eur J Cancer, 2011. **47**(3): p. 339-46.
306. Popple, A., et al., *The chemokine, CXCL12, is an independent predictor of poor survival in ovarian cancer.* Br J Cancer, 2012. **106**(7): p. 1306-13.
307. Ochiumi, T., et al., *Clinical significance of angiopoietin-2 expression at the deepest invasive tumor site of advanced colorectal carcinoma.* Int J Oncol, 2004. **24**(3): p. 539-47.
308. Standiford, T.J., et al., *TGF-beta-induced IRAK-M expression in tumor-associated macrophages regulates lung tumor growth.* Oncogene, 2011. **30**(21): p. 2475-84.
309. Bamba, H., et al., *High expression of cyclooxygenase-2 in macrophages of human colonic adenoma.* Int J Cancer, 1999. **83**(4): p. 470-5.
310. Lin, E.Y., et al., *Vascular endothelial growth factor restores delayed tumor progression in tumors depleted of macrophages.* Mol Oncol, 2007. **1**(3): p. 288-302.
311. Rolny, C., et al., *HRG inhibits tumor growth and metastasis by inducing macrophage polarization and vessel normalization through downregulation of PlGF.* Cancer Cell, 2011. **19**(1): p. 31-44.
312. De Palma, M. and C.E. Lewis, *Macrophage regulation of tumor responses to anticancer therapies.* Cancer Cell, 2013. **23**(3): p. 277-86.
313. Aharinejad, S., et al., *Colony-stimulating factor-1 antisense treatment suppresses growth of human tumor xenografts in mice.* Cancer Res, 2002. **62**(18): p. 5317-24.
314. Loberg, R.D., et al., *Targeting CCL2 with systemic delivery of neutralizing antibodies induces prostate cancer tumor regression in vivo.* Cancer Res, 2007. **67**(19): p. 9417-24.
315. Quail, D.F. and J.A. Joyce, *Microenvironmental regulation of tumor progression and metastasis.* Nat Med, 2013. **19**(11): p. 1423-37.
316. O'Neill, A.J., et al., *Characterisation and manipulation of docetaxel resistant prostate cancer cell lines.* Mol Cancer, 2011. **10**: p. 126.
317. *Lung cancer statistics*. CancerStats Updated 4 Dec 2013, Accessed 17 Dec 2013]; Available from: http://www.cancerresearchuk.org/cancer-info/cancerstats/types/lung/.
318. *Chemotherapy for non-small cell lung cancer* Cancer Information 1 Sep 2012 Accessed 17 Dec 2013]; Available from: http://www.macmillan.org.uk/Cancerinformation/Cancertypes/Lung/Treatingnon-smallcelllungcancer/Chemotherapy.aspx.

319. Friedrich, J., et al., *Spheroid-based drug screen: considerations and practical approach.* Nat Protoc, 2009. **4**(3): p. 309-24.
320. Hirschhaeuser, F., et al., *Multicellular tumor spheroids: an underestimated tool is catching up again.* J Biotechnol, 2010. **148**(1): p. 3-15.
321. van der Meer, J.W., et al., *Characteristics of human monocytes cultured in the Teflon culture bag.* Immunology, 1982. **47**(4): p. 617-25.
322. Lee, S.H. and L.B. Epstein, *Reversible inhibition by interferon of the maturation of human peripheral blood monocytes to macrophages.* Cell Immunol, 1980. **50**(1): p. 177-90.
323. Daigneault, M., et al., *The identification of markers of macrophage differentiation in PMA-stimulated THP-1 cells and monocyte-derived macrophages.* PLoS One, 2010. **5**(1): p. e8668.
324. Rehli, M., et al., *Carboxypeptidase M is identical to the MAX.1 antigen and its expression is associated with monocyte to macrophage differentiation.* J Biol Chem, 1995. **270**(26): p. 15644-9.
325. *Direct Hybridization Assay*. 2013 Accessed 21 Nov 2013]; Available from: http://www.illumina.com/technology/direct_hybridization_assay.ilmn.
326. Smyth, G.K., *Linear models and empirical bayes methods for assessing differential expression in microarray experiments.* Stat Appl Genet Mol Biol, 2004. **3**: p. Article3.
327. Fox, S.E., et al., *The effects and comparative differences of neutrophil specific chemokines on neutrophil chemotaxis of the neonate.* Cytokine, 2005. **29**(3): p. 135-40.
328. Wieder, H.A., et al., *Comparison of changes in tumor metabolic activity and tumor size during chemotherapy of adenocarcinomas of the esophagogastric junction.* J Nucl Med, 2005. **46**(12): p. 2029-34.
329. Lee, S.C., et al., *Chemotherapy-induced tumor gene expression changes in human breast cancers.* Pharmacogenet Genomics, 2009. **19**(3): p. 181-92.
330. Liebmann, J.E., et al., *Cytotoxic studies of paclitaxel (Taxol) in human tumour cell lines.* Br J Cancer, 1993. **68**(6): p. 1104-9.
331. Fizazi, K., et al., *Viable malignant cells after primary chemotherapy for disseminated nonseminomatous germ cell tumors: prognostic factors and role of postsurgery chemotherapy--results from an international study group.* J Clin Oncol, 2001. **19**(10): p. 2647-57.
332. Davis, D.W., et al., *Automated quantification of apoptosis after neoadjuvant chemotherapy for breast cancer: early assessment predicts clinical response.* Clin Cancer Res, 2003. **9**(3): p. 955-60.
333. Varghese, J., N.S. Khandre, and A. Sarin, *Caspase-3 activation is an early event and initiates apoptotic damage in a human leukemia cell line.* Apoptosis, 2003. **8**(4): p. 363-70.
334. Jedinak, A., S. Dudhgaonkar, and D. Sliva, *Activated macrophages induce metastatic behavior of colon cancer cells.* Immunobiology, 2010. **215**(3): p. 242-9.
335. Jeyaseelan, S., et al., *Transcriptional profiling of lipopolysaccharide-induced acute lung injury.* Infect Immun, 2004. **72**(12): p. 7247-56.
336. Koch, A.E., et al., *Epithelial neutrophil activating peptide-78: a novel chemotactic cytokine for neutrophils in arthritis.* J Clin Invest, 1994. **94**(3): p. 1012-8.

337. Jamieson, T., et al., *Inhibition of CXCR2 profoundly suppresses inflammation-driven and spontaneous tumorigenesis.* J Clin Invest, 2012. **122**(9): p. 3127-44.
338. Dwyer, J., et al., *Glioblastoma cell-secreted interleukin-8 induces brain endothelial cell permeability via CXCR2.* PLoS One, 2012. **7**(9): p. e45562.
339. Keane, M.P., et al., *Depletion of CXCR2 inhibits tumor growth and angiogenesis in a murine model of lung cancer.* J Immunol, 2004. **172**(5): p. 2853-60.
340. Balentien, E., et al., *Effects of MGSA/GRO alpha on melanocyte transformation.* Oncogene, 1991. **6**(7): p. 1115-24.
341. Wang, D., et al., *CXCL1 induced by prostaglandin E2 promotes angiogenesis in colorectal cancer.* J Exp Med, 2006. **203**(4): p. 941-51.
342. Lane, B.R., et al., *Human immunodeficiency virus type 1 (HIV-1)-induced GRO-alpha production stimulates HIV-1 replication in macrophages and T lymphocytes.* J Virol, 2001. **75**(13): p. 5812-22.
343. Hagemann, T., et al., *Ovarian cancer cells polarize macrophages toward a tumor-associated phenotype.* J Immunol, 2006. **176**(8): p. 5023-32.
344. Roh-Johnson, M., et al., *Macrophage contact induces RhoA GTPase signaling to trigger tumor cell intravasation.* Oncogene, 2013.
345. Chen, Q., X.H. Zhang, and J. Massague, *Macrophage binding to receptor VCAM-1 transmits survival signals in breast cancer cells that invade the lungs.* Cancer Cell, 2011. **20**(4): p. 538-49.
346. Nozawa, H., C. Chiu, and D. Hanahan, *Infiltrating neutrophils mediate the initial angiogenic switch in a mouse model of multistage carcinogenesis.* Proc Natl Acad Sci U S A, 2006. **103**(33): p. 12493-8.
347. Welch, D.R., et al., *Tumor-elicited polymorphonuclear cells, in contrast to "normal" circulating polymorphonuclear cells, stimulate invasive and metastatic potentials of rat mammary adenocarcinoma cells.* Proc Natl Acad Sci U S A, 1989. **86**(15): p. 5859-63.
348. Provencio, M., et al., *Inoperable stage III non-small cell lung cancer: Current treatment and role of vinorelbine.* J Thorac Dis, 2011. **3**(3): p. 197-204.
349. Melillo, R.M., et al., *Mast cells have a protumorigenic role in human thyroid cancer.* Oncogene, 2010. **29**(47): p. 6203-15.
350. Xu, J., et al., *Lymphatic endothelial cell-secreted CXCL1 stimulates lymphangiogenesis and metastasis of gastric cancer.* Int J Cancer, 2012. **130**(4): p. 787-97.
351. Persson-Dajotoy, T., et al., *Expression and production of the CXC chemokine growth-related oncogene-alpha by human eosinophils.* J Immunol, 2003. **170**(10): p. 5309-16.
352. Shirey, K.A., et al., *The TLR4 antagonist Eritoran protects mice from lethal influenza infection.* Nature, 2013. **497**(7450): p. 498-502.
353. Gay, L.J. and B. Felding-Habermann, *Contribution of platelets to tumour metastasis.* Nat Rev Cancer, 2011. **11**(2): p. 123-34.
354. Falanga, A., M. Panova-Noeva, and L. Russo, *Procoagulant mechanisms in tumour cells.* Best Pract Res Clin Haematol, 2009. **22**(1): p. 49-60.
355. Gil-Bernabe, A.M., et al., *Recruitment of monocytes/macrophages by tissue factor-mediated coagulation is essential for metastatic cell survival and premetastatic niche establishment in mice.* Blood, 2012. **119**(13): p. 3164-75.

356. Gil-Bernabe, A.M., S. Lucotti, and R.J. Muschel, *Coagulation and metastasis: what does the experimental literature tell us?* Br J Haematol, 2013. **162**(4): p. 433-41.
357. Stadtmann, A. and A. Zarbock, *CXCR2: From Bench to Bedside.* Front Immunol, 2012. **3**: p. 263.
358. Becker, S., et al., *Constitutive and stimulated MCP-1, GRO alpha, beta, and gamma expression in human airway epithelium and bronchoalveolar macrophages.* Am J Physiol, 1994. **266**(3 Pt 1): p. L278-86.
359. Schmidt, H., et al., *Elevated neutrophil and monocyte counts in peripheral blood are associated with poor survival in patients with metastatic melanoma: a prognostic model.* Br J Cancer, 2005. **93**(3): p. 273-8.
360. Inage, M., et al., *Levels of cytokeratin 19 fragments in bronchoalveolar lavage fluid correlate to the intensity of neutrophil and eosinophil-alveolitis in patients with idiopathic pulmonary fibrosis.* Respir Med, 2000. **94**(2): p. 155-60.
361. Atzpodien, J. and M. Reitz, *Peripheral blood neutrophils as independent immunologic predictor of response and long-term survival upon immunotherapy in metastatic renal-cell carcinoma.* Cancer Biother Radiopharm, 2008. **23**(1): p. 129-34.
362. Jablonska, J., et al., *Neutrophils responsive to endogenous IFN-beta regulate tumor angiogenesis and growth in a mouse tumor model.* J Clin Invest, 2010. **120**(4): p. 1151-64.
363. Zins, K., et al., *Colon cancer cell-derived tumor necrosis factor-alpha mediates the tumor growth-promoting response in macrophages by up-regulating the colony-stimulating factor-1 pathway.* Cancer Res, 2007. **67**(3): p. 1038-45.
364. Imaizumi, T., et al., *Expression of tumor necrosis factor-alpha in cultured human endothelial cells stimulated with lipopolysaccharide or interleukin-1alpha.* Arterioscler Thromb Vasc Biol, 2000. **20**(2): p. 410-5.
365. Gravestein, L.A. and J. Borst, *Tumor necrosis factor receptor family members in the immune system.* Semin Immunol, 1998. **10**(6): p. 423-34.
366. Haider, S. and M. Knofler, *Human tumour necrosis factor: physiological and pathological roles in placenta and endometrium.* Placenta, 2009. **30**(2): p. 111-23.
367. Canetti, C.A., et al., *IL-18 enhances collagen-induced arthritis by recruiting neutrophils via TNF-alpha and leukotriene B4.* J Immunol, 2003. **171**(2): p. 1009-15.
368. Chandrasekharan, U.M., et al., *Tumor necrosis factor alpha (TNF-alpha) receptor-II is required for TNF-alpha-induced leukocyte-endothelial interaction in vivo.* Blood, 2007. **109**(5): p. 1938-44.
369. Ulfhammer, E., et al., *TNF-alpha mediated suppression of tissue type plasminogen activator expression in vascular endothelial cells is NF-kappaB- and p38 MAPK-dependent.* J Thromb Haemost, 2006. **4**(8): p. 1781-9.
370. Mandron, M., et al., *Dendritic cell-induced apoptosis of human cytomegalovirus-infected fibroblasts promotes cross-presentation of pp65 to CD8+ T cells.* J Gen Virol, 2008. **89**(Pt 1): p. 78-86.

371. Frater-Schroder, M., et al., *Tumor necrosis factor type alpha, a potent inhibitor of endothelial cell growth in vitro, is angiogenic in vivo.* Proc Natl Acad Sci U S A, 1987. **84**(15): p. 5277-81.
372. Leibovich, S.J., et al., *Macrophage-induced angiogenesis is mediated by tumour necrosis factor-alpha.* Nature, 1987. **329**(6140): p. 630-2.
373. Malik, S.T., et al., *Cells secreting tumour necrosis factor show enhanced metastasis in nude mice.* Eur J Cancer, 1990. **26**(10): p. 1031-4.
374. Helsby, N.A., et al., *The combined impact of CYP2C19 and CYP2B6 pharmacogenetics on cyclophosphamide bioactivation.* Br J Clin Pharmacol, 2010. **70**(6): p. 844-53.
375. Hagemann, T., et al., *Enhanced invasiveness of breast cancer cell lines upon co-cultivation with macrophages is due to TNF-alpha dependent up-regulation of matrix metalloproteases.* Carcinogenesis, 2004. **25**(8): p. 1543-9.
376. Persson, T., et al., *Expression of the neutrophil-activating CXC chemokine ENA-78/CXCL5 by human eosinophils.* Clin Exp Allergy, 2003. **33**(4): p. 531-7.
377. Alzeer, J. and O.D. Scharer, *A modified thymine for the synthesis of site-specific thymine-guanine DNA interstrand crosslinks.* Nucleic Acids Res, 2006. **34**(16): p. 4458-66.
378. Nakagawa, H., et al., *Cytokine-induced neutrophil chemoattractant (CINC)-2 alpha, a novel member of rat GRO/CINCs, is a predominant chemokine produced by lipopolysaccharide-stimulated rat macrophages in culture.* Biochem Biophys Res Commun, 1996. **220**(3): p. 945-8.
379. Gijsbers, K., et al., *GCP-2/CXCL6 synergizes with other endothelial cell-derived chemokines in neutrophil mobilization and is associated with angiogenesis in gastrointestinal tumors.* Exp Cell Res, 2005. **303**(2): p. 331-42.
380. Malawista, S.E., et al., *Chemotactic activity of human blood leukocytes in plasma treated with EDTA: chemoattraction of neutrophils about monocytes is mediated by the generation of NAP-2.* J Leukoc Biol, 2002. **72**(1): p. 175-82.
381. Imai, Y., et al., *Neutrophils enhance invasion activity of human cholangiocellular carcinoma and hepatocellular carcinoma cells: an in vitro study.* J Gastroenterol Hepatol, 2005. **20**(2): p. 287-93.
382. Braun, D.A., M. Fribourg, and S.C. Sealfon, *Cytokine response is determined by duration of receptor and signal transducers and activators of transcription 3 (STAT3) activation.* J Biol Chem, 2013. **288**(5): p. 2986-93.
383. Ferreira, F.O., et al., *Association of CCL2 with lymph node metastasis and macrophage infiltration in oral cavity and lip squamous cell carcinoma.* Tumour Biol, 2008. **29**(2): p. 114-21.
384. Roca, H., et al., *CCL2 and interleukin-6 promote survival of human CD11b+ peripheral blood mononuclear cells and induce M2-type macrophage polarization.* J Biol Chem, 2009. **284**(49): p. 34342-54.
385. Dufresne, M., et al., *Pro-inflammatory type-1 and anti-inflammatory type-2 macrophages differentially modulate cell survival and invasion of human bladder carcinoma T24 cells.* Mol Immunol, 2011. **48**(12-13): p. 1556-67.
386. Chimal-Ramirez, G.K., et al., *MMP1, MMP9, and COX2 expressions in promonocytes are induced by breast cancer cells and correlate with*

collagen degradation, transformation-like morphological changes in MCF-10A acini, and tumor aggressiveness. Biomed Res Int, 2013. **2013**: p. 279505.
387. Wyckoff, J.B., et al., *Direct visualization of macrophage-assisted tumor cell intravasation in mammary tumors.* Cancer Res, 2007. **67**(6): p. 2649-56.
388. Li, J., et al., *TNF-alpha induces leukemic clonal evolution ex vivo in Fanconi anemia group C murine stem cells.* J Clin Invest, 2007. **117**(11): p. 3283-95.
389. Komori, J., et al., *Activation-induced cytidine deaminase links bile duct inflammation to human cholangiocarcinoma.* Hepatology, 2008. **47**(3): p. 888-96.
390. Stathopoulos, G.T., et al., *Tumor necrosis factor-alpha promotes malignant pleural effusion.* Cancer Res, 2007. **67**(20): p. 9825-34.
391. Slaney, C.Y., J. Rautela, and B.S. Parker, *The emerging role of immunosurveillance in dictating metastatic spread in breast cancer.* Cancer Res, 2013. **73**(19): p. 5852-7.
392. Sceneay, J., M.J. Smyth, and A. Moller, *The pre-metastatic niche: finding common ground.* Cancer Metastasis Rev, 2013. **32**(3-4): p. 449-64.
393. Wislez, M., et al., *Tumor-derived granulocyte-macrophage colony-stimulating factor and granulocyte colony-stimulating factor prolong the survival of neutrophils infiltrating bronchoalveolar subtype pulmonary adenocarcinoma.* Am J Pathol, 2001. **159**(4): p. 1423-33.
394. Crawford, J., D.C. Dale, and G.H. Lyman, *Chemotherapy-induced neutropenia: risks, consequences, and new directions for its management.* Cancer, 2004. **100**(2): p. 228-37.
395. Bochud, P.Y., et al., *Bacteremia due to viridans streptococcus in neutropenic patients with cancer: clinical spectrum and risk factors.* Clin Infect Dis, 1994. **18**(1): p. 25-31.
396. Chen, L.C., et al., *Tumour inflammasome-derived IL-1beta recruits neutrophils and improves local recurrence-free survival in EBV-induced nasopharyngeal carcinoma.* EMBO Mol Med, 2012. **4**(12): p. 1276-93.
397. Yang, X.D., et al., *Histamine deficiency promotes inflammation-associated carcinogenesis through reduced myeloid maturation and accumulation of CD11b+Ly6G+ immature myeloid cells.* Nat Med, 2011. **17**(1): p. 87-95.
398. Arnaout, M.A., *Structure and function of the leukocyte adhesion molecules CD11/CD18.* Blood, 1990. **75**(5): p. 1037-50.
399. Fleming, T.J., M.L. Fleming, and T.R. Malek, *Selective expression of Ly-6G on myeloid lineage cells in mouse bone marrow. RB6-8C5 mAb to granulocyte-differentiation antigen (Gr-1) detects members of the Ly-6 family.* J Immunol, 1993. **151**(5): p. 2399-408.
400. Hanninen, A., et al., *Ly6C supports preferential homing of central memory CD8+ T cells into lymph nodes.* Eur J Immunol, 2011. **41**(3): p. 634-44.
401. Sun, X., et al., *Phosphatidylinositol 3-kinase-gamma signaling promotes Campylobacter jejuni-induced colitis through neutrophil recruitment in mice.* J Immunol, 2013. **190**(1): p. 357-65.
402. Tate, M.D., A.G. Brooks, and P.C. Reading, *The role of neutrophils in the upper and lower respiratory tract during influenza virus infection of mice.* Respir Res, 2008. **9**: p. 57.

403. Carr, K.D., et al., *Specific depletion reveals a novel role for neutrophil-mediated protection in the liver during Listeria monocytogenes infection.* Eur J Immunol, 2011. **41**(9): p. 2666-76.
404. Tate, M.D., et al., *Neutrophils ameliorate lung injury and the development of severe disease during influenza infection.* J Immunol, 2009. **183**(11): p. 7441-50.
405. Daley, J.M., et al., *Use of Ly6G-specific monoclonal antibody to deplete neutrophils in mice.* J Leukoc Biol, 2008. **83**(1): p. 64-70.
406. Farooq, S.M., et al., *Therapeutic effect of blocking CXCR2 on neutrophil recruitment and dextran sodium sulfate-induced colitis.* J Pharmacol Exp Ther, 2009. **329**(1): p. 123-9.
407. Bertini, R., et al., *Noncompetitive allosteric inhibitors of the inflammatory chemokine receptors CXCR1 and CXCR2: prevention of reperfusion injury.* Proc Natl Acad Sci U S A, 2004. **101**(32): p. 11791-6.
408. Romieu, R., et al., *Passive but not active CD8+ T cell-based immunotherapy interferes with liver tumor progression in a transgenic mouse model.* J Immunol, 1998. **161**(10): p. 5133-7.
409. Sarau, H.M., et al., *Interleukin-8 receptor (CXCR2) antagonists* Progress in Respiratory Research. Vol. 31. 2001: Karger, Postfach, CH-4009 Basel, Switzerland.
410. Haney, D., et al., *Isolation of viable antigen-specific CD8+ T cells based on membrane-bound tumor necrosis factor (TNF)-alpha expression.* J Immunol Methods, 2011. **369**(1-2): p. 33-41.
411. Proebstl, D., et al., *Pericytes support neutrophil subendothelial cell crawling and breaching of venular walls in vivo.* J Exp Med, 2012. **209**(6): p. 1219-34.
412. Spriggs, D.R., et al., *Tumor necrosis factor expression in human epithelial tumor cell lines.* J Clin Invest, 1988. **81**(2): p. 455-60.
413. Porter, A.G. and R.U. Janicke, *Emerging roles of caspase-3 in apoptosis.* Cell Death Differ, 1999. **6**(2): p. 99-104.
414. Movahedi, K., et al., *Different tumor microenvironments contain functionally distinct subsets of macrophages derived from Ly6C(high) monocytes.* Cancer Res, 2010. **70**(14): p. 5728-39.
415. Kolar, M., et al., *Upregulation of IL-6, IL-8 and CXCL-1 production in dermal fibroblasts by normal/malignant epithelial cells in vitro: Immunohistochemical and transcriptomic analyses.* Biol Cell, 2012. **104**(12): p. 738-51.
416. Faber, J., et al., *Bacterial translocation is reduced by a specific nutritional combination in mice with chemotherapy-induced neutropenia.* J Nutr, 2011. **141**(7): p. 1292-8.
417. Ardestani, S., et al., *Membrane versus soluble isoforms of TNF-alpha exert opposing effects on tumor growth and survival of tumor-associated myeloid cells.* Cancer Res, 2013. **73**(13): p. 3938-50.
418. Zola, H., L. Flego, and H. Weedon, *Expression of membrane receptor for tumour necrosis factor on human blood lymphocytes.* Immunol Cell Biol, 1993. **71 (Pt 4)**: p. 281-8.
419. Gehr, G., et al., *Both tumor necrosis factor receptor types mediate proliferative signals in human mononuclear cell activation.* J Immunol, 1992. **149**(3): p. 911-7.

420. Ye, Q., et al., *Increased expression of tumor necrosis factor receptors in cryptogenic organizing pneumonia.* Respir Med, 2011. **105**(2): p. 292-7.
421. Faustman, D. and M. Davis, *TNF receptor 2 pathway: drug target for autoimmune diseases.* Nat Rev Drug Discov, 2010. **9**(6): p. 482-93.
422. Kieszko, R., et al., *Tumor necrosis factor receptors (TNFRs) on T lymphocytes and soluble TNFRs in different clinical courses of sarcoidosis.* Respir Med, 2007. **101**(3): p. 645-54.
423. Aderka, D., et al., *Stabilization of the bioactivity of tumor necrosis factor by its soluble receptors.* J Exp Med, 1992. **175**(2): p. 323-9.
424. Li, B., et al., *Low levels of tumor necrosis factor alpha increase tumor growth by inducing an endothelial phenotype of monocytes recruited to the tumor site.* Cancer Res, 2009. **69**(1): p. 338-48.
425. Ding, Y., et al., *NFAT1 mediates placental growth factor-induced myelomonocytic cell recruitment via the induction of TNF-alpha.* J Immunol, 2010. **184**(5): p. 2593-601.
426. Vieira, S.M., et al., *A crucial role for TNF-alpha in mediating neutrophil influx induced by endogenously generated or exogenous chemokines, KC/CXCL1 and LIX/CXCL5.* Br J Pharmacol, 2009. **158**(3): p. 779-89.
427. Murphy, P.M., et al., *International union of pharmacology. XXII. Nomenclature for chemokine receptors.* Pharmacol Rev, 2000. **52**(1): p. 145-76.
428. Yoo, S.Y., et al., *The degree of tumor volume reduction during the early phase of induction chemotherapy is an independent prognostic factor in patients with high-risk neuroblastoma.* Cancer, 2013. **119**(3): p. 656-64.
429. Kim, H.J. and W. Kim, *Method of tumor volume evaluation using magnetic resonance imaging for outcome prediction in cervical cancer treated with concurrent chemotherapy and radiotherapy.* Radiat Oncol J, 2012. **30**(2): p. 70-7.
430. Song, M.K., et al., *Prognostic value of metabolic tumor volume on PET / CT in primary gastrointestinal diffuse large B cell lymphoma.* Cancer Sci, 2012. **103**(3): p. 477-82.
431. Song, W.S., et al., *Tumor volume increase during preoperative chemotherapy as a novel predictor of local recurrence in extremity osteosarcoma.* Ann Surg Oncol, 2011. **18**(6): p. 1710-6.
432. Yang, X., et al., *Cyclophosphamide-induced apoptosis in A431 cells is inhibited by fucosyltransferase IV.* J Cell Biochem, 2011. **112**(5): p. 1376-83.
433. Weber, T.G., et al., *Noninvasive monitoring of pharmacodynamics and kinetics of a death receptor 5 antibody and its enhanced apoptosis induction in sequential application with doxorubicin.* Neoplasia, 2013. **15**(8): p. 863-74.
434. Reichel, C.A., et al., *Ccl2 and Ccl3 mediate neutrophil recruitment via induction of protein synthesis and generation of lipid mediators.* Arterioscler Thromb Vasc Biol, 2009. **29**(11): p. 1787-93.
435. *AC chemotherapy* Cancer Information Updated 1 Dec 2011, Accessed 24 Dec 2013]; Available from: http://www.macmillan.org.uk/Cancerinformation/Cancertreatment/Treatmenttypes/Chemotherapy/Combinationregimen/AC.aspx.

436. Feiken, E., et al., *Neutrophils express tumor necrosis factor-alpha during mouse skin wound healing.* J Invest Dermatol, 1995. **105**(1): p. 120-3.
437. Kanno, E., et al., *Wound healing in skin promoted by inoculation with Pseudomonas aeruginosa PAO1: The critical role of tumor necrosis factor-alpha secreted from infiltrating neutrophils.* Wound Repair Regen, 2011. **19**(5): p. 608-21.
438. Gruber, M., et al., *Prolonged progression-free survival in patients with chronic lymphocytic leukemia receiving granulocyte colony-stimulating factor during treatment with fludarabine, cyclophosphamide, and rituximab.* Ann Hematol, 2011. **90**(10): p. 1131-6.
439. Yu, J., et al., *Mobilization of Peripheral Blood Stem Cells Using Regimen Combining Docetaxel with Granulocyte Colony-stimulating Factor in Breast Cancer Patients.* Chin J Cancer Res, 2011. **23**(1): p. 49-53.
440. Martin, M., et al., *Toxicity and health-related quality of life in breast cancer patients receiving adjuvant docetaxel, doxorubicin, cyclophosphamide (TAC) or 5-fluorouracil, doxorubicin and cyclophosphamide (FAC): impact of adding primary prophylactic granulocyte-colony stimulating factor to the TAC regimen.* Ann Oncol, 2006. **17**(8): p. 1205-12.
441. Papaldo, P., et al., *Addition of either lonidamine or granulocyte colony-stimulating factor does not improve survival in early breast cancer patients treated with high-dose epirubicin and cyclophosphamide.* J Clin Oncol, 2003. **21**(18): p. 3462-8.
442. Ellis, G.K., et al., *Phase III comparison of standard doxorubicin and cyclophosphamide versus weekly doxorubicin and daily oral cyclophosphamide plus granulocyte colony-stimulating factor as neoadjuvant therapy for inflammatory and locally advanced breast cancer: SWOG 0012.* J Clin Oncol, 2011. **29**(8): p. 1014-21.
443. Staar, S., et al., *Intensified hyperfractionated accelerated radiotherapy limits the additional benefit of simultaneous chemotherapy--results of a multicentric randomized German trial in advanced head-and-neck cancer.* Int J Radiat Oncol Biol Phys, 2001. **50**(5): p. 1161-71.
444. Cairns, R.A., R. Khokha, and R.P. Hill, *Molecular mechanisms of tumor invasion and metastasis: an integrated view.* Curr Mol Med, 2003. **3**(7): p. 659-71.
445. Colombo, M.P., et al., *Granulocyte colony-stimulating factor gene transfer suppresses tumorigenicity of a murine adenocarcinoma in vivo.* J Exp Med, 1991. **173**(4): p. 889-97.
446. Xu, S., et al., *Granulocyte colony-stimulating factor (G-CSF) induces the production of cytokines in vivo.* Br J Haematol, 2000. **108**(4): p. 848-53.

APPENDIX

Supplementary Table 1 Top 150 upregulated and downregulated DEGs

	Probe_ID	Gene_Symbol	Gene_ID	logFC	pValue
	Upregulated				
1	ILMN_1672148	AKR1B10	57016	6.068605478	1.49E-03
2	ILMN_2278335	AKR1B15	441282	5.950108178	8.66E-04
3	ILMN_2412336	AKR1C2	1646	5.87972193	9.13E-04
4	ILMN_1801442	KRT81	3887	5.562068532	6.61E-04
5	ILMN_2060413	CD24	100133941	5.547963079	9.48E-04
6	ILMN_1665865	IGFBP4	3487	5.287727338	1.65E-03
7	ILMN_1720998	CA12	771	5.214947793	6.99E-04
8	ILMN_2133205	GPX2	2877	5.114019255	8.07E-03
9	ILMN_1746085	IGFBP3	3486	5.089582439	1.05E-02
10	ILMN_3307841	AGR2	10551	4.9036228	2.91E-03
11	ILMN_2371055	EFNA1	1942	4.883440678	2.04E-03
12	ILMN_1687757	AKR1C4	1109	4.868529694	4.00E-04
13	ILMN_1712082	GCNT3	9245	4.848964645	2.37E-04
14	ILMN_2315044	FGG	2266	4.654760779	3.58E-02
15	ILMN_1655595	SERPINE2	5270	4.578834173	1.23E-04
16	ILMN_1656487	FGA	2243	4.561850639	8.49E-03
17	ILMN_1713124	AKR1C3	8644	4.43627328	1.37E-04
18	ILMN_1753143	RHPN2	85415	4.372056429	2.73E-03
19	ILMN_1770338	TM4SF1	4071	4.32235871	7.24E-03
20	ILMN_1773567	LAMA5	3911	4.286644055	1.90E-04
21	ILMN_2382942	CA12	771	4.279721259	8.98E-04
22	ILMN_2396875	IGFBP3	3486	4.176009552	1.99E-02
23	ILMN_1771599	PLOD2	5352	4.126275561	2.33E-03
24	ILMN_2108735	EEF1A2	1917	4.060044566	6.99E-04
25	ILMN_1779017	FGA	2243	4.039377397	1.05E-02
26	ILMN_1670379	ANTXR1	84168	4.038274026	4.92E-04
27	ILMN_2387385	IGFBP1	3484	3.999221532	8.51E-04
28	ILMN_2041222	FLJ40504	284085	3.91322459	2.66E-03
29	ILMN_2381945	FGA	2243	3.869836384	1.48E-02
30	ILMN_1754795	FAT1	2195	3.857175958	2.37E-04
31	ILMN_1677511	PTGS2	5743	3.795429724	2.07E-03
32	ILMN_2174127	DCBLD2	131566	3.771386897	4.00E-04
33	ILMN_1721770	PAPPA	5069	3.767235047	1.20E-03
34	ILMN_2063168	MALL	7851	3.742252784	2.11E-02
35	ILMN_1694778	LOC646723	646723	3.719929515	1.16E-03
36	ILMN_2315780	TACC2	10579	3.677210775	5.79E-03
37	ILMN_1681983	RSPO3	84870	3.579048952	8.66E-04
38	ILMN_1666893	TRIML2	205860	3.5471121	3.14E-04
39	ILMN_1775830	TM4SF20	79853	3.536519575	3.86E-02
40	ILMN_3251672	DSG2	1829	3.497382598	1.03E-03
41	ILMN_1676278	ABCC2	1244	3.489174119	4.00E-04
42	ILMN_2171384	CXCL5	6374	3.47538525	1.36E-03
43	ILMN_2380237	C1QTNF1	114897	3.472773902	2.34E-03
44	ILMN_3305152	XAGE1A	653219	3.453159194	6.61E-04
45	ILMN_2054297	PTGS2	5743	3.437097065	8.66E-04
46	ILMN_1691494	XAGE1B	653220	3.404017398	4.00E-04
47	ILMN_1763196	WDR72	256764	3.344962239	1.48E-03
48	ILMN_1753584	KRT8	3856	3.343347519	1.92E-03
49	ILMN_1794863	CAMK2N1	55450	3.329647789	1.21E-02

50	ILMN_1729117	COL5A2	1290	3.323185412	4.20E-03
51	ILMN_3247578	FAT1	2195	3.321059116	9.77E-04
52	ILMN_2366192	FGL1	2267	3.308415833	2.43E-02
53	ILMN_1735499	DCBLD2	131566	3.299315505	7.78E-04
54	ILMN_2101832	LAPTM4B	55353	3.274211364	1.89E-03
55	ILMN_2139761	LIMCH1	22998	3.259611805	6.08E-03
56	ILMN_1656369	C8ORF4	56892	3.220160763	1.56E-03
57	ILMN_2041190	F2RL1	2150	3.196566671	4.43E-03
58	ILMN_1703593	BAIAP2L1	55971	3.186142725	1.04E-03
59	ILMN_1752562	CXCL5	6374	3.178668538	1.25E-02
60	ILMN_2269256	DNAJC12	56521	3.167815193	1.56E-03
61	ILMN_1742534	COL4A5	1287	3.155887774	1.98E-03
62	ILMN_1775829	PERP	64065	3.134424162	1.47E-03
63	ILMN_1691410	BAMBI	25805	3.123938596	8.75E-04
64	ILMN_2371053	EFNA1	1942	3.098001894	4.38E-02
65	ILMN_2400407	CNTN1	1272	3.092681751	2.76E-02
66	ILMN_2380163	PTPRF	5792	3.034912055	1.10E-03
67	ILMN_2149226	CAV1	857	3.01886244	8.51E-04
68	ILMN_1730487	CALD1	800	2.996332131	2.71E-03
69	ILMN_2411236	NRCAM	4897	2.943901991	1.98E-03
70	ILMN_1658499	SYT13	57586	2.907554143	1.97E-02
71	ILMN_1779228	CDH2	1000	2.903035218	1.22E-03
72	ILMN_1700031	PRAME	23532	2.89046379	1.14E-03
73	ILMN_1765966	CHGB	1114	2.864989977	2.03E-02
74	ILMN_1795342	MLPH	79083	2.851679823	5.09E-04
75	ILMN_1722809	NRCAM	4897	2.838917657	2.72E-03
76	ILMN_1709674	GFPT2	9945	2.822310424	2.32E-02
77	ILMN_1680196	LAPTM4B	55353	2.819217643	2.61E-03
78	ILMN_1680874	TUBB2B	347733	2.815008124	7.41E-04
79	ILMN_2398159	DKK3	27122	2.813630734	2.05E-03
80	ILMN_1806733	COL18A1	80781	2.805995674	4.36E-03
81	ILMN_1751161	COL7A1	1294	2.781632841	3.37E-05
82	ILMN_1682738	SMAD3	4088	2.779720994	2.37E-04
83	ILMN_1775448	PFN2	5217	2.759654271	4.66E-04
84	ILMN_1797776	PRSS23	11098	2.757678549	2.62E-03
85	ILMN_1789196	TPM2	7169	2.746844696	1.69E-02
86	ILMN_1844593	HS.551128		2.744415694	1.95E-03
87	ILMN_1750181	TESC	54997	2.722550049	2.21E-02
88	ILMN_1668052	FOXA2	3170	2.71790653	1.86E-03
89	ILMN_1719883	CYP4F11	57834	2.717374821	1.99E-04
90	ILMN_1779182	TMEM98	26022	2.709082152	9.36E-04
91	ILMN_1717793	C19ORF33	64073	2.703267192	1.48E-03
92	ILMN_1674620	SGCE	8910	2.702002622	9.13E-04
93	ILMN_1788874	SERPINA3	12	2.693242883	3.99E-03
94	ILMN_1700831	SLC27A2	11001	2.682760791	2.38E-03
95	ILMN_2384122	GPR56	9289	2.673658047	1.74E-02
96	ILMN_1757604	TPM2	7169	2.672197527	1.18E-02
97	ILMN_1837428	HS.25318		2.646052064	1.28E-03
98	ILMN_1792356	DPYSL4	10570	2.616251534	1.39E-03
99	ILMN_1803073	DNAJC12	56521	2.6140289	1.95E-03
100	ILMN_1682636	CXCL2	2920	2.602766696	4.73E-02
101	ILMN_1758164	STC1	6781	2.582168335	1.93E-02
102	ILMN_1854469	HS.100261		2.581511675	1.48E-03
103	ILMN_3263974	KRT18P13	392371	2.579487933	3.65E-03
104	ILMN_1671971	LOC644743	644743	2.575612154	2.66E-03
105	ILMN_2340259	PDE4B	5142	2.565843704	6.61E-04
106	ILMN_2041788	PLS3	5358	2.564675393	2.14E-03

107	ILMN_2081087	HSPA12A	259217	2.544854302	8.75E-04
108	ILMN_1791726	TUBB3	10381	2.498494504	1.26E-02
109	ILMN_2363165	TACC2	10579	2.488810936	1.90E-02
110	ILMN_1725485	RGS17	26575	2.482788011	5.32E-04
111	ILMN_1782439	CNN3	1266	2.481581768	3.58E-03
112	ILMN_1658289	WDR54	84058	2.4812945	1.19E-02
113	ILMN_1712545	S100A3	6274	2.464671407	2.13E-03
114	ILMN_1802808	LOC654103	654103	2.464293735	1.66E-03
115	ILMN_1790778	PNMA2	10687	2.449448243	1.47E-03
116	ILMN_1788416	FAM108C1	58489	2.441826607	2.91E-03
117	ILMN_1761858	MID1	4281	2.441745142	3.42E-03
118	ILMN_2120695	TSPAN7	7102	2.441264102	2.22E-03
119	ILMN_1815500	ITPR3	3710	2.436990774	1.20E-03
120	ILMN_1803348	EHBP1	23301	2.436051401	3.65E-03
121	ILMN_2376263	SMARCA1	6594	2.436039283	1.26E-03
122	ILMN_1672589	SEMA4B	10509	2.413716299	2.89E-03
123	ILMN_1740555	SNAP25	6616	2.413199559	3.86E-02
124	ILMN_2343774	XAGE1	9503	2.412778057	4.00E-04
125	ILMN_1788955	PDLIM1	9124	2.405846652	2.22E-03
126	ILMN_1716815	CEACAM1	634	2.398077381	1.59E-02
127	ILMN_1729563	UGDH	7358	2.396282961	1.83E-03
128	ILMN_1765574	TFAP2A	7020	2.386072134	3.14E-04
129	ILMN_1756071	MFGE8	4240	2.37621973	2.31E-03
130	ILMN_1695946	TRNP1	388610	2.369131319	1.56E-03
131	ILMN_2068104	TFPI2	7980	2.365494779	8.66E-04
132	ILMN_2163723	KRT7	3855	2.363897768	1.20E-03
133	ILMN_1796074	C18ORF56	494514	2.353759842	3.89E-03
134	ILMN_1782419	GNG11	2791	2.351761083	6.33E-03
135	ILMN_1673113	F2RL1	2150	2.348551863	5.63E-03
136	ILMN_1815673	DKK3	27122	2.342476532	8.14E-03
137	ILMN_1720282	NQO1	1728	2.336109972	4.66E-04
138	ILMN_2352097	GPR56	9289	2.335233727	1.93E-02
139	ILMN_2128770	CDR2L	30850	2.333485176	1.28E-03
140	ILMN_1705066	BTBD11	121551	2.326005325	2.59E-02
141	ILMN_1787897	CXCL1	2919	2.32072426	3.38E-02
142	ILMN_1663401	LARP6	55323	2.318288029	5.87E-04
143	ILMN_1659913	ISG20	3669	2.312972634	9.13E-04
144	ILMN_2113490	NTN4	59277	2.299948844	1.18E-03
145	ILMN_1769201	ELF3	1999	2.295579746	2.76E-03
146	ILMN_1701007	PON3	5446	2.294023766	4.09E-02
147	ILMN_1658709	LAMB1	3912	2.291446499	4.07E-03
148	ILMN_2093027	MYO1B	4430	2.287761696	1.59E-02
149	ILMN_1709479	YAP1	10413	2.27276551	1.56E-03
150	ILMN_1724658	BNIP3	664	2.263770441	9.29E-03
	Probe_ID	**Gene_Symbol**	**Gene_ID**	**logFC**	**pValue**
	Downregulated				
1	ILMN_1754121	CSK	1445	-0.284140672	4.61E-02
2	ILMN_3278157	LOC653156	653156	-0.289716204	4.36E-02
3	ILMN_1800543	SCFD1	23256	-0.304810559	4.27E-02
4	ILMN_1657148	C19ORF23	148046	-0.31013655	4.73E-02
5	ILMN_1755111	C6ORF199	221264	-0.310393389	4.56E-02
6	ILMN_1682711	LOC493754	493754	-0.314521009	3.79E-02
7	ILMN_2299843	ATP5S	27109	-0.316489628	3.71E-02
8	ILMN_3268564	C19ORF60	55049	-0.319941584	3.83E-02
9	ILMN_1670769	CENPQ	55166	-0.325616473	4.74E-02

10	ILMN_3251501	SERF2	10169	-0.326013676	4.28E-02
11	ILMN_1651735	TGOLN2	10618	-0.328636966	4.14E-02
12	ILMN_2191720	ZNF471	57573	-0.329571295	4.36E-02
13	ILMN_1806483	ZWILCH	55055	-0.33144606	4.88E-02
14	ILMN_2389445	ARHGEF10L	55160	-0.332162395	3.46E-02
15	ILMN_2364700	ENSA	2029	-0.332525146	4.80E-02
16	ILMN_2321634	RAD17	5884	-0.332830856	4.47E-02
17	ILMN_1667737	DNAHL1	284176	-0.333119929	3.29E-02
18	ILMN_1751143	C7ORF23	79161	-0.333236852	4.41E-02
19	ILMN_1695357	CCDC99	54908	-0.333947619	3.86E-02
20	ILMN_1755937	ANXA2	302	-0.335346044	3.97E-02
21	ILMN_1754423	C3ORF23	285343	-0.335614372	3.55E-02
22	ILMN_1776119	ABCC10	89845	-0.335937013	4.20E-02
23	ILMN_1820767	HS.293676		-0.336700336	4.90E-02
24	ILMN_1718610	ARHGAP17	55114	-0.337066429	4.52E-02
25	ILMN_1765500	NDUFV3	4731	-0.338814072	3.56E-02
26	ILMN_2130838	UTP11L	51118	-0.338994387	4.88E-02
27	ILMN_1770466	ATP5G3	518	-0.339319257	3.38E-02
28	ILMN_1657149	C8ORF46	254778	-0.339629423	3.58E-02
29	ILMN_1715908	NCAPH2	29781	-0.340504933	4.87E-02
30	ILMN_1808196	GSTO1	9446	-0.343223371	4.12E-02
31	ILMN_1656184	PI4KAP1	728233	-0.344733433	4.60E-02
32	ILMN_1727798	MOSPD1	56180	-0.345252566	3.90E-02
33	ILMN_3238623	LYRM7	90624	-0.345538684	4.42E-02
34	ILMN_1755983	NFATC3	4775	-0.345576572	4.03E-02
35	ILMN_1735075	PGBD2	267002	-0.345582564	4.16E-02
36	ILMN_1657144	C1ORF69	200205	-0.346692673	4.60E-02
37	ILMN_1684042	BET1	10282	-0.346985652	4.00E-02
38	ILMN_1715674	ITPK1	3705	-0.347425688	2.96E-02
39	ILMN_1782069	TRAK1	22906	-0.347898996	3.43E-02
40	ILMN_2130514	FAM76B	143684	-0.348230266	3.62E-02
41	ILMN_1789751	MFSD1	64747	-0.348453256	2.40E-02
42	ILMN_1710710	DEDD	9191	-0.349986596	4.50E-02
43	ILMN_1750101	S100A11	6282	-0.350152543	3.44E-02
44	ILMN_1788211	SNX19	399979	-0.3524995	4.91E-02
45	ILMN_1723793	PALB2	79728	-0.352804557	2.71E-02
46	ILMN_1767992	SLC12A6	9990	-0.353666053	3.78E-02
47	ILMN_1784523	ATP6V1G1	9550	-0.353794014	3.86E-02
48	ILMN_1725787	RFX1	5989	-0.353817753	3.00E-02
49	ILMN_1728676	KIAA0196	9897	-0.354221015	3.14E-02
50	ILMN_1755423	PTCRA	171558	-0.354982709	4.15E-02
51	ILMN_1654318	PTPN23	25930	-0.35609997	2.94E-02
52	ILMN_1714567	AHNAK	79026	-0.356360855	4.00E-02
53	ILMN_1758545	DNAJB12	54788	-0.356660665	2.87E-02
54	ILMN_1730416	CYCS	54205	-0.357081055	3.25E-02
55	ILMN_1670801	MTR	4548	-0.357252811	4.26E-02
56	ILMN_3236135	FAM86D	692099	-0.357908036	4.82E-02
57	ILMN_2193498	C1ORF25	81627	-0.358174061	2.69E-02
58	ILMN_1807662	IGF2R	3482	-0.358436655	2.35E-02
59	ILMN_3251312	TMEM69	51249	-0.3589313	4.65E-02
60	ILMN_1711383	STK4	6789	-0.359812997	2.67E-02
61	ILMN_2163732	ATG3	64422	-0.360712855	2.52E-02
62	ILMN_1655921	GTF2E1	2960	-0.360754682	2.83E-02
63	ILMN_1734895	SFT2D1	113402	-0.361460601	4.45E-02
64	ILMN_1658302	PIAS2	9063	-0.361526306	3.67E-02
65	ILMN_1662932	LCP1	3936	-0.362144268	4.96E-02
66	ILMN_2305544	DBI	1622	-0.362395537	4.61E-02

67	ILMN_1719158	CTBP1	1487	-0.3627983	2.56E-02
68	ILMN_1658684	ATP9B	374868	-0.363245972	4.52E-02
69	ILMN_1792305	ZNF318	24149	-0.363269288	4.29E-02
70	ILMN_3178529	FAM108A2	728917	-0.36377767	4.21E-02
71	ILMN_2140990	CAMK1	8536	-0.363949135	3.03E-02
72	ILMN_2124386	RGL2	5863	-0.36414336	3.41E-02
73	ILMN_1804820	ZNF431	170959	-0.364322664	2.39E-02
74	ILMN_1668619	KIAA1467	57613	-0.36462873	4.60E-02
75	ILMN_1782851	TAPBP	6892	-0.365616452	3.18E-02
76	ILMN_1689518	PECAM1	5175	-0.36666655	4.08E-02
77	ILMN_1768640	CRNKL1	51340	-0.367941707	4.01E-02
78	ILMN_2408240	DTNBP1	84062	-0.368480712	2.91E-02
79	ILMN_2362346	TRPV4	59341	-0.369235661	3.35E-02
80	ILMN_1742224	SLTM	79811	-0.369536331	2.25E-02
81	ILMN_2052335	MYOC	4653	-0.369698511	2.53E-02
82	ILMN_1724230	LOC642236	642236	-0.370196696	4.55E-02
83	ILMN_2398587	ZNRD1	30834	-0.370969239	3.38E-02
84	ILMN_1754051	RMI1	80010	-0.371029457	2.96E-02
85	ILMN_1741712	MS4A4A	51338	-0.371647105	2.67E-02
86	ILMN_1903049	HS.527071		-0.371997852	4.33E-02
87	ILMN_2117171	LMO4	8543	-0.373299982	4.05E-02
88	ILMN_1716821	GORASP1	64689	-0.374164704	2.28E-02
89	ILMN_1679577	SETD3	84193	-0.374257917	3.48E-02
90	ILMN_1694504	RNF220	55182	-0.374309152	4.50E-02
91	ILMN_1786843	KCTD13	253980	-0.374383445	1.90E-02
92	ILMN_2043569	MOSPD2	158747	-0.374412458	3.24E-02
93	ILMN_2337789	Mar-02	51257	-0.375243592	1.72E-02
94	ILMN_3266054	FLJ31306	379025	-0.375795275	2.21E-02
95	ILMN_1776109	ZNF622	90441	-0.375806096	2.74E-02
96	ILMN_1755909	C20ORF11	54994	-0.37584411	4.34E-02
97	ILMN_1670377	ZNF20	7568	-0.376377013	3.73E-02
98	ILMN_2411731	HPS5	11234	-0.37685832	1.88E-02
99	ILMN_1703573	DNAJC17	55192	-0.378414542	4.56E-02
100	ILMN_1717099	DSCR3	10311	-0.378896129	3.66E-02
101	ILMN_3201485	LOC644988	644988	-0.378966844	2.94E-02
102	ILMN_1745005	GGCT	79017	-0.379093812	2.63E-02
103	ILMN_1765746	SFT2D3	84826	-0.379658216	3.39E-02
104	ILMN_1802631	AGA	175	-0.381106329	3.10E-02
105	ILMN_1697024	LOC730432	730432	-0.381114863	2.39E-02
106	ILMN_1810289	FER1L3	26509	-0.381350562	3.62E-02
107	ILMN_1747598	PPP1R11	6992	-0.381844513	4.92E-02
108	ILMN_3199780	LOC401076	401076	-0.38193012	3.31E-02
109	ILMN_1801043	GSN	2934	-0.382274799	4.45E-02
110	ILMN_1797082	SNX13	23161	-0.382606274	1.82E-02
111	ILMN_1735788	TRIOBP	11078	-0.382858751	3.07E-02
112	ILMN_1801914	SH3BP2	6452	-0.38340176	3.10E-02
113	ILMN_2380967	DNASE1L1	1774	-0.384582065	2.17E-02
114	ILMN_1756910	PLA2G15	23659	-0.38463456	3.11E-02
115	ILMN_1745620	KRCC1	51315	-0.38496145	2.76E-02
116	ILMN_1733374	LOC642197	642197	-0.385140183	2.36E-02
117	ILMN_3247064	SNRNP40	9410	-0.385323943	2.16E-02
118	ILMN_1663664	MRPS10	55173	-0.385798395	3.48E-02
119	ILMN_2162234	NEK1	4750	-0.387059473	3.93E-02
120	ILMN_2367418	OSCAR	126014	-0.387206692	3.41E-02
121	ILMN_1653940	USP2	9099	-0.388524838	3.62E-02
122	ILMN_1744914	FUCA2	2519	-0.389163905	3.71E-02
123	ILMN_2365307	CD276	80381	-0.389854692	2.37E-02

124	ILMN_2141807	C15ORF23	90417	-0.389977963	4.78E-02
125	ILMN_1738604	ADH5	128	-0.389997431	3.55E-02
126	ILMN_3243011	LOC641844	641844	-0.390056305	2.76E-02
127	ILMN_2389347	NR3C1	2908	-0.390991345	3.75E-02
128	ILMN_1688753	PTDSS1	9791	-0.391244837	3.34E-02
129	ILMN_1655734	RPF1	80135	-0.393071157	4.19E-02
130	ILMN_2088410	PSMG2	56984	-0.393084781	3.02E-02
131	ILMN_1721704	FNTA	2339	-0.393170338	1.90E-02
132	ILMN_1780618	TMEM192	201931	-0.393413761	4.06E-02
133	ILMN_1810228	TTF2	8458	-0.393603248	2.98E-02
134	ILMN_2151579	HMGN1	3150	-0.394135477	4.16E-02
135	ILMN_1765021	TOP3B	8940	-0.394276259	4.50E-02
136	ILMN_1766247	ZBTB2	57621	-0.394414338	2.88E-02
137	ILMN_1671981	FLJ44076	401080	-0.395039178	2.03E-02
138	ILMN_1783469	LOC642197	642197	-0.395249021	3.56E-02
139	ILMN_3237721	TMCO7	79613	-0.395416716	3.44E-02
140	ILMN_1873300	HS.571245		-0.395609499	4.34E-02
141	ILMN_1655312	HPS5	11234	-0.396474864	2.83E-02
142	ILMN_1671387	C3ORF23	285343	-0.396627456	4.15E-02
143	ILMN_2276952	TSC22D3	1831	-0.396830739	3.38E-02
144	ILMN_2074258	BARD1	580	-0.397066646	4.93E-02
145	ILMN_3241758	POTEF	728378	-0.398191381	4.36E-02
146	ILMN_2167416	MR1	3140	-0.399294339	2.61E-02
147	ILMN_1733515	LOXL3	84695	-0.39944334	4.22E-02
148	ILMN_2178088	ZNF131	7690	-0.399637066	2.07E-02
149	ILMN_1768020	HAUS8	93323	-0.399780033	3.32E-02
150	ILMN_2383693	UPF2	26019	-0.400114189	1.90E-02

Supplementary Method 1 Immunohistochemistry protocol

DEPARAFFINIZATION

In a slide staining jar, perform the following procedures to remove paraffin and rehydrate tissues:

XYLENE/HISTOCLEAR - Wash 3X, 3 min each wash (replace solution in jar each time)

100% Ethanol – Wash 2X, 3 min each wash

95% Ethanol – Wash 1x, 2 min.

70% Ethanol – Wash 1x, 2 min.

Distilled Water – Wash 1x, 2 min.

PAP Section with pen, and add 1% hydrogen peroxide in water (*from 30% stock*), 10 min. to quench any endogenous peroxidase in tissue

10ml = 333ul 30% H2O2 into 9.7 ml H20

Meanwhile, prep moisture chamber (wet tissues and put parafilm on top)

Turn **ON** steamer, and warm antigen retrieval solution

(3.75 ml of either alkaline or citrate-based antigen retrieval solution + 400 ml of water (*Vector Labs, H3300 or H3301*))

Wash slides with PBS at least 3X, 3 min. each

ANTIGEN RETRIEVAL STEP

Put slides into warmed antigen retrieval solution and keep in closed steamer for 30 minutes

Remove steaming basket, and let cool at room temperature for 15-30 minutes

---

PRIMARY ANTIBODY STEP

Wash slides at least 1X with PBS

Block with pre-diluted 2.5% normal goat blocking serum for 20 minutes. (in humidified chamber)

Wash slides with PBS 3X

Add 2.5% normal goat blocking serum + primary antibody (~120ul per slide, use flexible coverslip to submerge slides and prevent drying out). Levae O/N at 4 deg C in moisture chamber.

RAT anti-PyMT- use at 1:200 overnight (in 2.5% NGS)

SECONDARY ANTIBODY STEP

Wash cover slips off with PBS, and incubate slides 2x in PBS for 5 min each

Drop ImmPRESS reagent (ex. anti-rat, mouse adsorbed) onto sections and incubate 30 minutes at room temp in moisture chamber.

Wash slides with PBS 2x, 5 min. each

DAB SUBSTRATE ADDITION

Prepare ImmPACT DAB substrate solution (*SK-4105, Vector Labs)*

Add 1 drop of ImmPACT DAB Chromogen concentrate to 1ml ImmPACT DAB Diluent. Mix well. Stable for 14 days at 2-8 deg C.

Incubate slides in DAB substrate solution for 5 minutes (or until developed).

Once staining intensity is achieved, immediately wash with cold tap water. Rinse slides at least 2x with cold tap water 5 min each.

HEMATOXYLIN QS COUNTER-STAIN

Use Hematoxylin QS (QuickStain – *H-3404 Vector Labs*) and apply on sections directly, for 5-45 seconds.

Wash with distilled water until it runs clear.

DEHYRADATION

Follow alcohol series in ***reverse*** from deparaffinization step:

70% Ethanol – 1x, 2 minutes

95% Ethanol – 1x, 2 minutes

100% Ethanol – 2x, 3 minutes

Xylene/Histoclear – 3x, 3 minutes

Mount with Cytoseal XYL (*Richard-Allen Scientific*)